

ECE 417/517 NANO-ELECTRONICS

Spring 2007

Lecture 1: Introduction

- Moore's Law, etc
- CMOS
 - Scaling
 - Nanoscale operation
 - Fundamental limits
- Nanoscale dimensions
- Density of states
- Nanoparticles

References:

- Mircea & Daniela Dragoman "Nanoelectronics: Principles & Devices" Artech House (2006)
 - Rainer Waser (ed) "Nanoelectronics & Information technology" Wiley-VCH (2003)
 - K.Goser, P. Glosekotter, & J. Dienstuhl "Nanoelectronics & Nanosystems" Springer (2004)
 - Mizuta & Tanoue "Physics & Applications of Resonant Tunnelling Diodes" Cambridge (1995)
 - Mahapatra & Ionescu "Hybrid CMOS Single-Electron-Transistor Device & Circuit Design" Artech House (2006)
 - Omar Manasreh "Semiconductor Heterojunctions & Nanostructures" McGraw-Hill (2005)
 - Bharat Bhushan (Ed) "Springer Handbook of Nanotechnology" Springer (2004)
 - Edward Wolf "Nanophysics & nanotechnology" Wiley-VCH ((2004)
- Selected contents from each of the above are included in the Course Pack
- Poole & Owens "Introduction to Nanotechnology" Wiley (2003)
 - Kwok Ng "Complete Guide to Semiconductor Devices (2e)" Wiley/IEEE (2002)
 - Christoph Wasshuber "Computational Single-Electronics" Springer (2001)
 - Grabert & Devoret (eds) "Single Charge Tunneling" NATO ASI B294, Kluwer/Plenum
 - Ferry & Goodnick "Transport in Nanostructures" Cambridge (1997)
 - Ferry, Barker, & Jacoboni (eds) "Granular Nanoelectronics" PlenumNATO Series 251 (1991)
 - Saito, Dresselhaus, & Dresselhaus "Physical Properties of Carbon Nanotubes" ICP (1998)
 - Forrest L. Carter (ed) "Molecular Electronic Devices" Marcel-Dekker (1982)

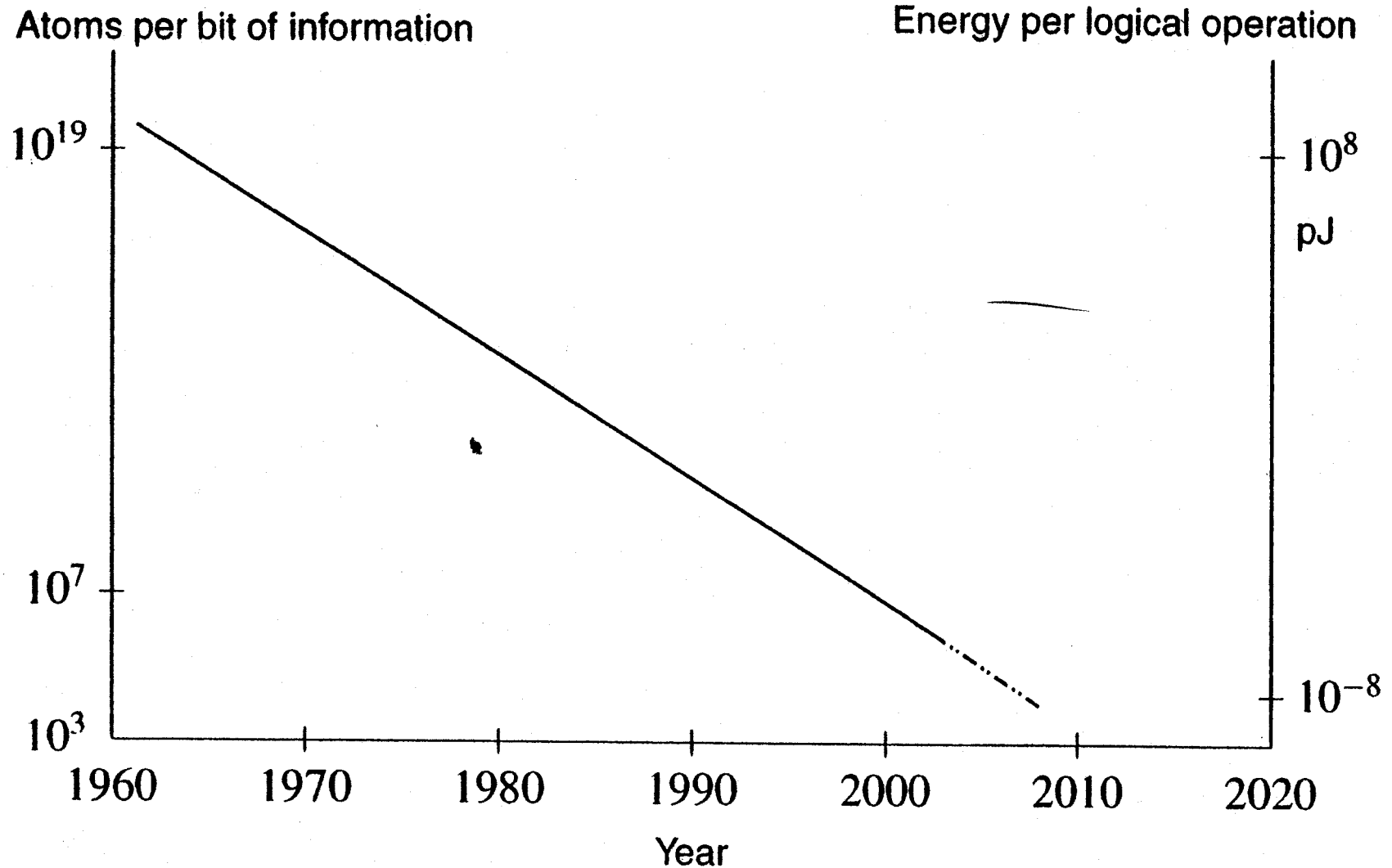


Fig. 1.2. The development of integrated circuits shows changes in the orders of magnitude. The number of atoms and the switching energy necessary for operating one bit are reduced by several powers of ten

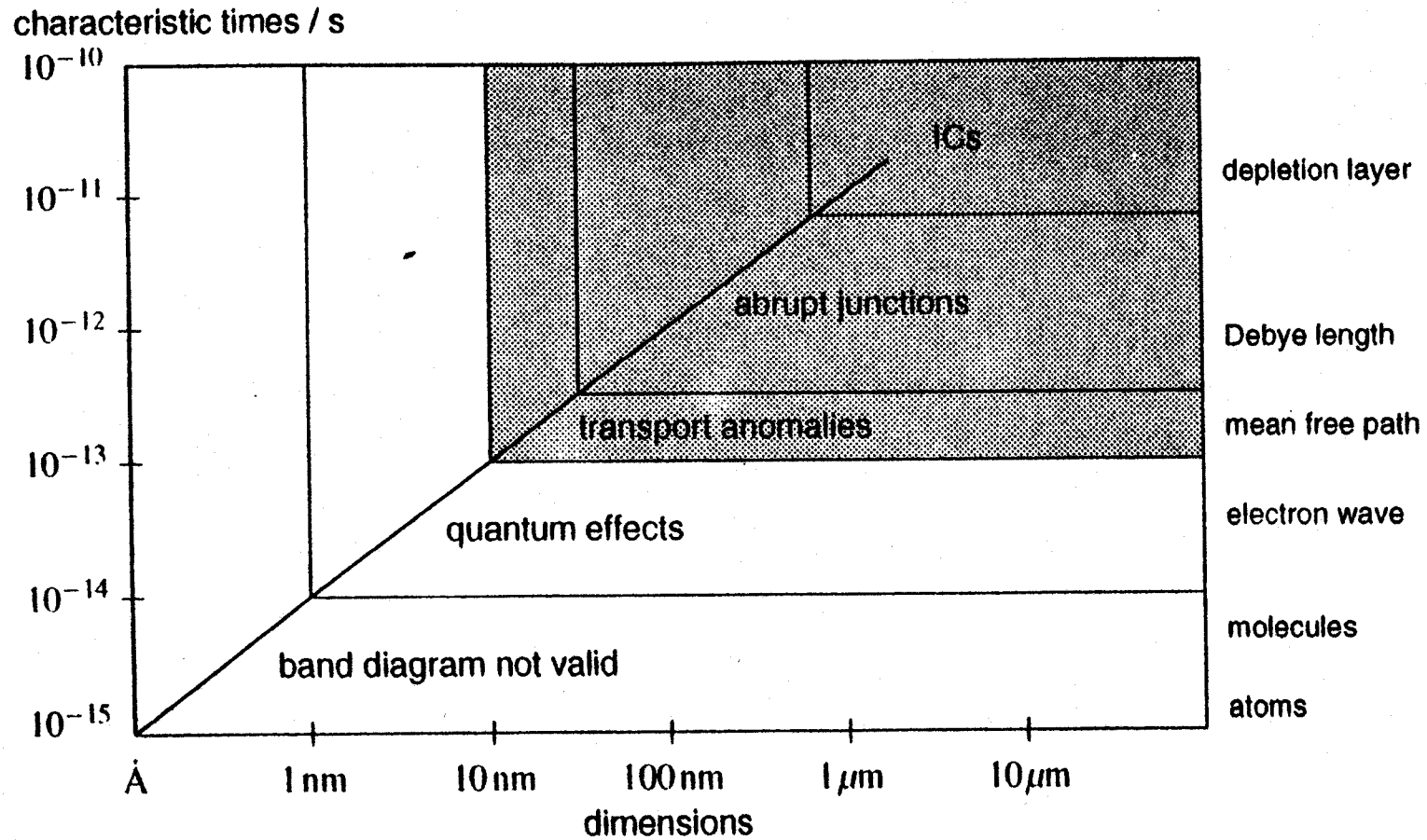


Fig. 1.4. Characteristic times and structures for semiconductor devices. The grey area concerns the present integrated circuits

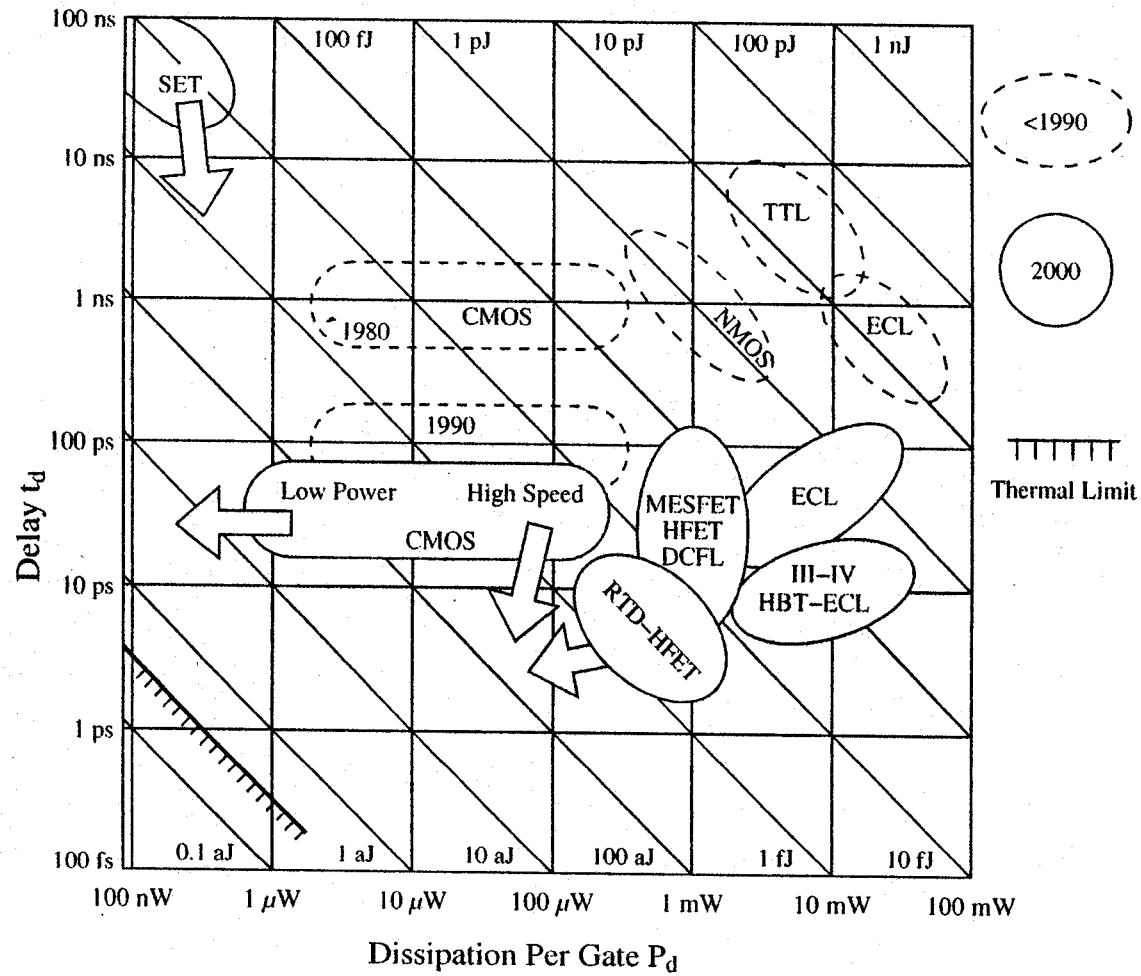


Fig. 2.15. Power-delay characteristic of current silicon technologies as well as more advanced SET and RTD technologies, which will be discussed later

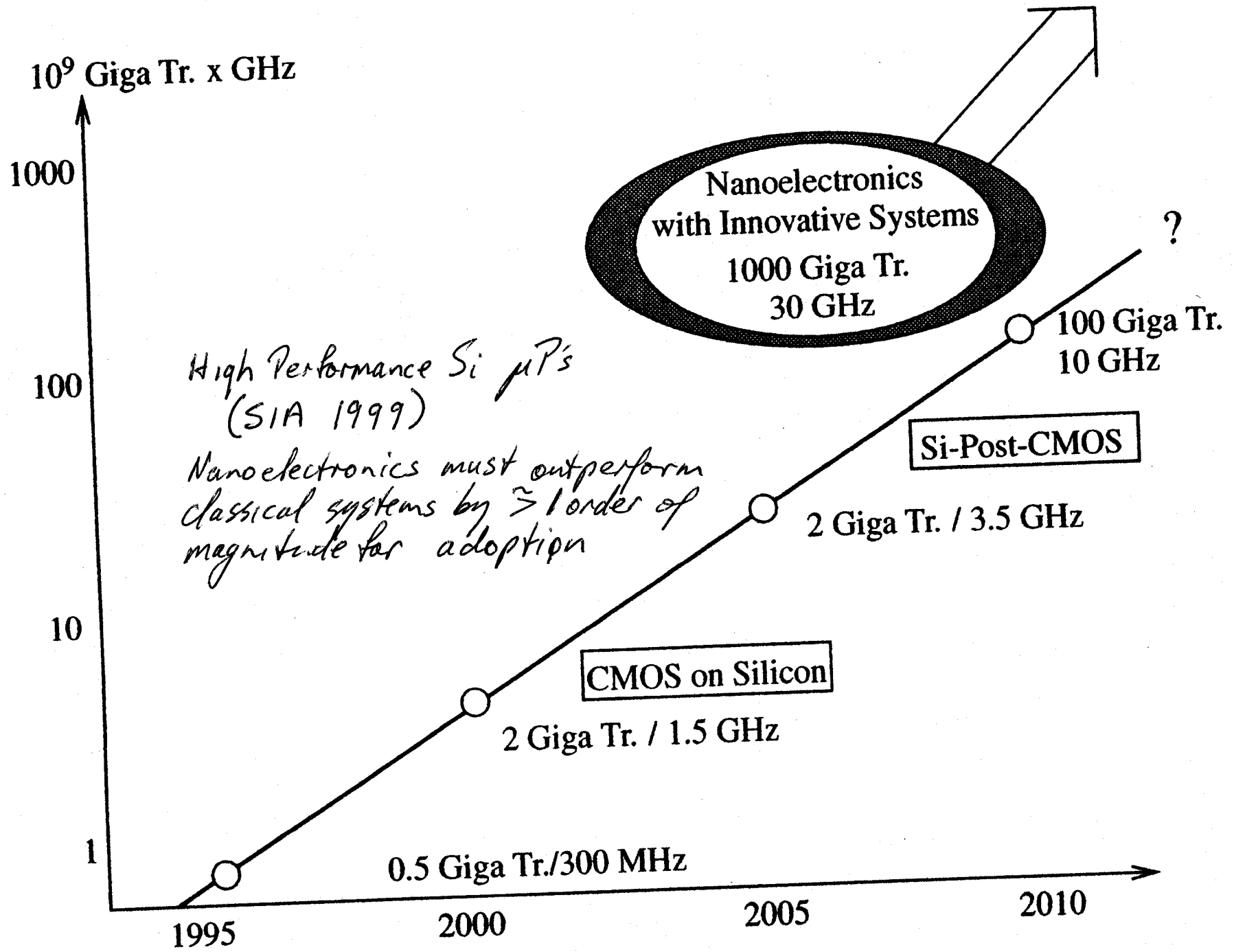


Table 2.1. Selected quantities of the SIA 1999 roadmap

Year	2000	2005	2010	2015
Feature size [nm]	130	100	50	35
Device density [$\frac{10^9}{cm^2}$]	0.5	1.7	10	24
Device density [$\frac{10^9}{Chip}$]	2	9	70	190
Clock frequency [GHz]	1.5	3.5	10	13

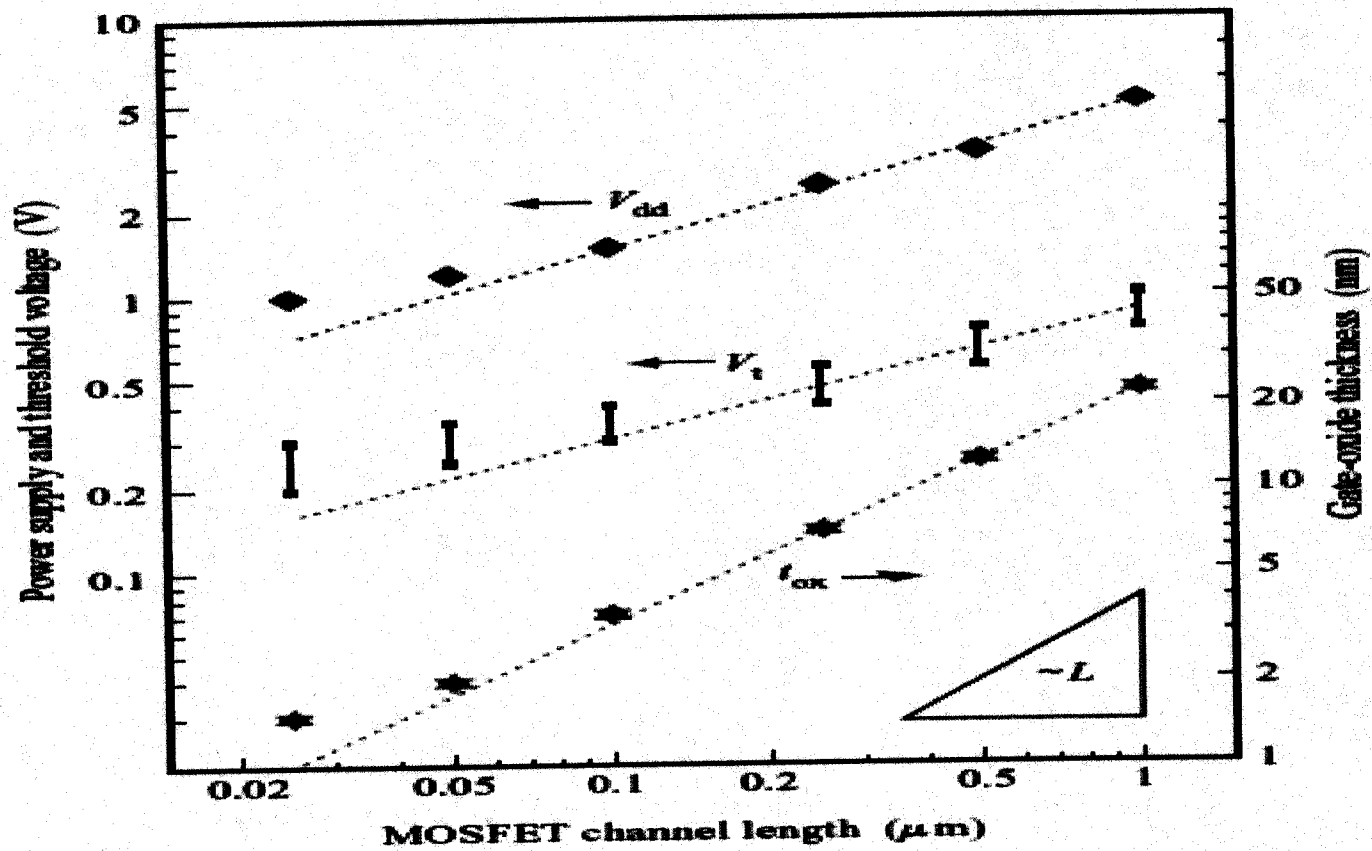
	MOSFET device and Circuit Parameters	Multiplicative Factor ($\alpha > 1$)
Scaling assumptions	Device dimensions (t_{ox}, L, w, x_j)	$1/\alpha$
	Doping concentration (N_a, N_d)	α
	Voltage (V_D)	$1/\alpha$
Derived scaling Behavior of device Parameters	Electric field (E)	1
	Depletion-layer width (w_d)	$1/\alpha$
	Capacitance ($C = \epsilon A/t_{ox}$)	$1/\alpha$
	Inversion-layer charge density (Q_i)	1
	Carrier velocity	1
	Current, drift (I)	$1/\alpha$
Derived scaling Behaviour of device Parameters	Circuit delay time ($\tau \sim CV_D/I_D$)	$1/\alpha$
	Power dissipation per circuit ($P \sim V_D I_D$)	$1/\alpha^2$
	Power-delay product per circuit ($P\tau$)	$1/\alpha^3$
	Circuit density ($\propto 1/A$)	α^2
	Power density (P/A)	1

Table 1: Device and circuit parameters resulting from constant field scaling [6].

MOSFET Scaling (From: [1, 3])

MOSFET parameter	Constant voltage scaling	Generalized scaling
Dimensions	$1/p$	$1/p$
Electric field	p	Q
Doping concentration	p	Pq
Voltage	1	q/p
Current	p	q^2/p
Capacitance	$1/p$	$1/p$
Delay	$1/p^2$	$1/pq$
Power density	p^3	q^3
Power dissipation	p	q^3/p^2

Scaling trend



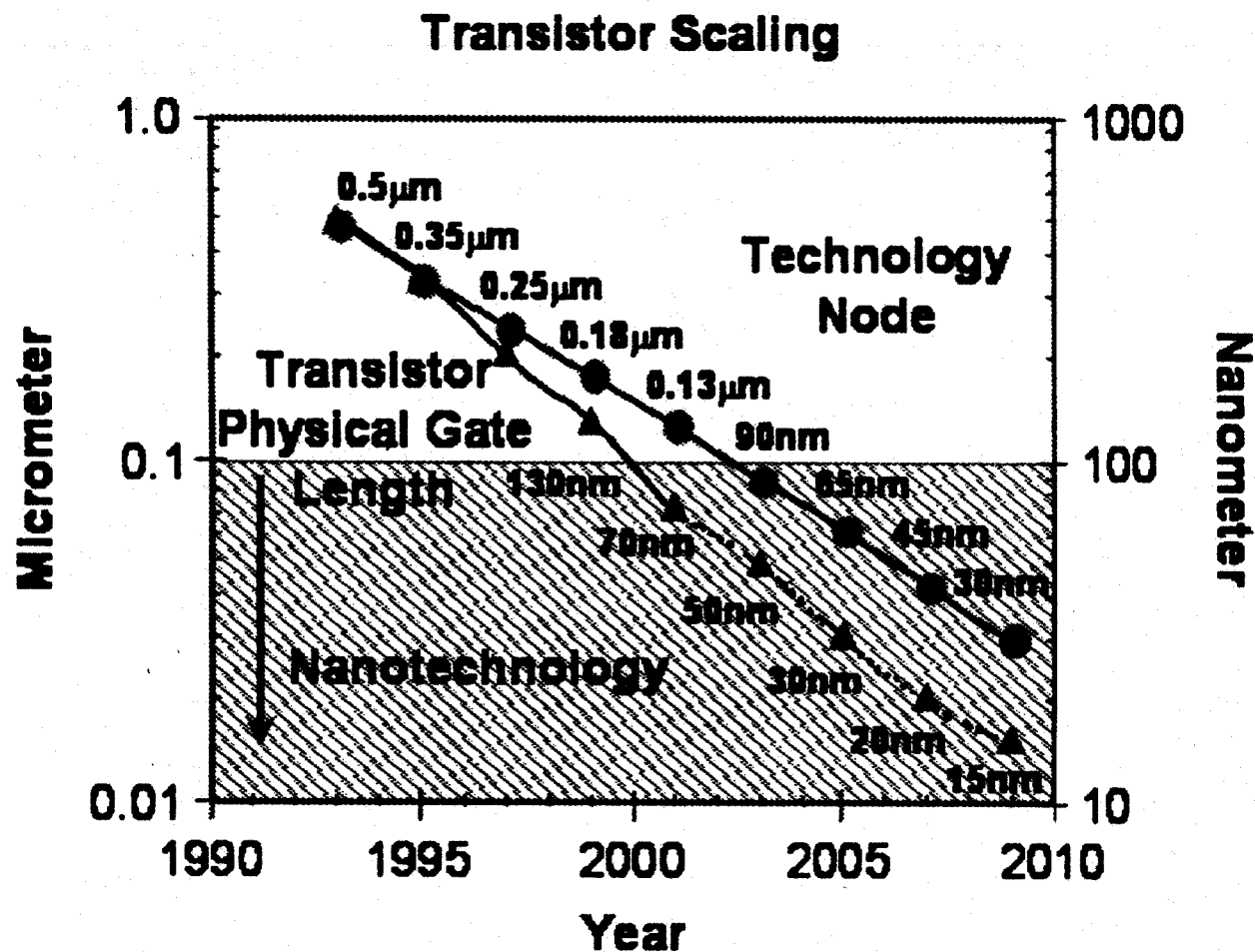


Fig. 1. Scaling of transistor size (physical gate length) with technology node to sustain Moore's Law. Nodes with feature size less than 100 nm can be referred to as nanotechnology. By 2011, the gate length is expected to be at or below 10 nm. Transistor scaling will be enabled by integration of emerging nanotechnology options on to the Si platform.

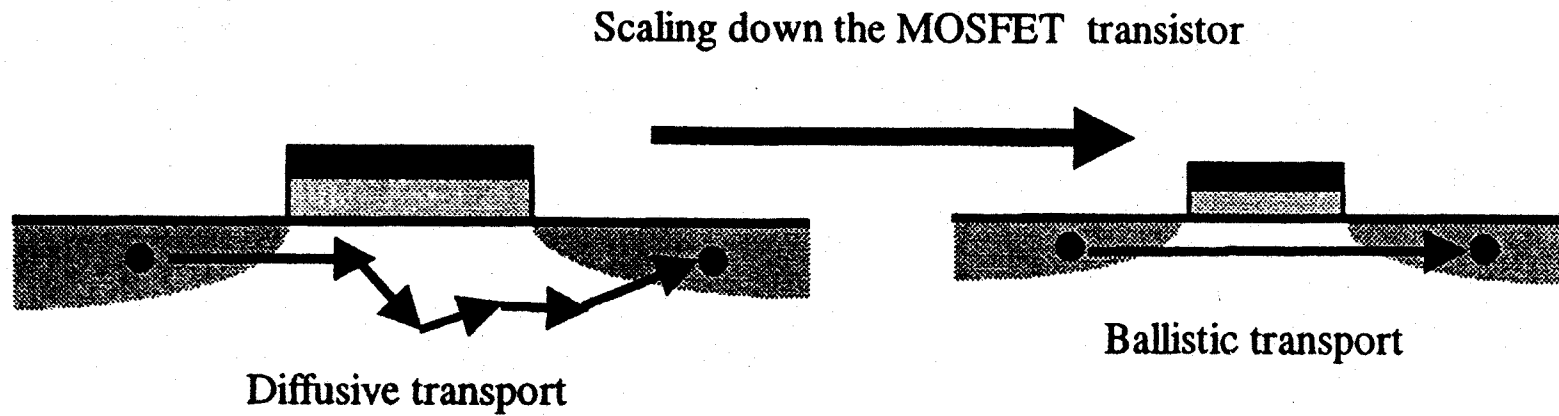


Figure 5.7 By scaling down the MOSFET transistor the diffusive transport transforms into ballistic transport.

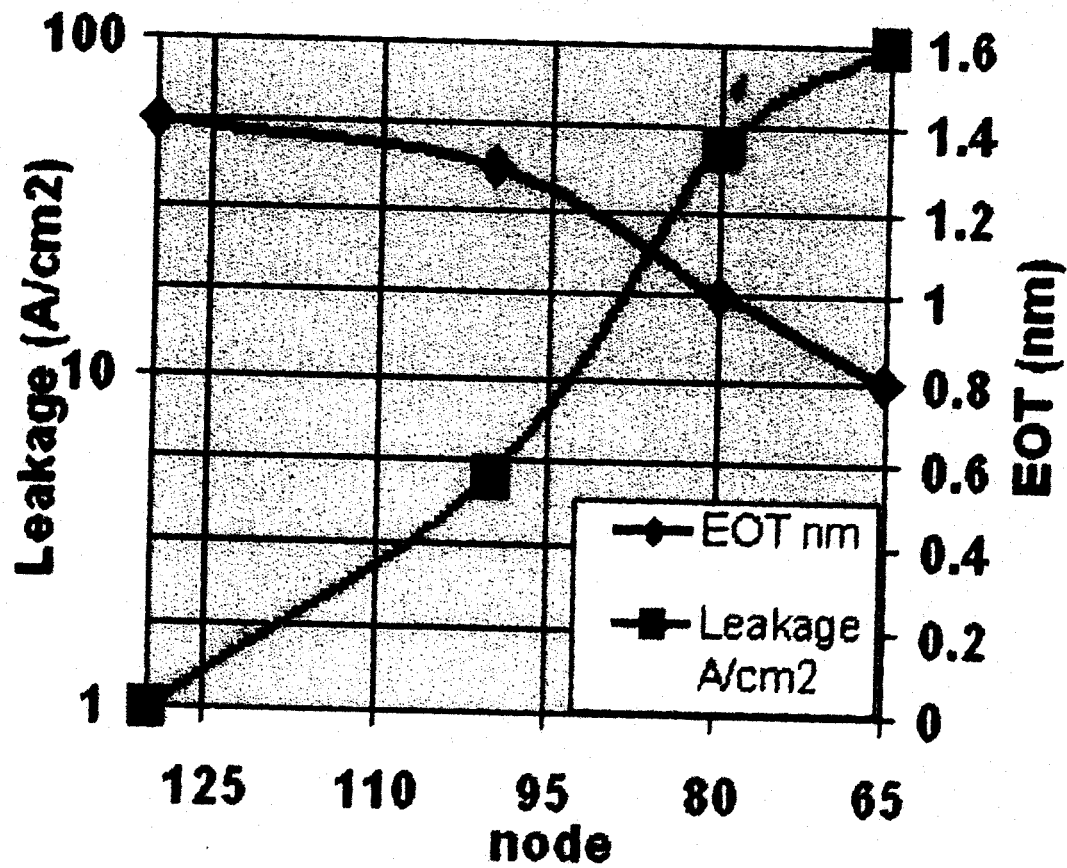
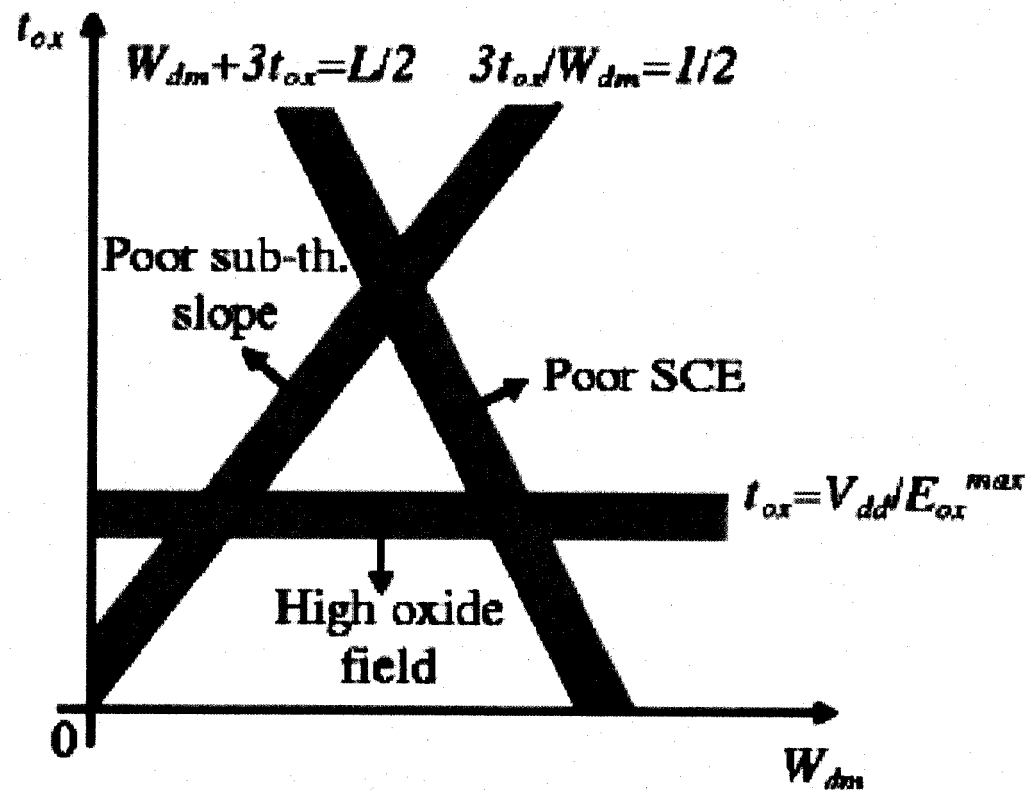


Figure 11: Gate leakage current and equivalent oxide thickness (EOT) versus technology node given in nm.

- Third condition is gate oxide reliability

$$t_{ox} = V_{dd} / E_{ox}^{max}$$



MOSFET Shrink

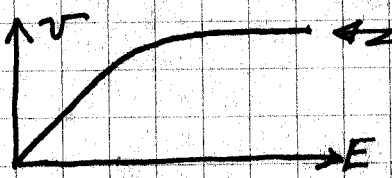
* Scaling: Constant voltage, constant field, and generalized scaling.
 Power density $\propto \rho^3$ ----- constant ----- $\propto \rho^3$

* Subthreshold leakage $I_{DS, leak} = I_0 \exp \frac{q(V_G - V_{th})}{m k_B T}$ $m \Rightarrow$ subthreshold slope
 (for $V_{DS} > kT/q$) $S = 2.3 m k_B T / q = 2.3 k_B T (1 + \frac{C_D}{C_{ox}})$
 ΔV_G change for ΔI_{DS} of one decade $\sim 80-100$ mV/decade
 S does not scale

* High electric field along channel \rightarrow high $K E_{elec}$ \rightarrow tunnelling into gate or gate oxide
 Hot electrons \rightarrow incr V_{th} (by trapping in oxide), m , S

* Short channel \leftarrow S, D junction depths and depletion widths
 V_D affects V_G near source \rightarrow "drain induced barrier lowering (DIBL)"

* Velocity saturation $v \propto E_{field}$



I becomes independent of V_{DS}, L
 Effective μ decreases

* Channel width very small \rightarrow depletion region below gate extends beyond W (y direction) & V_{th} increases.

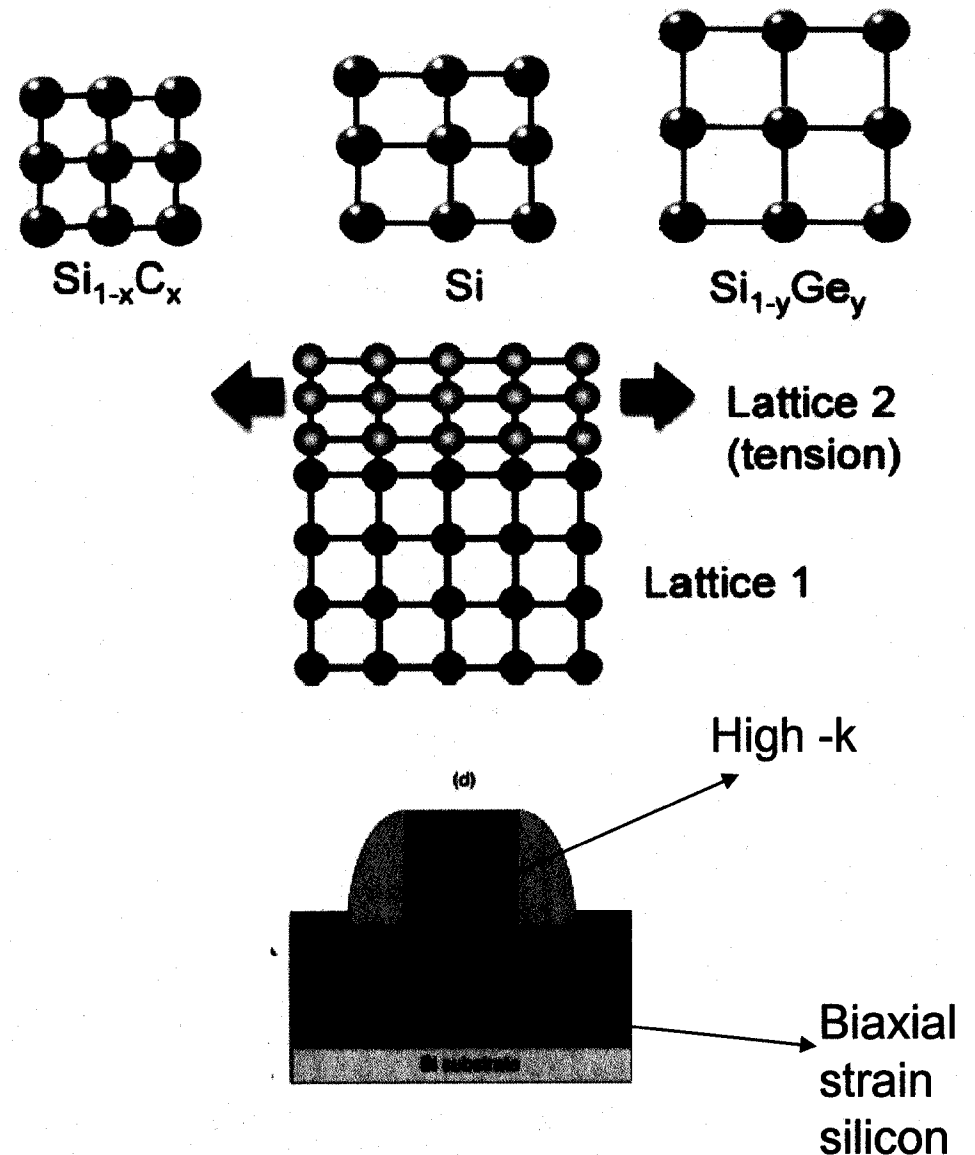
* Small area \rightarrow statistical variations in doping \rightarrow V_{th} variations.

Solutions: Silicon on insulator (SOI)

Double gate structures (standard nanoscale MOSFET)
 Reduced short channel effects; no DIBL

Strained silicon

- The mobility of the carriers increases with increase in strain
- Two types of strain : biaxial strain and uniaxial strain
- The size of silicon small than compound Silicon structure introduces the biaxial strain
- Uniaxial:Placing at the edge of the source or drain.
- The Ion of device improves 15% to 30% with out scaling
- 90nm and 65 nm technologies used strained silicon technology
- Next generation technology (45nm)uses High -k and metal gate with strain silicon



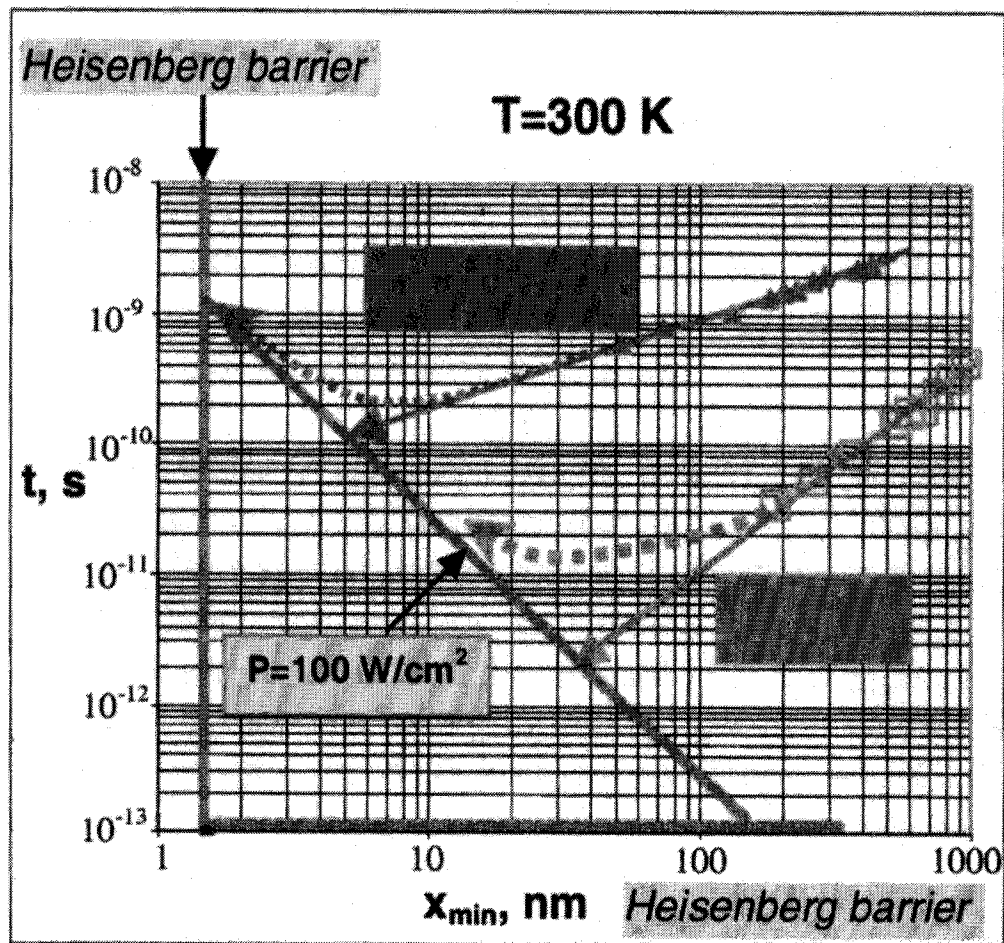


Fig. 3: Possible inflections of ITRS scaling vector for memory and logic devices by approaching limits of heat removal

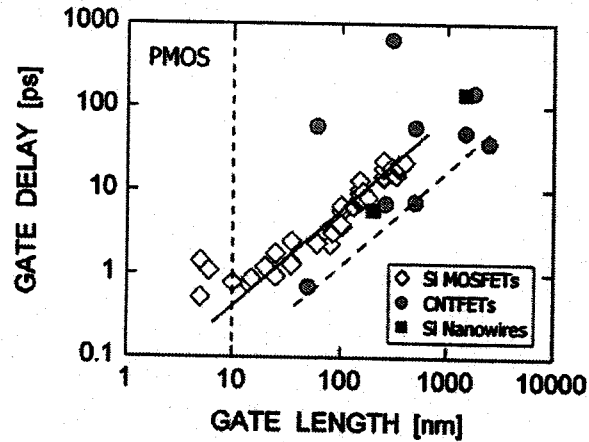


Fig. 4. Gate delay (intrinsic device speed CV/I) versus transistor physical gate length of PMOS devices.

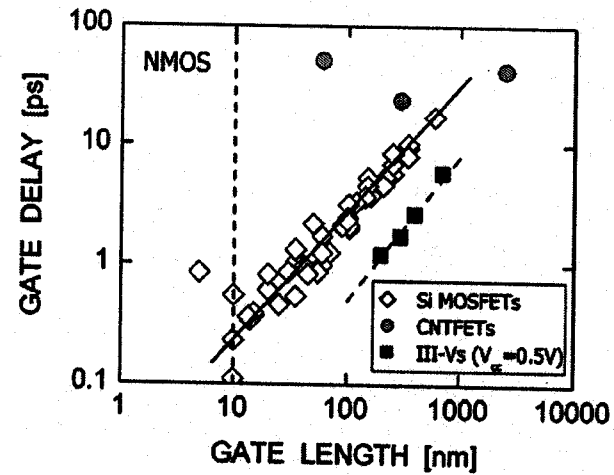


Fig. 5. Gate delay (intrinsic device speed, CV/I) versus transistor physical gate length of NMOS devices.

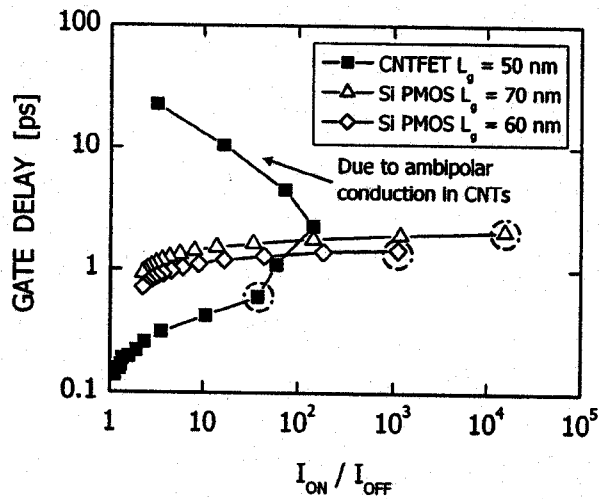


Fig. 11. Gate delay (intrinsic device speed, CV/I) versus on-to-off state current ratio I_{ON}/I_{OFF} of Si PMOS transistors with $L_g = 60$ nm and 70 nm at $V_{CC} = 1.3$ V, and a CNT PMOS transistor with $L_g = 50$ nm and $V_{CC} = 0.3$ V [15]. The three circled points were used in the PMOS CV/I versus L_g plot in Fig. 4, where the V_G swing is anchored around $V_G = V_T$.

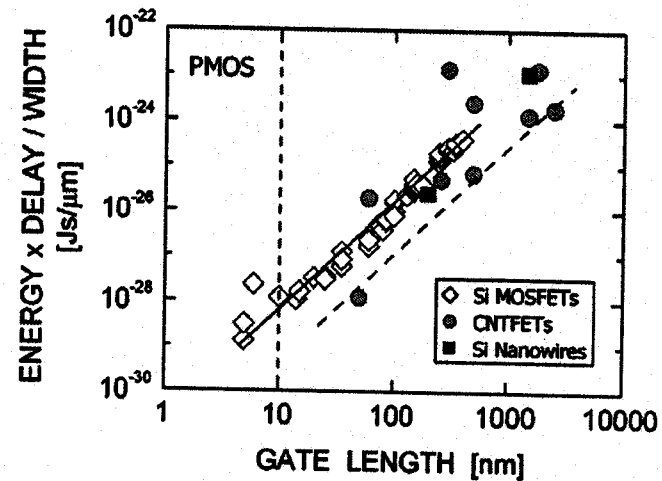


Fig. 6. Energy-delay product per device width versus transistor physical gate length of PMOS transistors.

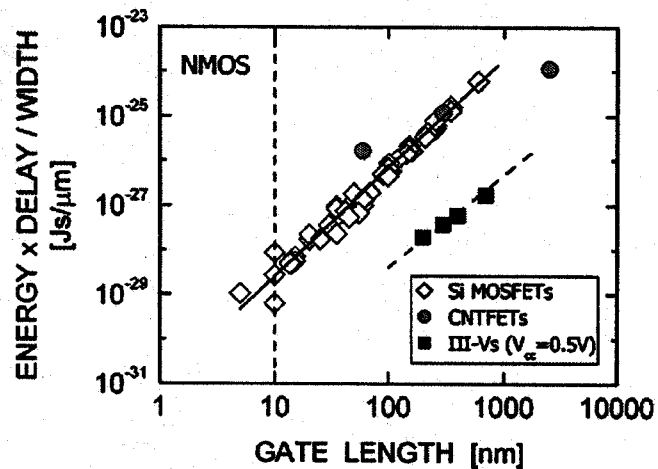


Fig. 7. Energy-delay product per device width versus transistor physical gate length of NMOS transistors.

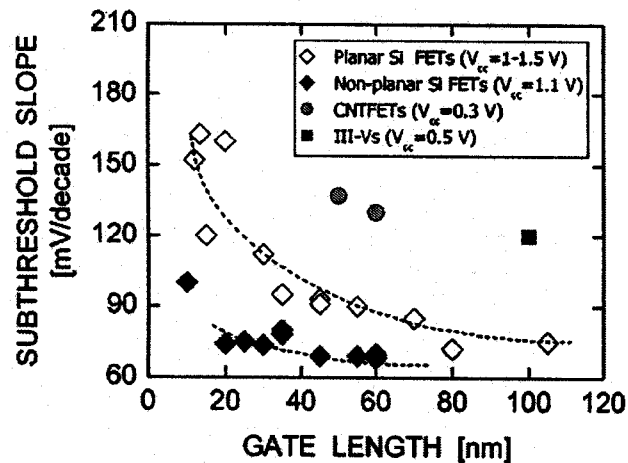


Fig. 8. Subthreshold slope versus transistor physical gate length. The planar and nonplanar Si FETs as well as the III-V planar devices are n-channel transistors, while the CNT FETs are p-channel transistors.

CNT FETs. The significant improvement of the III-V devices

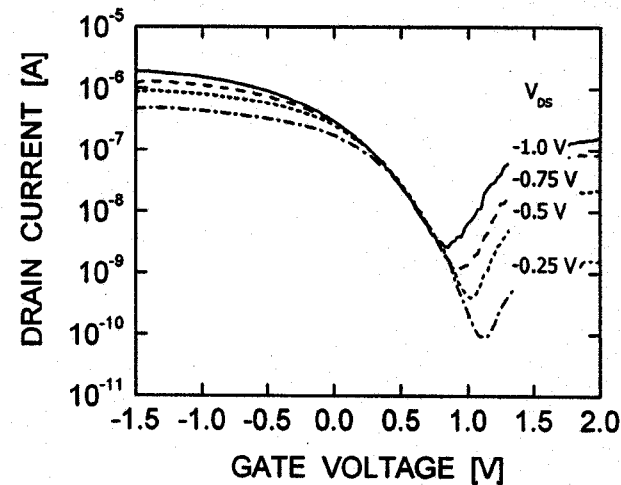


Fig. 9. I_D - V_G characteristics of an Si nanowire PMOS transistor with metal source-drain at different drain biases V_{DS} , illustrating ambipolar conduction.

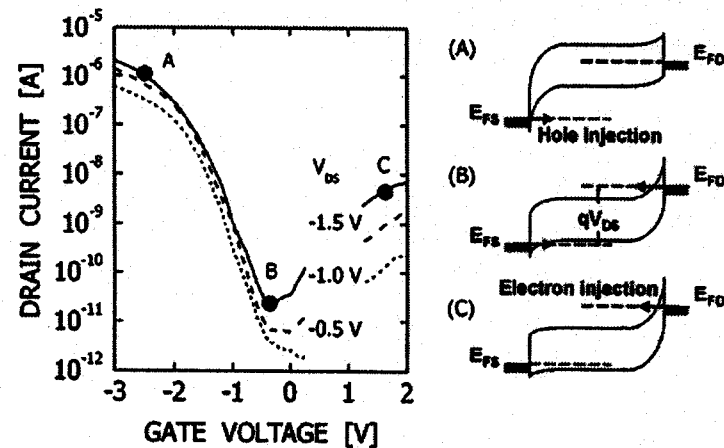


Fig. 10. I_D - V_G characteristics of a CNT PMOS transistor with Pd metal source-drain at different drain biases V_{DS} , illustrating ambipolar conduction. Pd has a p-type work function with respect to nanotubes. The energy band diagrams exhibit: (A) dominant hole injection in the on state, (B) equal hole and electron injection at the minimum current point, and (C) dominant electron injection in the ambipolar branch.

Table 1. Emerging Research Memory Devices

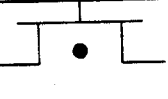
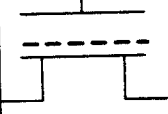
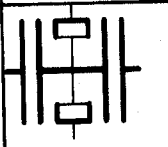
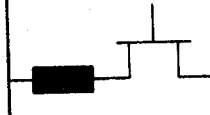
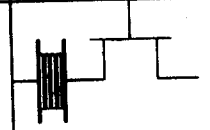
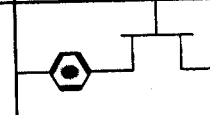

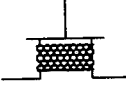
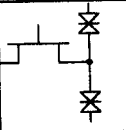
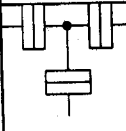
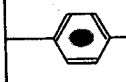
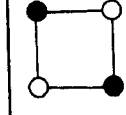
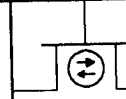
Device	Operation Mechanism	
I. Capacitive Memory Element		
Floating body DRAM	Charge stored in body of PDSOI MOSFET	
Nanofloating Gate Memory	FLASH with engineered tunnel barrier OR charge stored on silicon nano-crystals	
Single-electron memory	Charge stored on a quantum dot channel of an Single Electron Transistor	
II. Resistive Memory Element		
Phase-Change memory	$R=f(\text{crystalline- or amorphous- phase})$	
Insulator resistance change Memory	$R=f(\text{formation or dissolution of metal nanowire})$	
Molecular Memory	$R=f(\text{bias voltage})$	

Table 2. Emerging Research Logic Devices

Device	Operation mechanism	
Rapid Single Flux Quantum Devices (RSFQ)	Tunneling in superconducting structures	
1D structures	Drift electron transport in nanowires and nanotubes	
Resonant Tunneling Devices (RTD)	Resonant tunneling in semiconductor heterostructures	
Single Electron Transistors (SET)	Single electron tunneling and coulomb blockade	
Molecular devices	Electron transport in molecules	
Quantum Cellular Automata (QCA)	Electrostatic repulsion together with tunneling	
Spin Transistors	Spin transport in transistor structure	

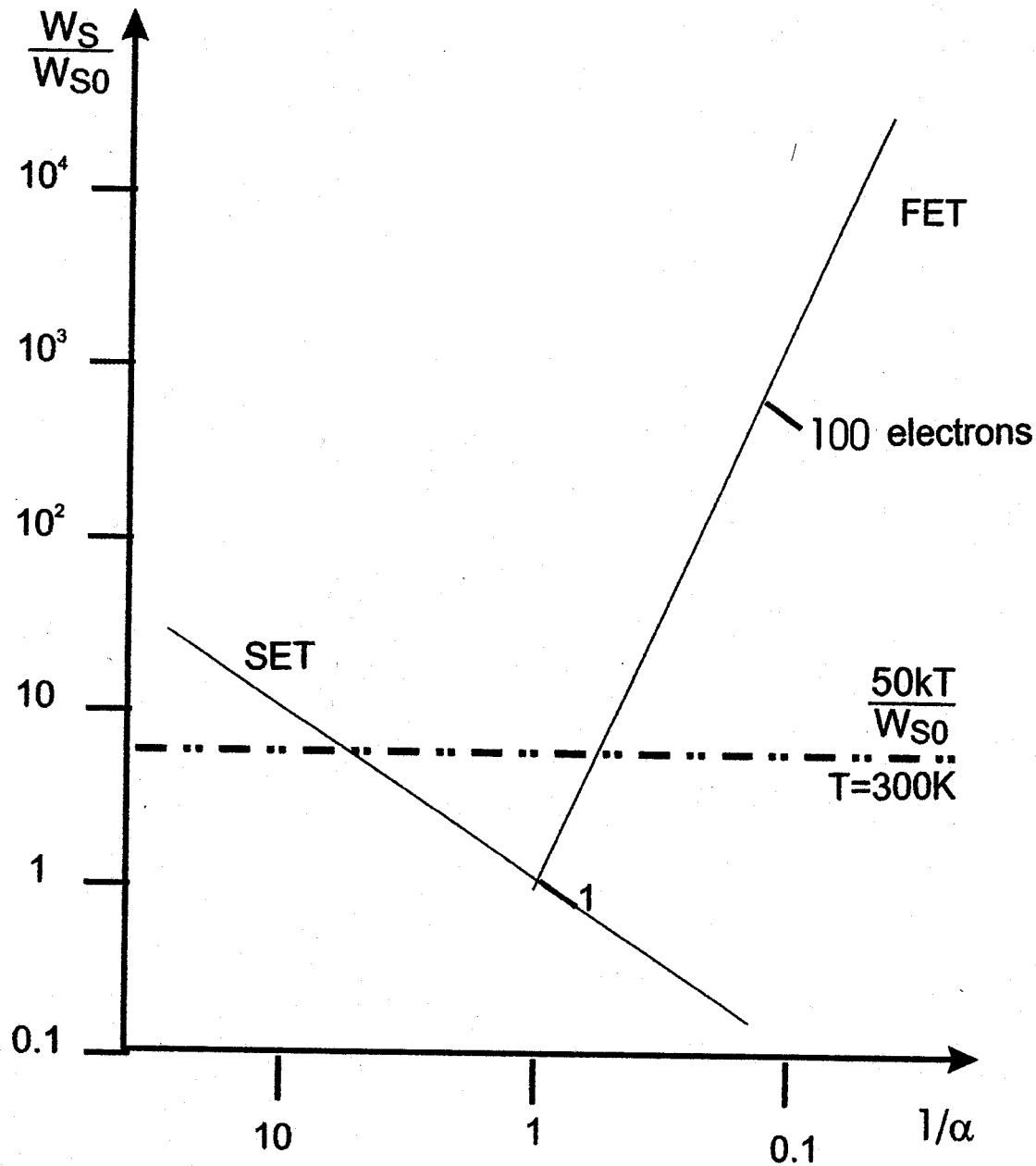


Fig. 13.17. The power-delay diagram reveals the impacts of scaling on the SET and FET

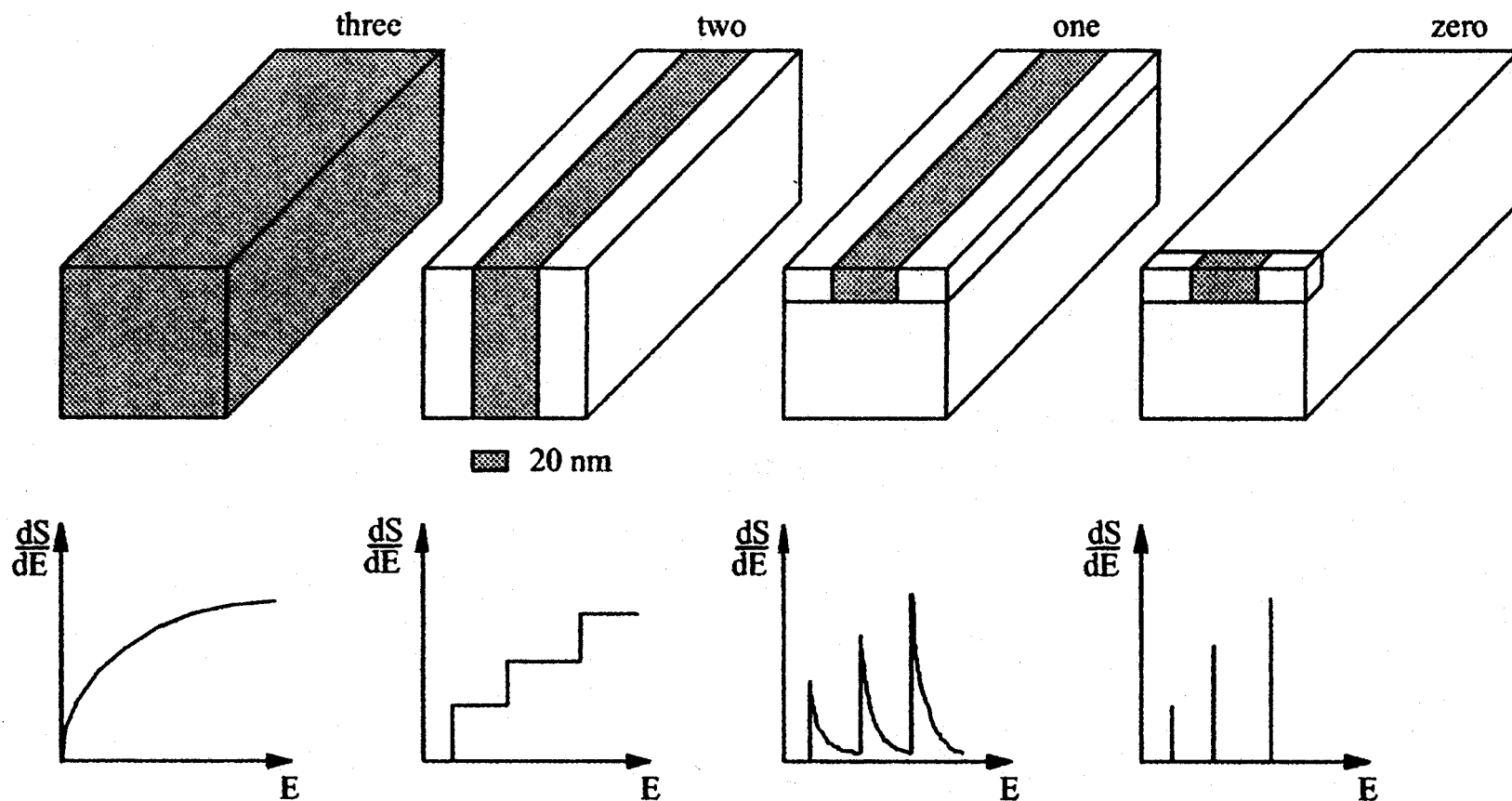


Fig. 10.4. Quantum structures with different dimensions: normal solid-state body, quantum well, quantum wire, and quantum dot, additionally their density of states are illustrated. The grid of the steps depends on the size of the quantum structure

ρ = Density of states = $D(E)$

Quantum dot: $\rho_{QD} \propto \delta(E - E_{s,pqr})$

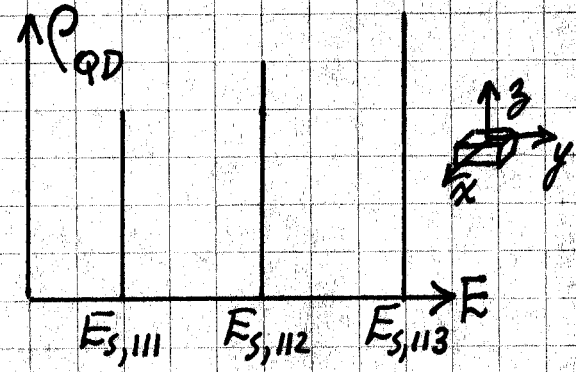
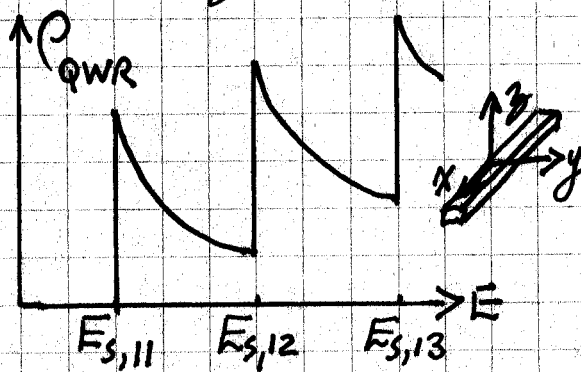
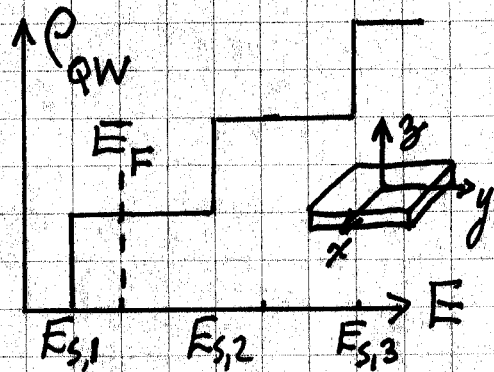
$$E(k_x, k_y, k_z) = E_c + \frac{\hbar^2}{2m} \left(\frac{p\pi}{L_x}\right)^2 + \frac{\hbar^2}{2m} \left(\frac{q\pi}{L_y}\right)^2 + \frac{\hbar^2}{2m} \left(\frac{r\pi}{L_z}\right)^2 = E_{s,pqr}$$

Quantum wire: $\rho_{QWR}(E) = \frac{(2m)^{1/2}}{\pi \hbar L_y L_z} \sum_{p,q} (E - E_{s,pq})^{-1/2}$

$$E(k_x, k_y, k_z) = E_c + \frac{\hbar^2}{2m} \left(\frac{p\pi}{L_x}\right)^2 + \frac{\hbar^2}{2m} \left(\frac{q\pi}{L_y}\right)^2 + \frac{\hbar^2}{2m} k_x^2 = E_{s,pq} + \frac{\hbar^2 k_x^2}{2m}$$

Quantum well: $\rho_{QW}(E) = \frac{m}{\pi \hbar^2 L_z} \sum_p \mathcal{V}(E - E_{s,p})$ \mathcal{V} = unit step

$$E(k_x, k_y, k_z) = E_c + \frac{\hbar^2}{2m} \left(\frac{p\pi}{L_z}\right)^2 + \frac{\hbar^2}{2m} (k_x^2 + k_y^2) = E_{s,p} + \frac{\hbar^2}{2m} (k_x^2 + k_y^2)$$



$$E_{kin} = E_F - E_{s,1} = \frac{\hbar^2 k_F^2}{2m} \quad \& \quad k_F = \sqrt{2\pi n} = 2\pi/\lambda_F$$

$$e^- \text{ density/unit area } n = \frac{m}{\pi \hbar^2} (E_F - E_{s,1})$$

Type	$N(\epsilon)$	$D(\epsilon)$	Dimensions	
	Number of electrons	Density of states	Delocalized	Confined
Dot	$N(\epsilon) = 2 \sum d_i \Theta(\epsilon - E_{i,w})$	$D(\epsilon) = 2 \sum d_i \delta(\epsilon - E_{i,w})$	0	3
Wire	$N(\epsilon) = \frac{2L}{\pi} \left(\frac{2m}{\hbar^2}\right)^{1/2} \sum d_i (\epsilon - E_{i,w})^{1/2}$	$D(\epsilon) = \frac{L}{\pi} \left(\frac{2m}{\hbar^2}\right)^{1/2} \sum d_i (\epsilon - E_{i,w})^{-1/2}$	1	2
Well	$N(\epsilon) = \frac{A}{2\pi} \left(\frac{2m}{\hbar^2}\right) \sum d_i (\epsilon - E_{i,w})$	$D(\epsilon) = \frac{A}{2\pi} \left(\frac{2m}{\hbar^2}\right) \sum d_i$	2	1
Bulk	$N(\epsilon) = \frac{V}{3\pi^2} \left(\frac{2m}{\hbar^2}\right)^{3/2} \epsilon^{3/2}$	$D(\epsilon) = \frac{V}{2\pi^2} \left(\frac{2m}{\hbar^2}\right)^{3/2} \epsilon^{1/2}$	3	0

$$V = L^3 \quad A = L^2$$

$$\Theta(x) = \begin{cases} 0 & x < 0 \text{ (left side)} \\ 1 & x > 0 \text{ (step function)} \end{cases}$$

$$\delta(x) = \begin{cases} 0, & x \neq 0 \\ \infty, & x = 0 \end{cases} \quad \left\{ \begin{array}{l} \text{Delta} \\ \text{function} \end{array} \right\}$$

$d_i \rightarrow$ confined (well) energy level degeneracies

$$D(\epsilon) = \frac{dN(\epsilon)}{d\epsilon}$$

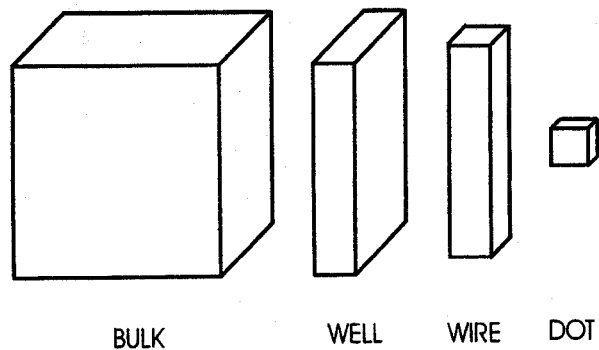


Figure 9.1. Progressive generation of rectangular nanostructures.

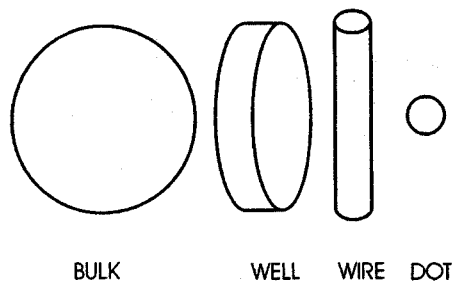


Figure 9.2. Progressive generation of curvilinear nanostructures.

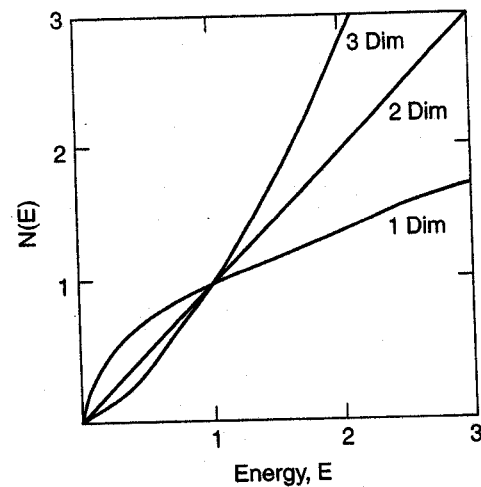


Figure 9.9. Number of electrons $N(E)$ plotted as a function of the energy E for conduction electrons delocalized in one (quantum wire), two (quantum well), and three dimensions (bulk material).

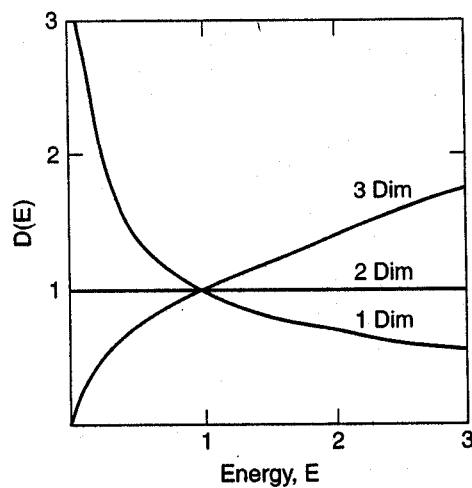


Figure 9.10. Density of states $D(E) = dN(E)/dE$ plotted as a function of the energy E for conduction electrons delocalized in one (Q-wire), two (Q-well), and three (bulk) dimensions.

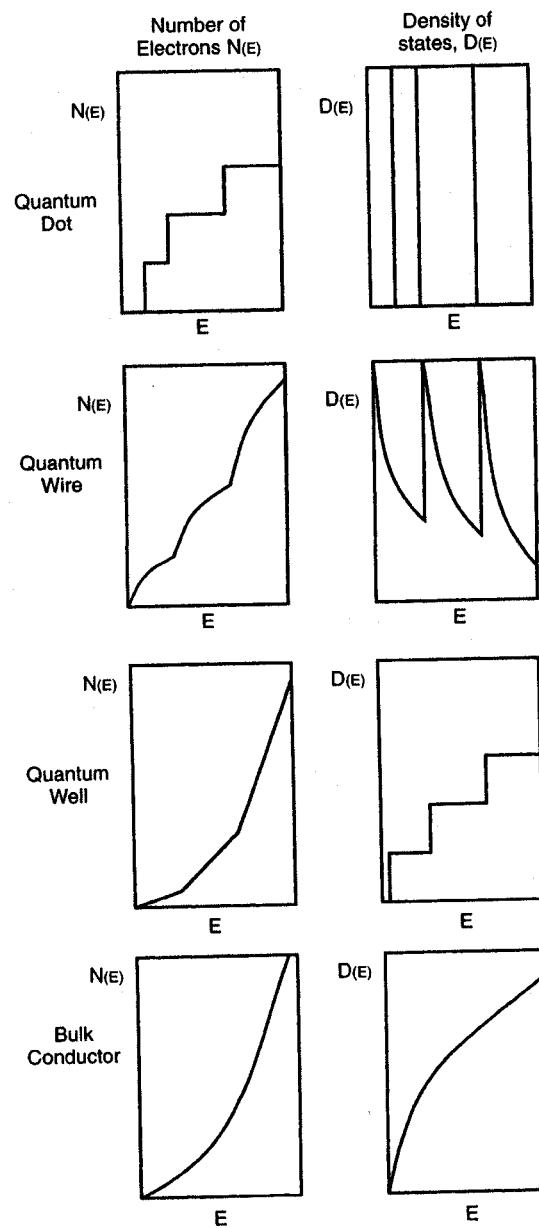


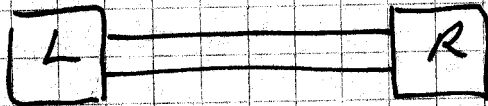
Figure 9.15. Number of electrons $N(E)$ (left side) and density of states $D(E)$ (right side) plotted against the energy for four quantum structures in the square well-Fermi gas approximations.

LANDAUER FORMULA (Resistance quantum)

Ballistic conductors \rightarrow only electrons near E_F conduct at equilibrium.

1D ballistic conductor \rightarrow quantum wire

V drives off equilibrium
 E_{FL} & E_{FR} in L & R electron reservoirs



Small $qV = E_{FL} - E_{FR}$ for $E_{FL} > E_{FR} \rightarrow$ electron flow at zero T
for $E_{FR} > E > E_{FL}$

Ballistic, i.e. no scattering

$I = qv S_n$ for each sub-band, where $S_n = \left(\frac{dn}{dE}\right) qV$

(greater electron density in L contact)

Velocity $v = \hbar^{-1} (dE/dk) \therefore I = \frac{q^2}{\hbar} v \frac{dE}{dR} \frac{dn}{dE}$

For the quantum wire, $n(E) = \frac{1}{\pi} \left(\frac{2m}{\hbar^2}\right)^{1/2} E^{1/2}$
of the form:

& $E = \hbar^2 k^2 / 2m$

$G = \frac{I}{V} = \frac{2q^2}{h} M \leftarrow M(E) \text{ sub-bands}$
 $= M G_0$

G_0 is (the Landauer resistance)⁻¹
Minimum resistance

$R_0 = h/2q^2 \approx 13 \text{ k}\Omega$

$$\Delta G = \frac{I}{U} = \frac{2q^2}{h}, \tag{10.8}$$

which is equivalent to the step of the staircase function.

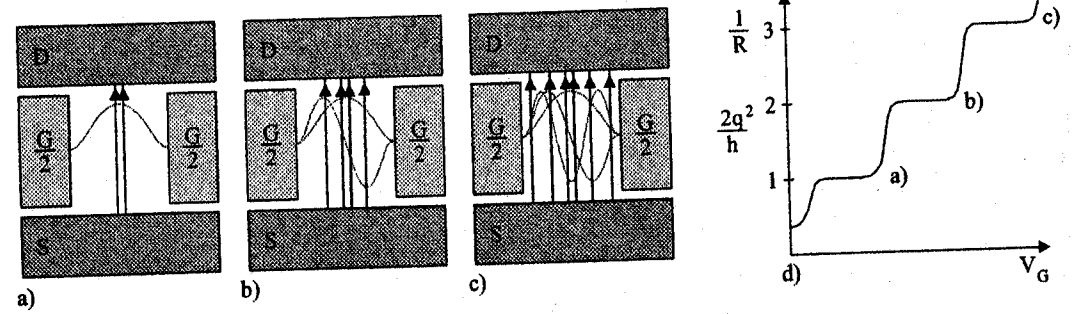


Fig. 10.8. Mesoscopic element: Split-gate transistor with three different operation conditions (a-c) and its GV_g characteristics (d) that can be described by Schrödinger's equation

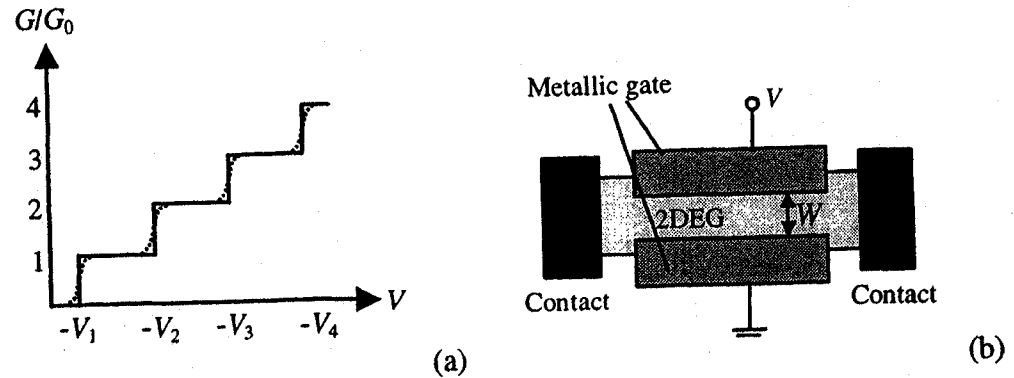


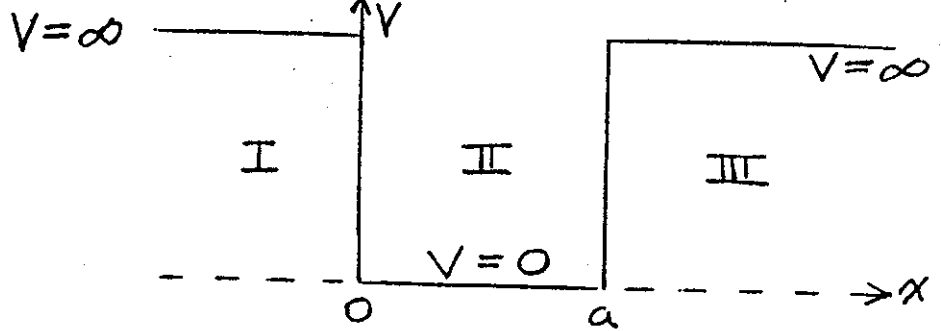
Figure 1.4. (a) The dependence on the gate voltage at zero temperature (solid line) and finite temperatures (dotted line) of the conductance of (b) a 1D ballistic conductor with variable width.

ECE 417/517
NANO ELECTRONICS
Spring 2007

Lecture 2:
Quantum Mechanics Review

- Electron wave function
- Schrödinger's equation
- Heisenberg Uncertainty Principle
- Infinite potential well
- Finite potential well
- Potential barrier

3.3 Infinite Potential Well



In region I: $V > E \quad \therefore \xi_{\text{I}} = \left[\frac{2m(V-E)}{\hbar^2} \right]^{1/2} \xrightarrow{V \rightarrow \infty} \infty$

$$\psi_{\text{I}} = C \exp \xi_{\text{I}} x + D \exp -\xi_{\text{I}} x$$

$C = 0$ since ψ_{I} must be finite

$$\therefore \psi_{\text{I}} = D \exp -\infty = 0 \text{ everywhere in region I}$$

In region III: $V > E$ again gives same result, $\psi_{\text{III}} = 0$

In region II: $V < E \quad \therefore \gamma = \left[\frac{2m(E-V)}{\hbar^2} \right]^{1/2} \xrightarrow{V \rightarrow 0} \left(\frac{2mE}{\hbar^2} \right)^{1/2}$

$$\psi_{\text{II}} = A \exp j\gamma x + B \exp -j\gamma x$$

At $x=0 \quad \psi_{\text{II}} = A + B = 0 \quad \therefore B = -A$

At $x=a \quad \psi_{\text{II}} = A \exp j\gamma a + B \exp -j\gamma a = 0$

ie. $A (\exp j\gamma a - \exp -j\gamma a) = 0$

ie. $2jA \sin \gamma a = 0$

Either $A = 0$ (trivial) or $\gamma a = n\pi$ ($n = 0, 1, 2, 3, \dots$)

$$\therefore \psi_{\text{II}}(x) = A (\exp j\gamma x - \exp -j\gamma x) = 2jA \sin \frac{n\pi}{a} x$$

Note that the trivial solutions give $\psi = 0$ everywhere & that

$$\therefore \int_{-\infty}^{\infty} \psi^* \psi dx \neq 1$$

\therefore Non-physical

(a) Normalization: $\psi_{II}^* \psi_{II} = A^* A (\exp j\delta x - \exp -j\delta x) \times (\exp -j\delta x - \exp j\delta x)$

$$= A^* A (1 - \exp 2j\delta x - \exp -2j\delta x + 1)$$

$$= 2A^* A (1 - \cos 2\delta x)$$

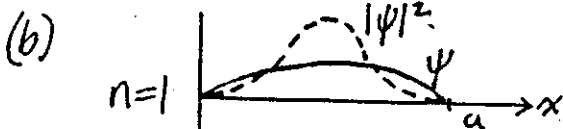
$$\therefore \int_0^a A^* A 2(1 - \cos 2\delta x) dx = 1$$

$$2A^* A \left(x - \frac{\sin 2\delta x}{2\delta} \right)_0^a = 1 \quad \text{gives } A^* A = \frac{1}{2a}$$

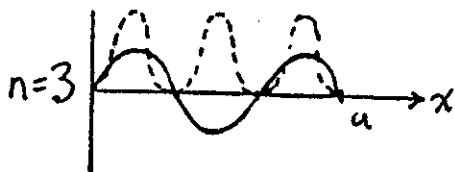
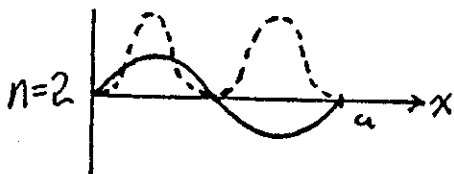
$$\text{ie. } A = \frac{-j}{\sqrt{2a}}$$

$$\therefore \psi_{II}(x) = \sqrt{\frac{2}{a}} \sin\left(\frac{n\pi}{a}\right)x$$

$n = 1, 2, 3, \dots$



Compare quantized solutions to standing wave on transmission line.



Note that as $n \rightarrow \infty$, develop uniform probability across potential well.

(c) Total solution

$$\begin{aligned}\Psi_n(x,t) &= \psi(x) \phi(t) \\ &= \sqrt{\frac{2}{a}} \cdot \sin \frac{n\pi}{a} x \cdot \exp -j \frac{E_n}{\hbar} t\end{aligned}$$

$$\text{i.e. } \Psi(x,t) = \sum_{n=1}^{\infty} \sqrt{\frac{2}{a}} \cdot \sin \frac{n\pi}{a} x \cdot \exp -j \frac{E_n}{\hbar} t$$

$$\begin{aligned}\text{where } E_n &= \frac{\gamma^2 \hbar^2}{2m} = \frac{1}{2m} \left(\frac{n\pi \hbar}{a} \right)^2 = \frac{1}{2m} \frac{n^2 \pi^2 \hbar^2}{a^2} \\ &= n^2 \frac{\hbar^2}{8ma^2}\end{aligned}$$

i.e. these are the permitted energies of a particle in a box or an electron in a potential well.

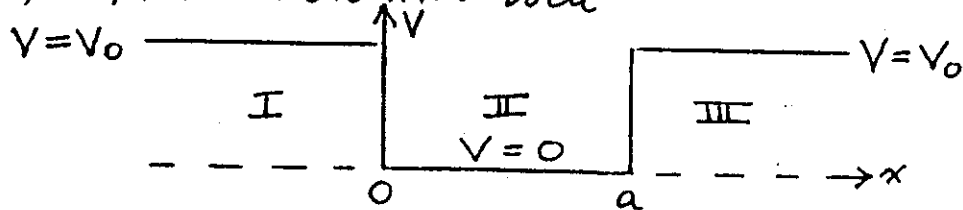
(d) Expected position:

$$\begin{aligned}\langle x \rangle &= \int_{-\infty}^{\infty} \psi^* x \psi dx \quad \left\{ \begin{array}{l} \text{Note: denominator} \\ \text{unnecessary since} \\ \psi \text{ already normalized.} \end{array} \right\} \\ &= \int_0^a \frac{2}{a} \left(\sin^2 \frac{n\pi x}{a} \right) x dx \\ &= \frac{2}{a} \int_0^a \frac{x}{2} (1 - \cos \frac{2n\pi x}{a}) dx = \frac{1}{a} \int_0^a x dx - \frac{1}{a} \int_0^a x \cos \frac{2n\pi x}{a} dx \\ &= \left[\frac{x^2}{2a} \right]_0^a - \frac{1}{a} \left[\int_{\uparrow=0} \right] = a/2\end{aligned}$$

i.e. the average position $x = a/2$ is the same as the classical result, even for small n —

& even for n even where $\psi(a/2) = 0$!!

3.4 Finite Potential Well



For $E > V_0$, particle is free over whole region
 \Rightarrow travelling wave.

For $E < V_0$

$$\begin{aligned}\psi_{\text{I}} &= C_{\text{I}} \exp \xi_{\text{I}} x + D_{\text{I}} \exp -\xi_{\text{I}} x \\ &= C_{\text{I}} \exp \xi_{\text{I}} x\end{aligned}$$

since $D_{\text{I}} = 0$ for finite ψ_{I}
 as $x \rightarrow -\infty$.

Similarly

$$\psi_{\text{III}} = D_{\text{III}} \exp -\xi_{\text{III}} x$$

since $C_{\text{III}} = 0$ as $x \rightarrow +\infty$.

ie. write $\psi_{\text{I}} = C \exp \xi x$
 $\psi_{\text{III}} = D \exp -\xi x$ where $\xi = \left[\frac{2m(V_0 - E)}{\hbar^2} \right]^{1/2}$

Also $\psi_{\text{I}} = A_{\text{I}} \exp j\delta_{\text{I}} x + B_{\text{I}} \exp -j\delta_{\text{I}} x$
 $= A \exp j\delta x + B \exp -j\delta x$ where $\delta = \left[\frac{2mE}{\hbar^2} \right]^{1/2}$

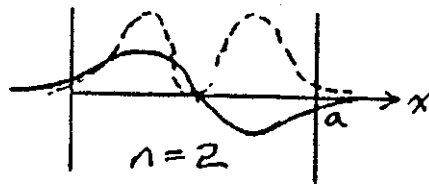
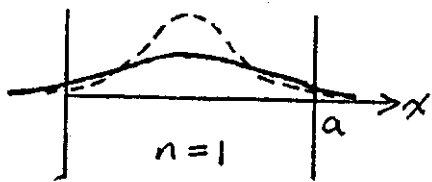
At $x=0$ $\psi_{\text{I}} = \psi_{\text{II}} \therefore C = A + B$

& $\frac{d\psi_{\text{I}}}{dx} = \frac{d\psi_{\text{II}}}{dx} \therefore C\xi = j\delta(A - B)$

At $x=a$ $\psi_{\text{II}} = \psi_{\text{III}} \therefore D \exp -\xi a = A \exp j\delta a + B \exp -j\delta a$

& $\frac{d\psi_{\text{II}}}{dx} = \frac{d\psi_{\text{III}}}{dx} \therefore -D\xi \exp -\xi a = j\delta(A \exp j\delta a - B \exp -j\delta a)$

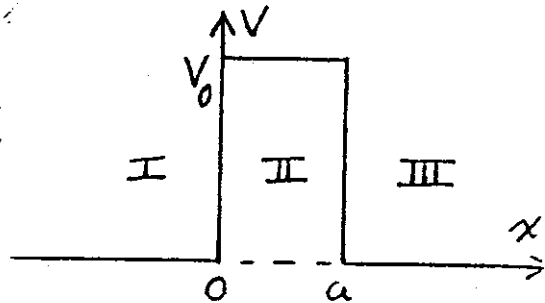
Solve & normalize!



For finite barrier height, there is a finite probability of finding a particle outside the box, even though $E < V_0$!!

3.5 Potential Barrier

For $E < V_0$:-



$$\psi_I = A_I \exp(j\delta_I x) + B_I \exp(-j\delta_I x)$$

$$\delta_I = \left(\frac{2mE}{\hbar^2}\right)^{1/2}$$

$$\psi_{II} = C_{II} \exp(\xi_{II} x) + D_{II} \exp(-\xi_{II} x)$$

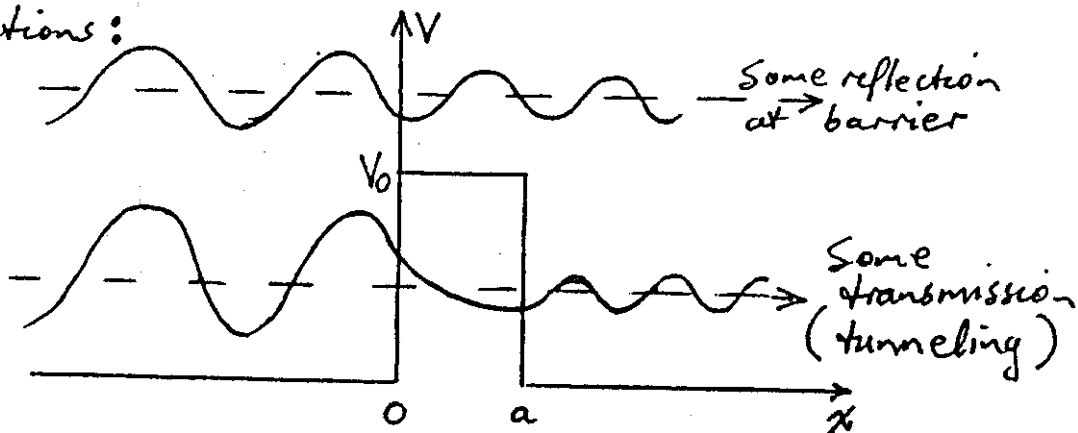
$$\xi_{II} = \left[\frac{2m(V_0 - E)}{\hbar^2}\right]^{1/2}$$

$$\psi_{III} = A_{III} \exp(j\delta_{III} x) + B_{III} \exp(-j\delta_{III} x)$$

$$\delta_{III} = \delta_I$$

Simplify by assuming an electron source at $x = -\infty$
 \therefore no travel from $x = +\infty$
 & $B_{III} = 0$

Solutions:



ECE 417/517
NANO ELECTRONICS
Spring 2007

Lecture 3:
Electron Tunneling

- Rectangular barrier
- WKB approximation
- Parabolic barrier
 - Image effect
- Tunneling time

4.1 Tunneling Coefficient - Rectangular Barrier

$$\text{At } x=0, \quad \psi_I = \psi_{II} \quad \text{and} \quad \frac{d\psi_I}{dx} = \frac{d\psi_{II}}{dx}$$

$$x=a \quad \psi_{II} = \psi_{III} \quad \text{and} \quad \frac{d\psi_{II}}{dx} = \frac{d\psi_{III}}{dx}$$

i.e. at $x=0$

$$\psi_{I,II}(0) = A_I + B_I = C_{II} + D_{II} \quad \dots (1)$$

$$\frac{d\psi_{I,II}(0)}{dx} = j\delta (A_I - B_I) = \xi (C_{II} - D_{II}) \quad \dots (2)$$

& at $x=a$ (assuming no electron wave $R \rightarrow L$, $B_{III}=0$)

$$\psi_{II,III}(a) = A_{III} \exp j\delta a = C_{II} \exp \xi a + D_{II} \exp -\xi a \quad \dots (3)$$

$$\frac{d\psi_{II,III}(a)}{dx} = j\delta A_{III} \exp j\delta a = \xi (C_{II} \exp \xi a - D_{II} \exp -\xi a) \quad \dots (4)$$

Want the transmitted ratio, i.e. find $|A_{III}/A_I|$

$$\therefore \text{Solve} \quad A_I + B_I = C_{II} + D_{II} \quad \dots (1)$$

$$A_I - B_I = \frac{\xi}{j\delta} (C_{II} - D_{II}) \quad \dots (2)$$

to get

$$A_I = \frac{1}{2} \left(1 + \frac{\xi}{j\delta}\right) C_{II} + \frac{1}{2} \left(1 - \frac{\xi}{j\delta}\right) D_{II} \quad \dots (5)$$

& substitute for C_{II} , D_{II} from (3), (4)

$$A_{III} = C_{II} \exp(\xi - j\delta)a + D_{II} \exp -(\xi + j\delta)a$$

$$\frac{j\delta}{\xi} A_{III} = C_{II} \exp(\xi - j\delta)a - D_{II} \exp -(\xi + j\delta)a$$

Solve, gives

$$2C_{II} \exp(\xi - j\delta)a = (1 + j\frac{\delta}{\xi}) A_{III}$$

$$2D_{II} \exp -(\xi + j\delta)a = (1 - j\frac{\delta}{\xi}) A_{III}$$

Substitute for C_{II} , D_{II} in (5) to get

$$A_I = \frac{1}{2} \left(1 + \frac{\xi}{j\delta}\right) \left(1 + j\frac{\delta}{\xi}\right) A_{III} \frac{1}{2} \exp -(\xi - j\delta)a + \frac{1}{2} \left(1 - \frac{\xi}{j\delta}\right) \left(1 - j\frac{\delta}{\xi}\right) A_{III} \frac{1}{2} \exp(\xi + j\delta)a$$

& rearrange & manipulate into the form

$$\frac{A_I}{A_{III}} = \frac{\exp j\delta a}{2} \left[2 \cosh \xi a - \left(\frac{\xi}{j\delta} + j\frac{\delta}{\xi}\right) \sinh \xi a \right]$$

Find magnitude (multiply by complex conjugate)

$$\left| \frac{A_I}{A_{III}} \right|^2 = \left(\frac{A_I}{A_{III}} \right)^* \left(\frac{A_I}{A_{III}} \right)$$

$$= \cosh^2 \xi a - \frac{1}{4} \left(\frac{j\delta}{\xi} + \frac{\xi}{j\delta} \right)^2 \sinh^2 \xi a$$

$$= \cosh^2 \xi a + \frac{1}{4} \left(\frac{\delta}{\xi} - \frac{\xi}{\delta} \right)^2 \sinh^2 \xi a$$

$$= \cosh^2 \xi a + \frac{1}{4} \frac{(V_0 - 2E)^2}{E(V_0 - E)} \sinh^2 \xi a$$

\therefore Tunneling transmission coefficient T is:

$$T = \left| \frac{A_{III}}{A_I} \right|^2 = \frac{1}{\cosh^2 \xi a + \frac{1}{4} \frac{(V_0 - 2E)^2}{E(V_0 - E)} \sinh^2 \xi a}$$

$$= \frac{\cosh^{-2} \xi a}{1 + \frac{(\frac{1}{2}V_0 - E)^2}{E(V_0 - E)} \tanh^2 \xi a}$$

& if $V_0 \sim E$, $\xi a \gg 0$ so $\tanh \xi a \sim 1$
 $\cosh \xi a \approx e^{\xi a}$

get $T \approx \frac{1}{2} \exp - 2 \xi a$

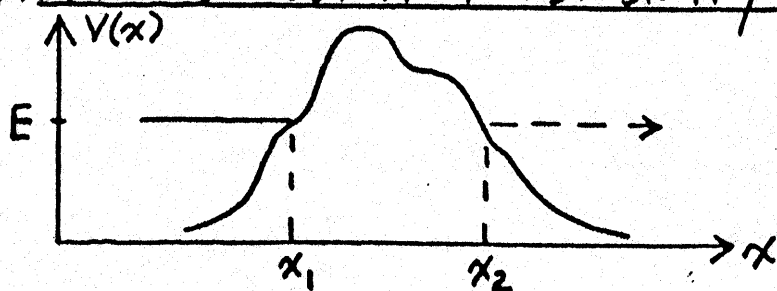
$$= \frac{1}{2} \exp - \frac{4\pi}{h} \sqrt{2m(V_0 - E)} \cdot a$$

This form is very similar to the WKB approximation for non-rectangular barriers.

ie. $T(E) = \exp - \frac{4\pi}{h} \int_{x_1}^{x_2} [V(x) - E]^{1/2} dx$

$$\rightarrow \exp - \frac{4\pi}{h} (2m\phi)^{1/2} a$$

4.2 TRANSMISSION PROBABILITY: Practical Barriers



$$\frac{d^2\psi}{dx^2} + \frac{2m}{\hbar^2} [E - V(x)]\psi = 0 \quad \longrightarrow \quad \frac{d^2\psi}{dx^2} = \frac{2m}{\hbar^2} [V(x) - E]\psi$$

through the barrier
where $E < V(x)$

Try solution of the form $\psi = A \exp \alpha(x)$

then $\frac{d\psi}{dx} = A \exp \alpha(x) \cdot \frac{d\alpha(x)}{dx}$

$$\frac{d^2\psi}{dx^2} = A \exp \alpha(x) \cdot \frac{d^2\alpha(x)}{dx^2} + \left[\frac{d\alpha(x)}{dx} \right]^2 A \exp \alpha(x)$$

$$\therefore \text{Schrodinger} \rightarrow \ddot{\alpha}(x) + [\dot{\alpha}(x)]^2 - \frac{2m}{\hbar^2} [V(x) - E] = 0$$

Wentzel-Kramers-Brillouin (WKB) approximation:

$\ddot{\alpha}(x) \ll [\dot{\alpha}(x)]^2$
ie. "slowly varying" potential barrier.

$$\therefore [\dot{\alpha}(x)]^2 \approx \frac{2m}{\hbar^2} [V(x) - E]$$

$$\& \quad \alpha(x) = \pm \int_{x_1}^x \left(\frac{2m}{\hbar^2} [V(x) - E] \right)^{1/2} dx$$

At x_2 $\psi^* \psi = A^2 \exp - 2 \left(\frac{2m}{\hbar^2} \right)^{1/2} \int_{x_1}^{x_2} [V(x) - E]^{1/2} dx$

-|| At x_1 $\psi^* \psi = A^2$

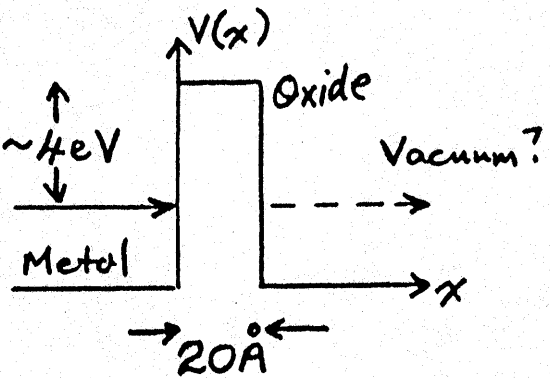
∴ Transmission probability $\psi^* \psi|_{x_2} / \psi^* \psi|_{x_1}$
 is $T(E) = \exp - 2 \left(\frac{2m}{\hbar^2} \right)^{1/2} \int_{x_1}^{x_2} (V(x) - E)^{1/2} dx$
 $\Rightarrow \exp - 2 \frac{(2m\phi)^{1/2}}{\hbar} d$

4.3 Example 1 (e^- from metal)

$$T \sim \exp - 2 \sqrt{\frac{2 \times 9.11 \times 10^{-31} \left(\frac{1}{2} \times 1.6 \times 10^{-19} \right)^{1/2}}{6.67^2 \times 10^{-68} / 4\pi^2} \times 20 \times 10^{-10} E_F}$$

$$\sim \exp - 40.7$$

$$\sim 2 \times 10^{-18}$$

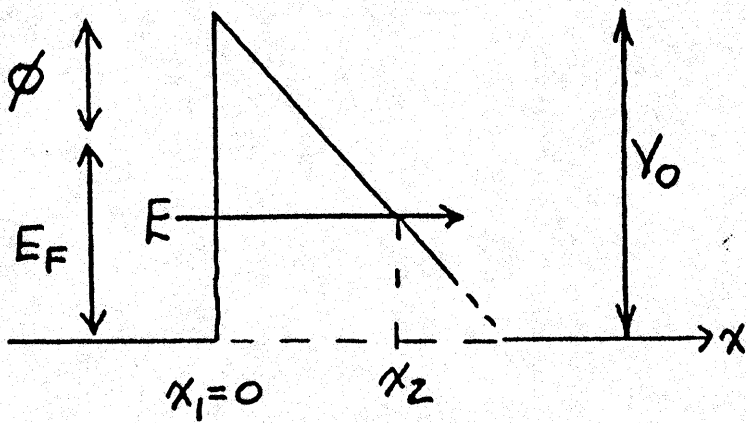


4.4 Example 2 (ball through wall)

Say $m \sim 0.1 \text{ Kg}$
 height $\sim 1 \text{ m}$ ∴ KE to go over $mgh \sim 4 \text{ J}$
 thickness 10 cm (init velocity $\sim 3 \text{ m/s}$)

$$\text{Here } T \sim \exp - 2 \sqrt{\frac{2 \times 0.1}{6.67^2 \times 10^{-68} / 4\pi^2}} \sqrt{4} (0.1) = \exp - 15 \times 10^{33} !!$$

4.5 Example 3 Field Emission Current Density



Barrier

$$V(x) = V_0 - qEx$$

\therefore For e^- with energy E , x_2 given by

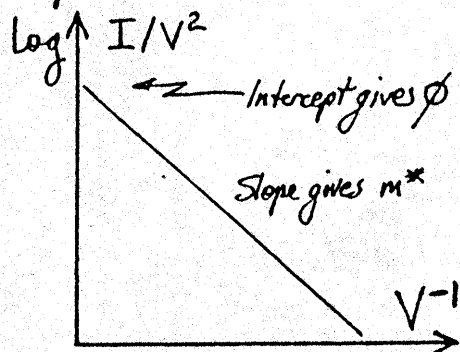
$$E = V_0 - qEx_2$$

$$\begin{aligned} \therefore T(E) &= \exp - 2 \left(\frac{2m}{\hbar^2} \right)^{1/2} \int_0^{(V_0-E)/qE} (V_0 - qEx - E)^{1/2} dx \\ &= \exp - 2 \left(\frac{2m}{\hbar^2} \right)^{1/2} \left[\frac{2}{3} (V_0 - qEx - E)^{3/2} \right]_0^{(V_0-E)/qE} \\ &= \exp - \frac{4}{3} \left(\frac{2m}{\hbar^2} \right)^{1/2} \frac{(V_0-E)^{3/2}}{qE} \end{aligned}$$

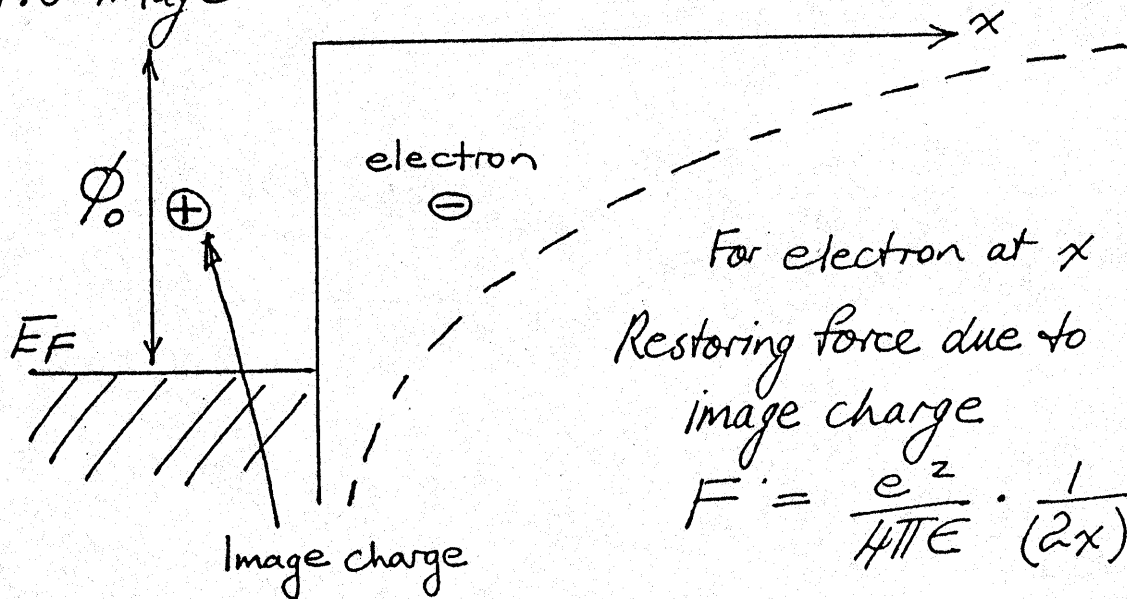
Integrating for electrons from E_F to ∞ gives

$$J = \frac{q^3 E^2}{18\pi h \phi} \exp - \left[\frac{4}{3} \left(\frac{2m}{\hbar^2} \right)^{1/2} \frac{\phi^{3/2}}{qE} \right]$$

Plot: $\log(J/E^2)$ vs $(1/E)$
 i.e. $\log(I/V^2)$ vs $(1/V)$
 to validate mechanism



4.6 Image Effect



\therefore Work done against restoring force in removal of electron to distance x

$$= \frac{e^2}{4\pi\epsilon} \cdot \frac{1}{4} \int_0^x x^{-2} dx$$

$$= -\frac{e^2}{16\pi\epsilon x} + \text{const (limits at } x=0)$$

\therefore Effective barrier (work function)

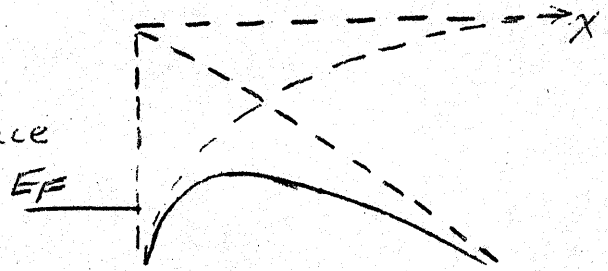
$$\phi = \phi_0 - \frac{e^2}{16\pi\epsilon x}$$

Schottky Effect

If now apply electric field to surface

$$q\phi(x) = q\phi_0 - \frac{q^2}{16\pi\epsilon x} - qFx$$

elec field



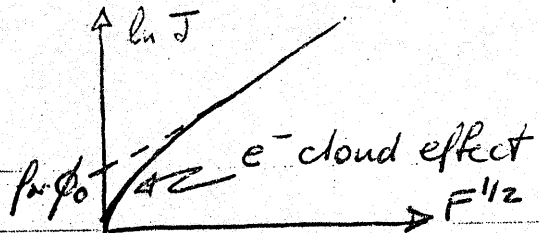
New effective work function - due to reduction in total barrier height

$$\frac{d}{dx} q\phi(x) = -\frac{q^2}{16\pi\epsilon} \left(-\frac{1}{x^2}\right) - qF = 0 \text{ at } \frac{q^2}{16\pi\epsilon x^2} = qF$$

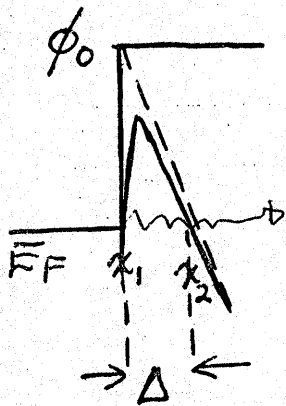
$$\therefore q\phi_{\max} = q\phi_0 - \frac{q^2}{16\pi\epsilon} \left(\frac{qF}{16\pi\epsilon}\right)^{1/2} - qF \left(\frac{q^2}{16\pi\epsilon qF}\right)^{1/2}$$

$$= q\phi_0 - q \left(\frac{qF}{4\pi\epsilon}\right)^{1/2}$$

Now $J = AT^2 \exp -q\phi_{\max}/kT$



④ Fowler-Nordheim Tunneling $J \propto e^{-(2m\phi)^{1/2} \Delta}$



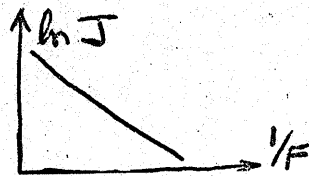
Find barrier width Δ at E_F

ie. set $q\phi(x) = q\phi_0 - \frac{q^2}{16\pi\epsilon x} - qFx = 0$

ie. at $x_1, x_2 = \left\{ -q\phi_0 \pm \left[(q\phi_0)^2 - \frac{4qFq^2}{16\pi\epsilon} \right]^{1/2} \right\} / (-2qF)$

$\Delta = x_2 - x_1 = \left[\left(\frac{\phi_0}{F} \right)^2 - \frac{q}{4\pi\epsilon F} \right]^{1/2} \approx \phi_0 / F$

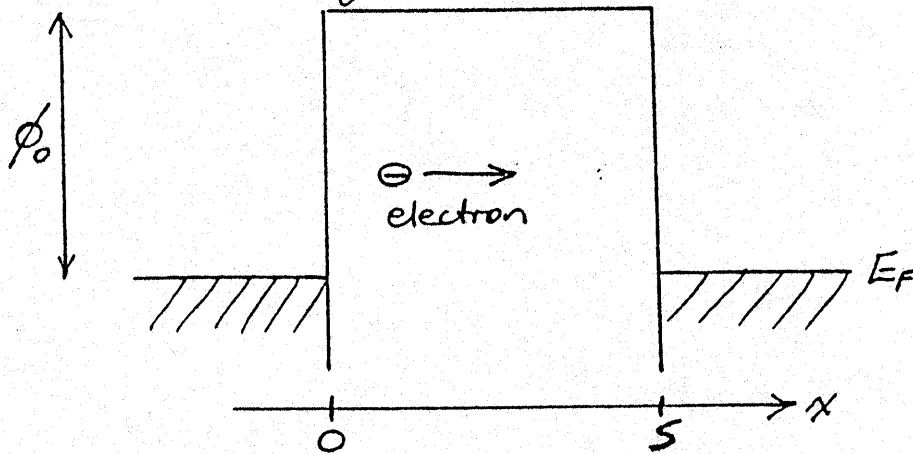
$\therefore J \propto \exp -\frac{\lambda}{F}$



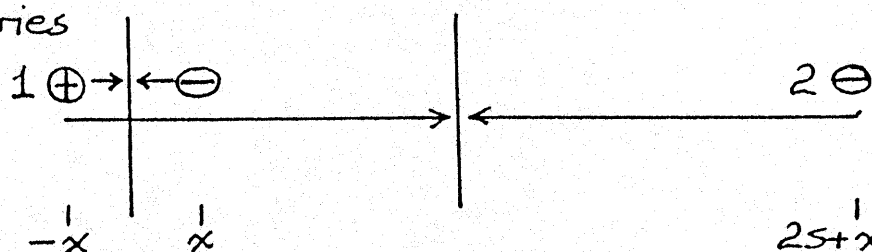
{ Field emission
microscopes

4.7 Parabolic barrier

Consider ideal rectangular barrier with image effects.

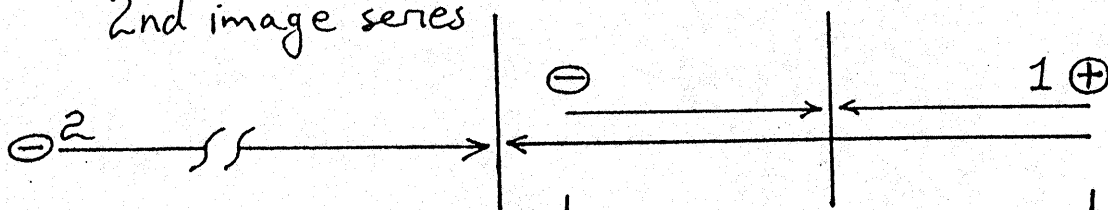


1st image series



$$F_1 = \text{Force} = \frac{e^2}{4\pi\epsilon} \left(\frac{1}{(2x)^2} - \frac{1}{(2s)^2} + \frac{1}{(2s+2x)^2} + \dots \right)$$

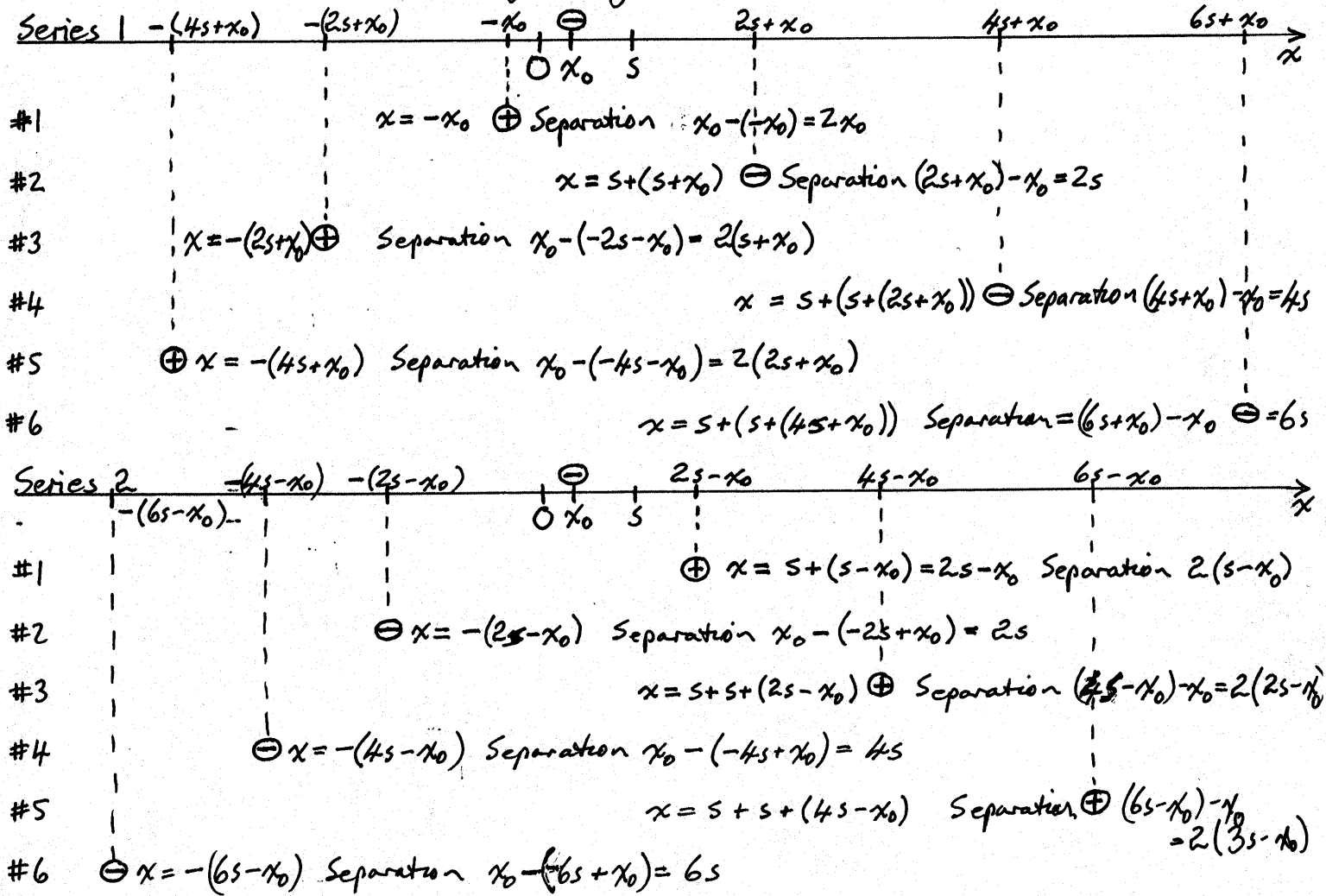
2nd image series



$$F_2 = \text{Force} = \frac{e^2}{4\pi\epsilon} \left(-\frac{1}{(2s-2x)^2} + \frac{1}{(2s)^2} - \frac{1}{(4s-2x)^2} + \dots \right)$$

$$\phi(x) = \phi_0 - \frac{e^2}{16\pi\epsilon} \left[\left(\frac{1}{x} + \frac{1}{s+x} + \frac{1}{2s+x} + \dots \right) - \left(\frac{1}{s-x} + \frac{1}{2s-x} + \dots \right) \right]$$

Image Charges



Force 1 (to left)

$$F_1 = \frac{e^2}{4\pi\epsilon} \left[\frac{1}{(2x_0)^2} + \frac{1}{(2(s+x_0))^2} + \frac{1}{(2(2s+x_0))^2} + \dots \right. \\ \left. + \frac{1}{(2s)^2} + \frac{1}{(4s)^2} + \frac{1}{(6s)^2} + \dots \right]$$

Force 2 (to right)

$$F_2 = \frac{e^2}{4\pi\epsilon} \left[\frac{1}{(2(s-x_0))^2} + \frac{1}{(2(2s-x_0))^2} + \frac{1}{(2(3s-x_0))^2} + \dots \right. \\ \left. + \frac{1}{(2s)^2} + \frac{1}{(4s)^2} + \frac{1}{(6s)^2} + \dots \right]$$

\therefore Net force (to left) = $F_1 - F_2$

$$= \frac{e^2}{4\pi\epsilon} \cdot \frac{1}{4} \left[\frac{1}{x_0^2} + \frac{1}{(s+x_0)^2} - \frac{1}{(s-x_0)^2} \right. \\ \left. + \frac{1}{(2s+x_0)^2} - \frac{1}{(2s-x_0)^2} \right. \\ \left. + \frac{1}{(3s+x_0)^2} - \frac{1}{(3s-x_0)^2} \dots \right]$$

$$= \frac{e^2}{16\pi\epsilon} \left[\frac{1}{x_0^2} + \sum_{n=1}^{\infty} \left(\frac{1}{(ns+x_0)^2} - \frac{1}{(ns-x_0)^2} \right) \right]$$

$$\therefore \text{Potential } \phi(x) = \phi_0 - \frac{e^2}{16\pi\epsilon} \left[\frac{1}{x_0} + \sum_{n=1}^{\infty} \left(\frac{1}{ns+x_0} + \frac{1}{ns-x_0} \right) \right]_{x_0}^{x_0}$$

$$= \phi_0 - \frac{e^2}{16\pi\epsilon} \left[\frac{1}{x_0} + \sum_{n=1}^{\infty} \frac{2ns}{(ns)^2 - x_0^2} = \frac{2}{ns} + \text{pole} \right]_{x_0=0}$$

$$= \phi_0 - \frac{e^2}{8\pi\epsilon} \left[\frac{1}{2x_0} + \sum_{n=1}^{\infty} \frac{ns}{(ns)^2 - x_0^2} = \frac{1}{ns} \right]$$

At $x_0 = s/2$

$$\rightarrow \phi_0 - \frac{e^2}{8\pi\epsilon s} \left[1 + \sum_{n=1}^{\infty} \frac{1}{(n^2-1/4)} \right] \rightarrow \phi_0 - \frac{e^2}{6\pi\epsilon s}$$

$$\phi(x) = \phi_0 - \frac{e^2}{16\pi\epsilon_s} \left[\frac{1}{x_0} + \sum_{n=1}^{\infty} \frac{1}{ns+x_0} + \frac{1}{ns-x_0} - \frac{2}{ns} \right]$$

At $x = s/2$

$$\Rightarrow \phi_0 - \frac{e^2}{8\pi\epsilon_s} \left[1 + \sum_{n=1}^{\infty} \frac{1}{2n+1} + \frac{1}{2n-1} - \frac{1}{n} \right]$$

$$= \phi_0 - \frac{e^2}{8\pi\epsilon_s} \left[1 + \frac{1}{3} + \frac{1}{5} + \frac{1}{7} + \frac{1}{9} + \dots \right. \\ \left. + 1 + \frac{1}{3} + \frac{1}{5} + \frac{1}{7} + \dots \right. \\ \left. - 1 - \frac{1}{2} - \frac{1}{3} - \frac{1}{5} - \frac{1}{7} - \dots \right]$$

$$= \phi_0 - \frac{e^2}{8\pi\epsilon_s} \left[1 - \frac{1}{2} + \frac{1}{3} - \frac{1}{5} + \frac{1}{7} - \dots \right]$$

$$= \phi_0 - \frac{e^2}{8\pi\epsilon_s} \ln 2$$

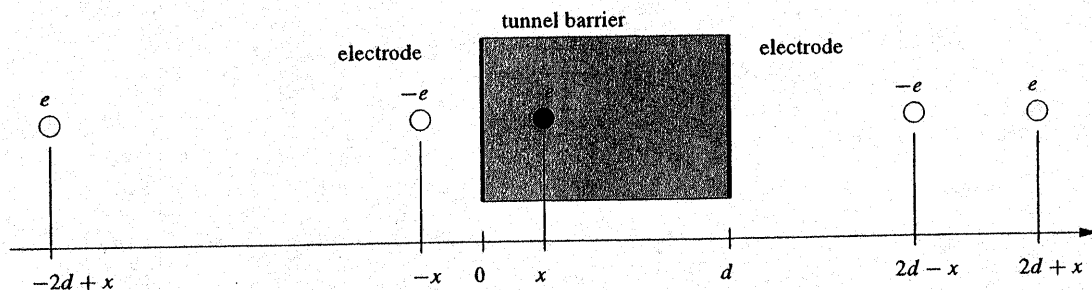


Fig. 17. The effect of two infinite parallel planes on a point charge between the conductors can be replaced with an infinite number of image charges of which the first four are shown

example, has a distance of $2x$ to position x , and a charge of $-e$. The series of image charges with charge e come in pairs with distances $2nd$, for $n = 1, 2, \dots$, and with d as the distance of the plate electrodes. Image charges with charge $-e$ come with distances $2nd \pm 2x$. Summing all point potentials, the potential energy due to image charges at the location of the electron is given by

Note error;
should be
 $8\pi\epsilon$

$$V_{\text{im}}(x) = -\frac{e^2}{4\pi\epsilon} \left[\frac{1}{2x} + \sum_{n=1}^{\infty} \left(\frac{nd}{n^2d^2 - x^2} - \frac{1}{nd} \right) \right]. \quad (2.89)$$

No closed-form expression is possible for this sum. However, if the tunneling electron is exactly in the middle of the tunnel barrier, image charges are symmetrically positioned and the sum can be calculated. For $x = d/2$ image charges have distances of multiples of d . The potential is then

$$V_{\text{im}}(d/2) = -\frac{e^2}{2\pi\epsilon d} \sum_{n=1}^{\infty} \frac{(-1)^n}{n} = -\frac{e^2}{2\pi\epsilon d} \ln(2). \quad (2.90)$$

Compare 8πϵs

A good approximation to (2.89) was given by Simmons [282]:

$$V_{\text{im}}(x) \approx -\frac{1.15e^2 \ln(2)d}{8\pi\epsilon x(d-x)}. \quad (2.91)$$

Figure 18 shows the exact image charge potential for different relative dielectrics and compares it to the approximation (2.91). Thin barriers with low dielectric constant will exhibit the strongest modification due to image charges. A 1 nm thick Al_2O_3 barrier, with $\epsilon_r = 9.4$, will have an effective barrier height reduction of about 0.21 eV.

The exact expression (2.89) as well as the approximation (2.91) have a pole at $x = 0$ and $x = d$. This is an artifact which stems from the assumption of an abrupt barrier. On the atomic scale abrupt barriers do not exist. This

4.9 Tunneling Time

Controversial topic for many years.

Only consensus is "fast."

Model 1: Wave function describes probability of electron position, \therefore electron "exists" on both sides of junction, $\therefore t_t = 0$

Model 2: Electron wave travels at velocity of light, c .
 $\therefore t_t = s/c \sim \frac{30 \text{ \AA} \times 10^{-10} \text{ m}}{3 \times 10^8 \text{ m/s}}$ for 30 \AA
 $\approx 10^{-17} \text{ sec.}$

Model 3: Heisenberg Uncertainty Principle

$$\Delta E \Delta t \sim \hbar$$

$$\text{ie. } t_t = 2\Delta t = 2\hbar / \Delta E$$

$$\Delta E \sim 0.1 \text{ eV}$$

$$\sim \frac{2 \times 6.67 \times 10^{-34}}{2\pi \times 0.1 \times 1.6 \times 10^{-19}}$$

$$\sim \cancel{2} \times 10^{-14} \text{ sec}$$

Model 4: Sequential calculations of barrier changes as localized electron tunnels through.
 \Rightarrow slower

ECE 417/517
NANO ELECTRONICS
Spring 2007

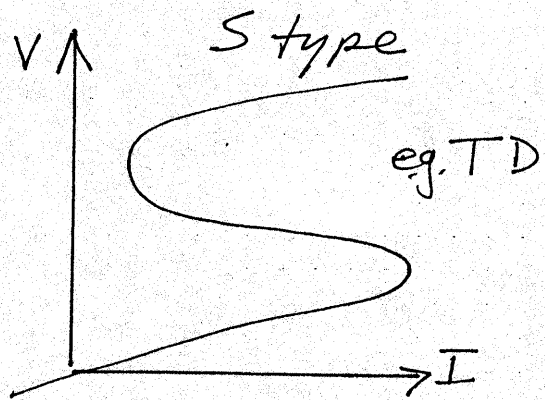
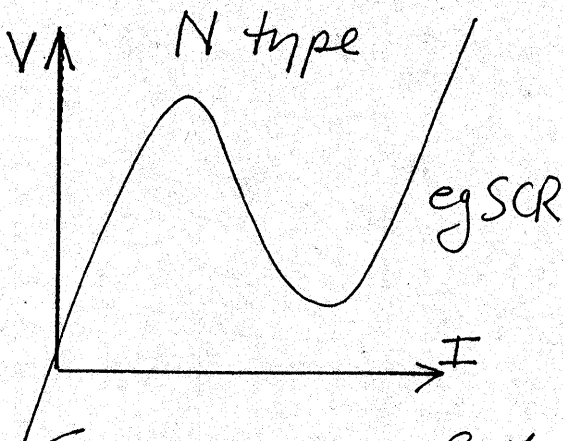
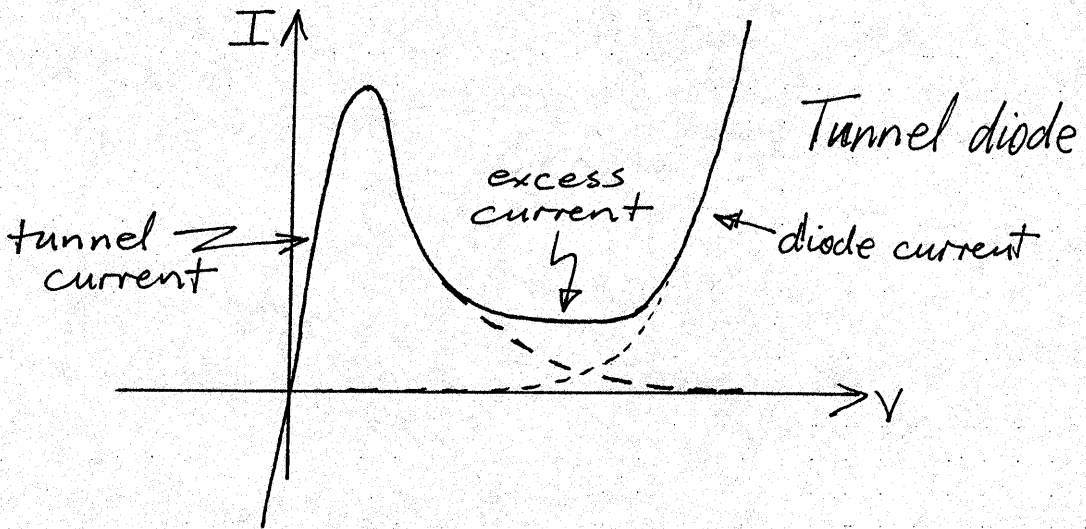
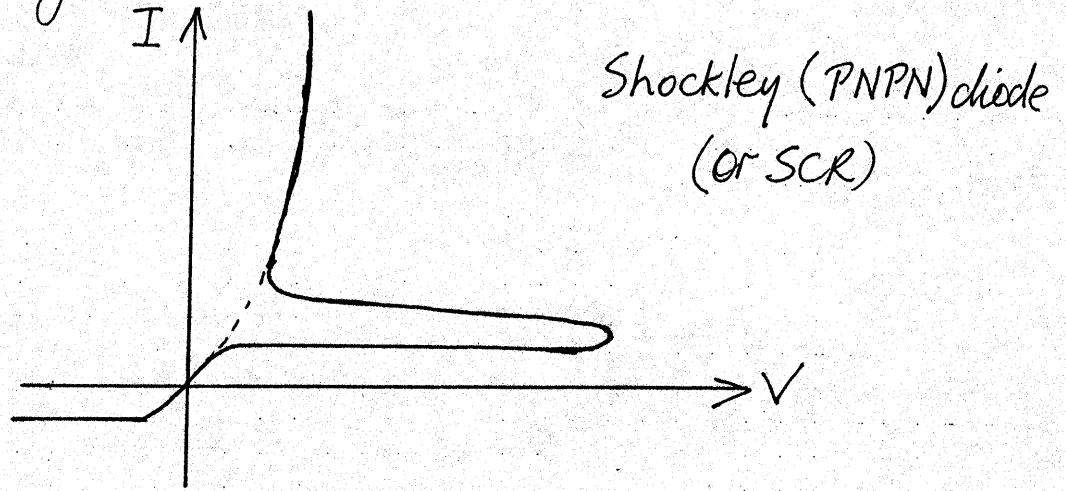
Lecture 4:

Tunnel Diode & Resonant TD

- Esaki tunnel diode (TD)
- Resonant tunneling
- RTD characteristics
- Equivalent circuits

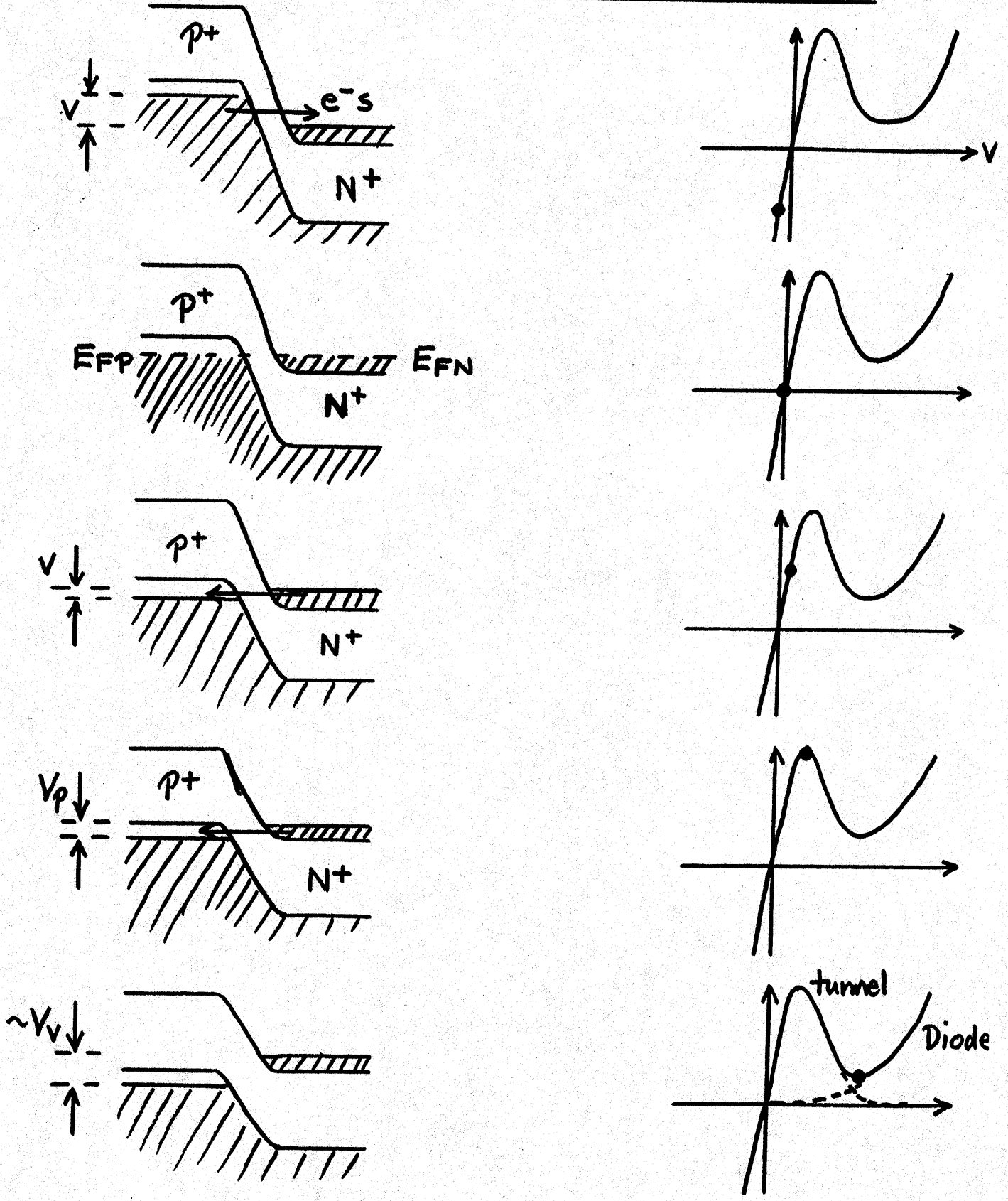
B

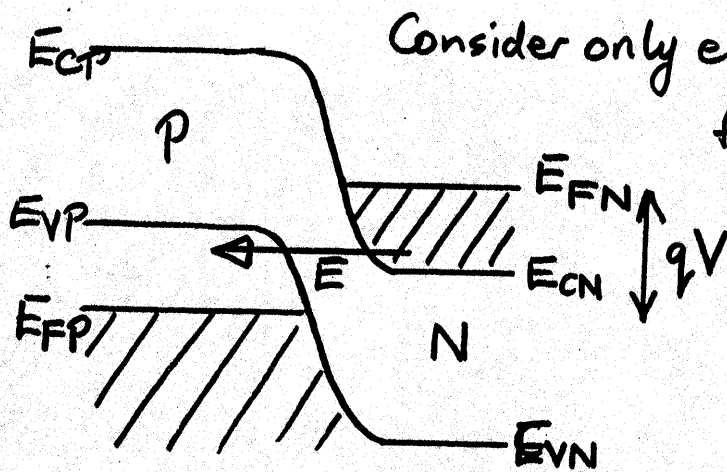
1.1 Negative resistance devices



Semiconductors & thermal runaway as neg. resist.

1.2 TUNNEL DIODE CHARACTERISTICS





Consider only electrons:

In range E to $E+dE$
from N to P :

$dI_{nN} \propto \left\{ \begin{array}{l} \text{No. of } e^- \text{ in} \\ \text{cond. band of } N \end{array} \right\}$

$\times \left\{ \begin{array}{l} \text{No. of holes in} \\ \text{valence band of } P \end{array} \right\}$

in range E to $E+dE$.

$$\therefore dI_{nN} = A D(E) \underbrace{F_N(E) S_N(E)}_{\text{in cond band of } N \text{ type}} \underbrace{(1 - F_P(E)) S_P(E)}_{\text{in valence band of } P \text{ type}} dE$$

$$\& I_{nN} = A \int_{E_{CN}}^{E_{VP}} D(E) S_N(E) S_P(E) F_N(E) (1 - F_P(E)) dE$$

Similarly can find the electron current I_{nP} from P to N .

$$I_{nP} = A \int_{E_{CN}}^{E_{VP}} D(E) S_N(E) S_P(E) F_P(E) (1 - F_N(E)) dE$$

So the net electron current is $I_n = I_{nN} - I_{nP}$

$$I_n = A \int_{E_{CN}}^{E_{VP}} D(E) S_N(E) S_P(E) [F_N(E) - F_P(E)] dE$$

We know $S_N(E) = B (E - E_{CN})^{1/2}$

$\& S_P(E) = B (E_{VP} - E)^{1/2}$

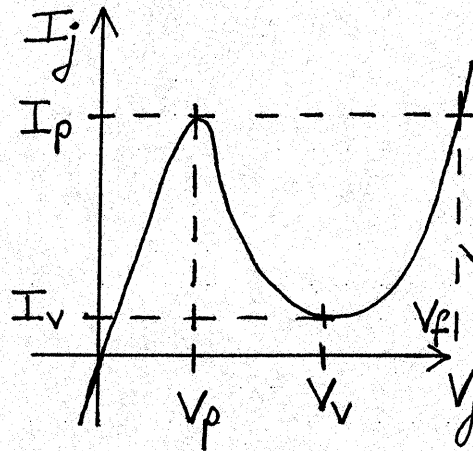
Let $E_{FN} = E_{CN} + \lambda_N$

$\& E_{FP} = E_{VP} - \lambda_P$

$\& qV = E_{FN} - E_{FP} = E_{CN} - E_{VP} + (\lambda_N + \lambda_P)$

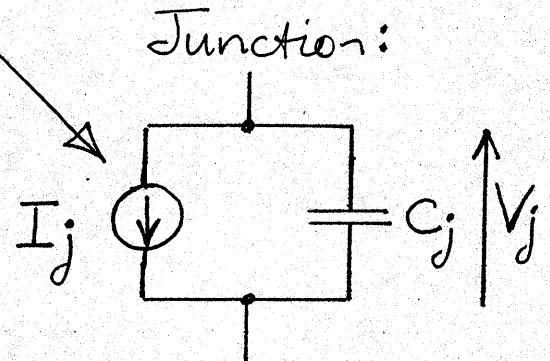
Hence $E_{VP} = E_{CN} + (\lambda_N + \lambda_P) - qV$

1.3 Equivalent Circuit



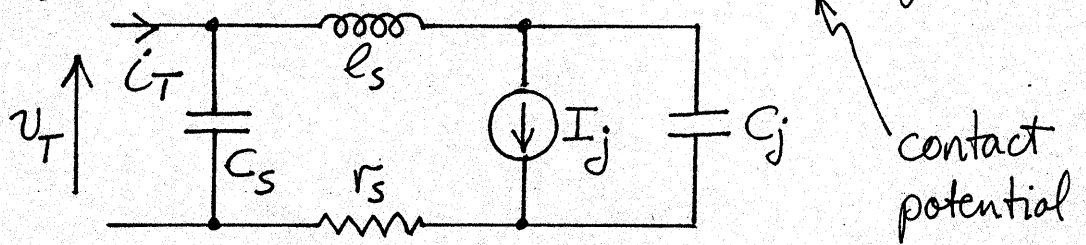
Static characteristic of junction itself

For Ge: $V_p \sim 60\text{mV}$, $V_v \sim 340\text{mV}$
 $V_{p1} \sim 500\text{mV}$
 $I_p/I_v \sim 5 \text{ to } 10$ $I_p \sim 1 \text{ to } 50\text{mA}$



$$C_j = \left(\frac{V_0 - V_v}{V_0 - V_j} \right)^{1/2}$$

Packaged device:



$$C_s \approx 1\text{pF}$$

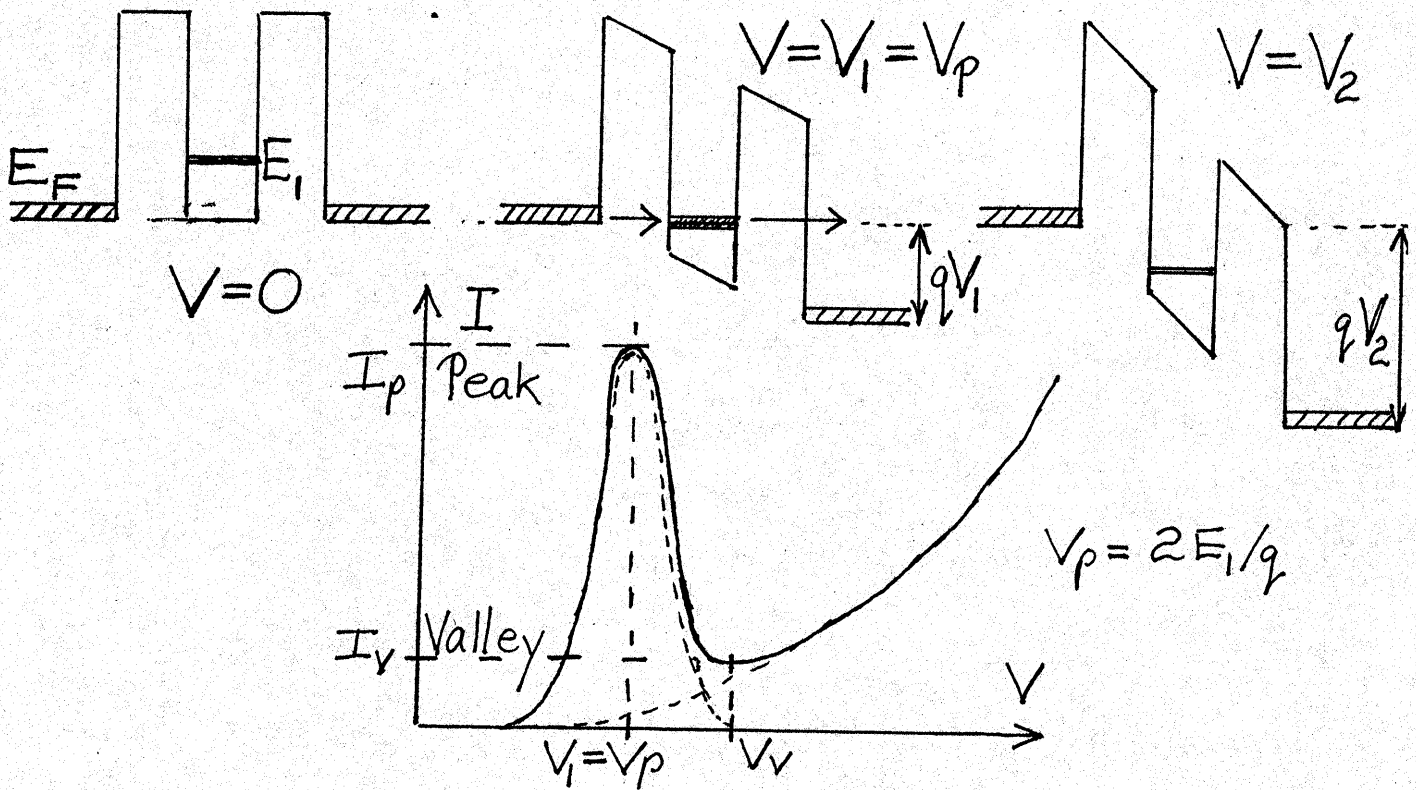
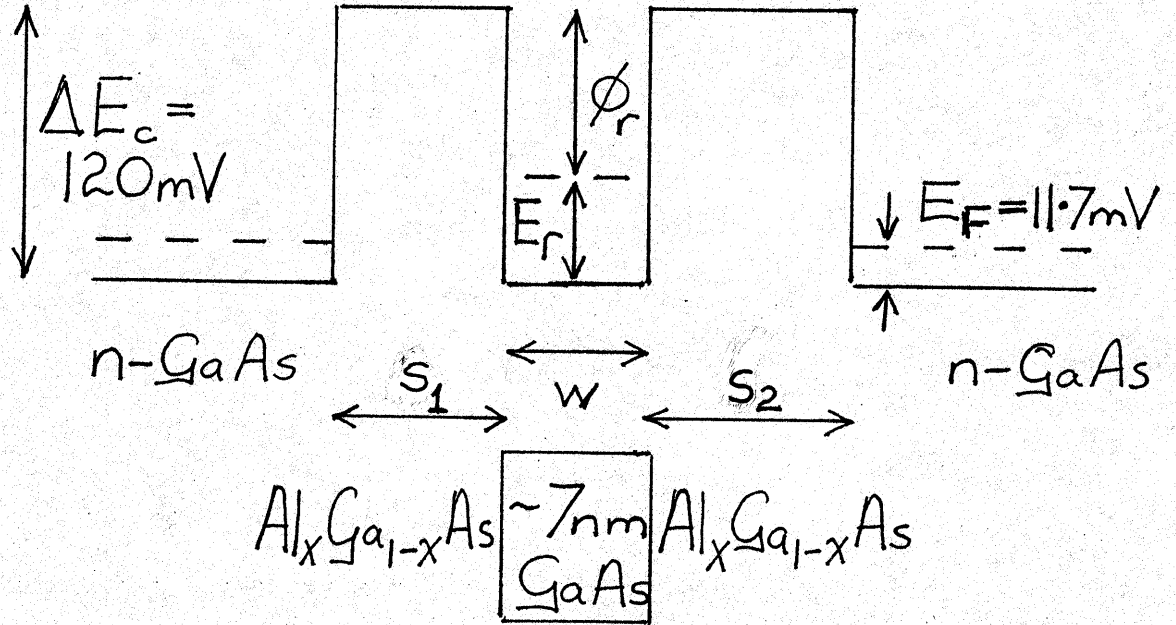
$$r_s \sim 1\Omega$$

$$l_s \sim 1\text{nH (stripline)}$$

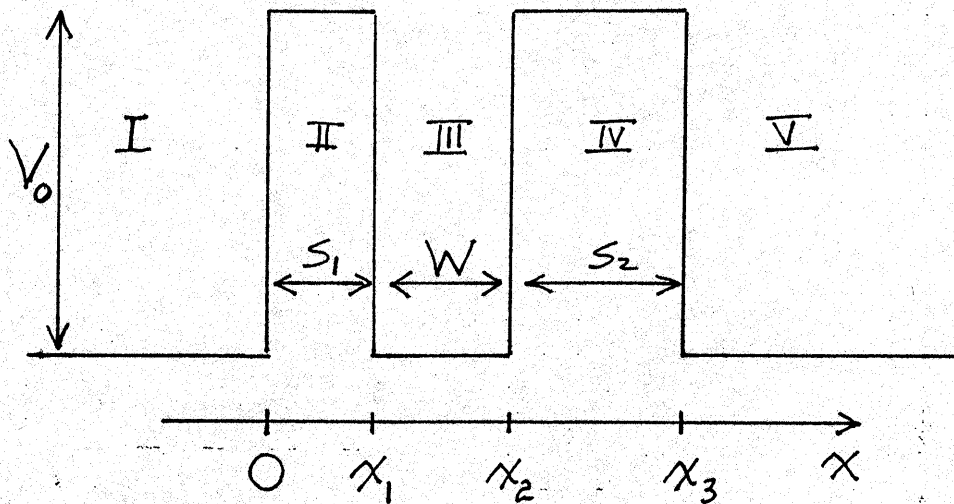
$$\sim 8\text{nH (lead package)}$$

1. Resonant Tunnel Diode (RTD) ^A

Typical structure:



5. RTD Characteristics



5.1. Follow same procedure as before

$$\text{i.e. set } \psi_I(0) = \psi_{II}(0) \quad \frac{d\psi_I(0)}{dx} = \frac{d\psi_{II}(0)}{dx}$$

$$\psi_{II}(x_1) = \psi_{III}(x_1) \quad \frac{d\psi_{II}(x_1)}{dx} = \frac{d\psi_{III}(x_1)}{dx}$$

$$\psi_{III}(x_2) = \psi_{IV}(x_2) \quad \frac{d\psi_{III}(x_2)}{dx} = \frac{d\psi_{IV}(x_2)}{dx}$$

$$\psi_{IV}(x_3) = \psi_V(x_3) \quad \frac{d\psi_{IV}(x_3)}{dx} = \frac{d\psi_V(x_3)}{dx}$$

where $\psi_I = A_I e^{j\delta x} + B_I e^{-j\delta x}$

$$\psi_{II} = C_I e^{g x} + D_I e^{-g x}$$

$$\psi_{III} = A_{III} e^{j\delta x} + B_{III} e^{-j\delta x}$$

$$\psi_{IV} = C_{IV} e^{\gamma x} + D_{IV} e^{-\gamma x}$$

$$\psi_{V} = A_{V} e^{j\delta x}$$

and $\delta = \frac{2\pi}{h} (2mE)^{1/2}$

$$\gamma = \frac{2\pi}{h} (2m(V_0 - E))^{1/2}$$

5.2. Simplification — assume barriers of equal width
 $S_1 = S_2 = S$

Then
$$T = \frac{1}{1 + \left[\frac{V_0}{2E(V_0 - E)} \right]^2 H^2 \sinh^2 \gamma S}$$

where
$$H = 2[E(V_0 - E)]^{1/2} \cdot \cosh \gamma S \cdot \cos \delta W - (2E - V_0) \cdot \sinh \gamma S \cdot \sin \delta W$$

When $H = 0$, $T \rightarrow 1$

This is the resonant tunneling condition and occurs at energies E_n which satisfy

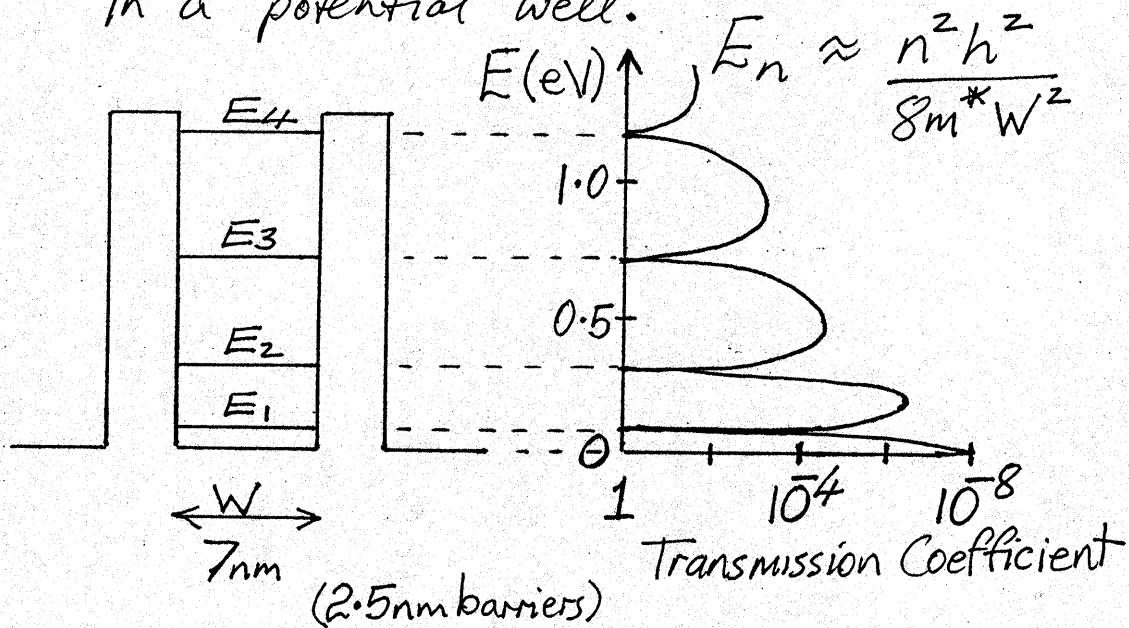
$$\frac{2[E_n(V_0 - E_n)]^{1/2}}{(2E_n - V_0)} = \tan \delta W \cdot \tanh \gamma S.$$

5.3. Notes:

(1) There are no impurity levels required for this process — it is fundamental to the idealized 2-barrier structure.

(2) Ideally T is not only increased, but it becomes unity, i.e. there is NO attenuation — T exceeds the single barrier transmission.

(3) To a first order, these critical/resonant energy levels match the permitted levels in a potential well:



— but they are not the same! The actual levels are affected by the tunneling process (& bias)

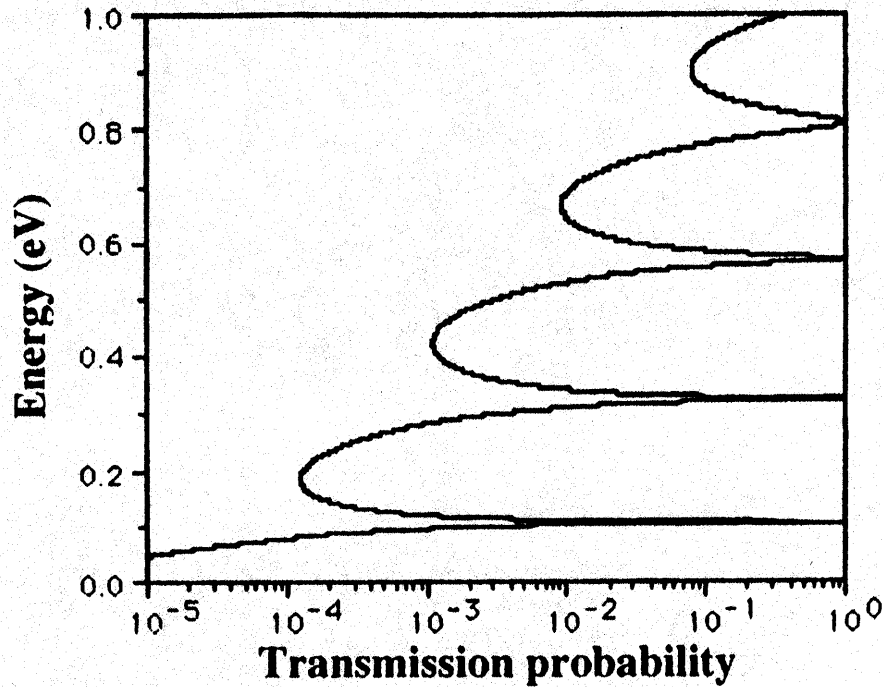
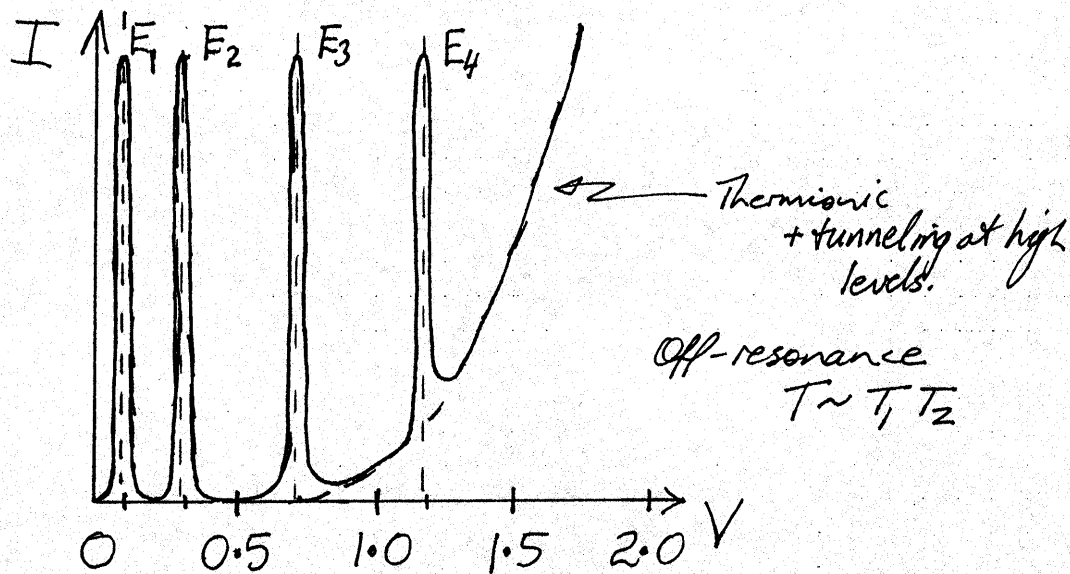
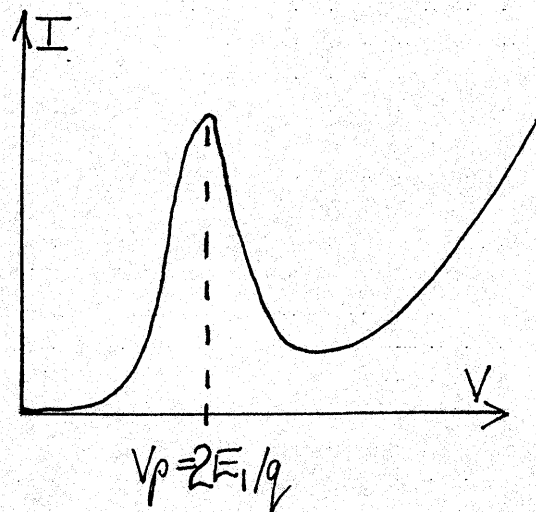


Figure 2.5 Transmission probability $T(E_z)$ versus energy E_z calculated for Material 1 under zero external bias.

From ^{RTD} Mizuta & Tanoue
 (All figures this lecture from Mizuta & Tanoue unless otherwise indicated)



Usually see first peak



How can this work? How can we have $T=1$ through
 TWO barriers, each of which have $T' \sim 10^{-8}$??
 Interference / standing wave in the well.
 Carrier population high in the well

- takes time to build up (dynamic response)
- represent by equivalent circuit inductance
- need level lifetime $\tau_0 >$ scattering time τ_s
- peak width $\Delta E \sim \hbar/\tau_0$
 (Heisenberg)

2.2 Theory of global coherent RT

27

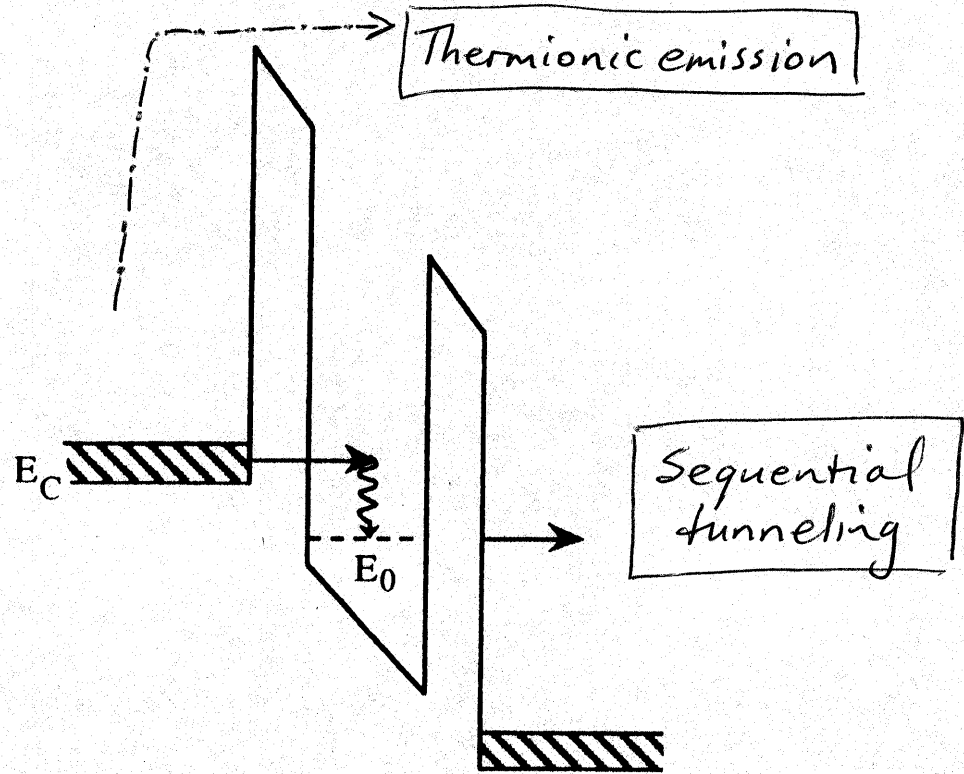


Figure 2.10 Schematic sequential tunnelling process mediated by an energy relaxation process (see Section 2.6), thought to give rise to the discrepancy between measured valley currents and those predicted by the global coherent tunnelling model.

5.4 Asymmetrical barriers

Full expression gives

$$T = \frac{T_{\min}}{T_{\max}}$$

at resonance, where

T_{\min} is tunneling coeff of thicker barrier

T_{\max} " " " " thinner "

& $T \rightarrow 1$ when $T_{\min} = T_{\max}$
(identical barriers)

QUANTUM WELL ELECTRON

- DWELL TIME
- LEVEL LIFETIME
- ESCAPE TIME

Classical view:

$$\tau_0 = \frac{q \sigma_w}{J}$$

← sheet e^- concentration (number/area)
 ← current density (current/area)

ie. $J = (q \sigma_w) / \tau_0$ rate of "recharge" of electrons in well.

Quantum view:

$$\tau_0 = \hbar \frac{\partial \delta(E)}{\partial E}$$

where δ is electron wave function phase shift

$$\frac{\psi_{II}}{\psi_I} = \left| \frac{\psi_{II}}{\psi_I} \right| \exp j\delta$$

* It can be shown that for $E \approx E_n$ and energy width Γ_n of level E_n

$$\left. \begin{array}{l} \text{for } E \approx E_n \text{ and} \\ \text{energy width } \Gamma_n \text{ of level } E_n \end{array} \right\} \frac{\psi_{II}}{\psi_I} \approx \frac{\Gamma_n}{(E - E_n) + j\Gamma_n} \exp -jS_n(W + 2s)$$

so $\delta = -S_n(W + 2s) - \tan^{-1} \left(\frac{\Gamma_n}{E - E_n} \right)$

$$\therefore \tau_0(E) = \hbar \frac{\Gamma_n}{(E - E_n)^2 + \Gamma_n^2} \xrightarrow{E = E_n} \frac{\hbar}{\Gamma_n}$$

(See back, and compare Heisenberg)

* It can also be shown that $\Gamma_n \approx 2\hbar \cdot T_{SB}(E_n)$.

← electron velocity in well v_n
 $W + \frac{2}{S_n}$ ←

$$\text{so } \tau_0(E_n) = \frac{W + \frac{2}{S_n}}{v_n} [2T_{SB}(E_n)]^{-1}$$

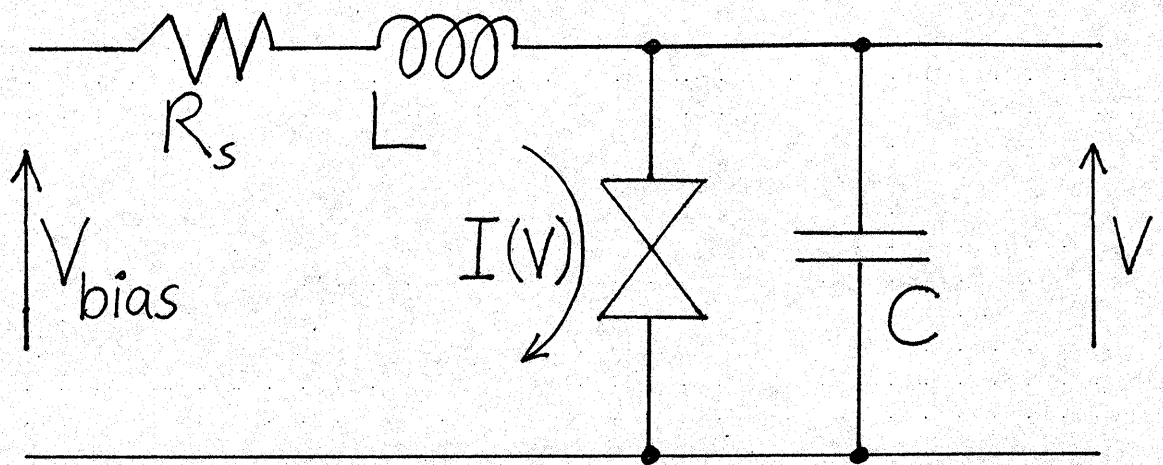
↑
Single barrier tunneling coefficient

← correction term for e^- wave penetration into barriers.

OR argue backwards from this "multiple reflection time" for the electron to get Γ_n !

$$\tau_0(E_n) = \frac{W + \frac{2}{S_n}}{2v_n} \exp + \frac{4\hbar S_n}{h} [2qm(V_0 - E_n)]^{1/2} \approx \tau_{esc} \text{ (see back)}$$

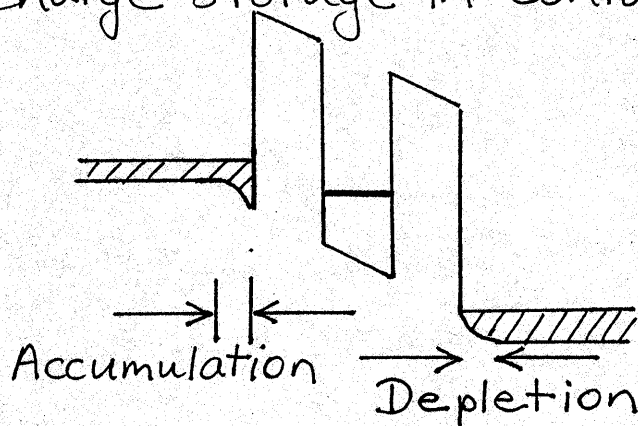
5.6. Equivalent Circuit



$I(V)$ given by static characteristic
(ie. tunneling current)

L — lead parasitics
— non-zero transit time

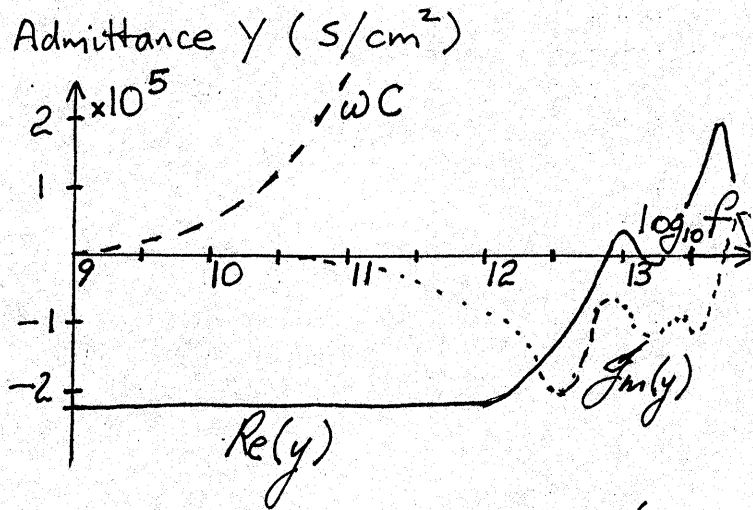
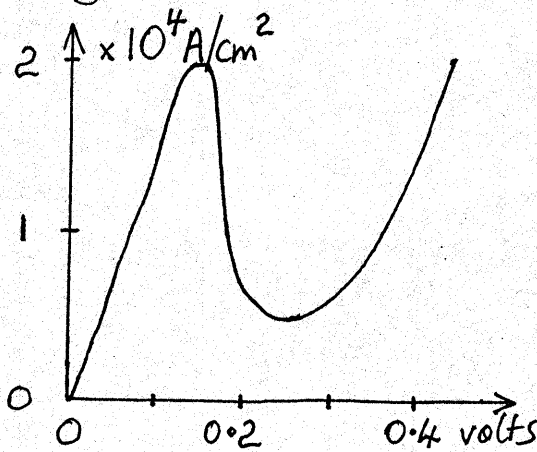
C — charge storage in contact regions



R_s — lead resistance, source resistance

5.7 CAPACITANCE

(a) Typical values



Device $10 \mu\text{m} \times 10 \mu\text{m}$ $I_p \sim 20 \text{ mA}$ $C \sim \frac{0.5 \times 10^5 \text{ S/cm}^2 \times 10^{-6} \text{ cm}^2}{2\pi \times 10^{10} \text{ rad/s}} \text{ at } 10^{10} \text{ Hz}$
 $\rightarrow 1 \text{ pF}$

Notes (1) RTD capacitance above $1 \rightarrow 2$ orders smaller than for similar I_p

"Esaki" tunnel diodes!

\therefore expect switching times $1 \rightarrow 2$ orders smaller
 ie. $< 100 \text{ ps}$

Check:

$$\tau_c = C \frac{dV_c}{dI_c}$$

$$\Delta t \sim C \frac{\Delta V}{I_c} \Rightarrow 10^{-12} \frac{0.2}{2 \times 10^{-2}}$$

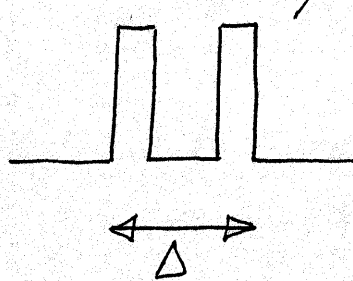
$\leftarrow \sim (I_p^+ - I_v)$ for $10 \mu\text{m}$ geometry

$= 10 \text{ ps}$

- (2) ωC above non-linear; C less at lower frequencies
- (3) C & I scale with area; speed independent of area.

(b) Calculation

(i) $C/\text{unit area} \sim \frac{\epsilon_r \epsilon_0}{\Delta} = C_p$



eg. Frensky, Appl Phys Lett
51 (6) 10 Aug 1987
pp 448-450

(ii) From depletion layer capacitances C_d
Standard semiconductor theory — requires
knowledge of semiconductor parameters,
materials used.

(c) "Quantum" capacitance

Hu & Stapleton Appl Phys Lett 58 (2) 1991 pp 167-169

Luryi Appl Phys Lett 59 (18) 1991 pp 2335-6

Charge exists in the potential well — Q_w

$$C_w = \frac{dQ_w}{dV}$$

$$C = C_d + C_w$$

5.8 Inductance

Electron "inertia"

High frequency semiconductor effects.

"Lead" inductance

- Self inductance
- Skin effect
- External inductance

RTD "Quantum Well" Inductance

Very little explanation or calculation in the research literature.

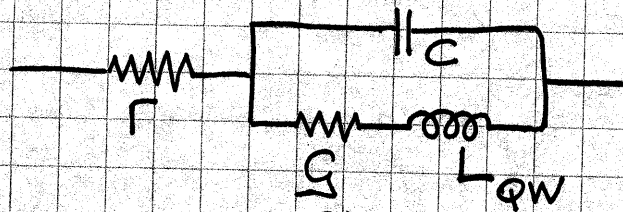
L_{QW} associated with changes in QW stored charge.

Apply voltage \rightarrow charge increases σ_w
 \rightarrow current increases $J = q\sigma_w/\tau_0$

$$\frac{dV}{dI} = g^{-1} \text{ and } dV = L \frac{dI}{dt} \rightarrow L_{QW} \frac{dI}{\tau_0}$$

$$\text{So } L_{QW} = \tau_0/g$$

RTD SMALL SIGNAL EQUIVALENT CIRCUIT



$$I = f(V)$$

$$G = dI/dV$$

$G < 0$ in NDR

$$z(f) = R + \left(j\omega C + \frac{1}{j\omega L + 1/G} \right)^{-1}$$

$$\Rightarrow \frac{[R(1 - \omega^2 LC) + j\omega C/G] + (j\omega L + 1/G)}{(1 - \omega^2 LC)^2 + \omega^2 C^2/G^2} [1 - \omega^2 LC - \frac{j\omega C}{G}]$$

Power consumed = $I^2 R(f) \rightarrow R(f) < 0$ implies gain

f_{MAX} defined as frequency where $R = 0$

$$\text{ie. } (1 - \omega^2 LC) [R(1 - \omega^2 LC) + 1/G] + \frac{\omega C}{G} (\omega L + \frac{\omega RC}{G}) = 0$$

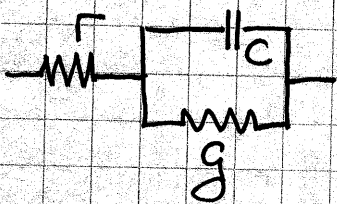
$$\Rightarrow \omega^4 - \omega^2 \left(\frac{2R}{LC} - \frac{1}{L^2 G^2} \right) + \frac{1}{L^2 C^2} \left(1 + \frac{R}{G} \right) = 0$$

$$\omega^2 = \frac{1}{2} \left\{ \frac{2R}{LC} - \frac{1}{L^2 G^2} \pm \left[\left(\frac{2R}{LC} - \frac{1}{L^2 G^2} \right)^2 - \frac{4}{L^2 C^2} \left(1 + \frac{R}{G} \right) \right]^{1/2} \right\}$$

$$= \left(\frac{1}{2L^2 C} \right) \left\{ \left(2L - \frac{C}{G^2} \right) + \left[\left(2L - \frac{C}{G^2} \right)^2 - 4L^2 \left(1 + \frac{R}{G} \right) \right]^{1/2} \right\}$$

$$\text{So } f_{max} = \frac{1}{2\pi} \left(\frac{1}{2L^2 C} \right)^{1/2} \left\{ \left(2L - \frac{C}{G^2} \right) + \left[\left(2L - \frac{C}{G^2} \right)^2 - 4L^2 \left(1 + \frac{R}{G} \right) \right]^{1/2} \right\}^{1/2}$$

If L_{QW} negligible: $z(f) = R + (G + j\omega C)^{-1} = \frac{[R + j\omega RC][G - j\omega C]}{G + \omega^2 C^2}$



$$R(f) = 0 \text{ when } G(1 + R/G) + \omega^2 RC^2 = 0$$

$$\text{ie. } f_{max} = \frac{1}{2\pi C} \left(\frac{|G|}{R} - |G|^2 \right)^{1/2} \text{ in the NDR}$$

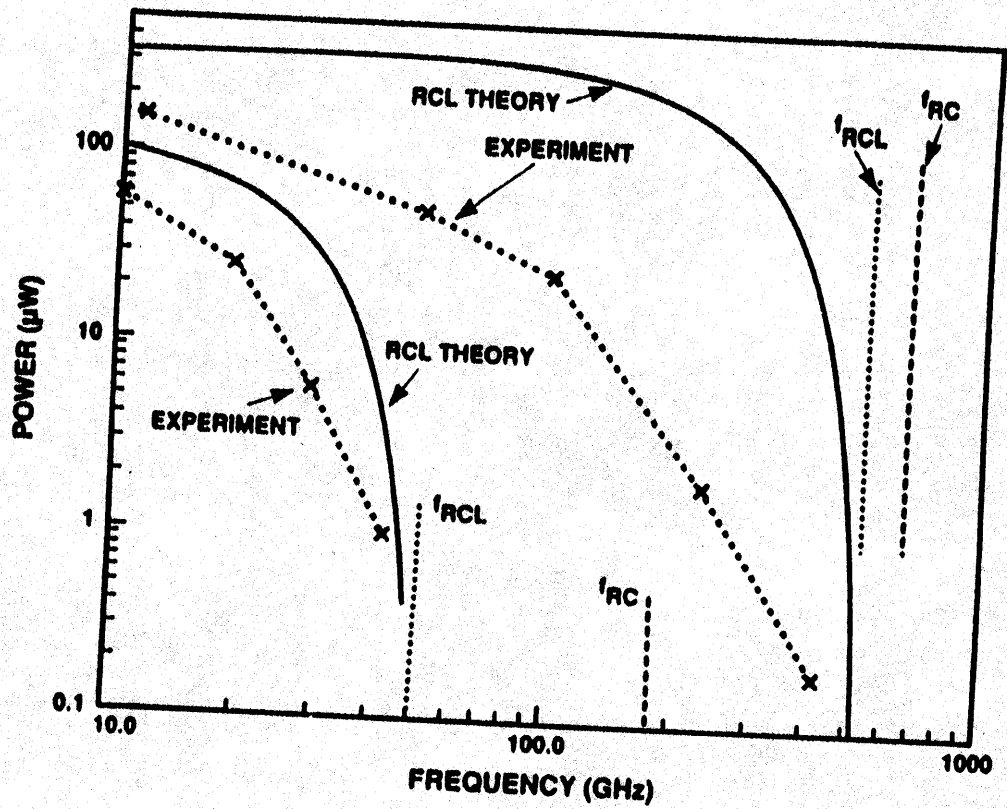
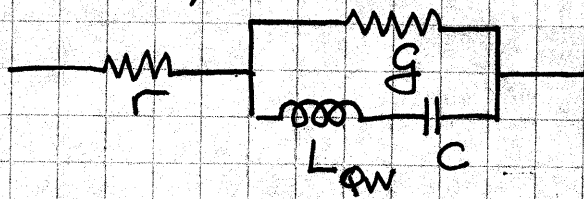


Figure 5.2 Output power as a function of frequency for two different double-barrier structures and their theoretical limits. The quantum well inductance is included in f_{RCL} but not in f_{RC} [3]. Reprinted with permission of MIT Lincoln Laboratory, Lexington, Massachusetts.

Another possible equivalent circuit:



L_{QW} represents charging of the QW

$$Z(f) = r + \left[g + \frac{1}{j\omega L + \frac{1}{j\omega C}} \right]^{-1}$$

$$= \frac{[(1 - \omega^2 LC)^2 (1 + rg)g + \omega^2 r C^2] - j\omega C [-\omega^2 LC]}{g^2 (1 - \omega^2 LC)^2 - \omega^2 C^2}$$

$$R \rightarrow 0 \quad (1 - \omega^2 LC)^2 (1 + rg)g + \omega^2 r C^2 = 0$$

$$\omega^4 - \omega^2 \left[\frac{2}{LC} - \frac{1}{L^2} \frac{r}{g(1+rg)} \right] + \frac{1}{L^2 C^2} = 0$$

Gives

$$f_{\max} = \frac{1}{2\pi} \left(\frac{1}{L^2 C} \right)^{1/2} \left\{ \left(2L - \frac{C}{g(g+r-1)} \right) + \left[\left(2L - \frac{C}{g(g+r-1)} \right)^2 - 4L^2 \right]^{1/2} \right\}^{1/2}$$

which is similar in form to the previous result but not the same.

Question: Where should L_{QW} go in the equiv. ckt.?

Must be consistent with physical interpretation.

5.5 Tunneling time

$$t_T = \frac{s}{\sqrt{2q(V_0 - E)/m}} \quad \text{ie. } \frac{\text{distance}}{\text{velocity}}$$

\uparrow
 $2 \times \text{KE} / \text{mass}$

Carrier lifetime in the well

$$\tau_{esc} = \frac{\hbar}{E} e^{+\frac{4\pi}{\hbar} \sqrt{2mq(V_0 - E)} \cdot s}$$

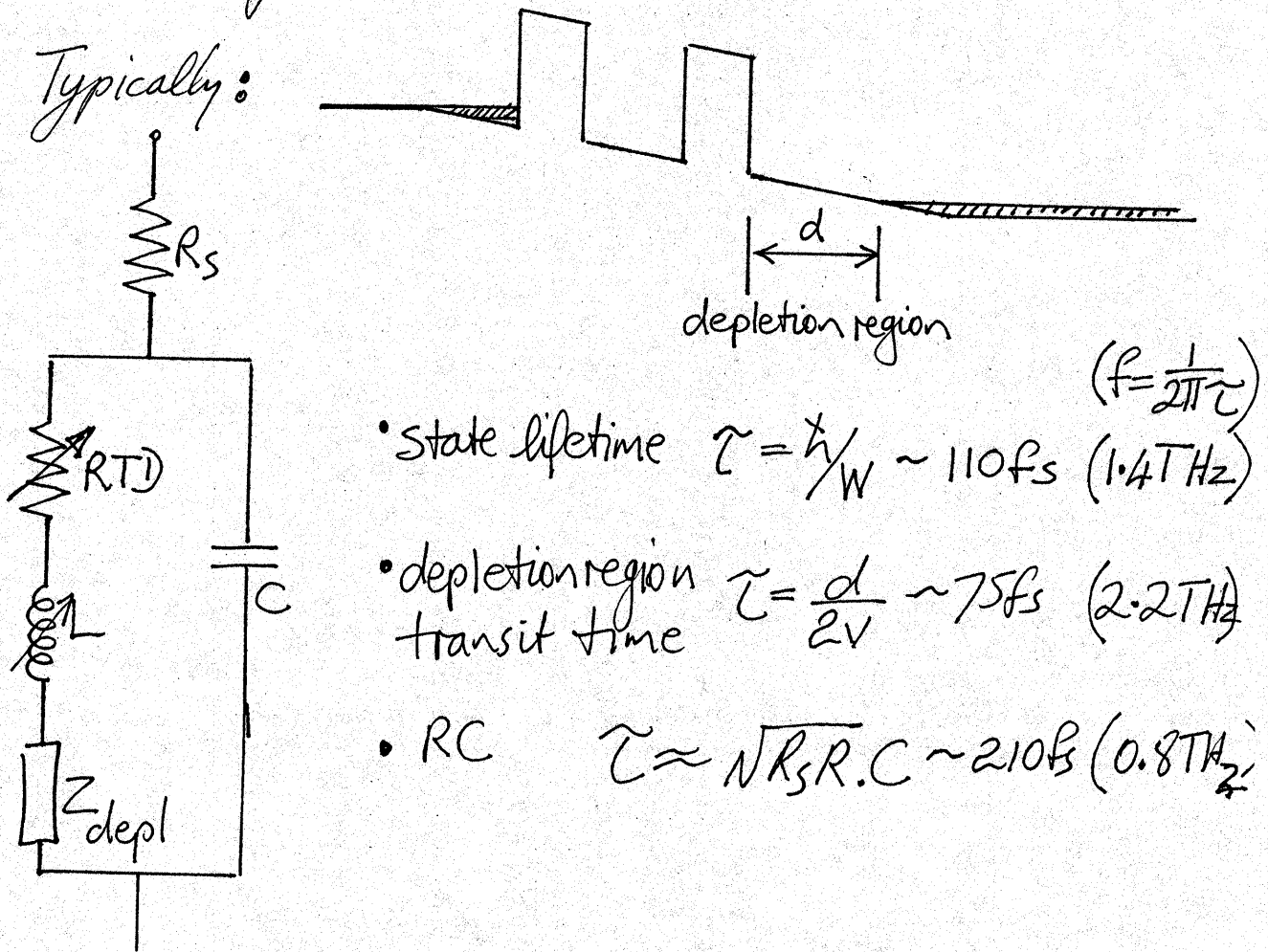
$$= \frac{mW^2}{\pi \hbar} e^{+\frac{4\pi}{\hbar} \sqrt{2mq(V_0 - E)} \cdot s}$$

(using $E \approx \frac{\hbar^2 k^2}{2ma^2}$)

& need $t_T \ll \tau_{esc}$

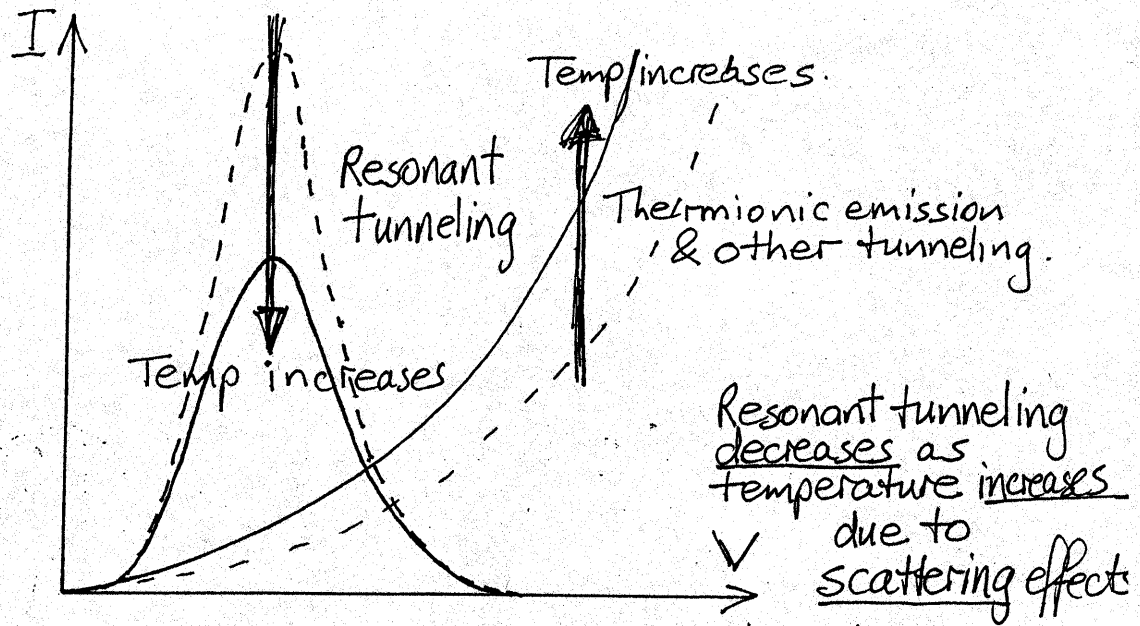
ie. tunneling time does not limit device response

Typically:



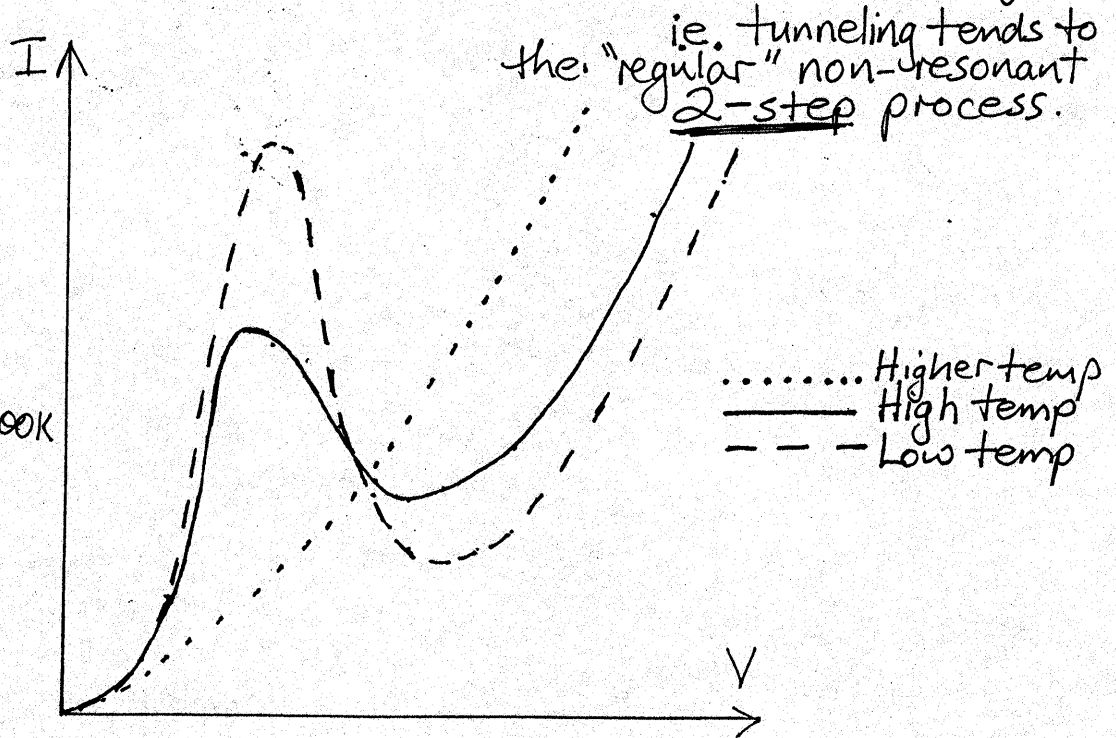
- state lifetime $\tau = \hbar/W \sim 110 \text{ fs}$ ($f = \frac{1}{2\pi\tau}$) (1.4 THz)
- depletion region transit time $\tau = \frac{d}{2v} \sim 75 \text{ fs}$ (2.2 THz)
- RC $\tau \approx \sqrt{R_s R} \cdot C \sim 210 \text{ fs}$ (0.8 THz)

5.9 TEMPERATURE



For example:-

- Room temp 300K
- LN2 77K
- Liq. He ~4K



Temperature increases :-
 peak/valley ratio decreases &
 eventually resonant tunneling disappears.

Applications: Room temperature or cooling required??

6. RTD Implications

Tunnel diodes were the fastest devices in mid-1960's.
Why weren't they more successful?

TD switching speed $\sim 1\text{ns}$
RTD switching speed $\sim 0.2\text{ps}$ } limited by device capacitance

6.1 Physical dimensions

In 1ns , signal travels $\sim 10^8\text{m/s} \times 10^{-9}\text{s} \approx 10\text{cm}$
 \therefore Devices must be closer than 10cm to take advantage of speed. If computer transmission lines up to 1m , cycle time limited to $\sim 10\text{ns}$ & no advantage to faster devices.

For RTD's - fabricate on monolithic substrates, but need dimensions (max line length)
 $\leq 0.2 \times 10^{-12} \times 10^8 \approx 20\mu\text{m}$.

So probably can't use full speed, but still faster than competitors if run slower.

6.2 Isolation

Two-terminal devices; same terminal is input & output; risk of retriggering by reflected output pulse.

Need 3-terminal isolation device, which then determines system speed.

(Note possible resonant 3-terminal devices)

6.3 Stray inductance

Radiotron Handbook: straight wire inductance

$$L (\mu\text{H}) \approx 5 \times 10^{-3} \ell (\text{in}) 2.3 \log_{10} \left[4 \frac{\ell}{d} - 0.75 \right]$$

Say 10 μm long, 0.5 μm diameter

$$L \sim 5 \times 10^{-3} \frac{10^{-3}}{2.5} 2.3 \log_{10}(80) \mu\text{H}$$
$$\sim 10 \text{ pH}$$

If device switches 5mA in 0.2ps

$$V_L \sim 10 \times 10^{-12} \frac{5 \times 10^{-3}}{0.2 \times 10^{-12}} = 0.25 \text{ volts}$$

Compare RTD device voltages ~ 0.5 volts

\therefore Expect problems with stray inductances.

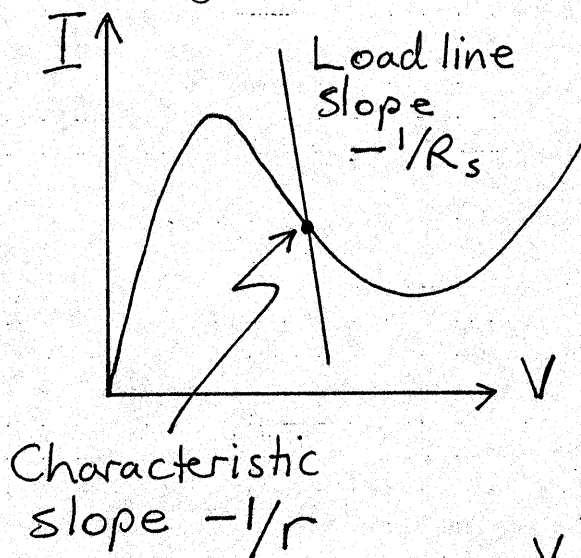
(Compare TD, $V_L \sim 20 \times 10^{-9} \frac{5 \times 10^{-3}}{10^{-9}} = 0.1$ volt,

ECE 417/517
NANOELECTRONICS
Spring 2007

Lecture 5:
TD & RTD Circuits

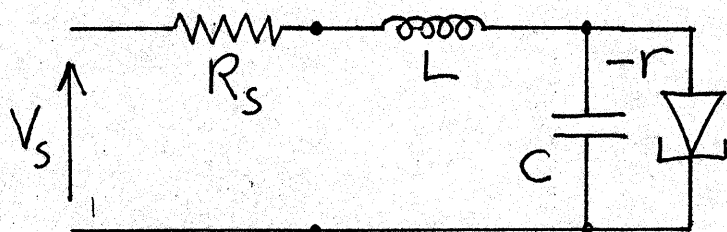
- Oscillators & amplifiers
- Curve tracing
- Modeling
- Switching waveforms
- Multivibrators
- Logic
- Counters
- Pulse generators

2.1 Negative Resistance Oscillators



Bias in negative resistance region.

$$R_s < |r|$$



$$Z_{IN} = R_s + j\omega L + \frac{(-r)(j\omega C)^{-1}}{-r + (j\omega C)^{-1}}$$

$$\Rightarrow R_s - \frac{r}{1 + \omega^2(rC)^2} + j\omega \left[L - \frac{r^2 C}{1 + \omega^2(rC)^2} \right]$$

$$= a + jb$$

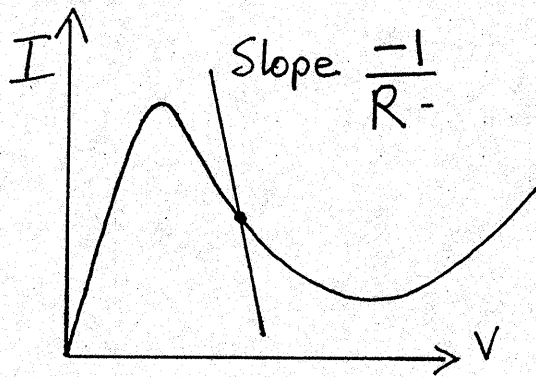
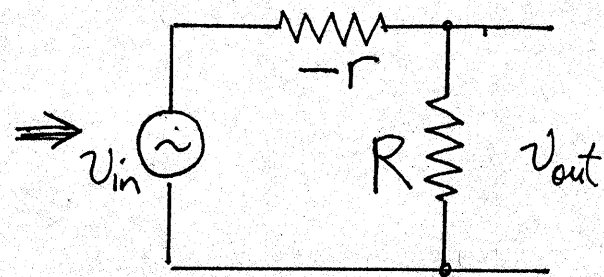
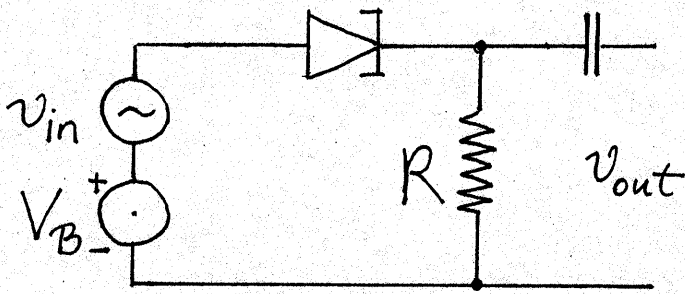
Spontaneous oscillations if $b=0$, $a < 0$

ie. oscillates at $\omega^2 = \frac{1}{LC} \left[1 - \frac{L}{r} \cdot \frac{1}{rC} \right]$

if $r > R_s (1 + (\omega r C)^2)$

\rightarrow if $r > R_s \frac{r^2 C}{L}$ ie. $R_s < \frac{L}{rC}$

2.2. Tunnel diode amplifier



$$\text{Gain} = \frac{R}{R-r} > 0$$

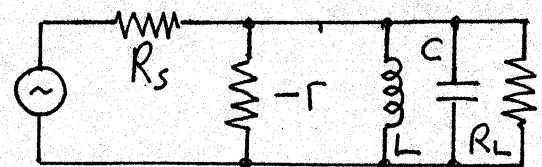
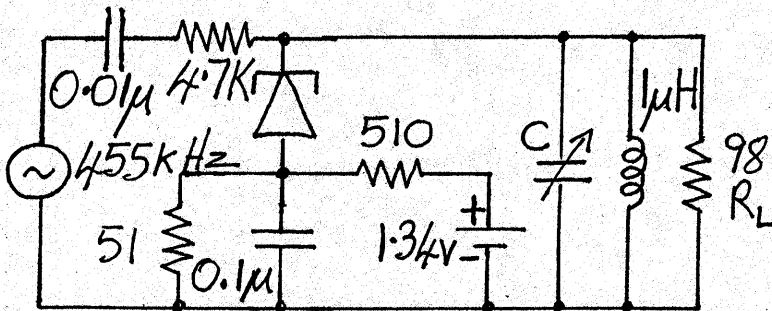
$$\text{Max voltage swing} = V_v - V_p$$

$$\text{Max current swing} = I_p - I_v$$

$$\therefore \text{Max power } P_{\text{max}} = \frac{(V_v - V_p)(I_p - I_v)}{8}$$

Stray l_s can cause parasitic oscillations,
need $l_s < rRC$

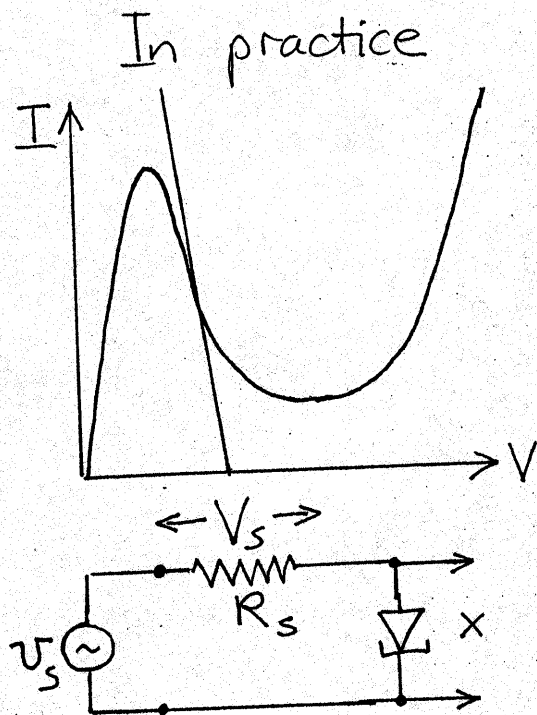
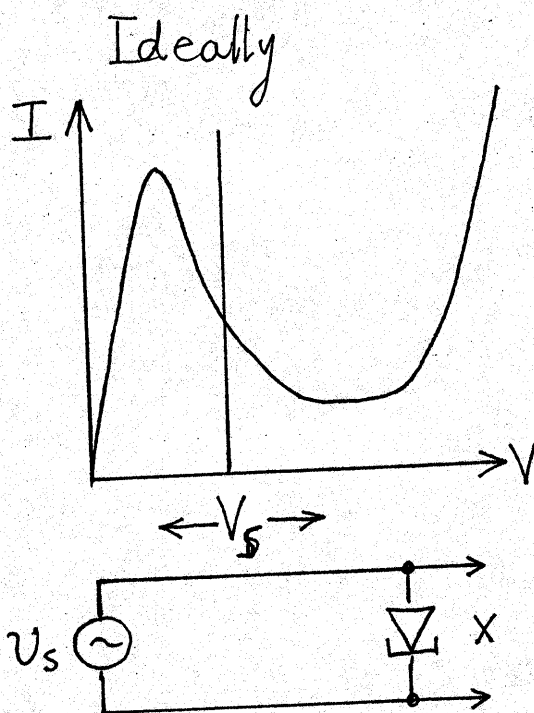
e.g. tuned amplifier



$$\text{At } \omega_0 = 1/\sqrt{LC}$$

$$A = \frac{R_L}{R_L + R_s} \cdot \frac{1}{1 - \frac{(R_s // R_L)}{r}}$$

2.3 Curve tracing



Requires $R_s < |r|$

Usual practical problem is oscillation due to stray inductance

Need $l_s < rR_s$ i.e. $\frac{l_s}{rC} < R_s < r$

This condition cannot be met if l_s too high

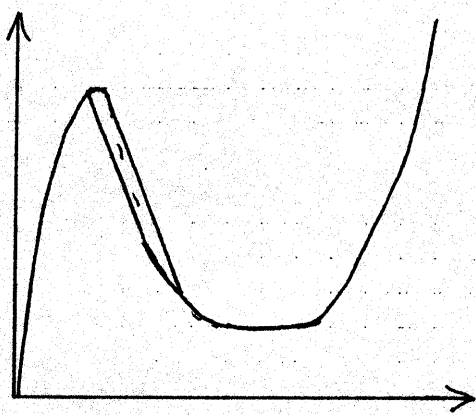
Check order of magnitude: say $r \sim \frac{50\text{mV}}{10\text{mA}} = 5\Omega$

& $C_j \approx 20\text{pF}$, Use max value of R_s , say 5Ω OK

Then $l_s < 5^2 \times 20 \times 10^{-12} = 1\text{nH} !!!$

Need short leads (typically $\sim 25\text{nH/inch}$) but usually intrinsic resistor inductance greater than the limit. Need low inductance mounts, carbon disc resistors, etc

2.4. Typical curve tracing problems



R_s too big
 $R_s > r$

$$(l_s/rC < r < R_s)$$

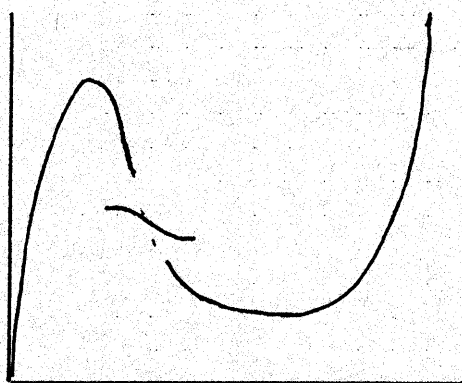


$R_s < r$
but

l_s too big

$$l_s > rR_sC$$

$$(R_s < l_s/rC < r)$$



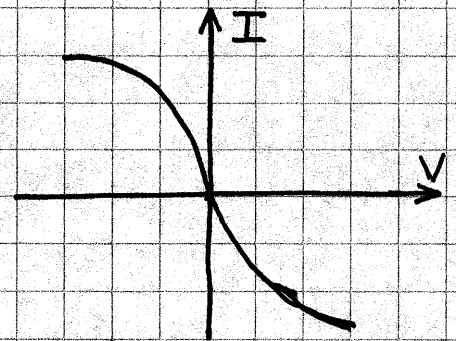
l_s too big

$$l_s > r^2C$$

$$(R_s < r < l_s/rC)$$



For bias at or near the saddle point



Shift origin

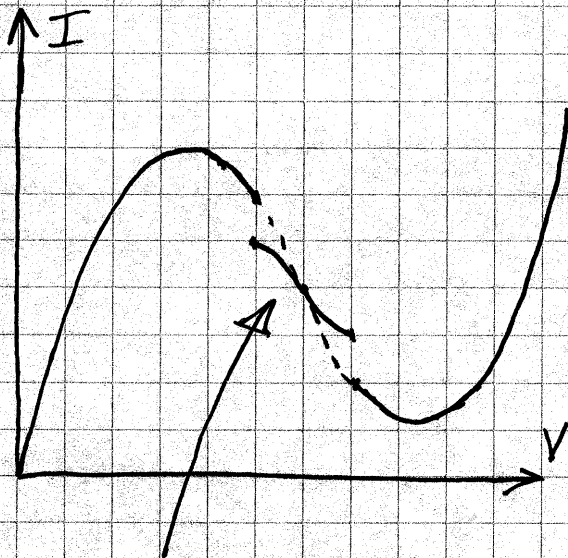
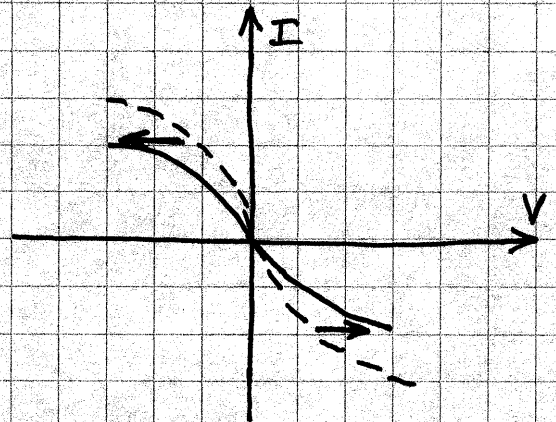
$$V = -\lambda I^3$$

For oscillation $i = A \cos \omega t$

$$\text{then } v = -\lambda (A \cos \omega t)^3$$

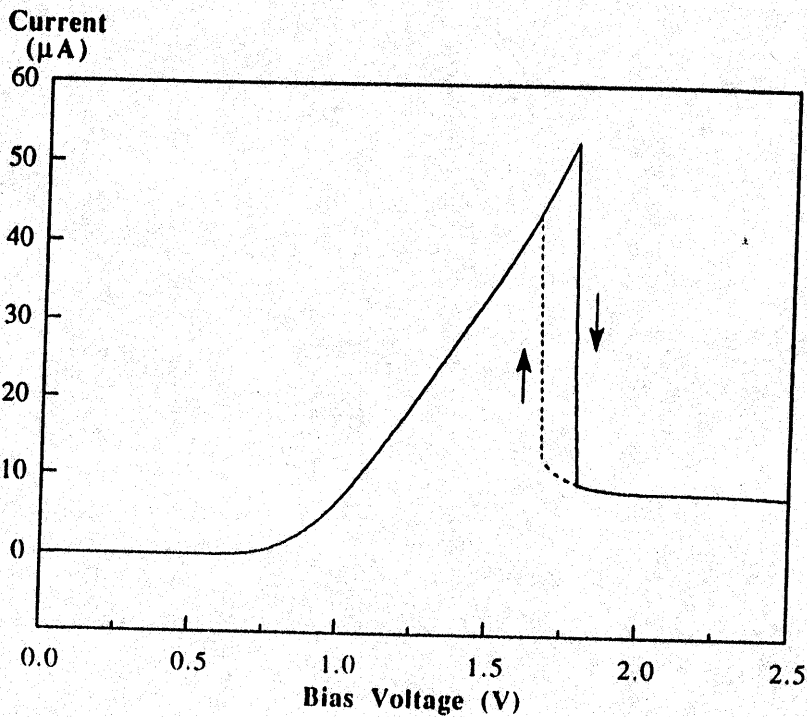
$$= -\frac{\lambda A^3}{4} (1 + 2 \cos \omega t + \cos 3\omega t)$$

ie. dc shift $-\lambda A^3/4$



DC shift over oscillation region
 ("Rectification" of self oscillation by non-linear characteristic)

(a)



(b)

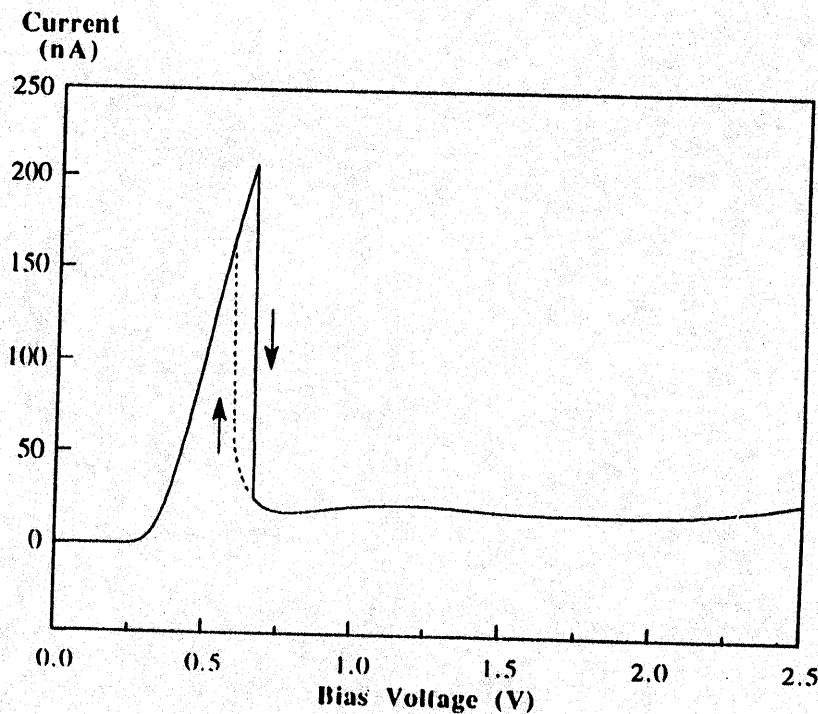


Figure 4.15 I - V characteristics for (a) Material 2 and (b) Material 3 at 4.2 K. The bias voltage was swept in both directions to show the hysteresis - the solid lines are for increasing voltage and the dashed line for decreasing voltage. Where the lines overlay, only the solid curve is shown. After Goodings *et al.* [16], with permission.

RTD
Intrinsic
Bistability
 ???

Sheet electron density in well

$$\sigma_w = \frac{J \cdot \tau_0}{q}$$

Argument claims possibility of 2 stable states at single voltage:

High current at large σ_w
 Low current at low σ_w

due to charge induced energy shifts.

But there ARE examples of single-plot characteristics in the literature.

Intrinsic bistability?

116

Fs dynamics and non-equilibrium distribution

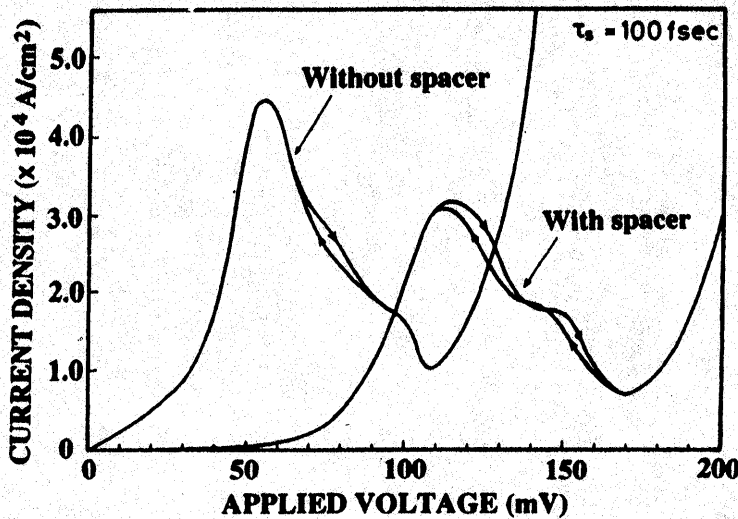


Figure 4.16 I - V characteristics calculated for RTDs with and without spacer layers. The applied bias is decreased after it reaches a maximum in order to see hysteresis. Bistability observed in the negative differential conductance region arises from dynamic electron redistribution in the quantum well.

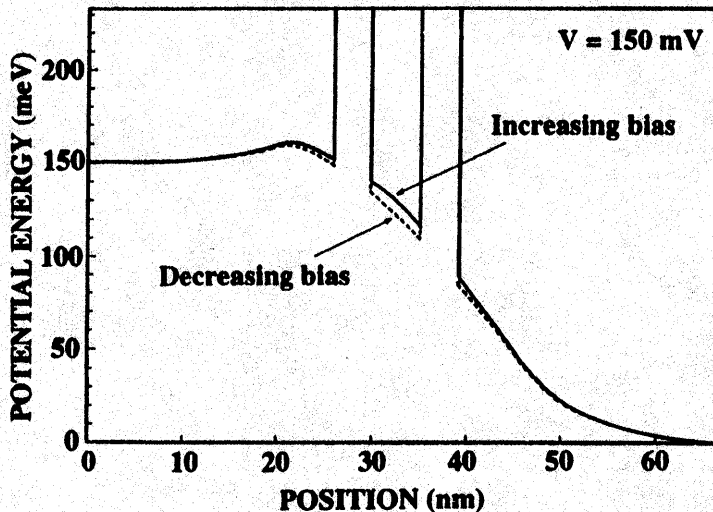
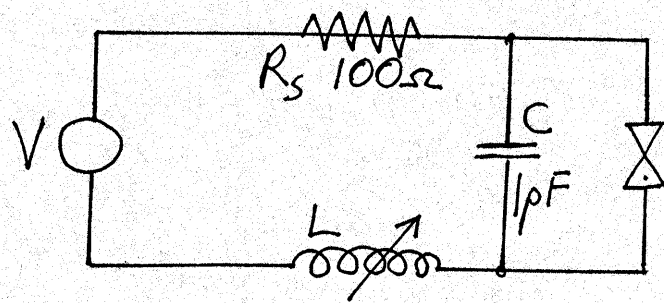
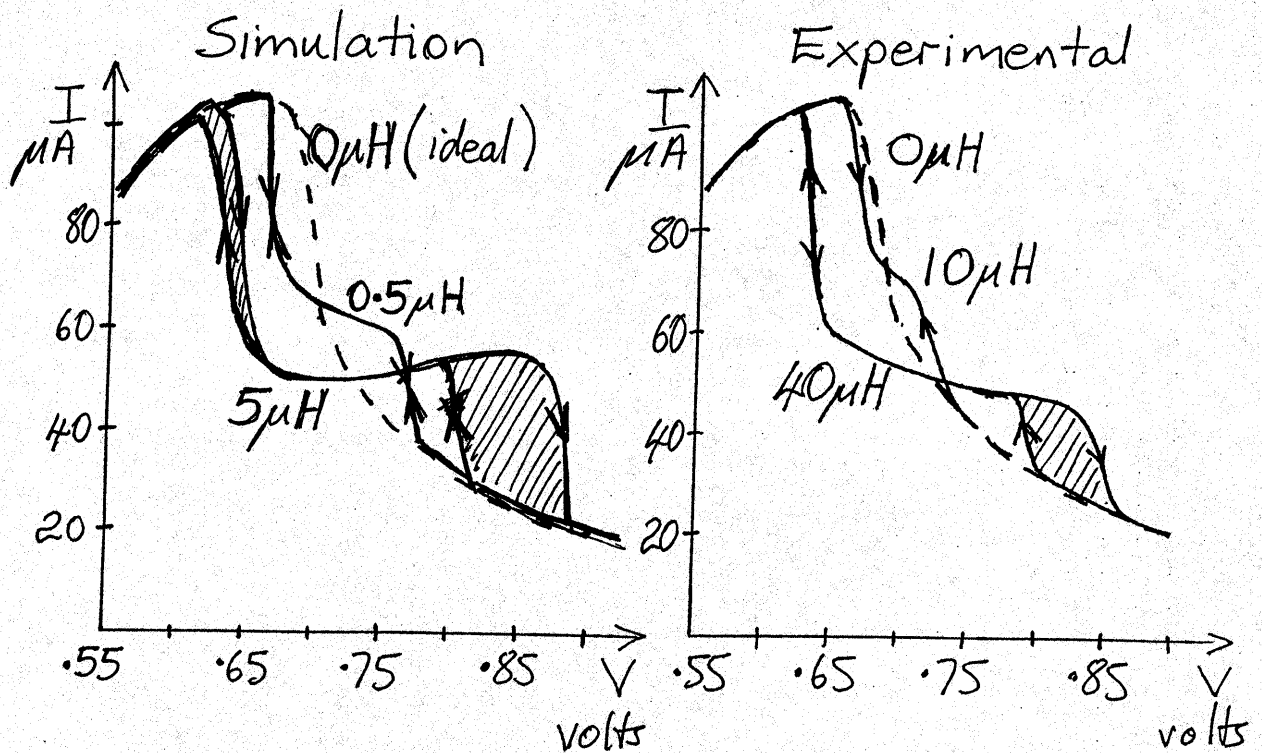


Figure 4.17 Self-consistent energy-band diagrams calculated at two stable states under an applied bias of 0.15 V. The upper curve corresponds to the larger current state, and the lower curve to the smaller current state.

"Spacer" layers: undoped regions in emitter/collector adjacent to barriers.

2.5. Belhadj et al (Potter)
 Appl. Phys. Lett. 57 (1) 2 July 1990 pp. 58-60

→ RTD negative resistance region curve tracing:
 inductive effects



Negative resistance
 r
 $\approx 3.11\text{K}\Omega$
 $= \frac{V_V - V_P}{I_P - I_V}$

3.1. Characteristics Modelling

(a) Physical equations

$$\text{e.g. } I_j = \frac{I_p}{4} \frac{V_j}{V_p} \left(3 - \frac{V_j}{V_p}\right)^2$$

But — this is already an approximation
— also does not include: diode forward current
or "excess" current

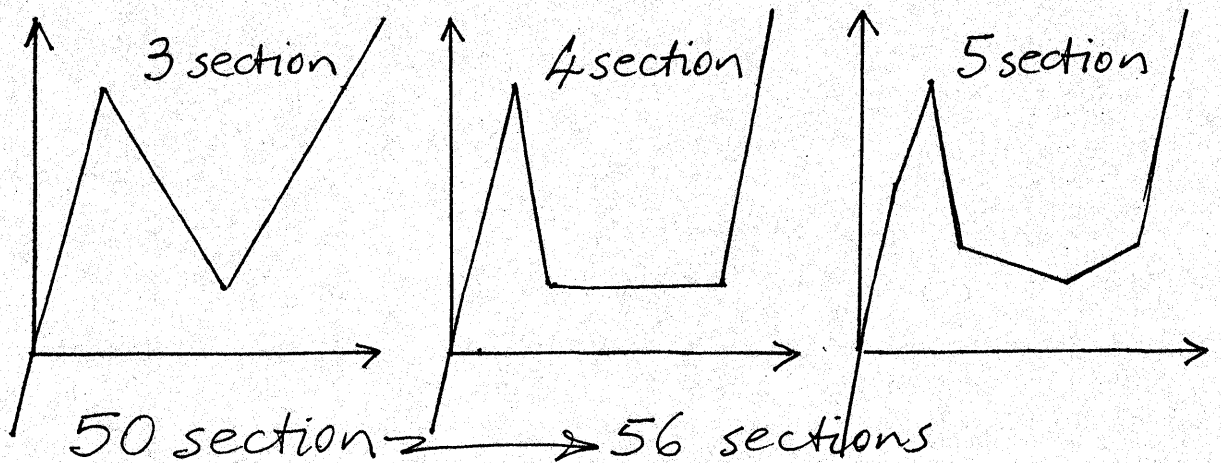
(b) Empirical equations for better fit

$$\text{e.g. } I_j = A \frac{V_j}{V_p} \exp -a \frac{V_j}{V_p}$$

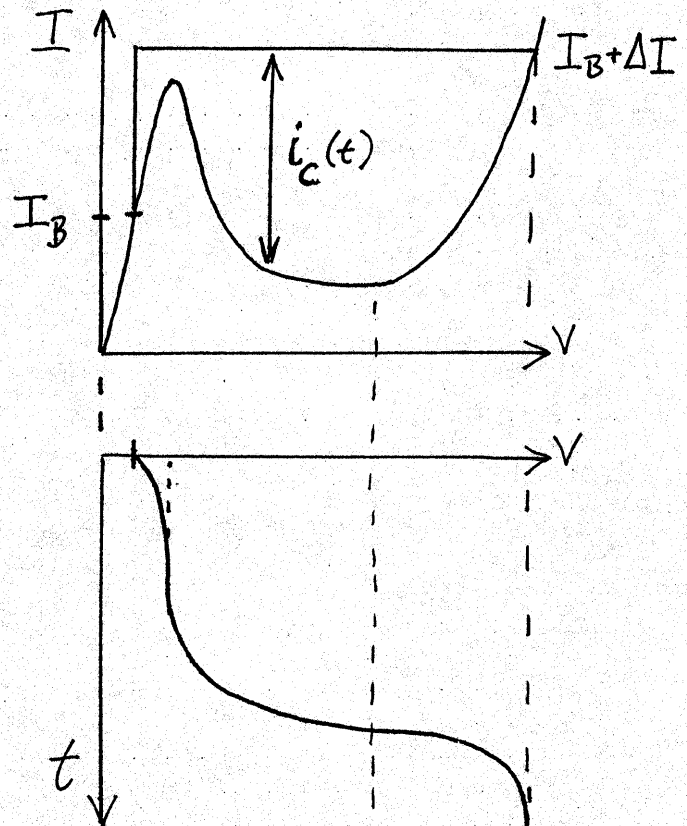
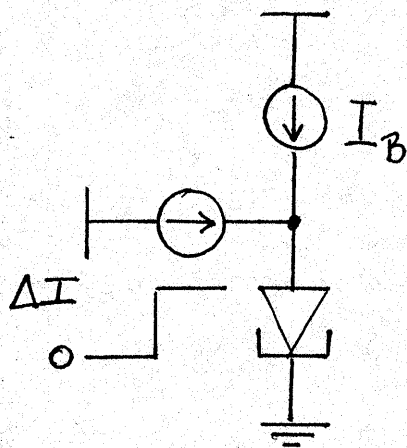
(c) Polynomial approximations (SPICE)

Curve fit — 5% accuracy needs 7 terms
 $i = a_0 + a_1 v + a_2 v^2 + \dots$ 2% accuracy needs 9 terms

(d) Linear piecewise (PSPICE)



3.2 Basic Switching Waveform



$$I_B + \Delta I = I_j(t) + i_c(t)$$

$$i_c(t) = C \frac{dV_j(t)}{dt}$$

Estimate switching time:

$$I_c \sim I_p - I_v \sim 5 \text{ mA}$$

$$C_j \sim 20 \text{ pF} \quad \Delta V \sim 400 \text{ mV}$$

$$\therefore \Delta t \approx \frac{C \Delta V}{I_c} = \frac{20 \times 10^{-12} \times 400 \times 10^{-3}}{5 \times 10^{-3}} \sim 1.6 \text{ ns}$$

Significant delay time

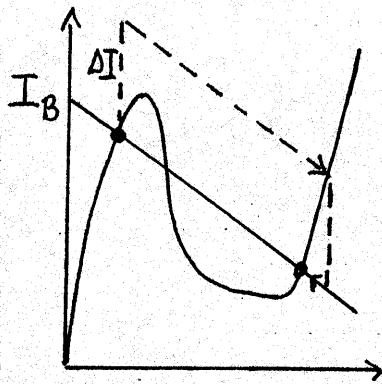
Compare accuracy of calculated switching waveforms with experiment. Agreement poor with 3, 4, 5, AND "regular" 50-section linear piecewise models.

Problem: accuracy most sensitive to delay — need accuracy where i_c smallest, i.e. at the peak.

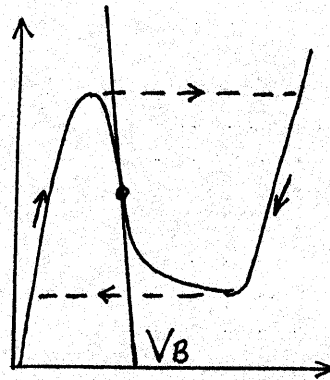
\therefore Add peak detail \rightarrow 56-sections.

Polynomials: curve fitting \rightarrow use more points at peak.

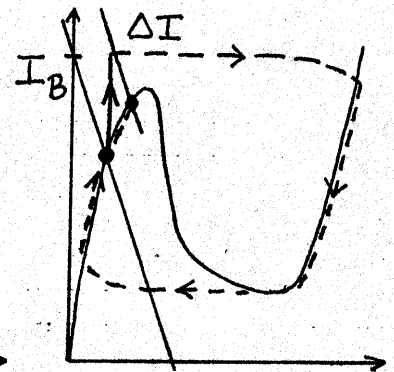
4.1 Basic Multivibrators



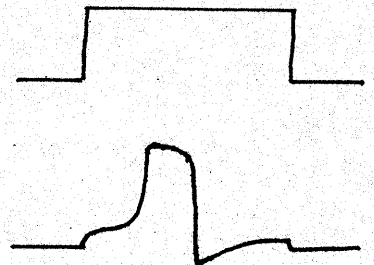
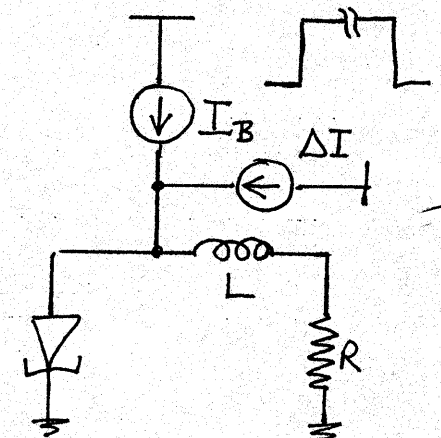
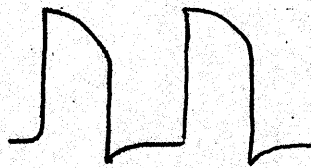
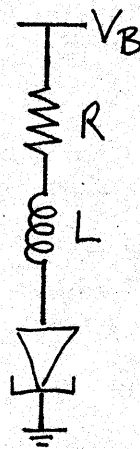
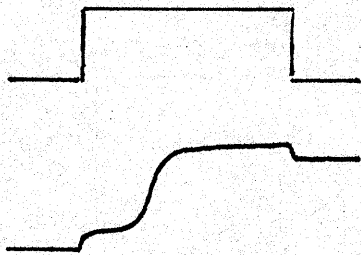
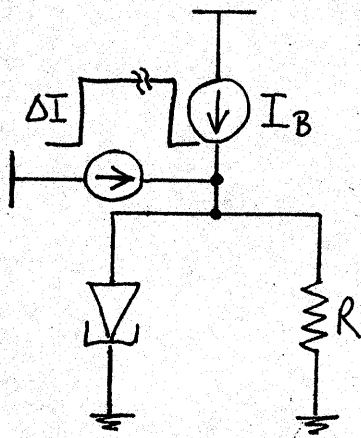
Bistable



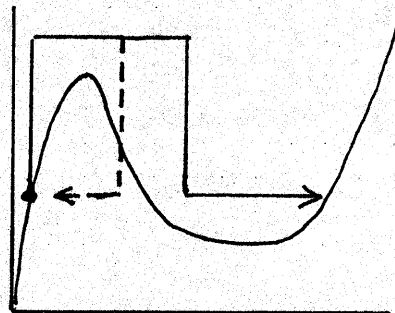
Astable



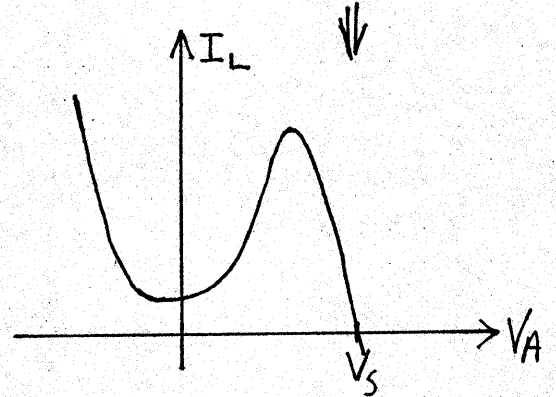
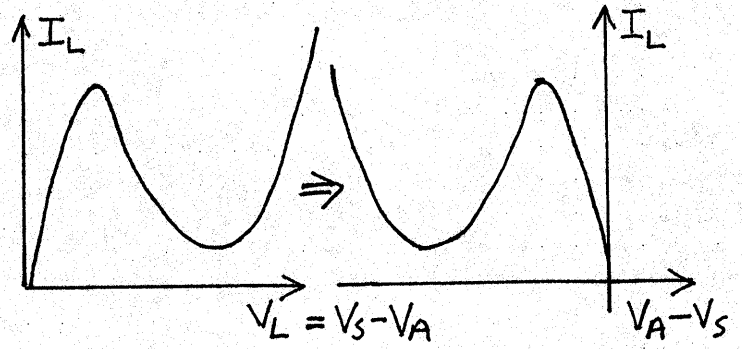
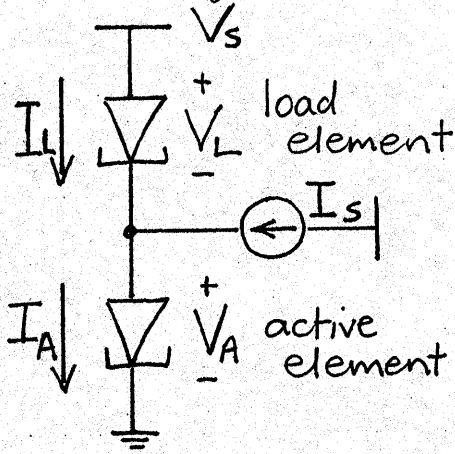
Monostable



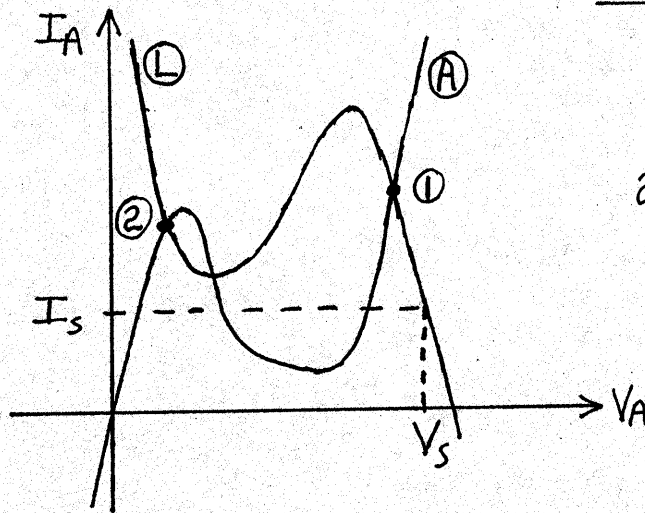
Note pulse width dependence



H.2 Goto Pair — load line example



and $I_A = I_L + I_s$



2 stable intersections
— complementary bistable

If I_s increases above level shown → forced to state ①
 V_A high, V_L low

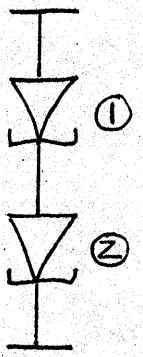
If I_s large & negative → forced to state ②
 V_A low, V_L high

RTD → known as the "MOBILE" circuit

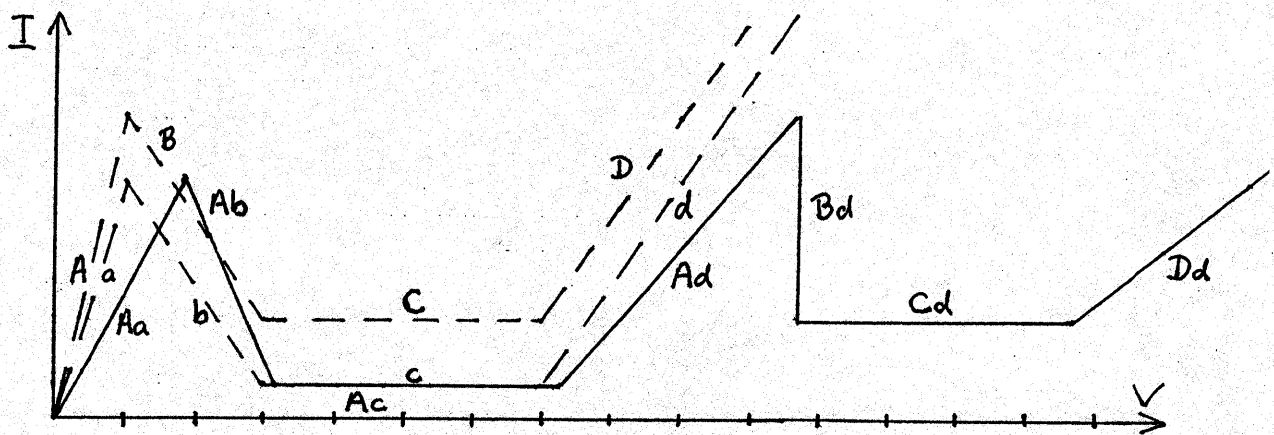
4.3 Series connected tunnel diodes —

* the tunnel diode scaler/counter

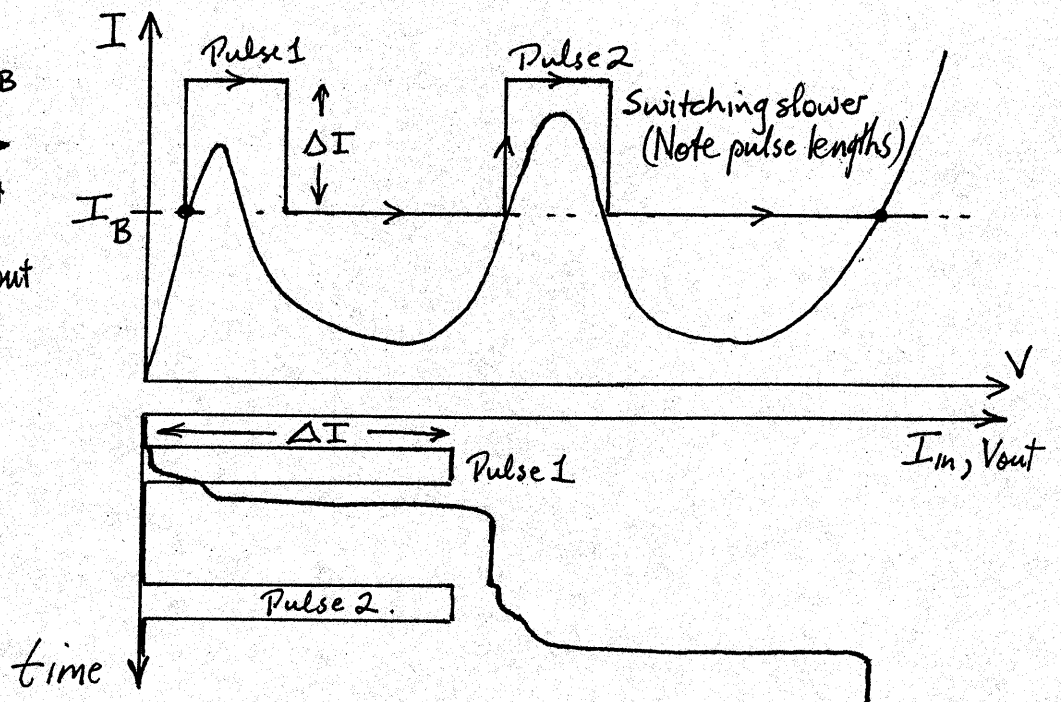
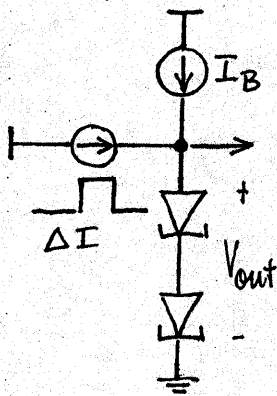
* example of composite characteristics



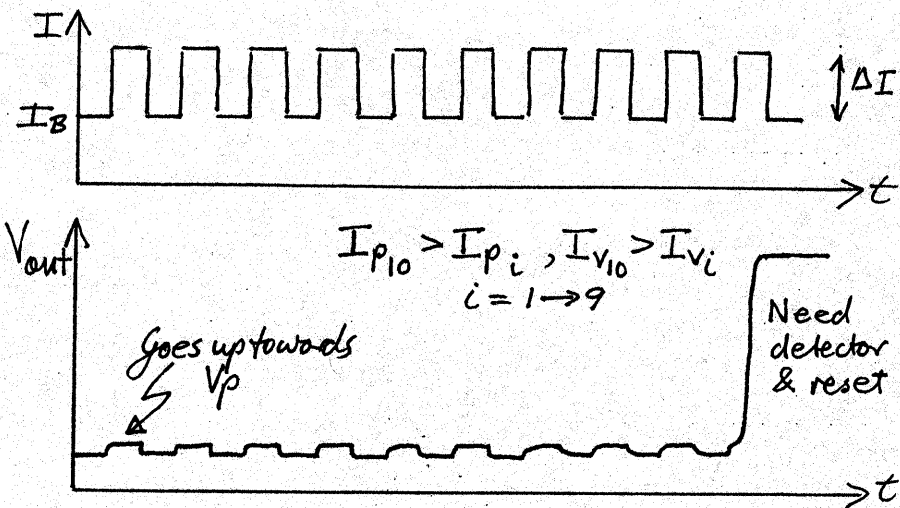
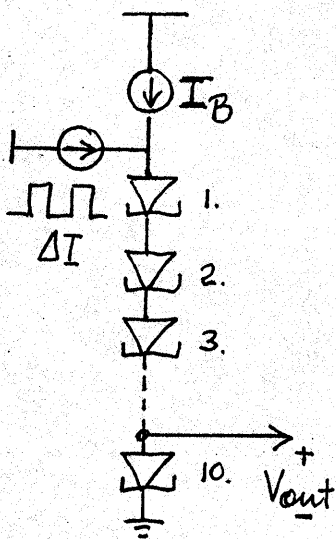
(a) the "regular" case — $I_{p1} < I_{p2}$
& $I_{v1} < I_{v2}$



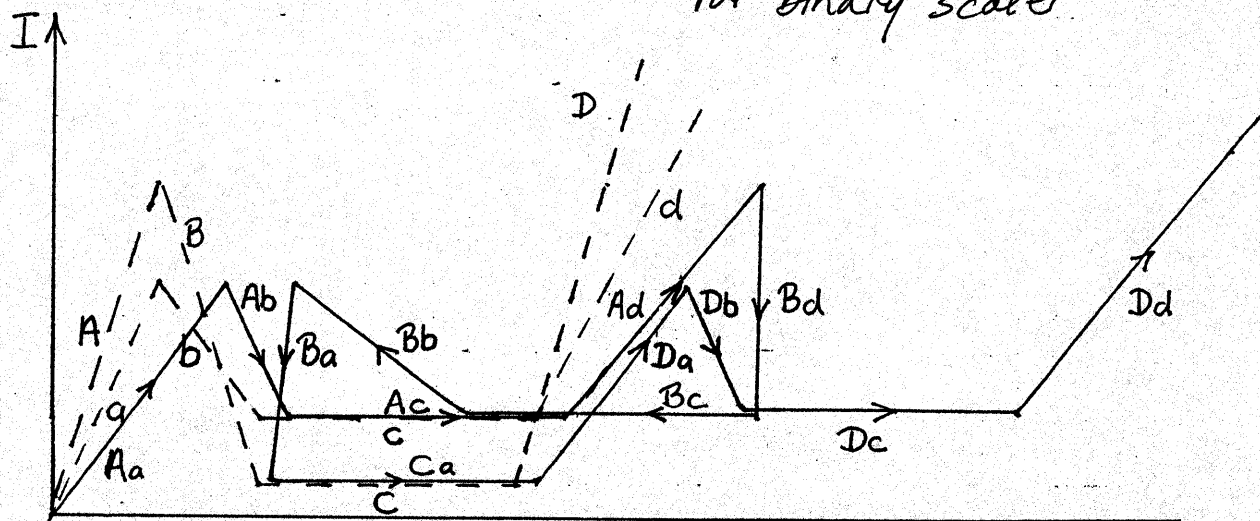
Application:



Multiple t.d. chains eg. decade scaler



(b) "Irregular" case: consider $I_{P1} < I_{P2}, I_{V1} > I_{V2}$ for binary scaler.



Note appearance of multiple peaks

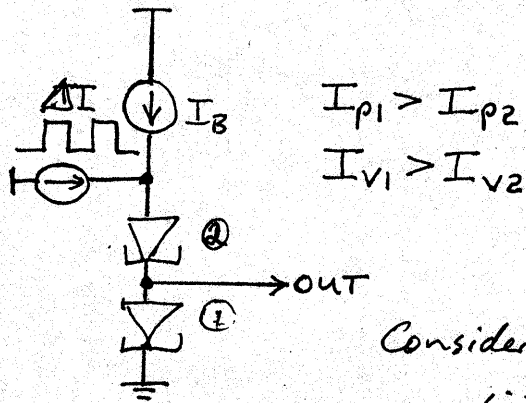
In general, for n series connected t.d.'s get:

1 regular case

$(n-1)$ irregular cases

& the "most" irregular case will have $2^n - 1$ peaks

(c) "Regular" case revisited.



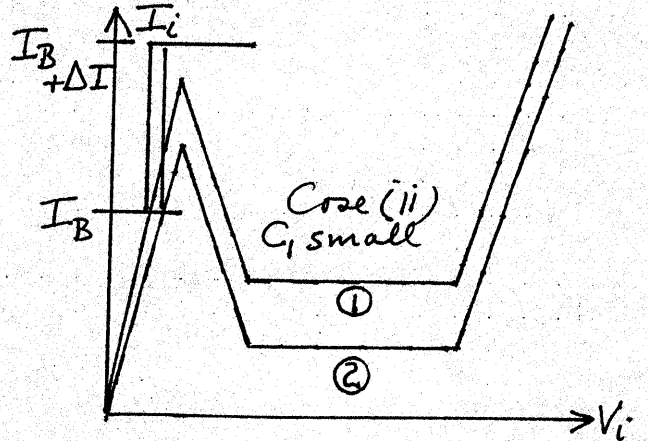
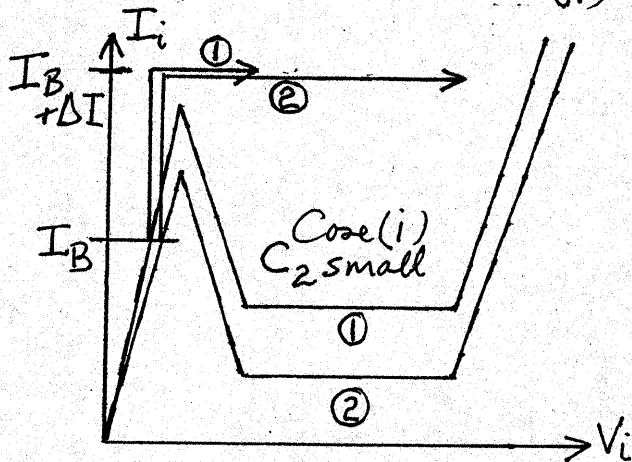
$$I_{p1} > I_{p2}$$

$$I_{v1} > I_{v2}$$

Note: Composite characteristic is plotted quasi-statically
 — actual circuit responses are dynamic.

Consider cases

- (i) $C_1 > C_2$
- (ii) $C_1 < C_2$



Bias current flows through both diodes
 Trigger current flows through both diodes.

For correct operation, need TD #1 to switch last.

$$\frac{dV_i}{dt} = \frac{I_B + \Delta I - I}{C_i}$$

Case (i) C_2 small & $I_B + \Delta I - I_2 > I_B + \Delta I - I_1$
 $\therefore dV_2/dt > dV_1/dt$ & operation correct.

Case (ii) C_1 small $\therefore dV_1/dt$ MAY be $> dV_2/dt$ & get output on first pulse

Need

$$I_{p1} > I_{p2} > I_{p3} > \dots > I_{pn}$$

$$I_{v1} > I_{v2} > I_{v3} > \dots > I_{vn}$$

$$\& C_1 > C_2 > C_3 > \dots > C_n$$

↑
* last t.d. to switch

* Use for detection

* Others can be any sequence.

Discrete devices (eg. t.d.'s)

Must test each device to ensure I_p, I_v, C conditions met — not practical for mass production.

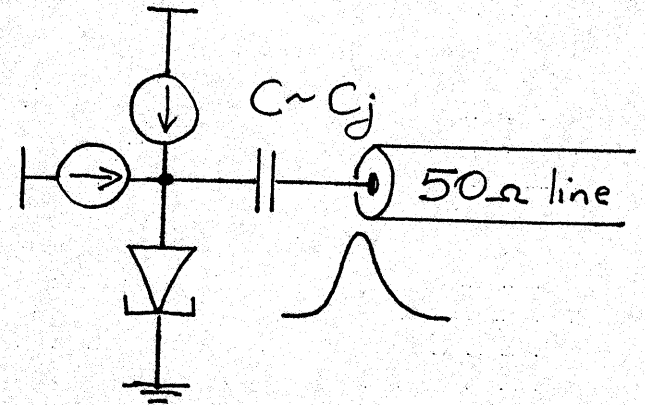
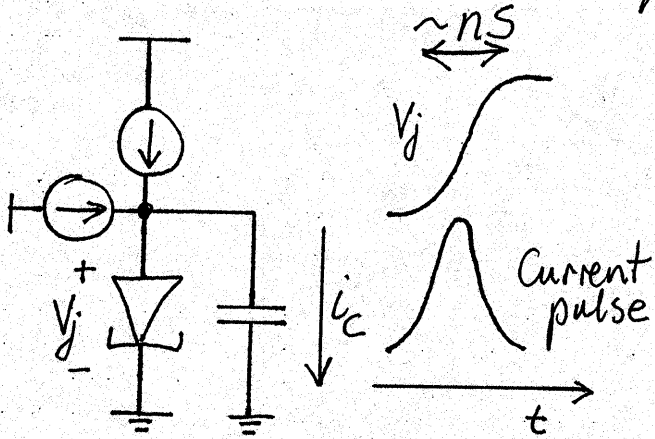
Monolithic devices (eg. RTDs)

If characteristics approx. uniform, can force I_p, I_v & C sequences correct by scaling areas

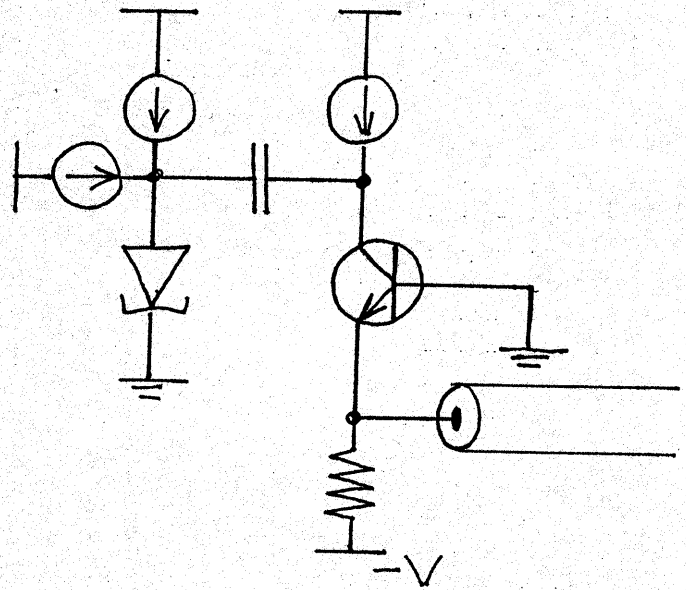
ie. I_p, I_v & C / unit area constant

then $A_1 > A_2 > A_3 > \dots > A_n$.

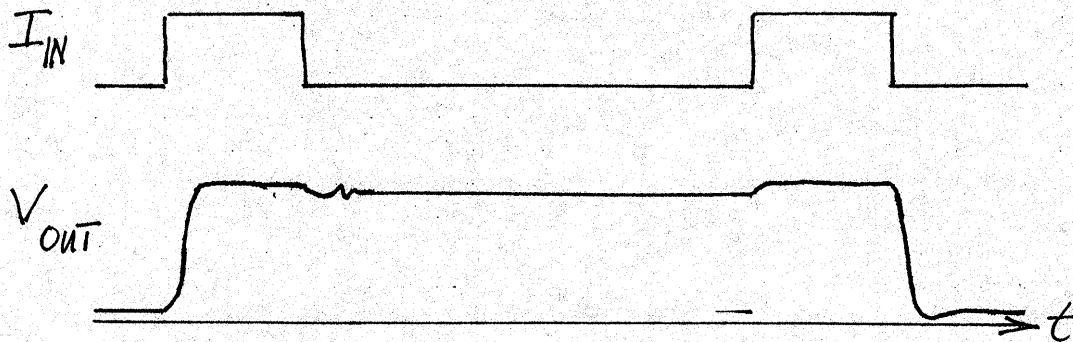
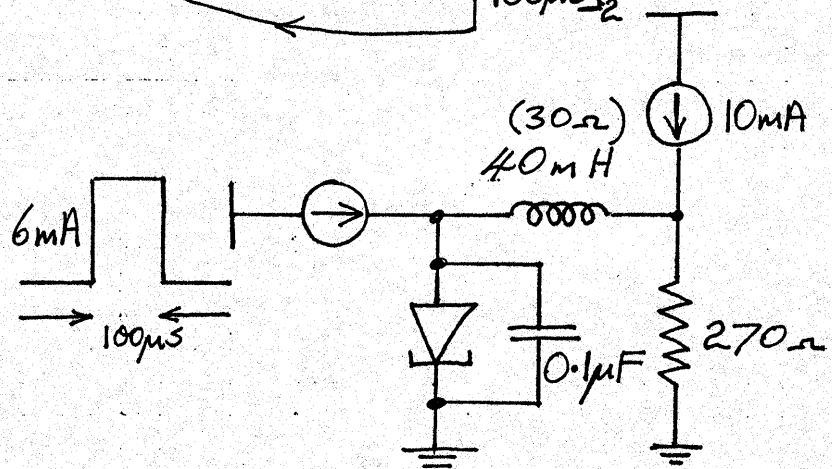
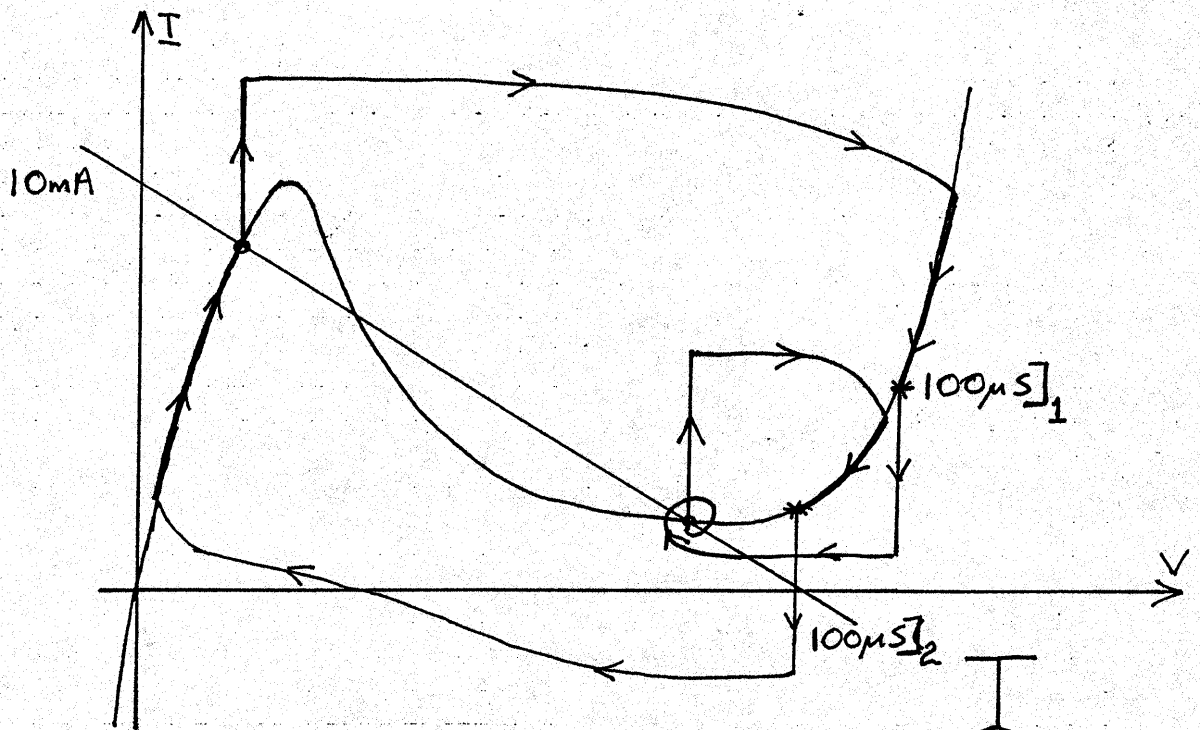
H.4 Tunnel diode pulse generator



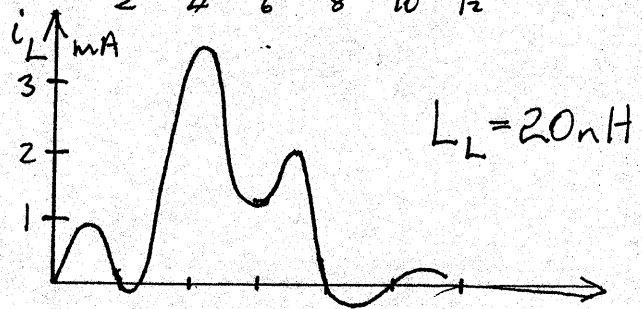
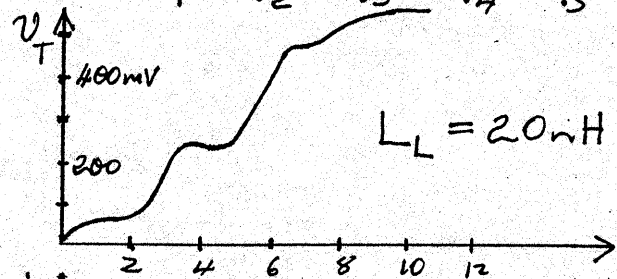
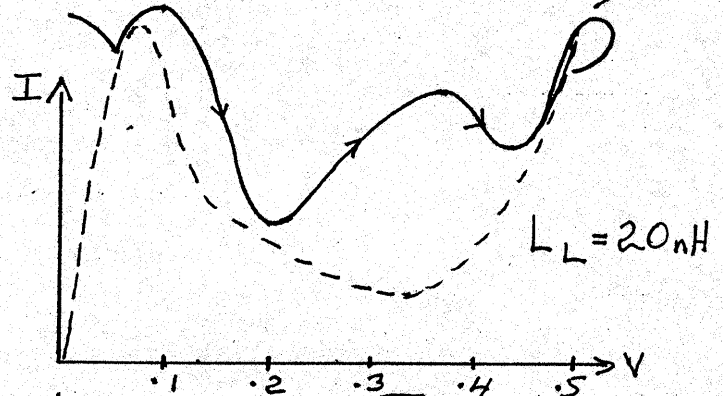
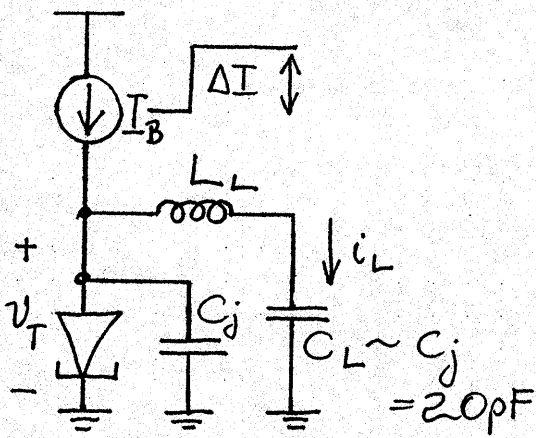
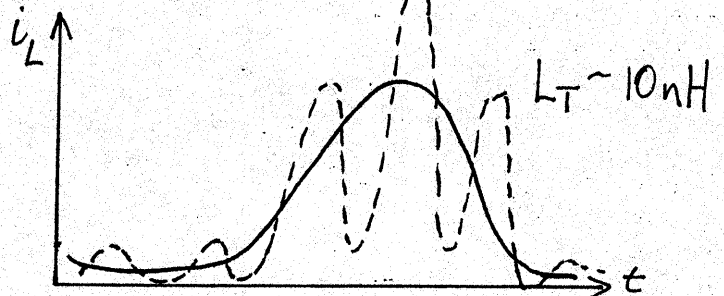
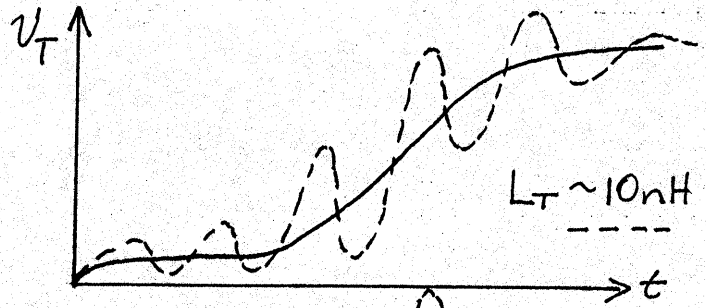
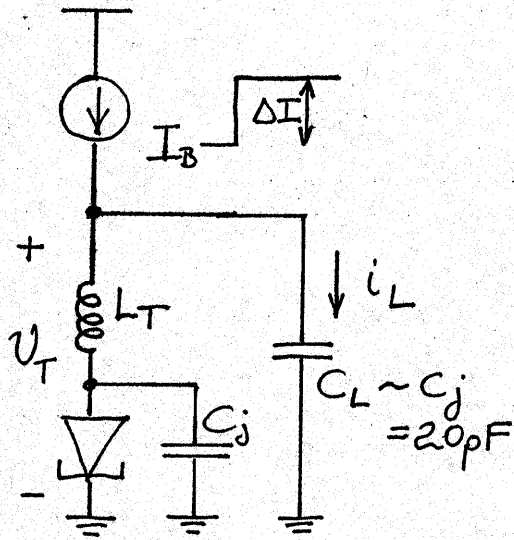
Isolation circuitry:



4.6 One td flip flop (Kaenel)



5.1 Effects of stray/lead inductances e.g. current pulse generator.



ECE 417/517
NANOELECTRONICS
Spring 2007

Lecture 7:

Single Electron Transistor

- **Nanoparticles**
- **Coulomb Block**
- **Electron box**
- **Single electron transistor**
- **SET characteristics**

Nanoparticles

High $\frac{\text{Surface area}}{\text{Volume}}$ ratio \rightarrow

High surface energy

Reactivity, catalysts

Small radius of curvature

Surface self-diffusion

Sintering

Field enhancement

Electron emission

Melting point depression

Energy level quantization

Electrostatic charging energy

Optical spectra (sizes $\sim \frac{\lambda_{\text{visible}}}{100}$)

Energy quantization $E_n = \frac{n^2 h^2}{8ma^2}$

$$a \approx 2r$$

Electrostatic charging energy $E_c = \frac{q^2}{4\pi\epsilon r}$

For $E_n \geq E_c$

$$\frac{h^2}{32m r^2} \geq \frac{q^2}{4\pi\epsilon r}$$

$$r \leq \left(\frac{8q^2 m}{\pi h^2 \epsilon} \right)^{-1} = \frac{\pi 6.67 \cdot 8.85 \cdot 10^{-68-11+38.31}}{8.256 \cdot 9.11}$$

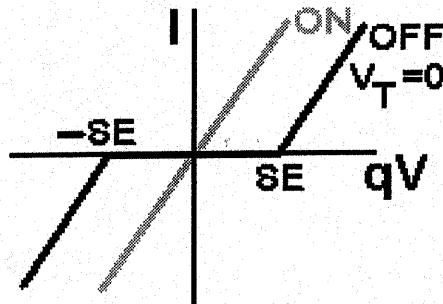
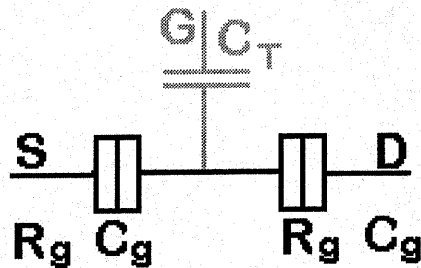
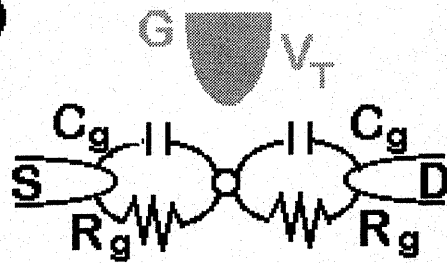
$$r \leq 6.63 \times 10^{-10} = 0.663 \text{ nm}$$

i.e. can ignore quantization effects for $r \gtrsim 1 \text{ nm}$
for nanoparticle charging devices

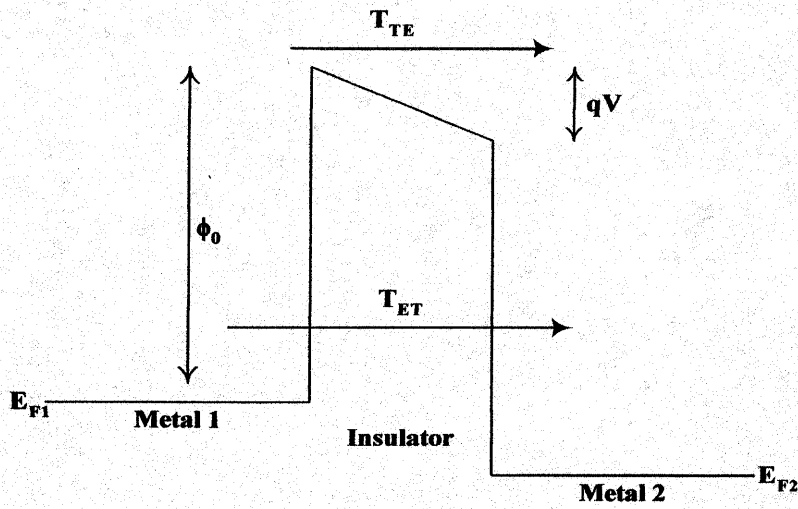
COULOMB BLOCK (ADE):

Source/drain electrodes
Nanodot/nanoparticle charging
Tunneling

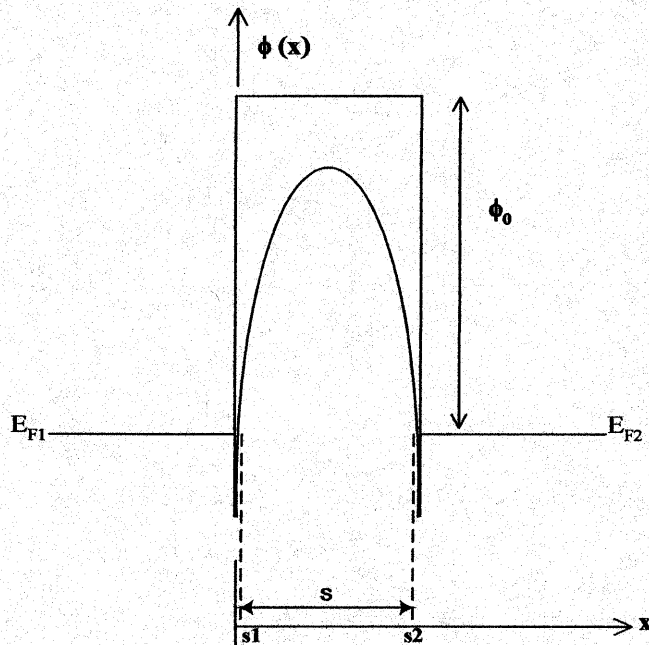
(a)



SINGLE ELECTRON TRANSISTOR (SET)
Add gate electrode



(a)



(b)

Figure 1. Electron energy diagrams of the potential barrier between two metal electrodes separated by an insulator (or vacuum,) with applied bias V . (a) Thermionic emission *over* the barrier (e.g. through the conduction band of the insulator) requires high energy; tunneling *through* the barrier is possible at lower energies near the Fermi Level, E_F , (where there are more electrons) if the barrier is sufficiently thin. (b) Electron image effects in the electrodes convert the rectangular barrier to a parabolic function.

COULOMB BLOCK at 0°K

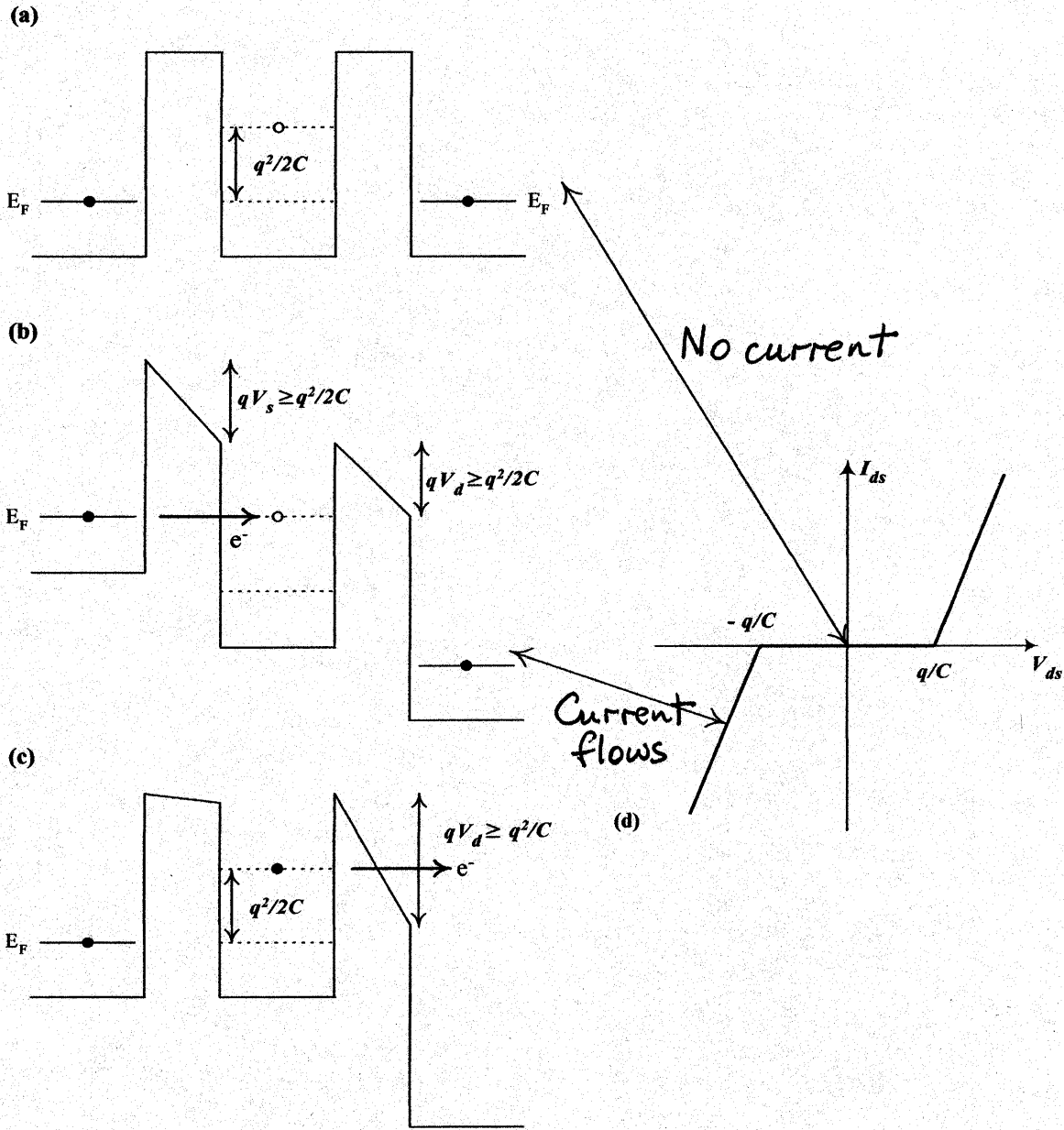


Figure 4. Electron energy diagram for the double tunnel junction Coulomb Block. (a) Zero bias, showing charging energy ΔE relative to the barrier height. (b) An electron can tunnel to the island when $qV > \Delta E$. (Assumes equal gap widths.) (c) With the island charged, E_F is raised ΔE , and the electron tunnels on with high probability. (d) CB characteristic at absolute zero, showing zero current below $2\Delta E/q$.

At finite $T \rightarrow$ tunneling possible due to Fermi-Dirac energy distribution $n(E)$ for $E > E_F$

Requirements

$$\Delta E = \frac{q^2}{2C} \gg kT \quad (\text{see later})$$

and localization of electrons
on the nanodot
(in the potential well)

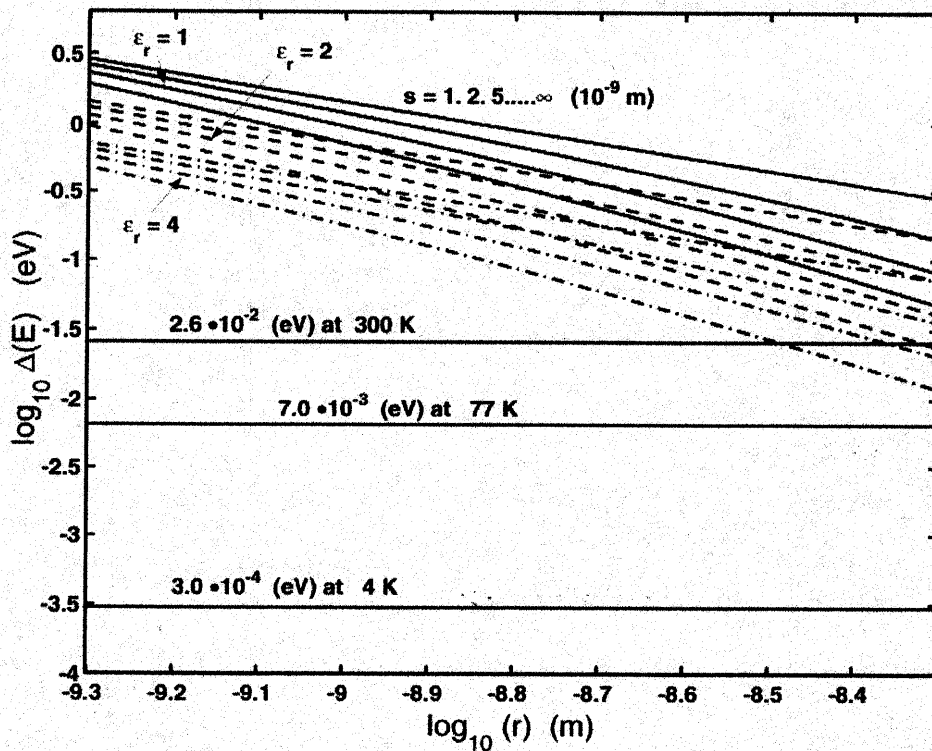
Heisenberg: $\Delta E \cdot \Delta t > h$

$$\frac{1}{2} \frac{q^2}{C} \cdot R_t C > h$$

$$\therefore R_t \gg 2 \frac{h}{q^2} \approx 2 \times 26 \text{ k}\Omega$$

where $\frac{h}{q^2}$ is the "von Klitzing resistance"
(Glosser & Gloesekoetter)

which is 2x the "Quantum Resistance" $= h/2q^2$
(Landauer formula)



$$\Delta E = \frac{1}{2} \frac{q^2}{C}$$

$$= \frac{q^2}{4\pi\epsilon} \left(\frac{1}{r} - \frac{1}{r+s} \right)$$

$$C = 2\pi\epsilon r \left(1 + \frac{r}{s} \right)$$

Figure 2. Electrostatic charging energy ΔE as a function of island radius, r , gap width, $s=1, 2, 5,$ and ∞ nm, and relative dielectric constant $\epsilon_r=1, 2,$ and 4 . (Dielectric constant $\epsilon = \epsilon_r \epsilon_0$ where ϵ_0 is the dielectric constant of free space.) The three clusters of lines correspond to ϵ_r values, with $\epsilon_r=1$ at the top, and within each cluster, the four lines correspond to s values, with $s=1$ nm at the bottom.

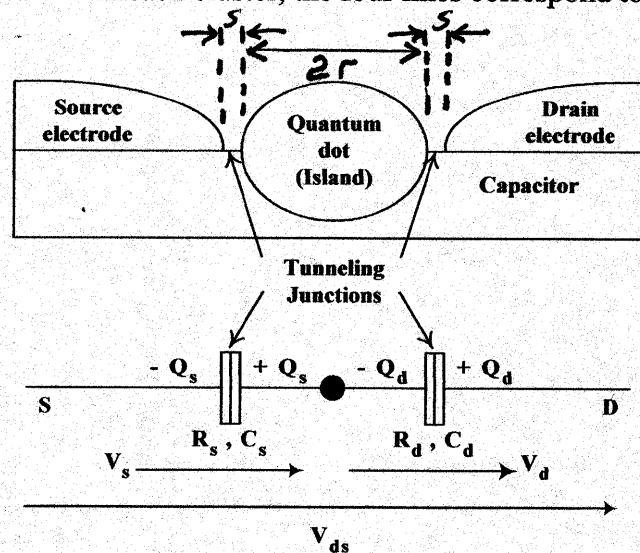
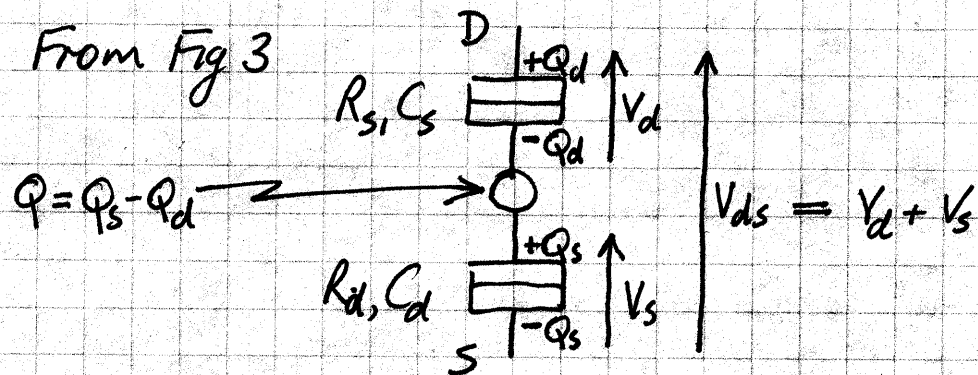


Figure 3. Coulomb Block: physical structure and equivalent circuit, with tunnel junction symbols.

COULOMB BLOCK



$$Q_d = C_d V_d \quad \text{and} \quad Q_s = C_s V_s$$

$$\begin{aligned} \therefore Q &= Q_s - Q_d = C_s V_s - C_d V_d \\ &= C_s V_s - C_d (V_{ds} - V_s) \quad \text{OR} \quad C_s (V_{ds} - V_d) - C_d V_d \end{aligned}$$

$$\Downarrow$$
$$\therefore V_s = \frac{C_d V_{ds} + Q}{C_s + C_d} \quad \& \quad V_d = \frac{C_s V_{ds} - Q}{C_s + C_d}$$

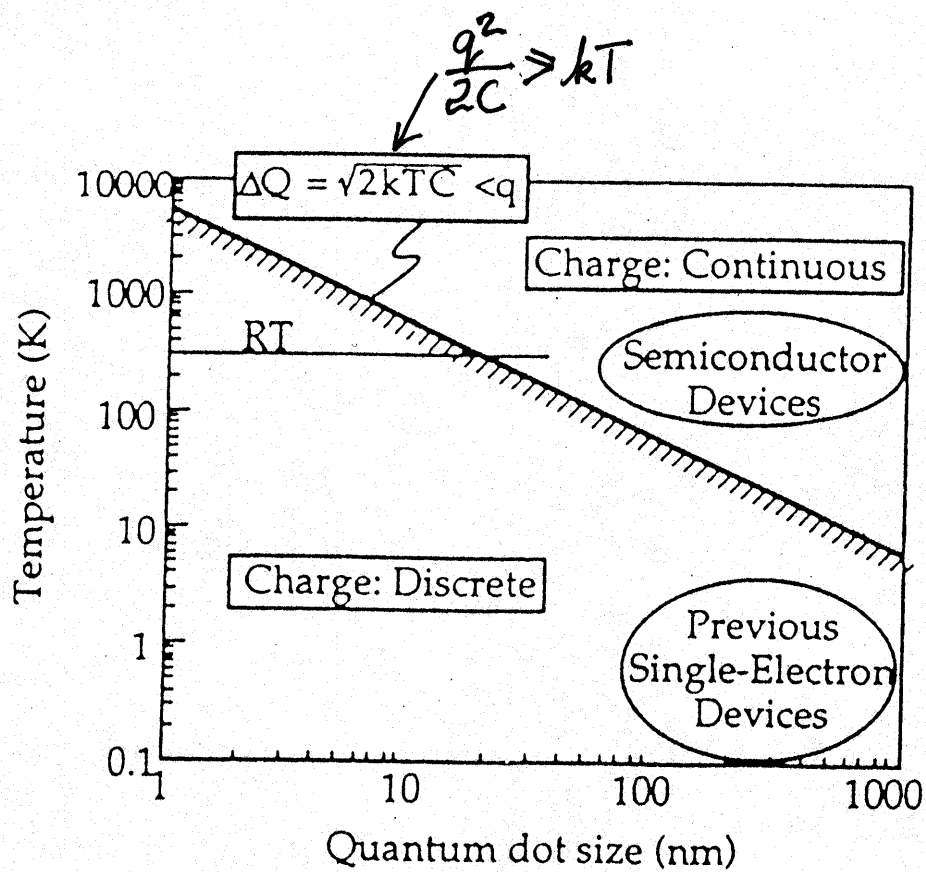
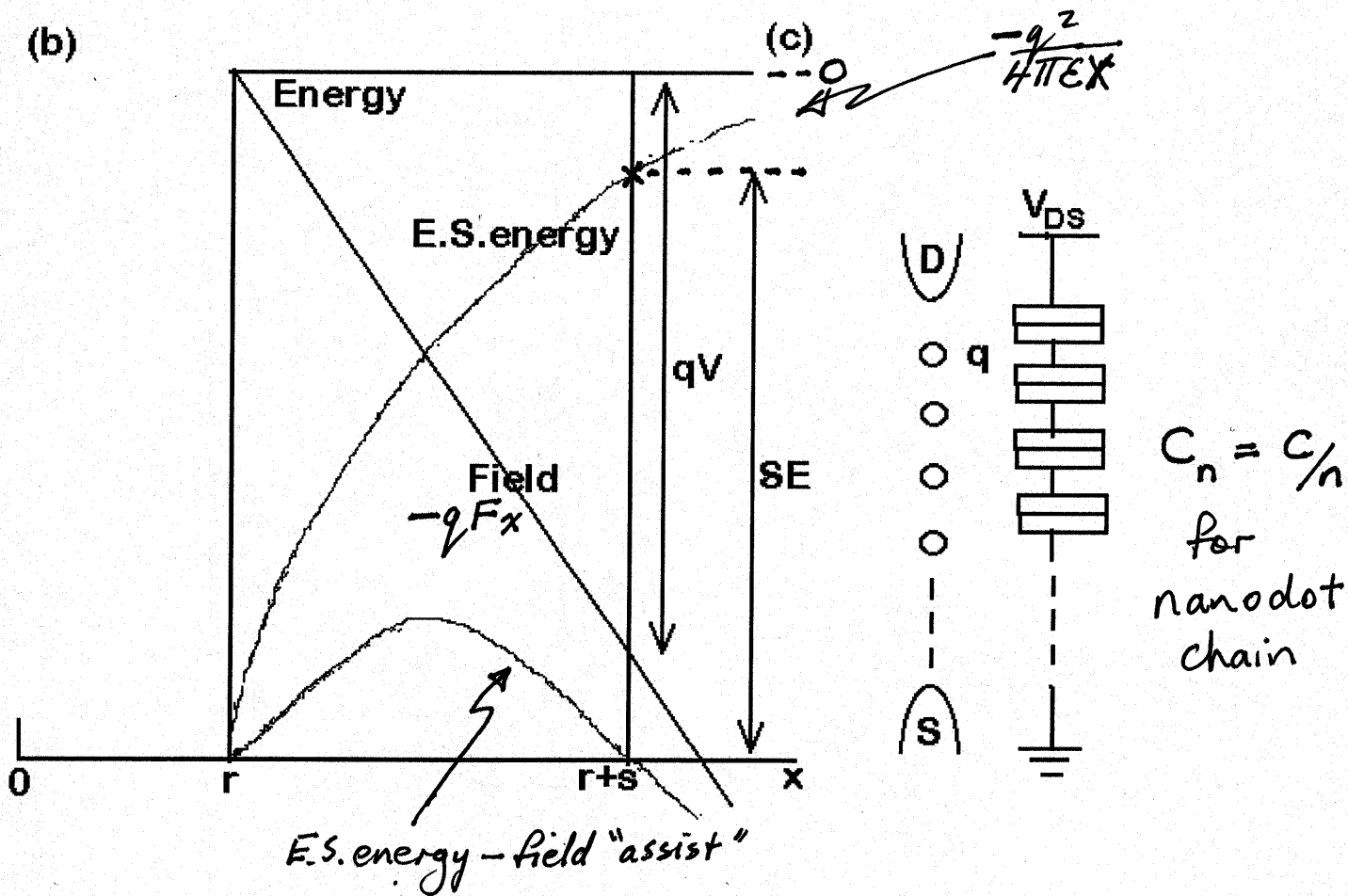


Fig. 2. Conditions for the Coulomb blockade. The self-capacitance of a uniformly charged sphere is assumed in the calculation.

Another look at the relationship between the electrostatic charging energy, electric field, and T



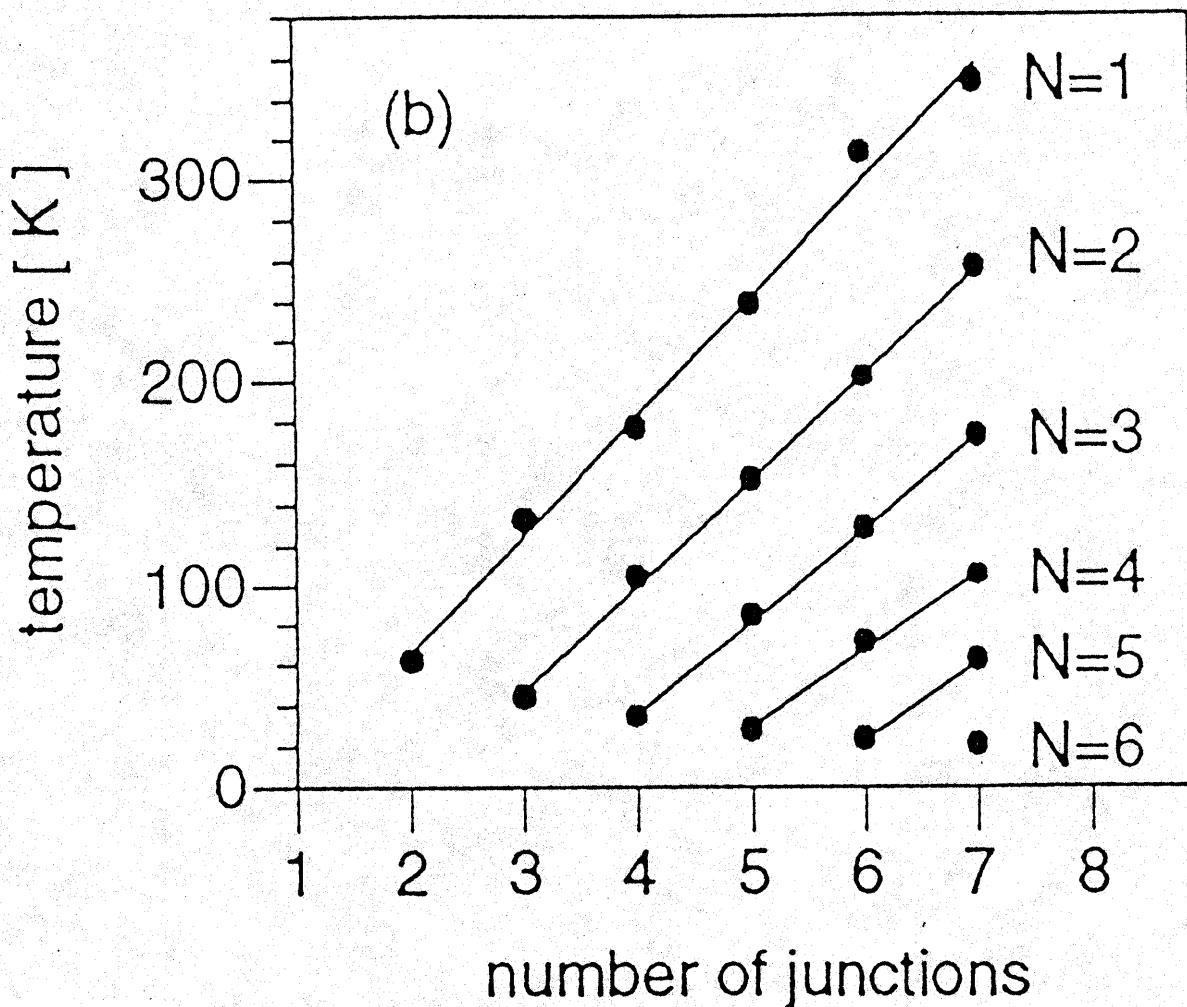
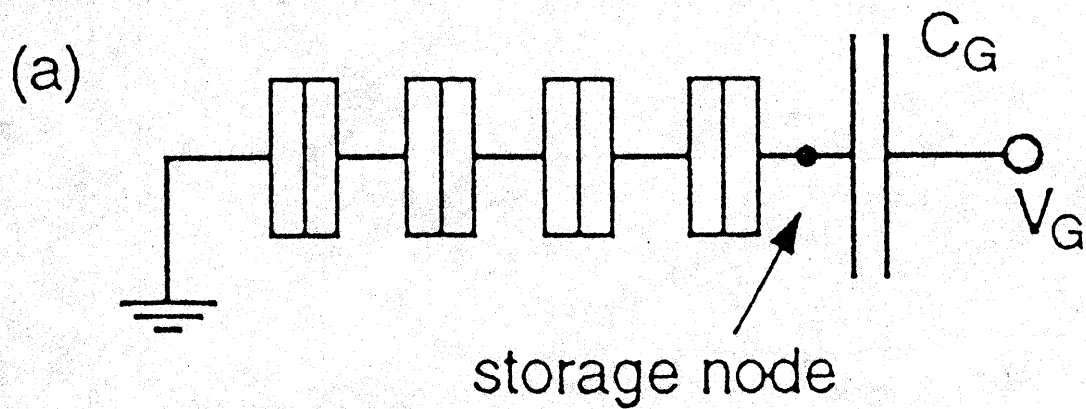


Figure 6. Single electron memory (a) and maximum temperature for keeping N electrons in the storage node (b).

YANO *et al.*: ROOM-TEMPERATURE SINGLE-ELECTRON MEMORY

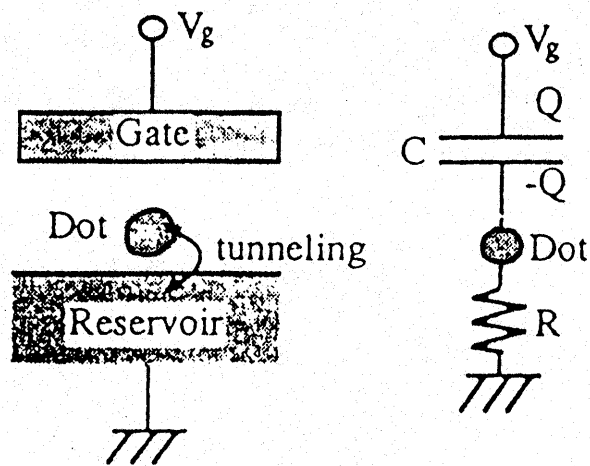


Fig. 1. The equivalent circuit of the single-electron box.

Single electron box

Capacitance $C \rightarrow$ too thick/wide for tunneling

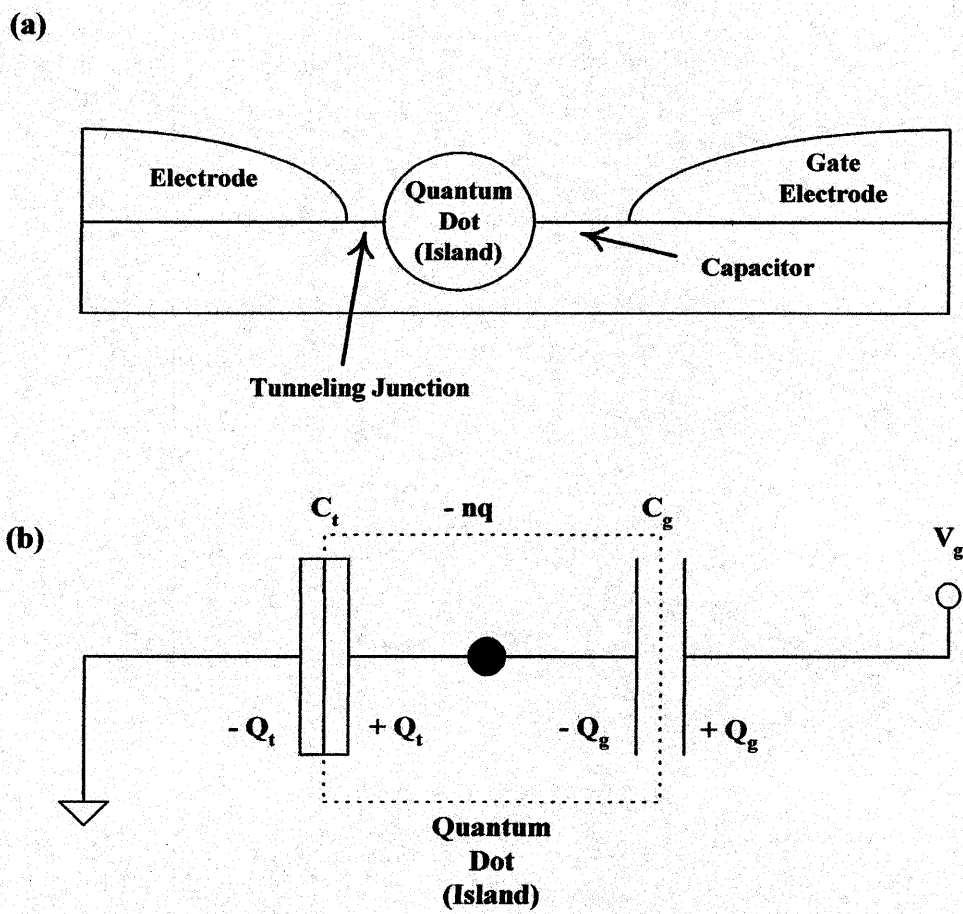


Figure 5. Single electron box: physical structure and equivalent circuit. [7]

(a)

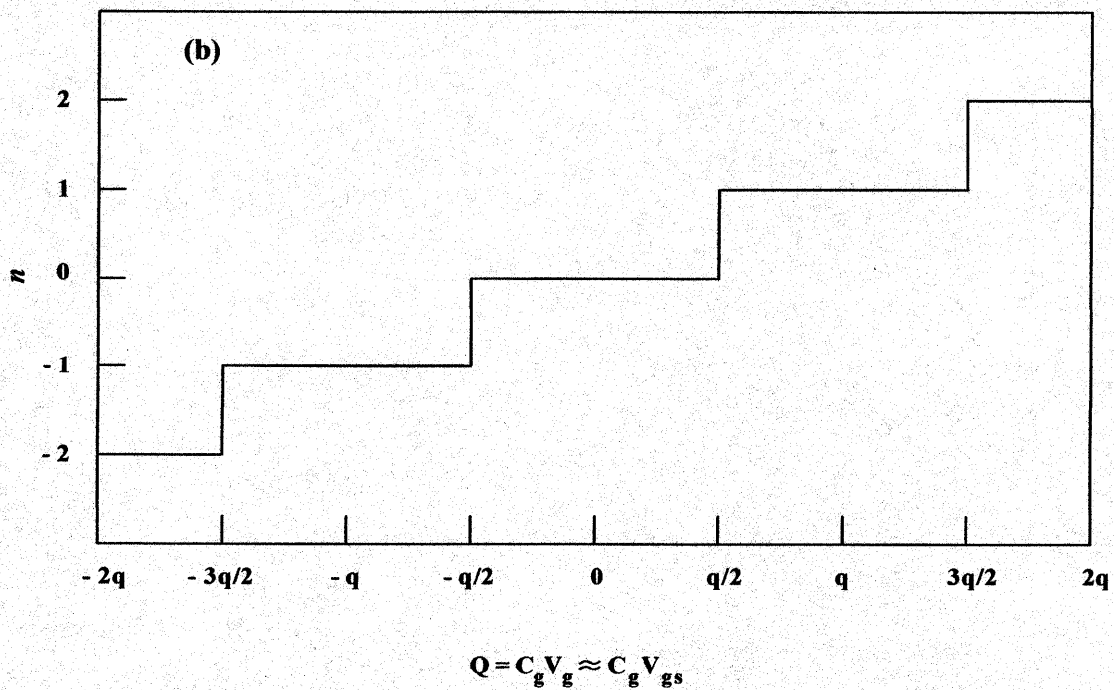
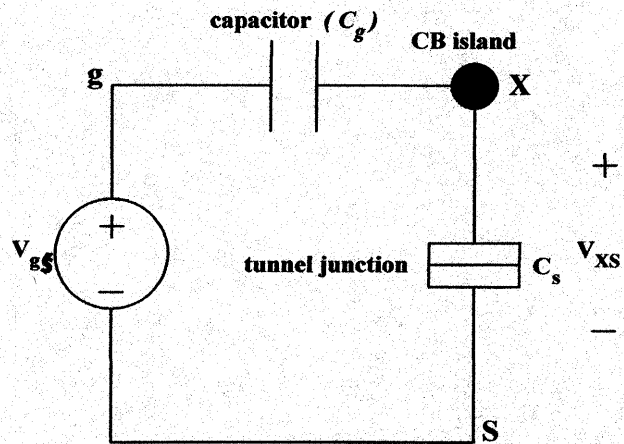
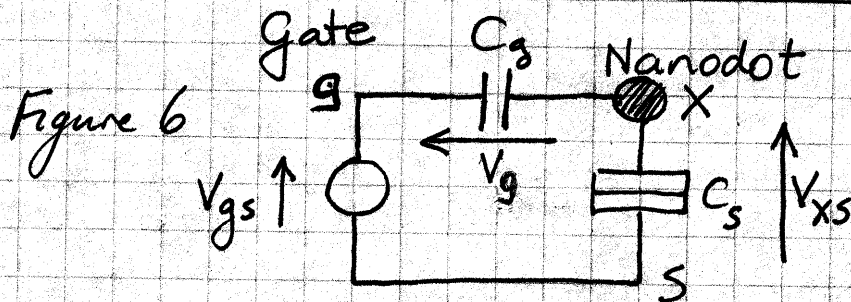


Figure 6. Single electron box: (a) circuit for analysis, and (b) stability diagram.

SINGLE ELECTRON BOX



$$C_g V_g = C_s V_{xs}$$

$$\therefore V_{xs} = \frac{C_g}{C_g + C_s} V_{gs} = \frac{C_g}{C_g + C_s} (V_{gs} - V_{xs})$$

Rearranging

$$= \frac{(C_g / C_s) V_{gs}}{1 + (C_g / C_s)}$$

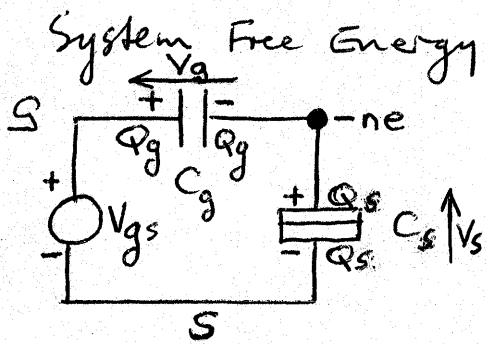
$$= \frac{C_g}{C_g + C_s} V_{gs}$$

We get tunneling through the source barrier

$$\text{when } V_{xs} \geq \Delta E / q$$

i.e. when $V_{gs} \geq \left(1 + \frac{C_s}{C_g}\right) \frac{\Delta E}{q}$ to charge nanodot

Electron Box (see Waser)



$$F(n) = W_c(n) - A(n)$$

↑
charging energy

↑
work done by gate voltage source to charge island

$$Q_s - Q_g = -ne \quad (1)$$

$$V_{gs} (= V_g + V_s) = \frac{Q_g}{C_g} + \frac{Q_s}{C_s} \quad (2)$$

$$W_c(n) = \frac{Q_s^2}{2C_s} + \frac{Q_g^2}{2C_g} \quad (3)$$

Solve (1) & (2): Eliminate $Q_s = (V_{gs} Q_g / C_g) C_s = Q_g - ne$
to get $Q_g = (C_s V_{gs} + ne) C_g / C_\Sigma$ (where $C_\Sigma = C_s + C_g$) (4)

& substitute back to get $Q_s = (C_g V_{gs} - ne) C_s / C_\Sigma$ (5)

Substitute Q_g & Q_s in (3) and expand/simplify to get

$$W_c(n) = n^2 e^2 / 2C_\Sigma + C_s C_g V_{gs}^2 / 2C_\Sigma \quad (6)$$

Now $A(n) = Q_g V_{gs}$; substitute from (4) gives $A(n) = ne C_g V_{gs} / C_\Sigma + C_s C_g V_{gs}^2 / C_\Sigma$ (7)

$$\therefore F(n) = [n^2 e^2 - 2(ne) C_g V_{gs} - C_s C_g V_{gs}^2] / 2C_\Sigma \quad (8)$$

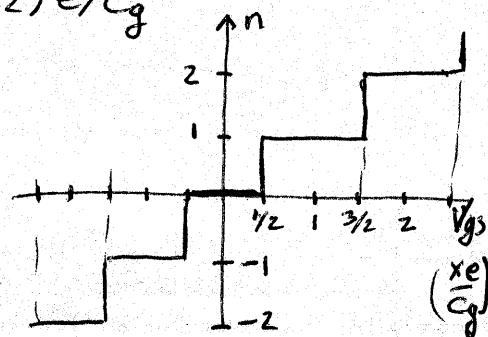
To maintain a stable charge ne on the island for given V_g requires

$$F(n) < F(n-1) \quad \text{and} \quad F(n) < F(n+1)$$

$$\begin{aligned} \text{i.e. } (ne)^2 - 2(ne) C_g V_{gs} &< (n-1)^2 e^2 - 2(n-1) e C_g V_{gs} && \text{and similarly;} \\ [n^2 - (n-1)^2] e &< C_g V_{gs} [2n - 2(n-1)] && \text{for } n, n+1 \\ (2n-1) e / C_g &< 2V_{gs} && 2V_{gs} < (2n+1) e / C_g \\ \therefore (n-1/2) e / C_g &< V_{gs} < (n+1/2) e / C_g \end{aligned}$$

which gives the electron box stability diagram for

$$\begin{array}{l} n=0 \quad -e/2C_g < V_{gs} < +e/2C_g \\ n=\pm 1 \quad -3e/2C_g \quad \quad \quad 3e/2C_g \\ n=\pm 2 \quad -5e/2C_g \quad \quad \quad 5e/2C_g \\ \text{etc} \end{array}$$



The SET combines the Coulomb Block with the Single Electron Box

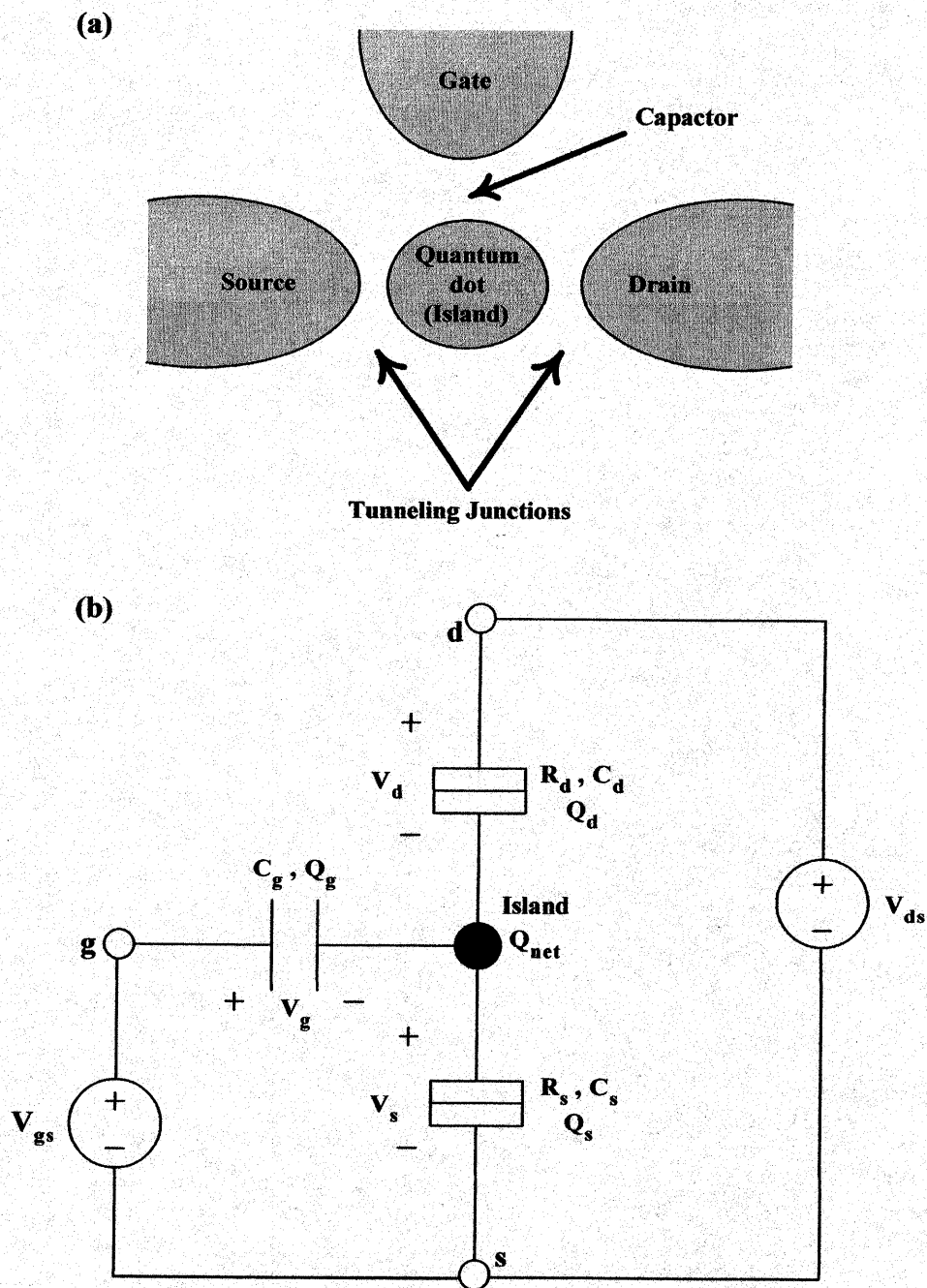
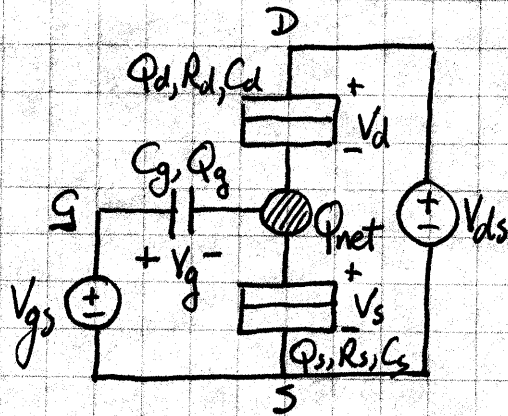


Figure 7. Single electron transistor: (a) physical structure, and (b) circuit for analysis.

SINGLE ELECTRON TRANSISTOR

For Fig 7



$$Q = Q_{net} = Q_s - Q_d - Q_g$$

$$= C_s V_s - C_d V_d - C_g V_g$$

$$= C_s V_s - C_d (V_{ds} - V_s) - C_g (V_{gs} - V_s)$$

$$\therefore (C_s + C_d + C_g) V_s = C_d V_{ds} + C_g V_{gs} + Q$$

and similarly $(C_s + C_d + C_g) V_d = (C_g + C_s) V_{ds} - C_g V_{gs} - Q$

give $V_{ds} = \frac{C_g}{C_g + C_s} V_{gs} + \left(1 + \frac{C_d}{C_g + C_s}\right) V_d + \frac{Q}{C_g + C_s}$

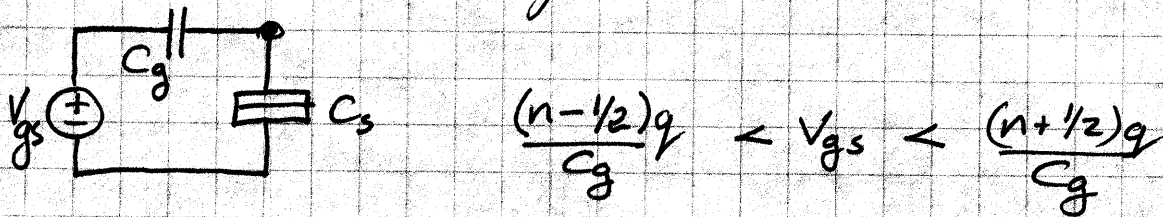
& $V_{ds} = -\frac{C_g}{C_d} V_{gs} + \left(1 + \frac{C_g + C_s}{C_d}\right) V_s - \frac{Q}{C_d}$

which are two lines $V_{ds} = f(V_{gs})$ of slope $\frac{C_g}{C_g + C_s}$ & $-\frac{C_g}{C_d}$

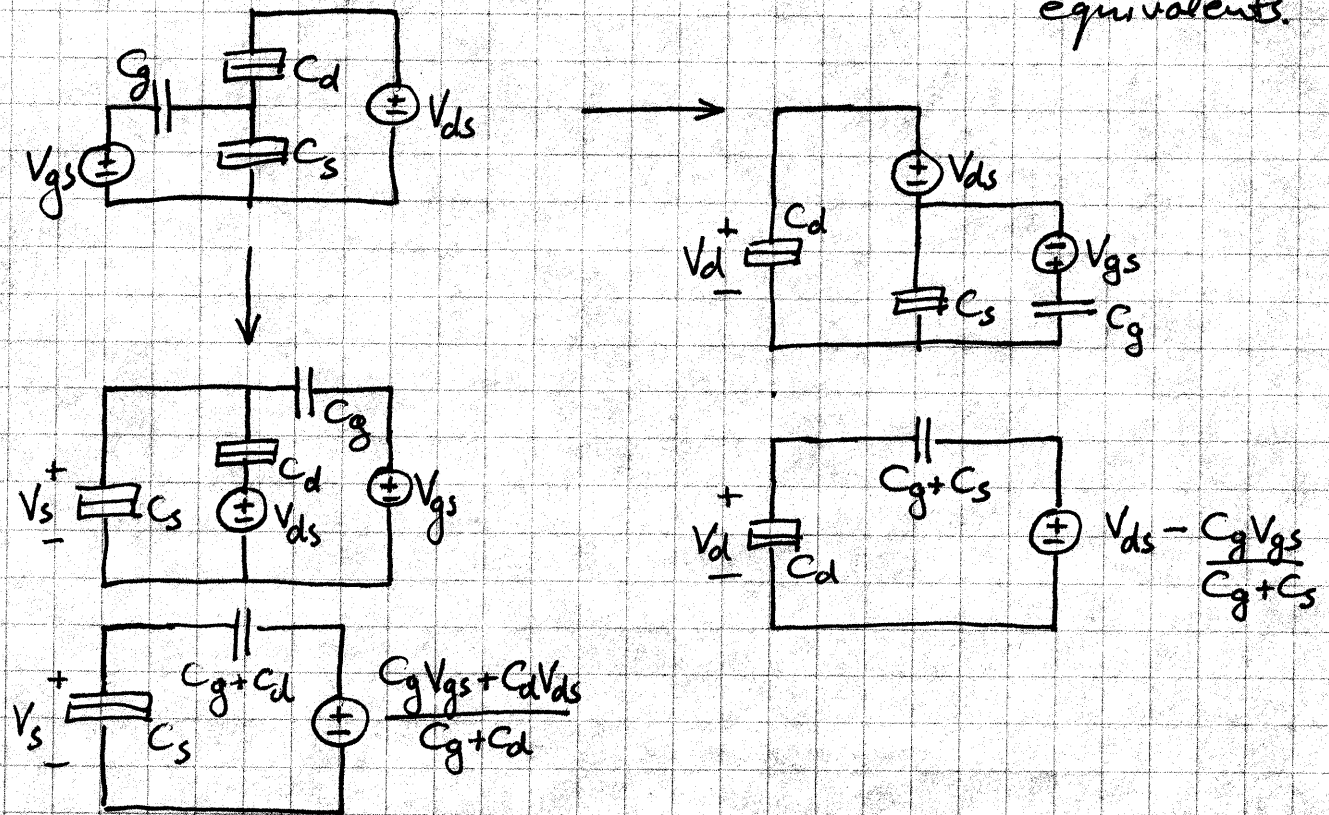
defining the circuit relationship as V_d, V_s vary
for $Q = \pm nq, n = 0, 1, 2, \dots$

But we still don't know how V_s, V_d might be constrained
with Q quantization

Return to the single electron box case



and transform the SET circuit to Thevenin equivalents.



So now there are two stability conditions by analogy

$$\frac{(n-1/2)q}{C_g + C_d} < \frac{C_g V_{gs} + C_d V_{ds}}{C_g + C_d} < \frac{(n+1/2)q}{C_g + C_d}$$

ie. $\frac{1}{C_d} \left((n-1/2)q - C_g V_{gs} \right) < V_{ds} < \frac{1}{C_d} \left((n+1/2)q - C_g V_{gs} \right)$

and

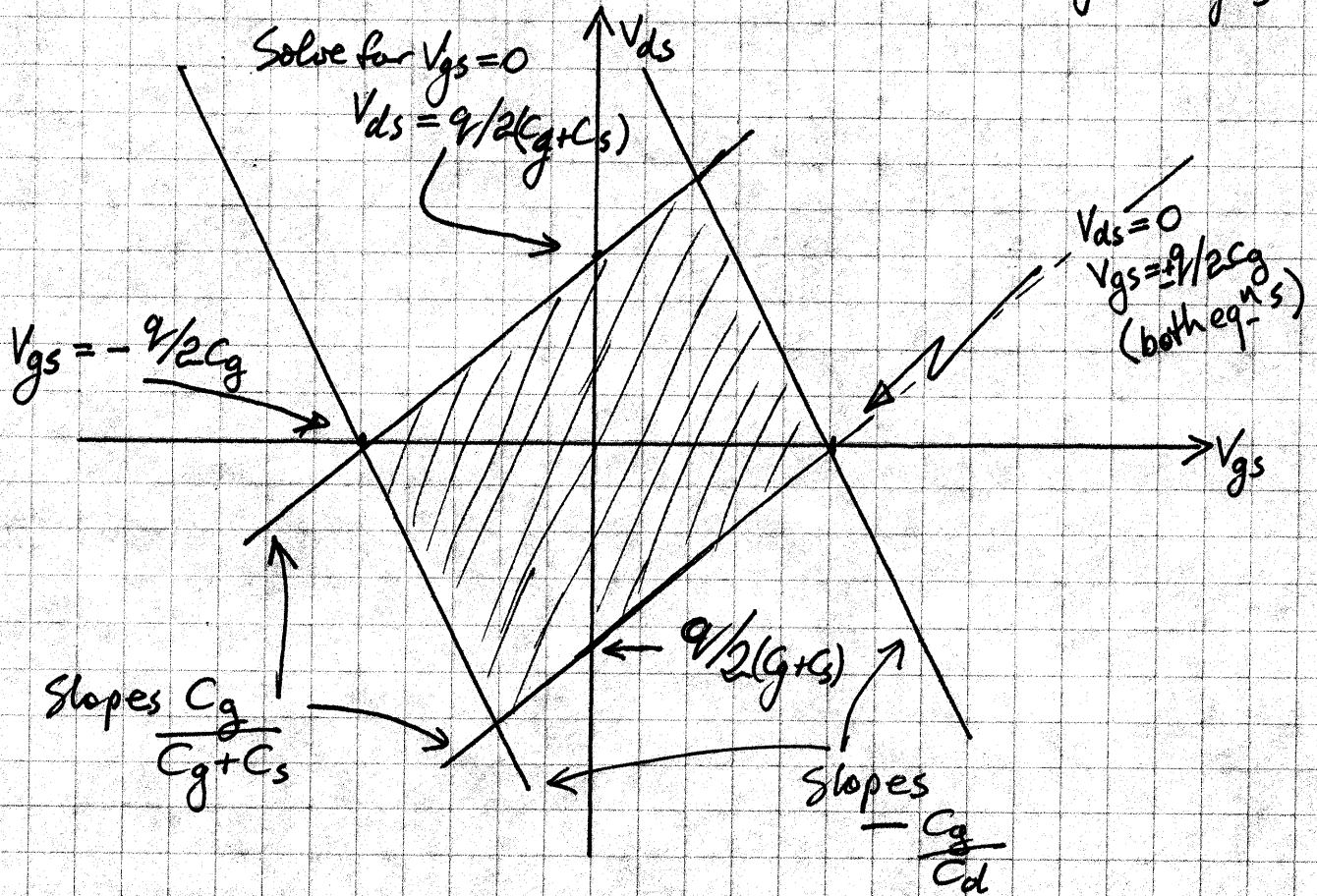
$$\frac{(n-1/2)q}{C_g + C_s} < V_{ds} - \frac{C_g V_{gs}}{C_g + C_s} < \frac{(n+1/2)q}{C_g + C_s}$$

$$\frac{1}{C_g + C_s} \left((n-1/2)q + C_g V_{gs} \right) < V_{ds} < \frac{(n+1/2)q + C_g V_{gs}}{C_g + C_s}$$

For $n=0$

$$\frac{-q}{2C_d} - \frac{C_g}{C_d} V_{gs} < V_{ds} < \frac{+q}{2C_d} - \frac{C_g}{C_d} V_{gs}$$

$$\& \frac{-q}{2(C_g+C_s)} + \frac{C_g}{C_g+C_s} V_{gs} < V_{ds} < \frac{+q}{2(C_g+C_s)} + \frac{C_g}{C_g+C_s} V_{gs}$$



Diamond meets both criteria for $n=0$

This is the stable region, i.e. no conduction.

Compare Coulomb Block with $V_{gs} = 0$

$$\text{Conducts } |V_{ds}| > \frac{q}{2(C_g+C_s)}$$

and SET threshold for $V_{ds} = 0$

$$|V_{gs}|_{\text{SET}} = q/2C_g$$

Note |slope| $\rightarrow \frac{C_g}{C_g+C_s} < \frac{C_g}{C_d}$ for $C_s \sim C_d$ Typ $C_g < C_s, C_d$

Note error on slopes as shown.

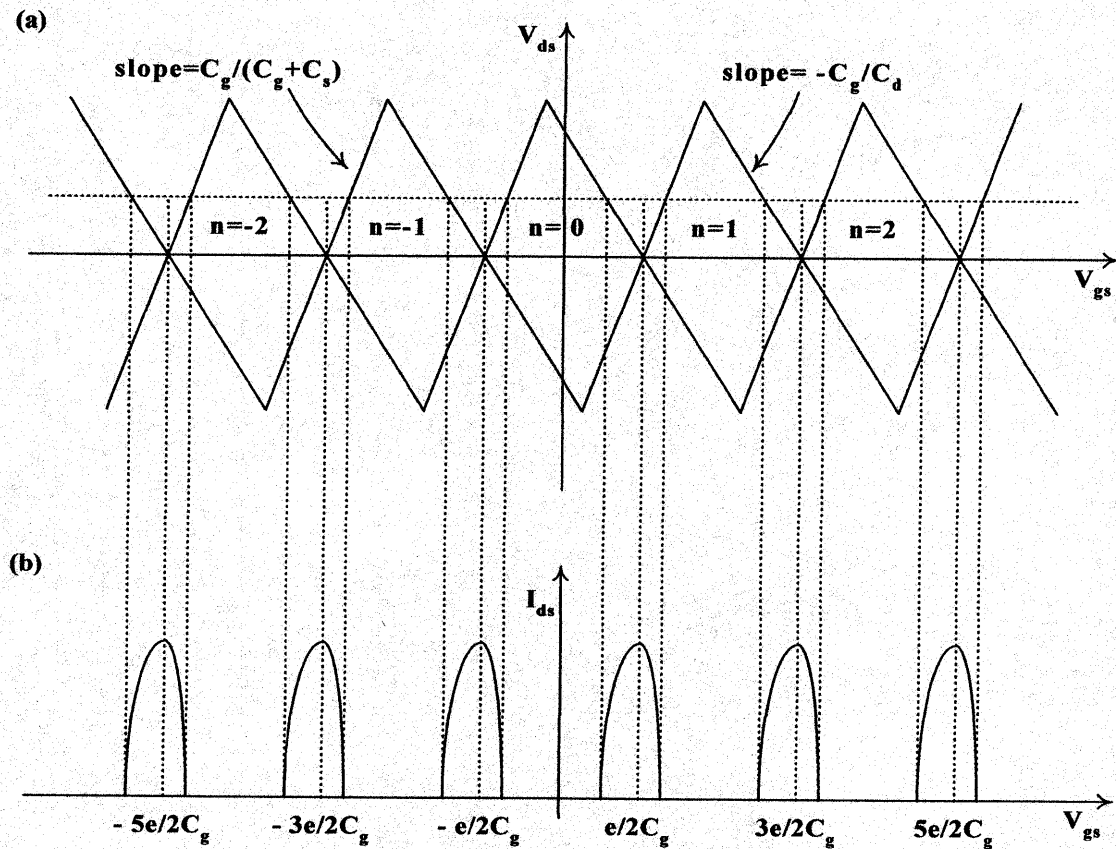


Figure 8. SET stability diagram. (a) Current can flow outside the periodic diamonds, as shown for finite V_{ds} in (b). [7, 8]

Lots of minor differences in figures and formulae
in different references.

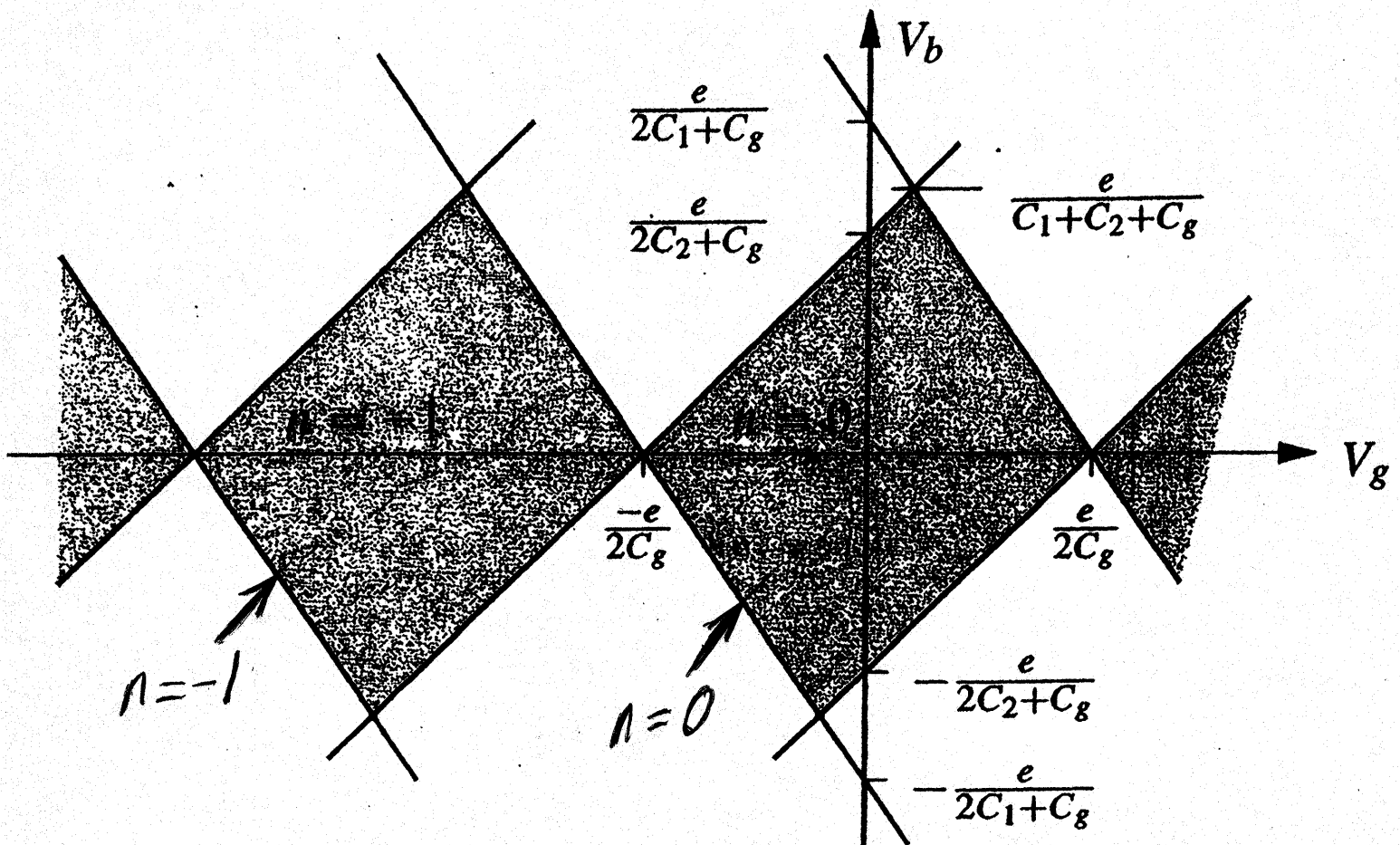


Fig. 53. Stability diagram of a SET. Only grey areas are stable

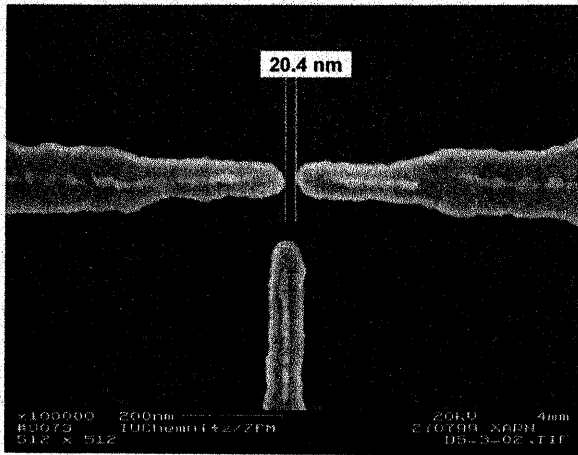
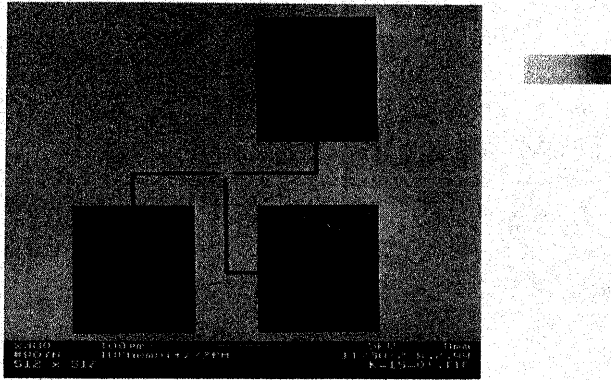


Figure 9. Electron micrographs of the SET structure [9].

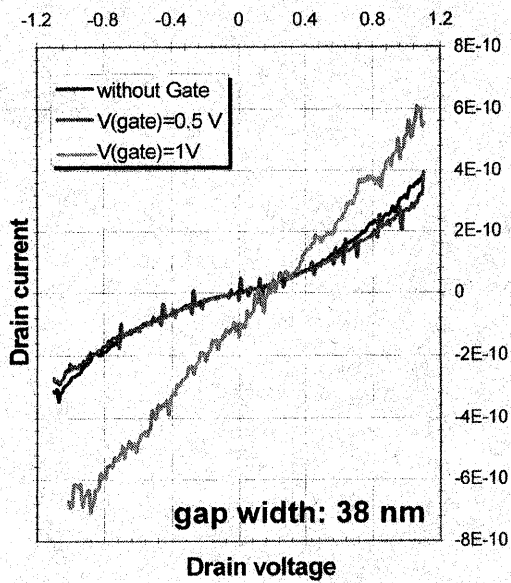


Figure 10. SET characteristics for a device similar to that of Figure 9 [9].

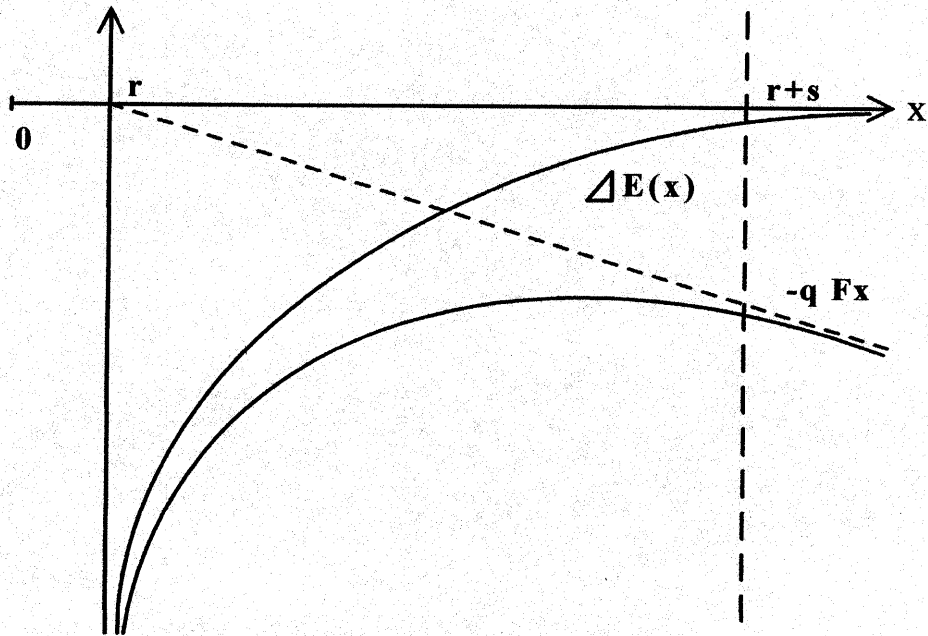


Figure 11. Electrostatic charging energy for island of radius r . The composite function $\Delta E(x) - qFx$ develops a maximum at high fields, where $\Delta E(x) = q^2/4\pi\epsilon x$.

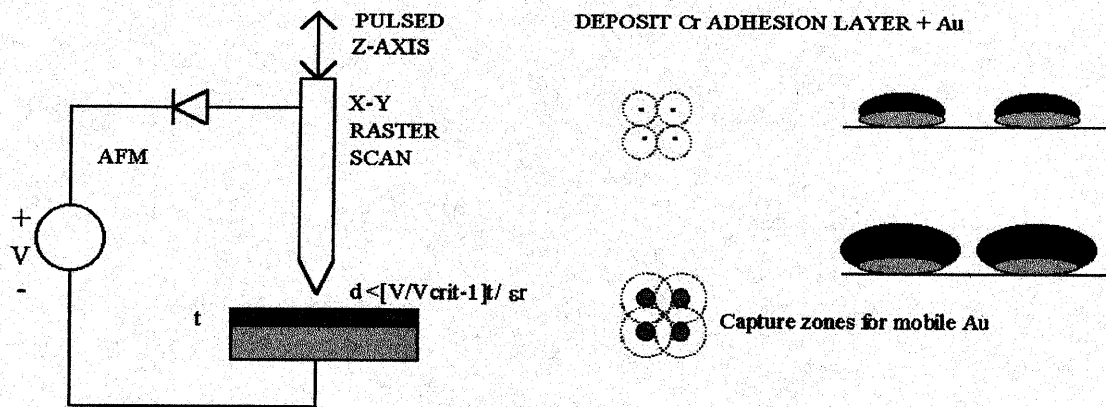


Figure 12. (a) AFM-piezoelectric drive system and (b) deposition model. [23]

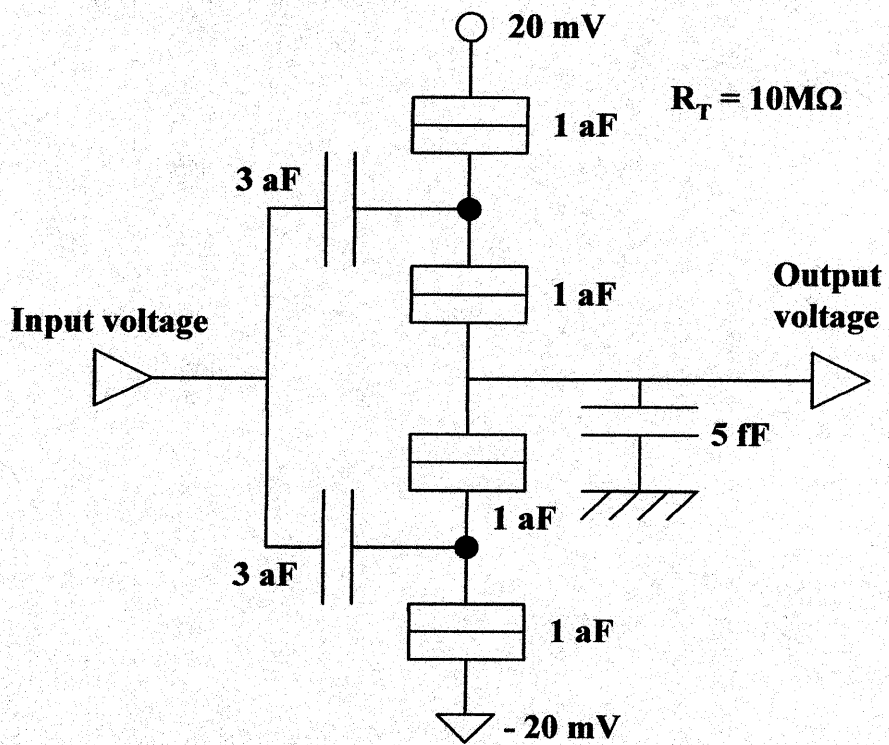


Figure 13. Simple SET inverter [7].

ECE 417/517 NANOELECTRONICS

Spring 2007

Lecture 8: SET Circuits

- Frequency response
- Basic circuits
- Memory
- Logic circuits
- Modeling
- Negative differential resistance
- Quantum cellular automata
- Multi-dot systems

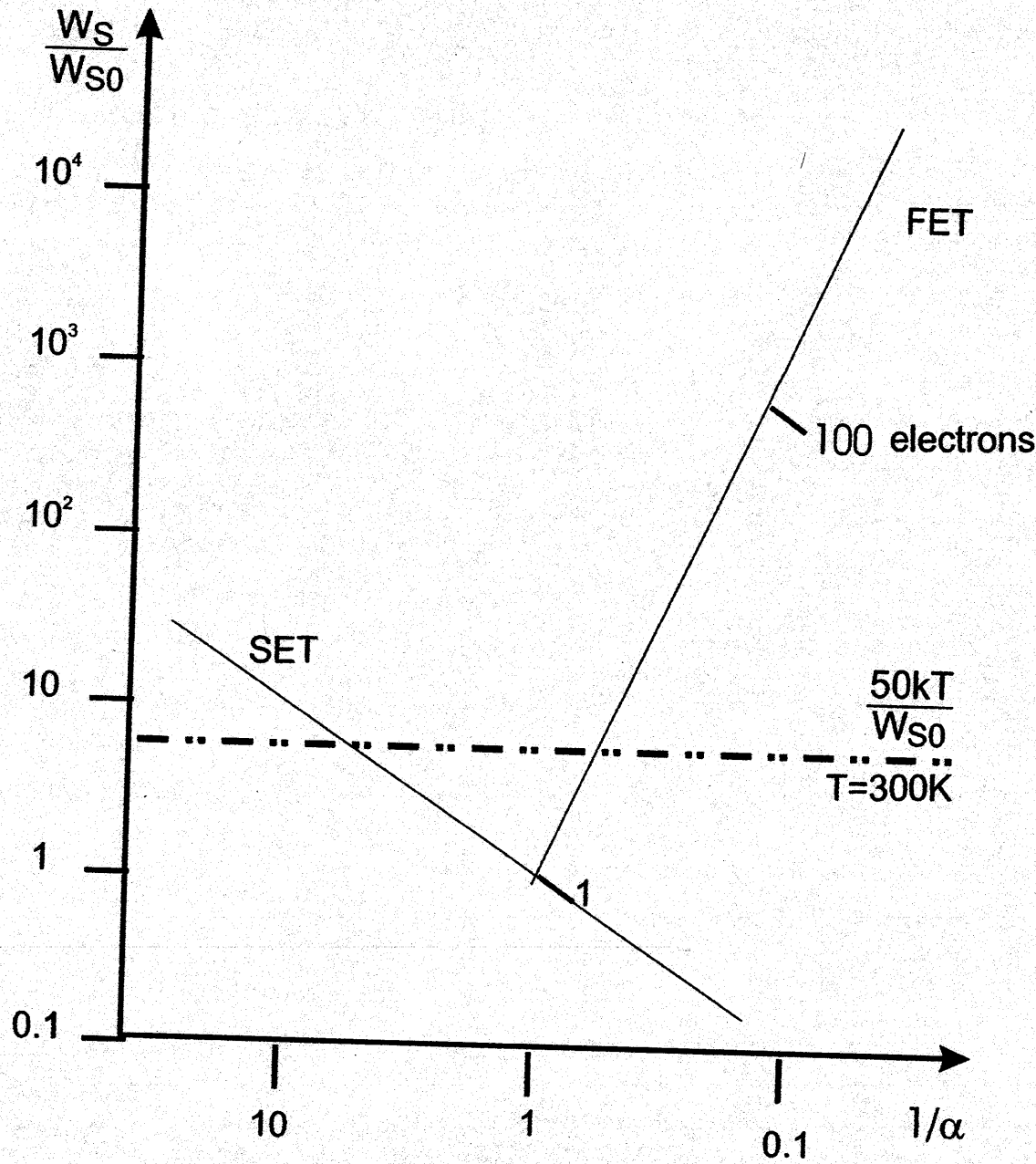


Fig. 13.17. The power-delay diagram reveals the impacts of scaling on the SET and FET

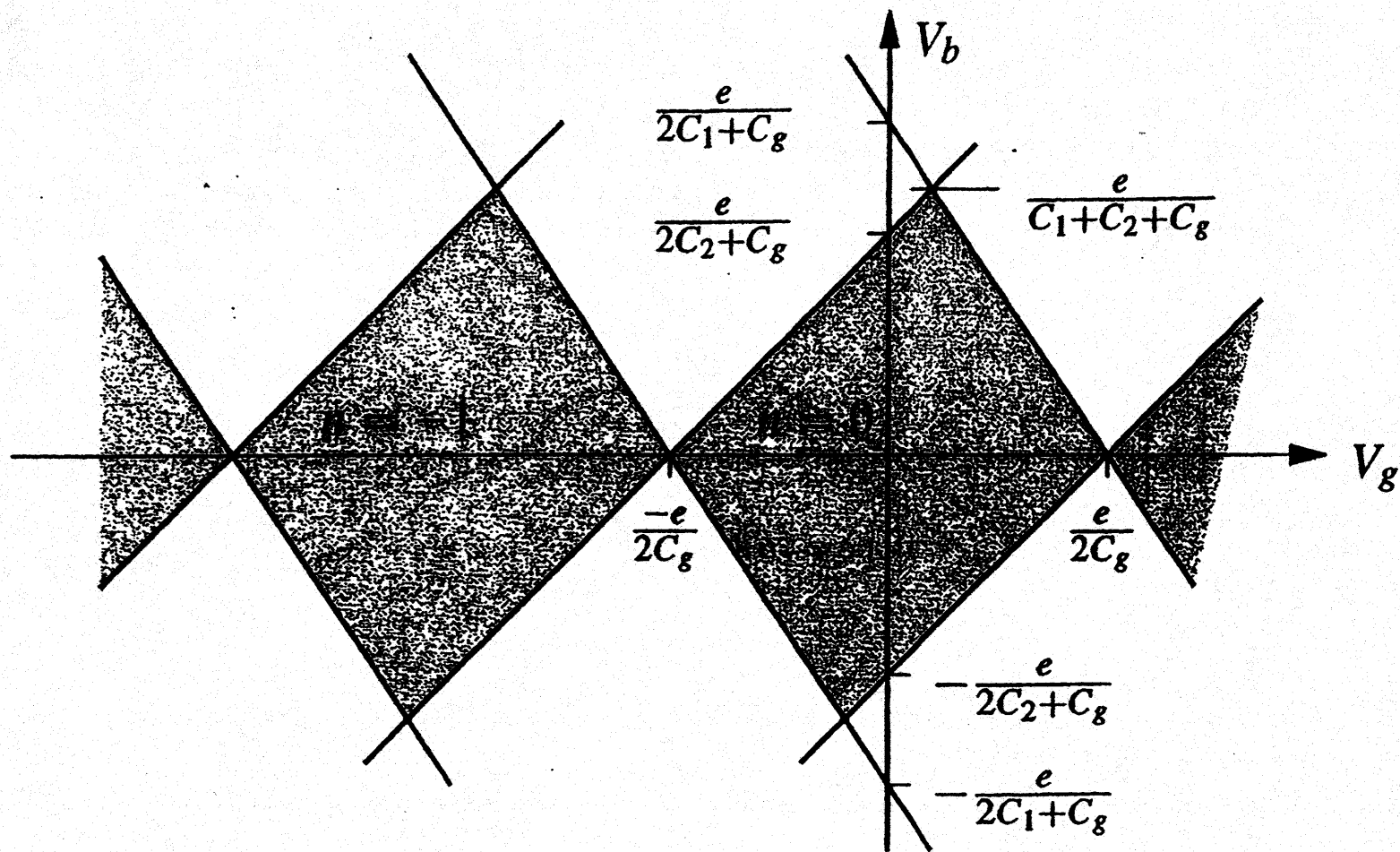
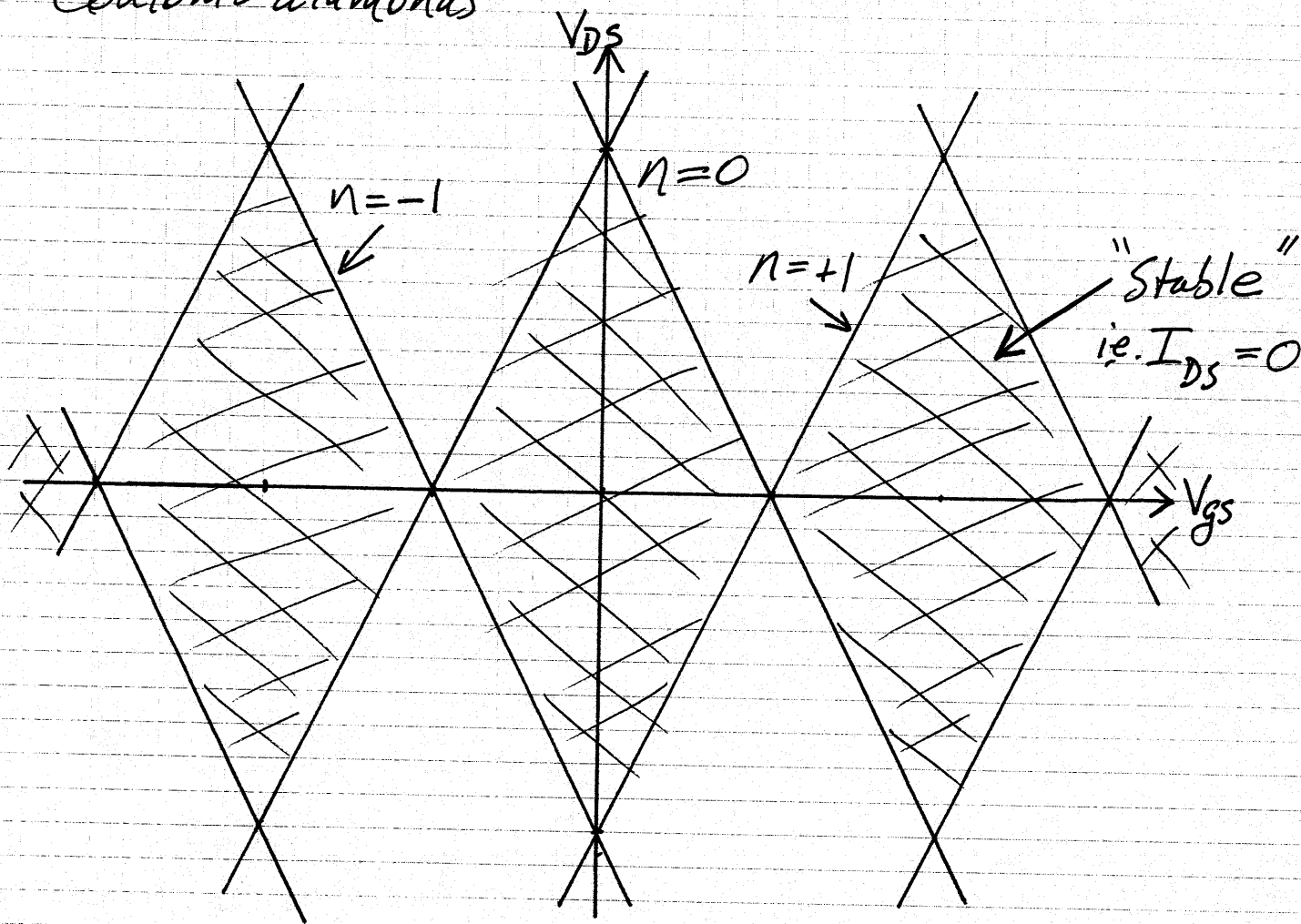


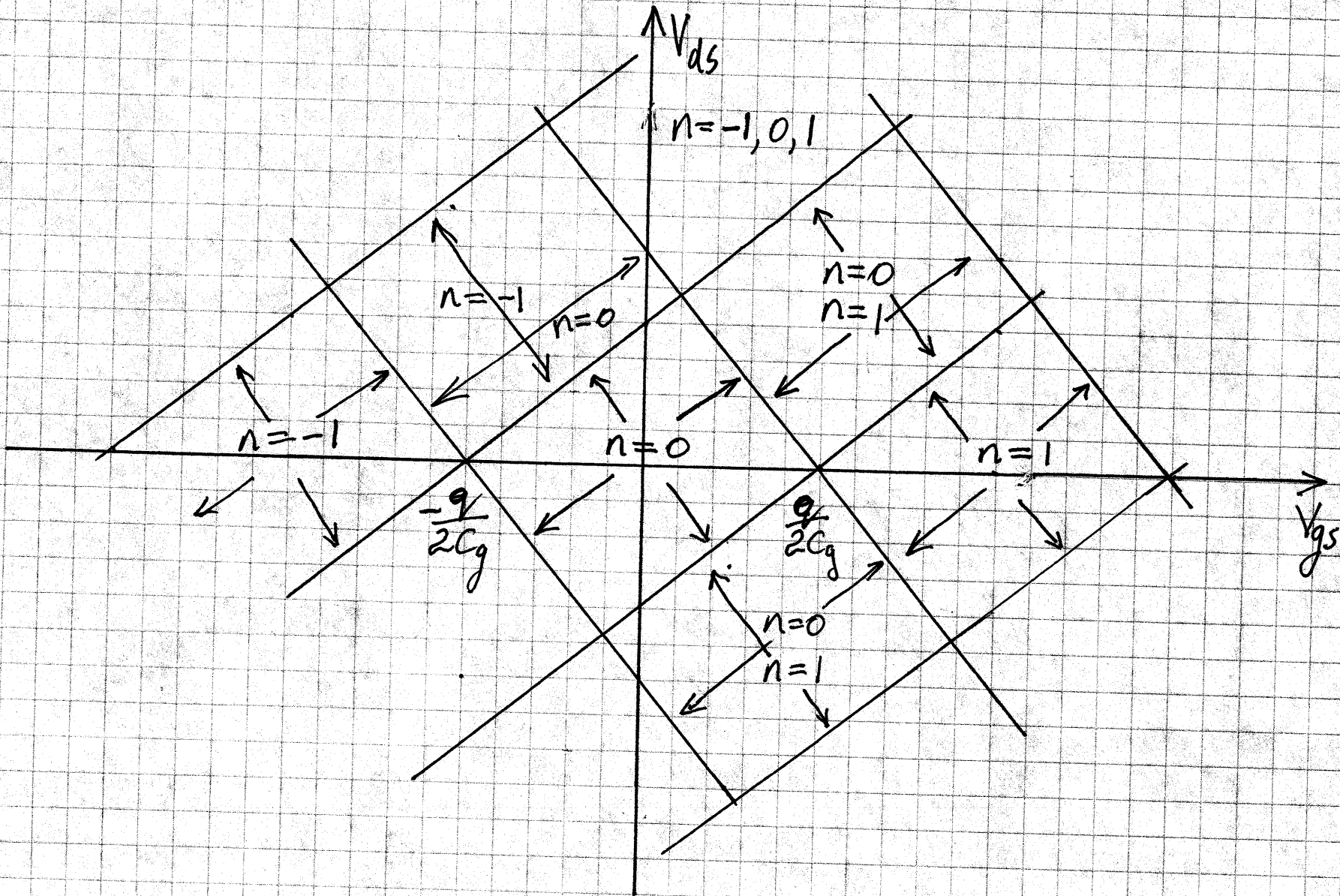
Fig. 53. Stability diagram of a SET. Only grey areas are stable

"Coulomb diamonds"



Simplify $\rightarrow C_S = C_D$ & $C_G \approx 0$ OR $C_S = C_G = C, C_D = 2C$

Note: At $V_{GS} = 0$, $-\frac{q}{2C} < V_{DS} < +\frac{q}{2C}$ for stability
ie. Coulomb Block region



SET / Coulomb Block Frequency Response

$$\frac{q^2}{2C} = \frac{q^2}{4\pi\epsilon r} \sim 1\text{eV}$$

$$\text{ie. } C \sim \frac{1.6 \times 10^{-19}}{2} \sim 8 \times 10^{-20} \text{ F} \\ = 0.08 \text{ aF}$$

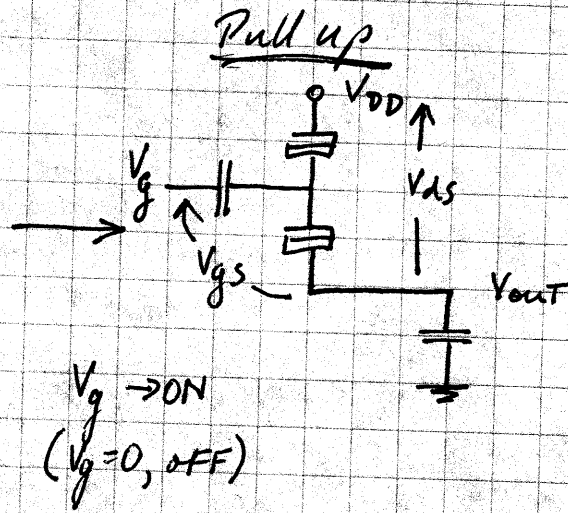
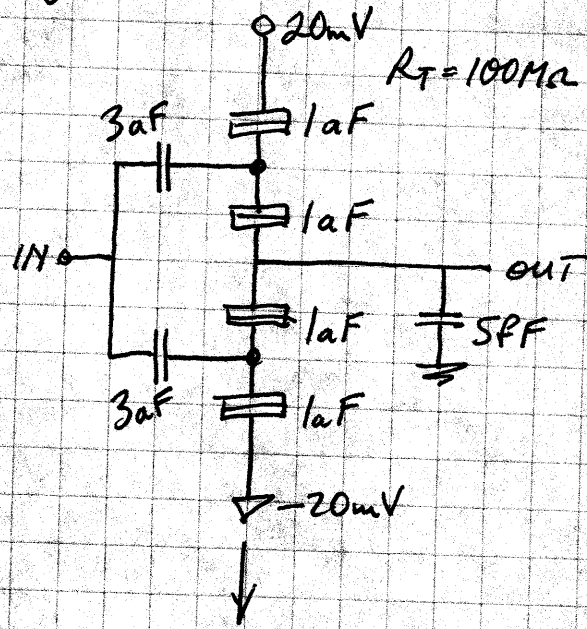
$$R \approx 28.5 \text{ k}\Omega$$

$$\therefore RC \approx 2 \times 10^{-15} \text{ s}$$

$$\therefore f \sim \frac{\omega_c}{2\pi} = \frac{1}{2\pi \times 2 \times 10^{-15}} \sim \frac{10^{15}}{12.5} \\ = 8 \times 10^{13} \\ = 80 \text{ THz}$$

Note: For small C, small island r
Island size incr \rightarrow max freq decr.

LOGIC INVERTER



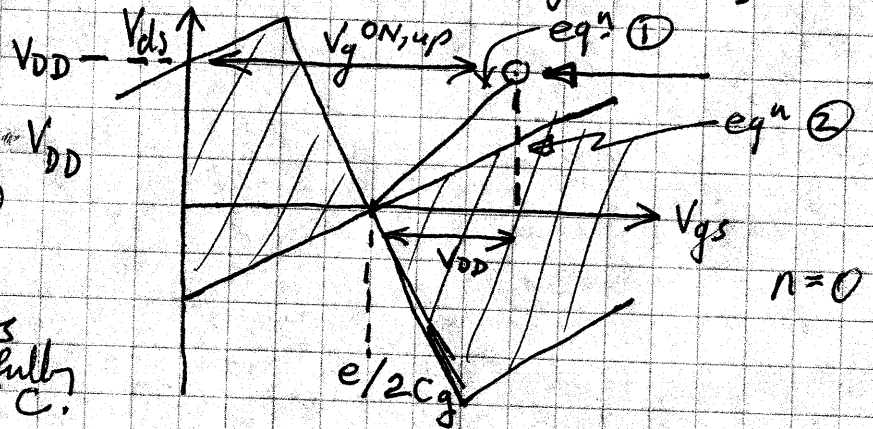
$V_g \rightarrow ON$
 $(V_g = 0, OFF)$

$$\left. \begin{aligned} V_{ds} &= V_{DD} - V_{out} \\ V_{gs} &= V_g^{ON, up} - V_{out} \end{aligned} \right\} V_{gs} = V_g^{ON, up} - V_{DD} + V_{ds}$$

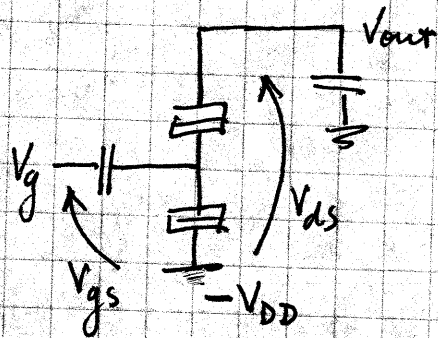
Need $V_{gs} = (n + 1/2)e/C_g$ for turn-on at $V_{ds} = 0$

$$\therefore V_g^{ON, up} = V_{DD} + (n + 1/2)e/C_g$$

$$\& V_{gs} = V_{ds} + (n + 1/2)e/C_g \quad \text{① (subtracting)} \quad (V_s = V_{out})$$



Pull down



$(V_g = 0, OFF)$
 $V_g \rightarrow ON$

$$V_g^{ON, down} = (n + 1/2)e/C_g = V_{gs} - V_{DD} \quad \text{②}$$

$$V_{gs} = V_{DD} + (n + 1/2)e/C_g$$

Pull up \rightarrow as V_{out} incr, V_{ds} decr along ① \rightarrow conducts
 Pull down \rightarrow as V_{out} decr, V_{ds} decr along ② \rightarrow cannot fully discharge C.

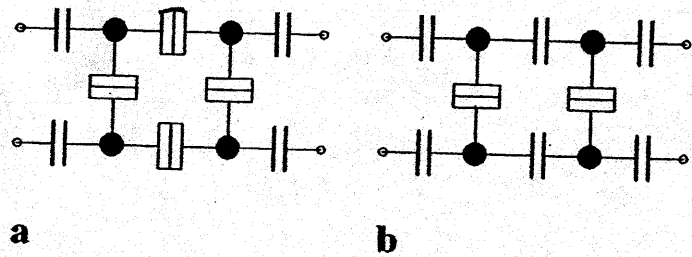


Fig. 97. *a* Typical realization of a quantum cellular automata cell consisting of four tunnel junctions and coupling capacitors to left and right neighbor. *b* Two-junction variation

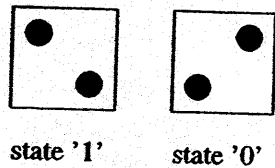


Fig. 98. The two excess electrons in a single cell can take on two stable configurations. The black dots represent electrons

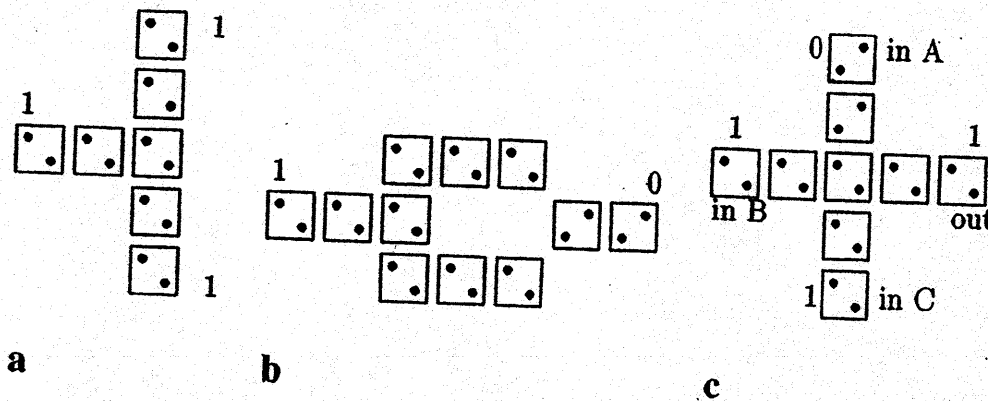


Fig. 99. *a* Fanout circuit, *b* inverter, *c* majority logic gate

Note:
Background
charge effects

operate at mK T's
 Relaxation to one of 2 ground states
 Increase T to be able to switch out of metastable states, but
 then ground state unstable

ECE 417/517 NANOELECTRONICS

Spring 2007

Lecture 9: Molecular Electronics; Scanning Probe Microscopy

- Introduction:
 - Conductors
 - Insulators
 - Diodes
 - Memory
- Transistors
- Self-assembly

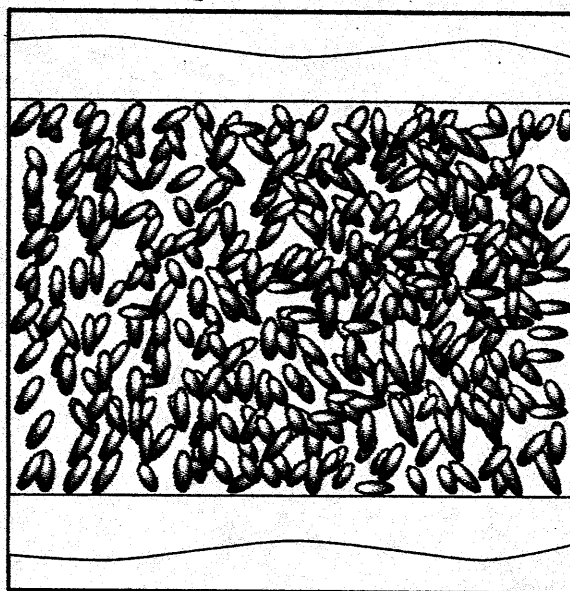
SPM:

Scanning tunneling microscope (STM) &
atomic force microscope (AFM)

Molecular Electronics

Bulk Molecular Systems

eg. OLEDs



- amorphous or polycrystalline structure
- most molecules in (random) contact to other molecules
- molecules not individually addressable



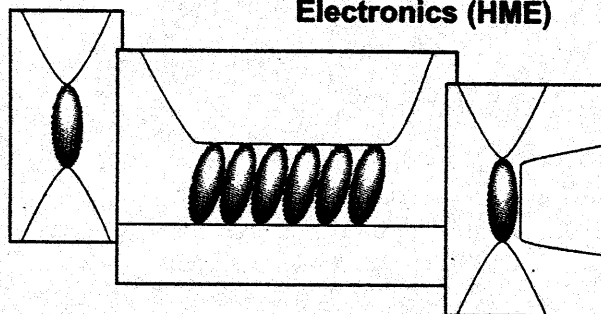
Electrode



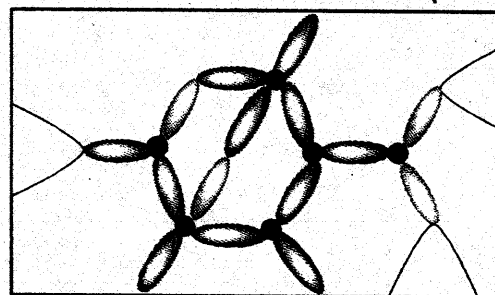
Molecule

Single Molecular Systems

Hybrid Molecular Electronics (HME)



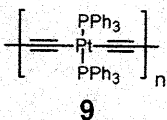
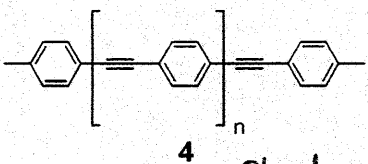
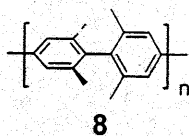
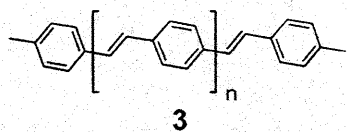
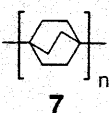
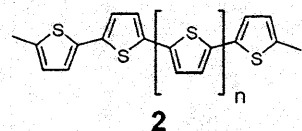
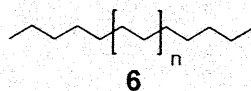
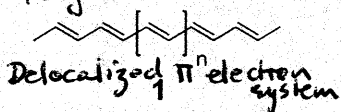
Mono-Molecular Electronics (MME)



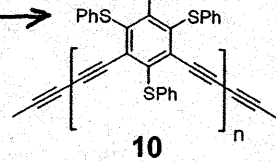
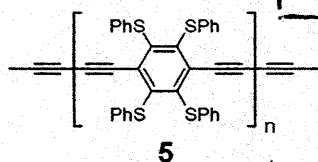
- single molecules or perfectly ordered films
- HME: molecule(s) in direct contact to electrodes
- MME: microscopically designed molecular network

Wires:
 conjugation active motives
 Alternating single/double bonds
 Polyene
 Delocalized π^n electron system

Insulators:
 conjugation passive motives



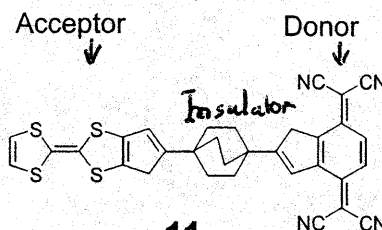
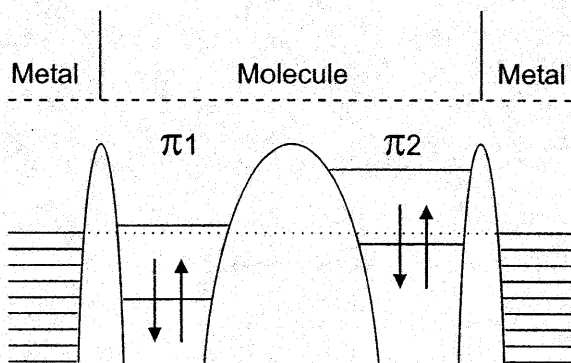
Closely related systems*
 para- meta-



Various aromatic/benzene chains

Figure 2: Molecular structural motives described in the text. Motives 1-5 are delocalized conjugated systems with the potential to act as molecular wires. Motives 6-10 are barely conjugated - even so in the case of 7-10 still rigid - systems, rather acting as insulating spacers.

* para- meta- | diacetylene connected thiophenyl-substituted benzene



Bias $\begin{matrix} + & \xrightarrow{11} & - \\ - & \xleftarrow{\quad} & + \end{matrix}$

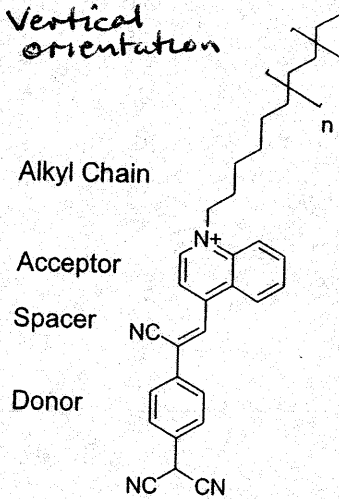
Figure 3: The first approach to molecular electronics [2]. Molecules with a donor and an acceptor group, separated by an insulating spacer, are predicted to behave as diodes. The upper panel displays the electron energies in the system, when no bias voltage is applied: In the metallic electrodes outside, electrons are filled up to the Fermi energy. The π -systems of the donor and acceptor units are confined in two potential wells. If a positive voltage is applied, the potential of the left lead is slightly increased and the potential of the right lead is correspondingly lowered: current can flow from the left to LUMO1, then to HOMO2 and further to the right electrode, going towards lower energies at each step. If the opposite voltage is applied, conduction take place only at much higher voltages. This is the behavior of a diode with the favourable current direction from the acceptor to the donor.

Problems to get molecules lined up the right way
 Hence LB Films better \rightarrow

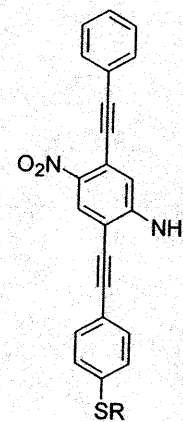
Basic Electrical Elements

- Conductors
- Insulators (spacers)
- Acceptor (p-type)
- Donor (n-type)

Vertical orientation



12

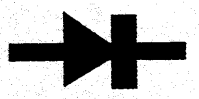


13

Figure 4: The LB-Film molecule 12 and the rod-like molecule 13.

Langmuir-Blodgett

a)



b)

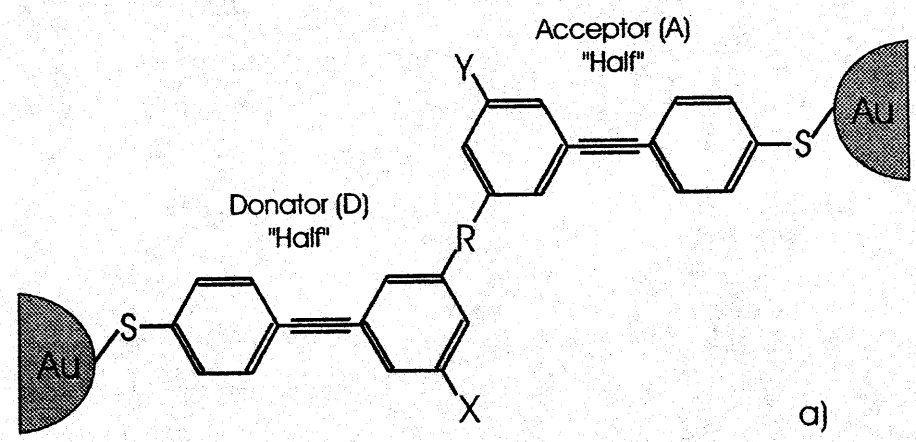
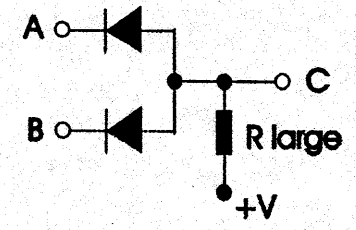


Fig. 11.15. Molecular structure of a diode

Electronic devices

a)



b)

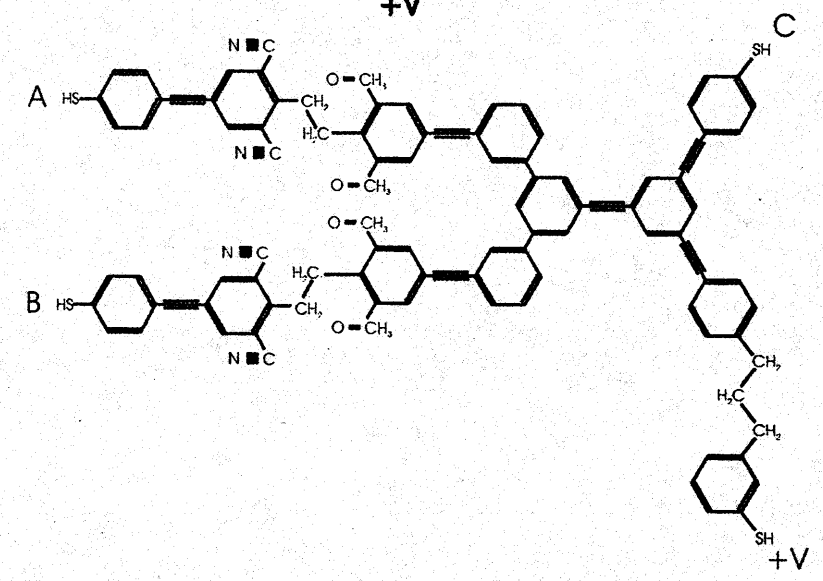


Fig. 11.16. Polymer structure of a logic AND gate: By reversing the diodes' polar and by applying a negative supply voltage the gate turns into a logic OR gate

processes	example of bistable systems
redox process	
configuration change	
conformation change	
electronic excitation (lifetime)	
magnetic spin orientation	
logic states	"0" "1"

Figure 5: Illustration of bistable molecular structures.

- (a) redox states, where A denotes an acceptor group and D is a donor group of the molecule;
- (b) configurations obtained by a re-arrangement where Z is the wandering group;
- (c) example of cis and trans conformations;
- (d) ground state A and excited state A* of a molecule;
- (e) parallel and anti-parallel spin states within a molecule.

*Bi-stable elements
Storage/switching*

*Triggering by light or chemistry (pH)
Few can be electrically triggered yet.*

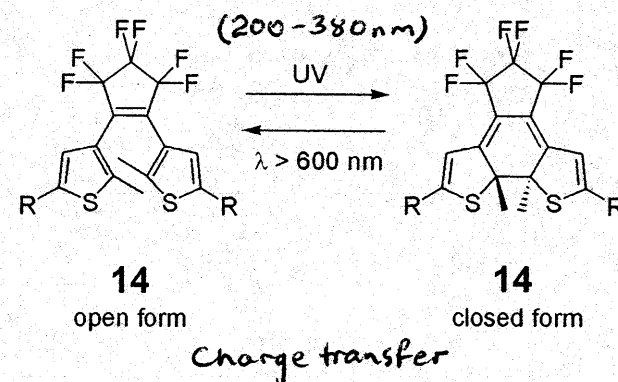


Figure 6: The light-triggered switch by Masahiro Irie [25].

Molecular FET → Molecule in gap gives SET characteristics

Figure 9: SEM picture of a Au electrode pair on top of an Al gate electrode, which is covered by an Al_2O_3 insulator. Such a setup was used as a molecular field effect transistor [47].

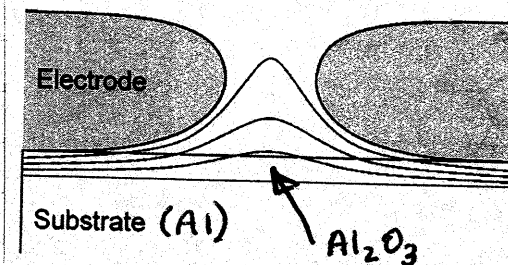
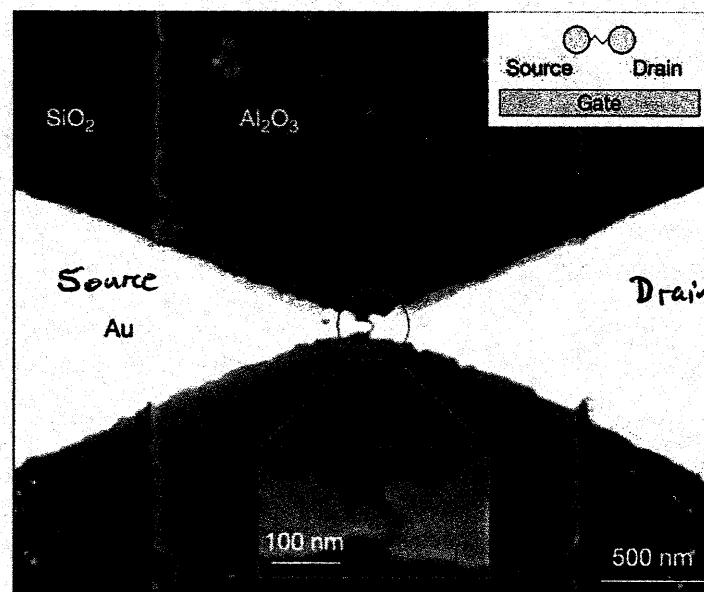
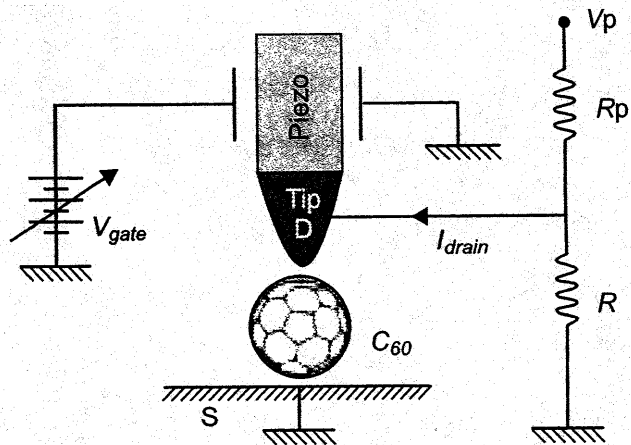


Figure 10: Scheme of an electrode gap with a buried gate electrode formed by the substrate (covered by an insulating layer). When a gate voltage is applied, the equipotential lines (red) are not homogeneous in the gap region. If the molecule is far away from the surface, high gate voltages are needed to affect the potential at the molecule's position. If the distance from the gate electrode is not well controlled, this will result in strongly varying switching voltages.



← Example of a mechanically controlled junction

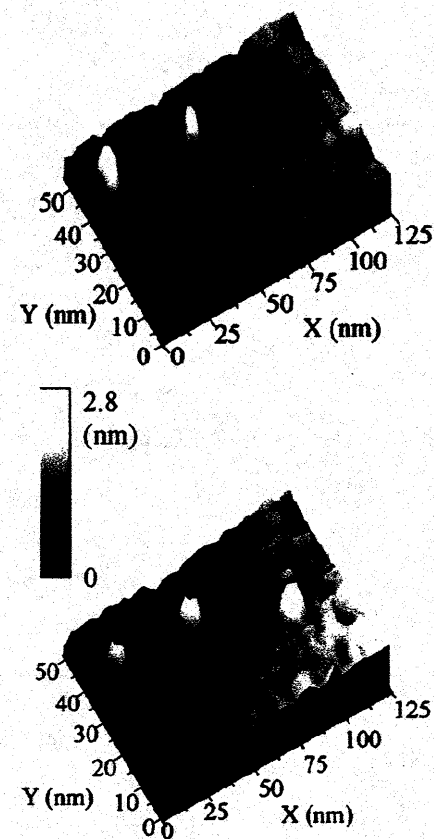
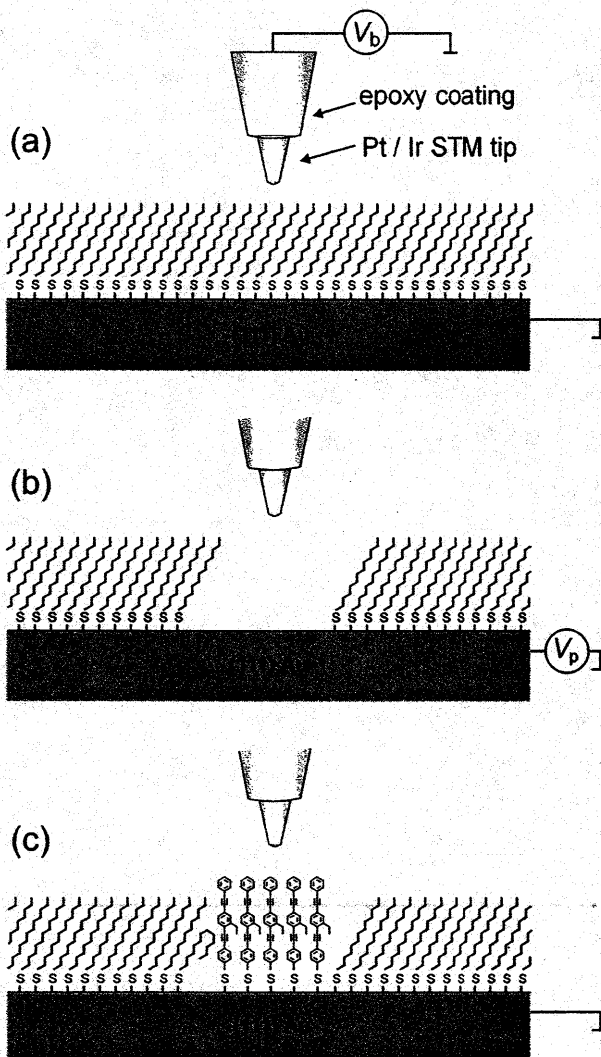
Figure 11: A nanomechanical three-terminal device [41]. The C_{60} molecule is contacted by the metallic substrate on one side, and by the STM tip from the opposite side. The steering parameter which replaces the third electrode is the force which acts on the STM tip. By pushing on the C_{60} molecule, the conductance varies by two orders of magnitude per nano-newton.

Figure 13:

Left: Illustration of the patterning of the SAM layer and the placement of electronically conducting 16 molecules in the alkanethiol matrix:

- (a) normal STM imaging of the SAM surface with a tip bias V_b ;
- (b) SAM removal by applying a pulse V_p to the substrate;
- (c) filling of the pit by 16 molecules from the solution (adapted from Ref. [36]).

Right: (top) the image of a dodecanethiol SAM surface after consecutive patterning, three pits show two peaks indicating adsorbed 16 and one pit without adsorption; (bottom) image taken few minutes later showing adsorption onto the third remaining pit.



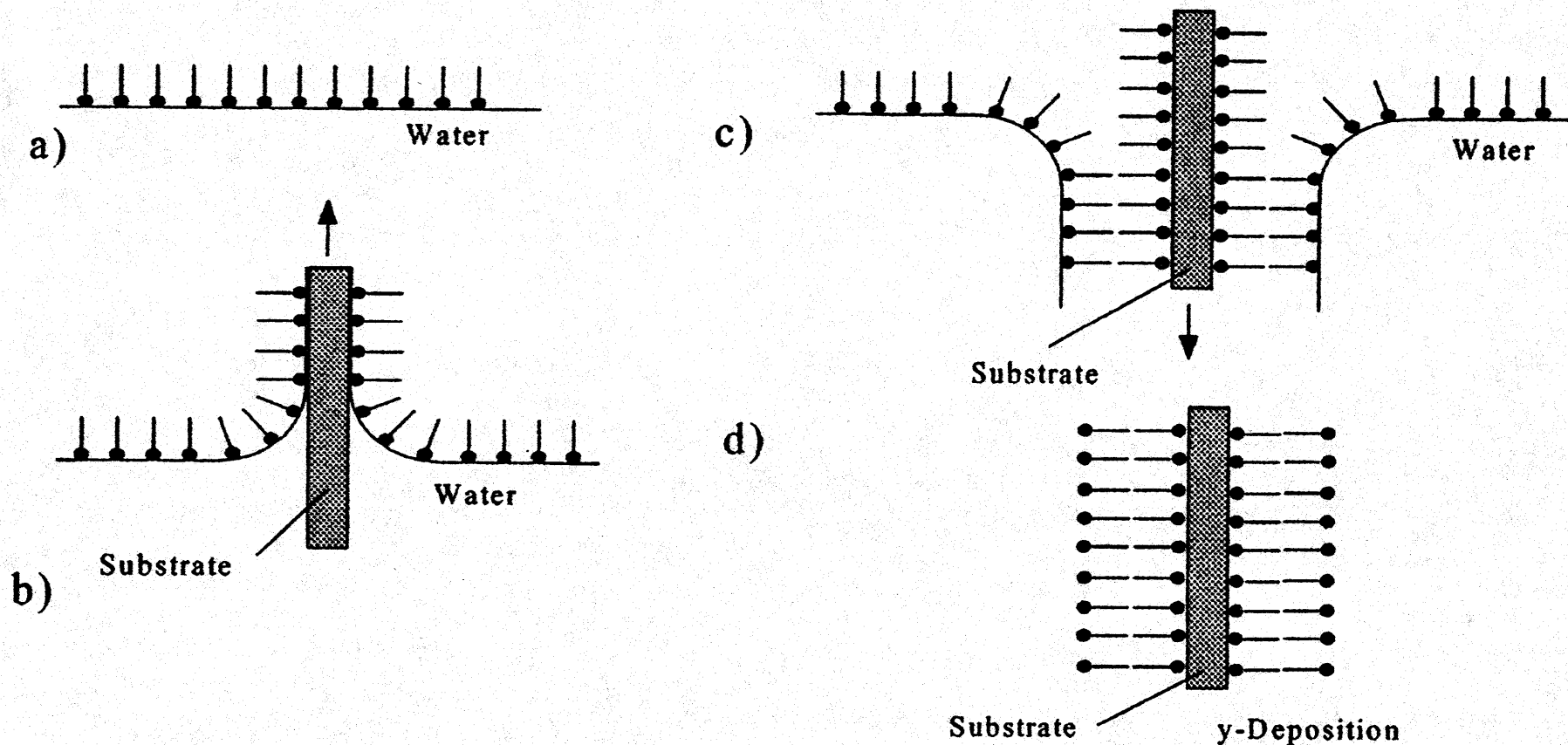


Fig. 11.2. Realization of artificial Langmuir-Blodgett films: (a) molecules align with their hydrophobic side on top of a water surface, (b) the aligned molecules attach to a substrate via adhesion, (c) and (d) by means of a further process step a double layer can be realized

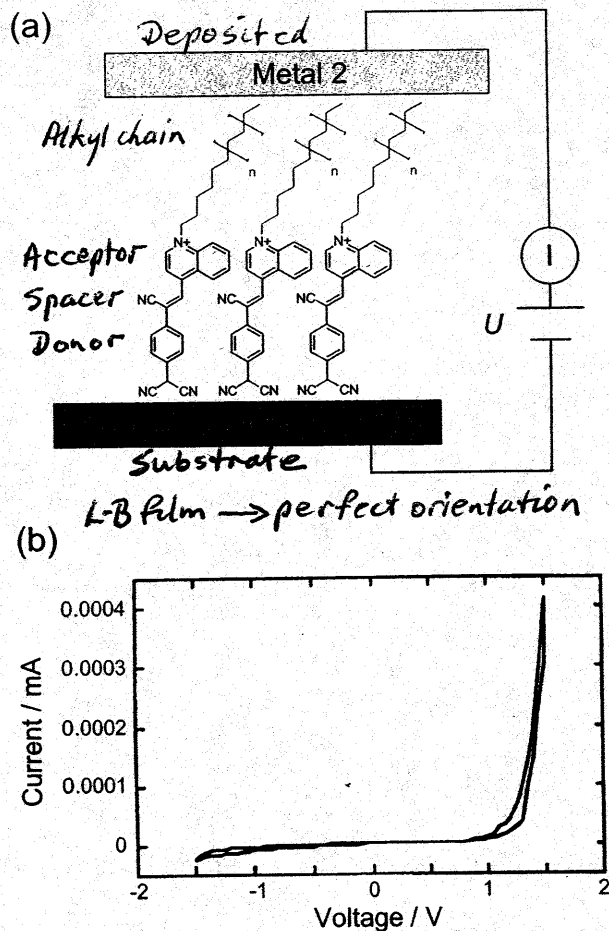


Figure 14:
 (a) Schematic presentation of a rectifying device based on an LB-film of the donor-acceptor molecule 12.
 (b) The $I-V$ curve of the sandwiched LB-monolayer displaying rectifying character.

Can also get NDR characteristics from LB films.

← L-B Diode

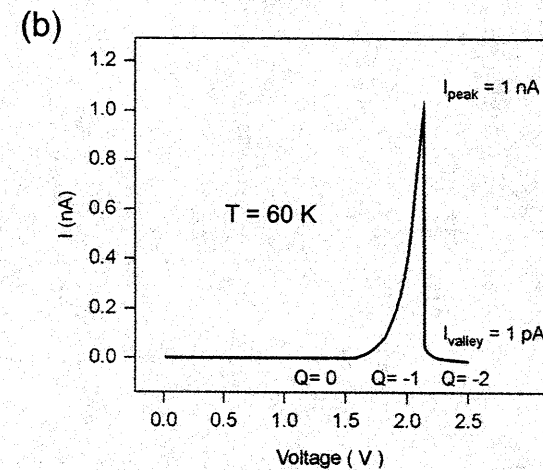
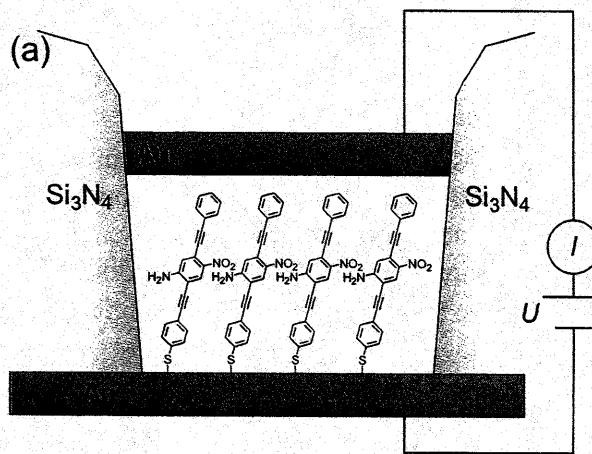


Figure 18:
 (a) Schematic presentation of the NDR-device. SAM of 13 between two Au electrodes laterally limited by Si_3N_4 walls.
 (b) The $I-V$ characteristics of the device displaying an negative differential conductance (NDR). The Q values are suggested to refer to the charge (in electrons) set by the bias voltage according to the theoretical studies [54].

Negative Differential Resistance NDR ↑

I-V curves :

Note similarity to Coulomb Block characteristic

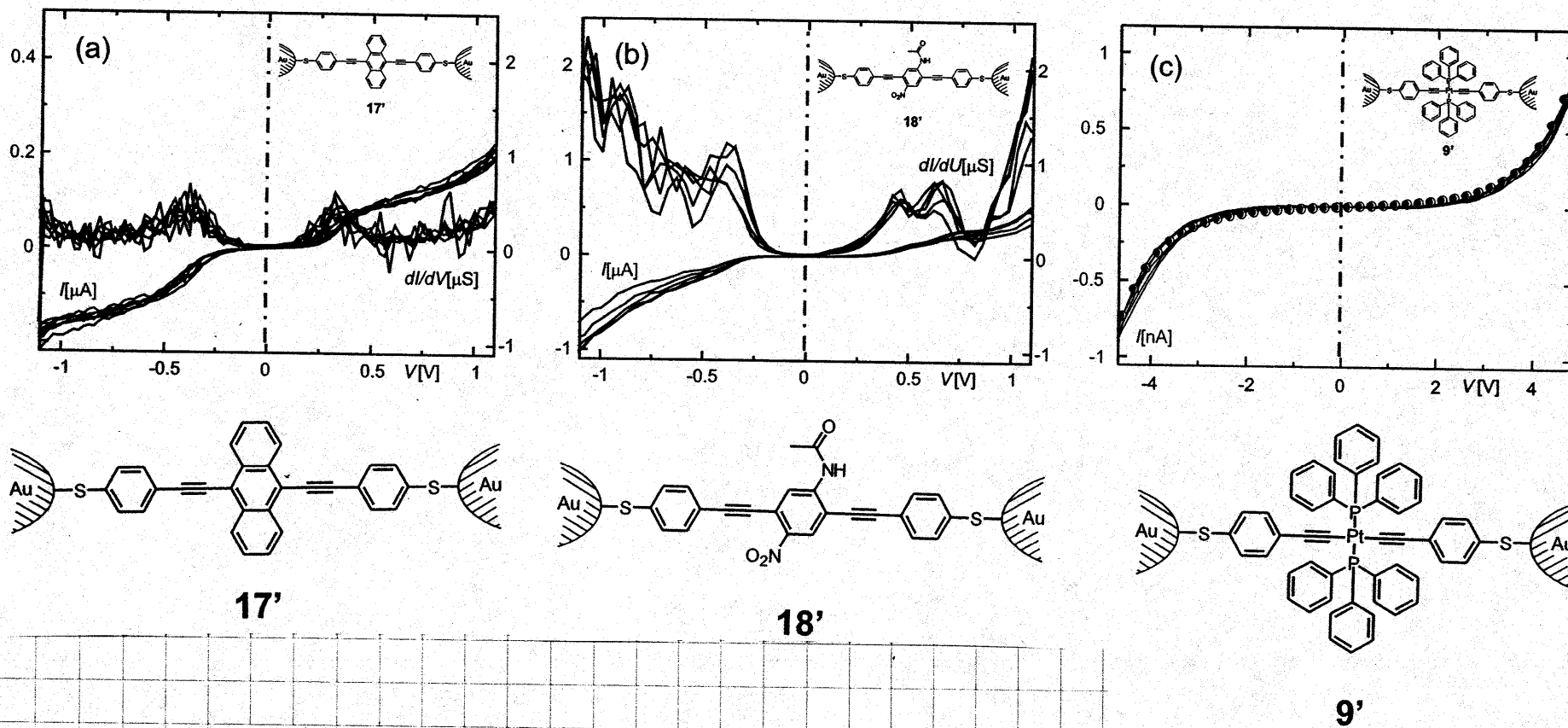


Figure 21: I - V curves (red) and differential conductance dI/dV (blue) for a) Au-17'-Au and b) Au-18'-Au. c) I - V curve (red) for Au-9'-Au and simulated current with a barrier height of 2.5 eV (blue circles) are shown.

Figure 20: Rigid molecular rods 17', 18' and 9' immobilized between two gold electrodes with terminal sulfur groups.

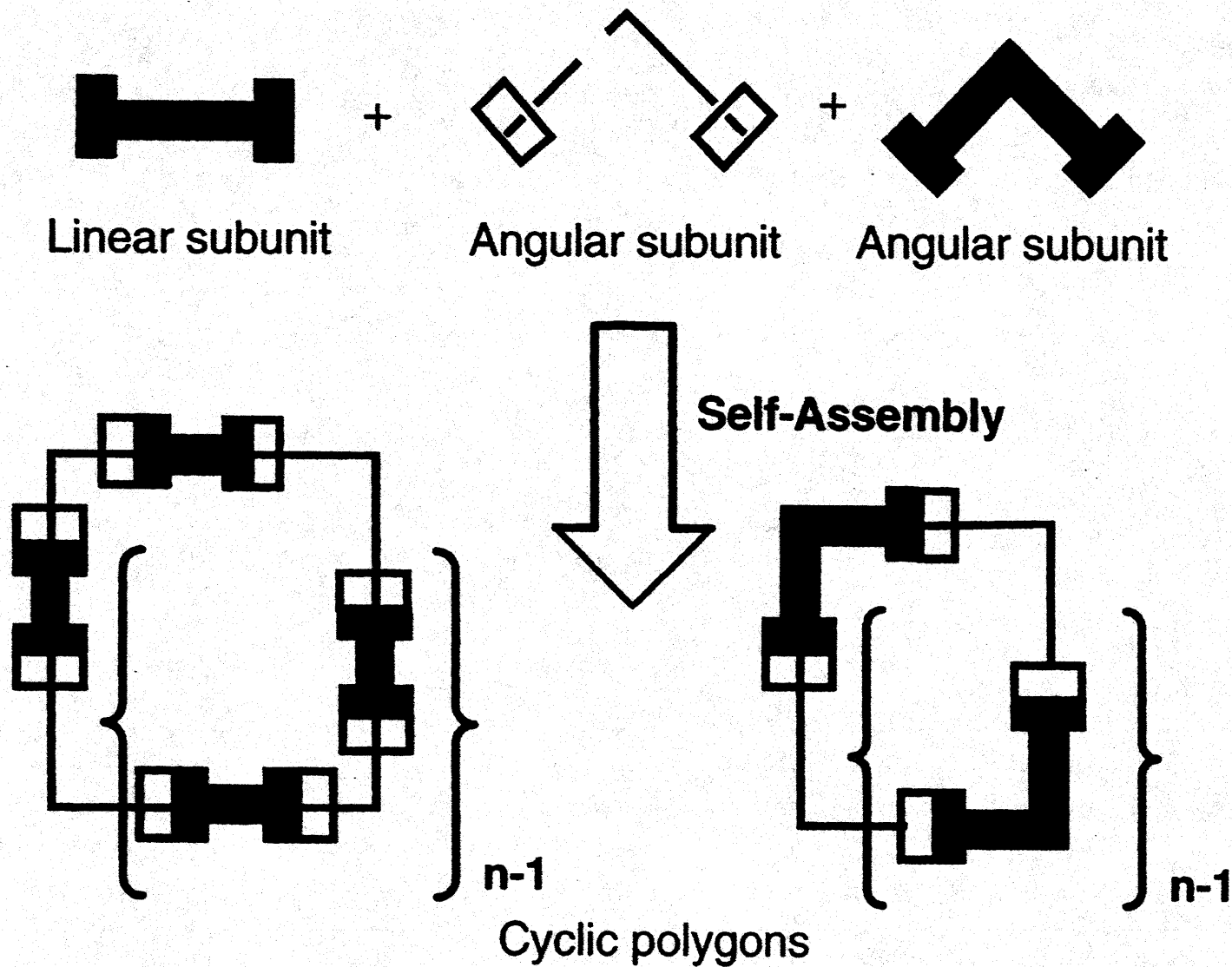
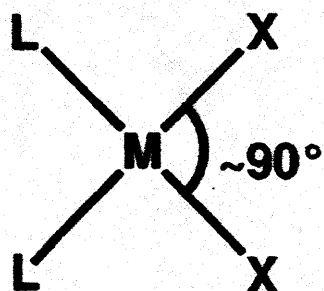
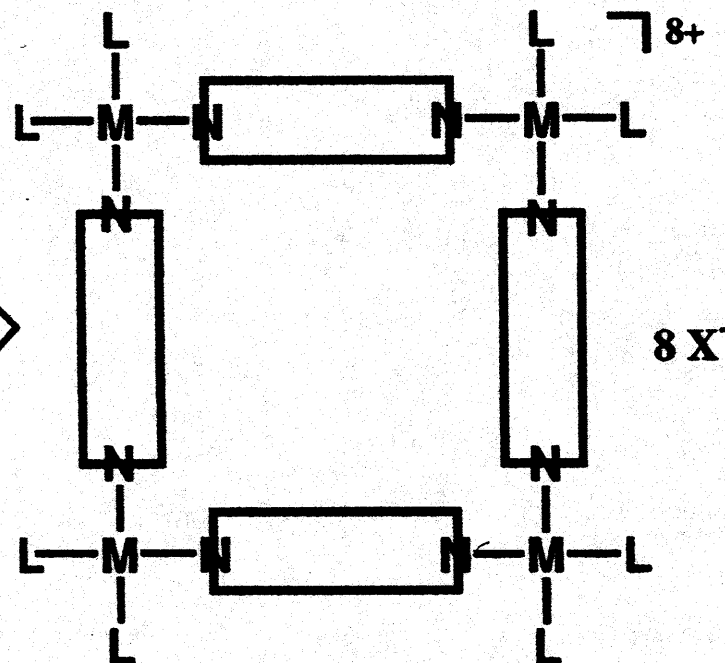
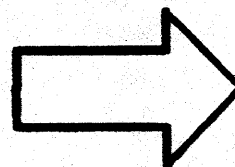


Figure 11.11. Cyclic polygons (bottom) constructed from building blocks (top) by the use of linear and angular subunits (lower left), and by the use of the two types of angular subunits (lower right). [From P. J. Stang and B. Olenyuk, in Nalwa (2000), Vol. 5, Chapter 2, p. 169.]



+



M=Pd, Pt
X= OTf^- , H_2O , NO_3^-
L= Et_3P , 1/2 dppp,
1/2 $\text{H}_2\text{N}(\text{CH}_2)_2\text{NH}_2$

Figure 11.12. Programmed self-assembly of four linear and four 90° angular subunits to form a molecular square. [From Stang and Olenyuk, Nalwa (2000), p. 171.]

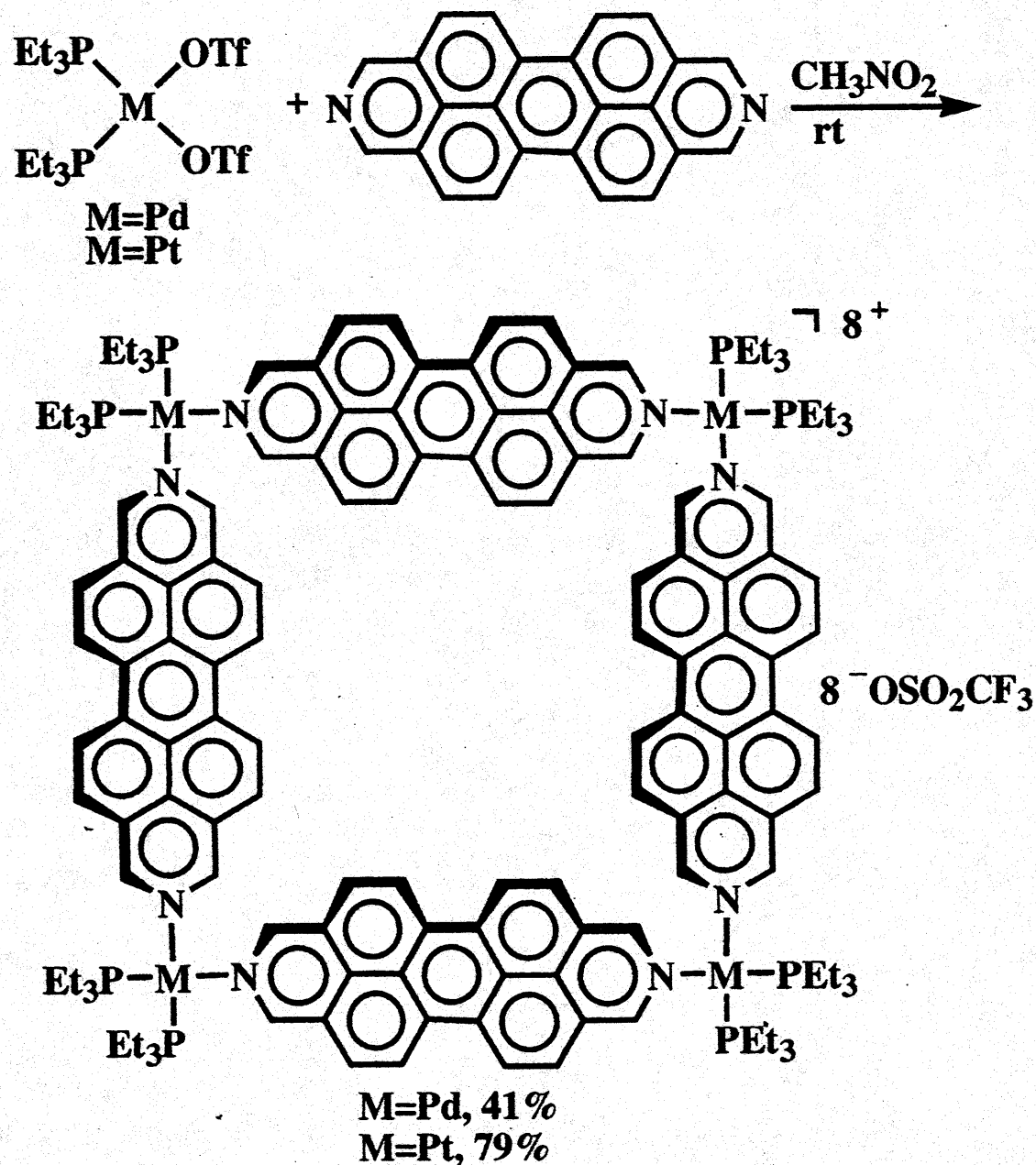


Figure 11.13. Molecular square formed by the self-assembly process of Fig. 11.11 from the subunits acyclic bisphosphane on the upper left and 2,9-diazabenzoc[cd,m]perylene on the upper right, where Et denotes an ethyl group $-\text{C}_2\text{H}_5$, and M can be either a Pd or a Pt atom. The overall +8 charge of the structure is balanced by eight $-\text{OSO}_2\text{CF}_3$ counterions, as indicated.

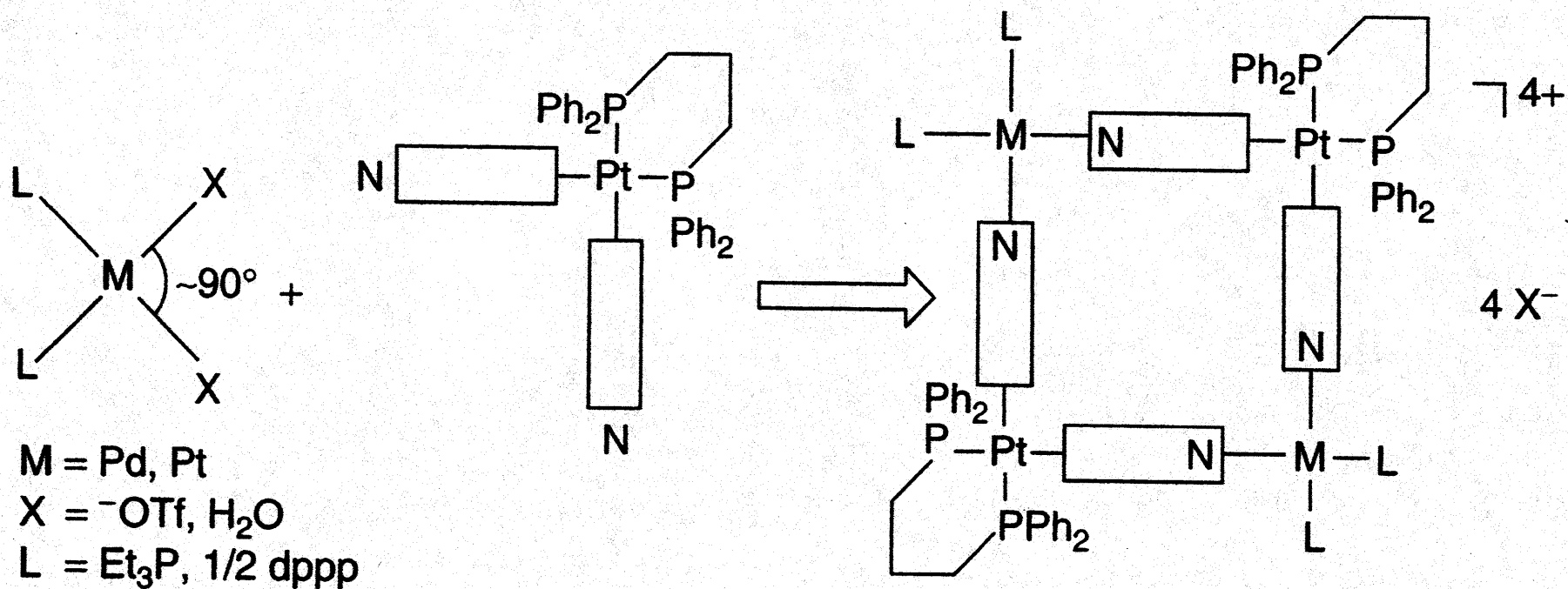


Figure 11.14. Programmed self-assembly of two types of angular subunits to form a molecular square [From Stang and Olenyuk (2000), p. 180.]

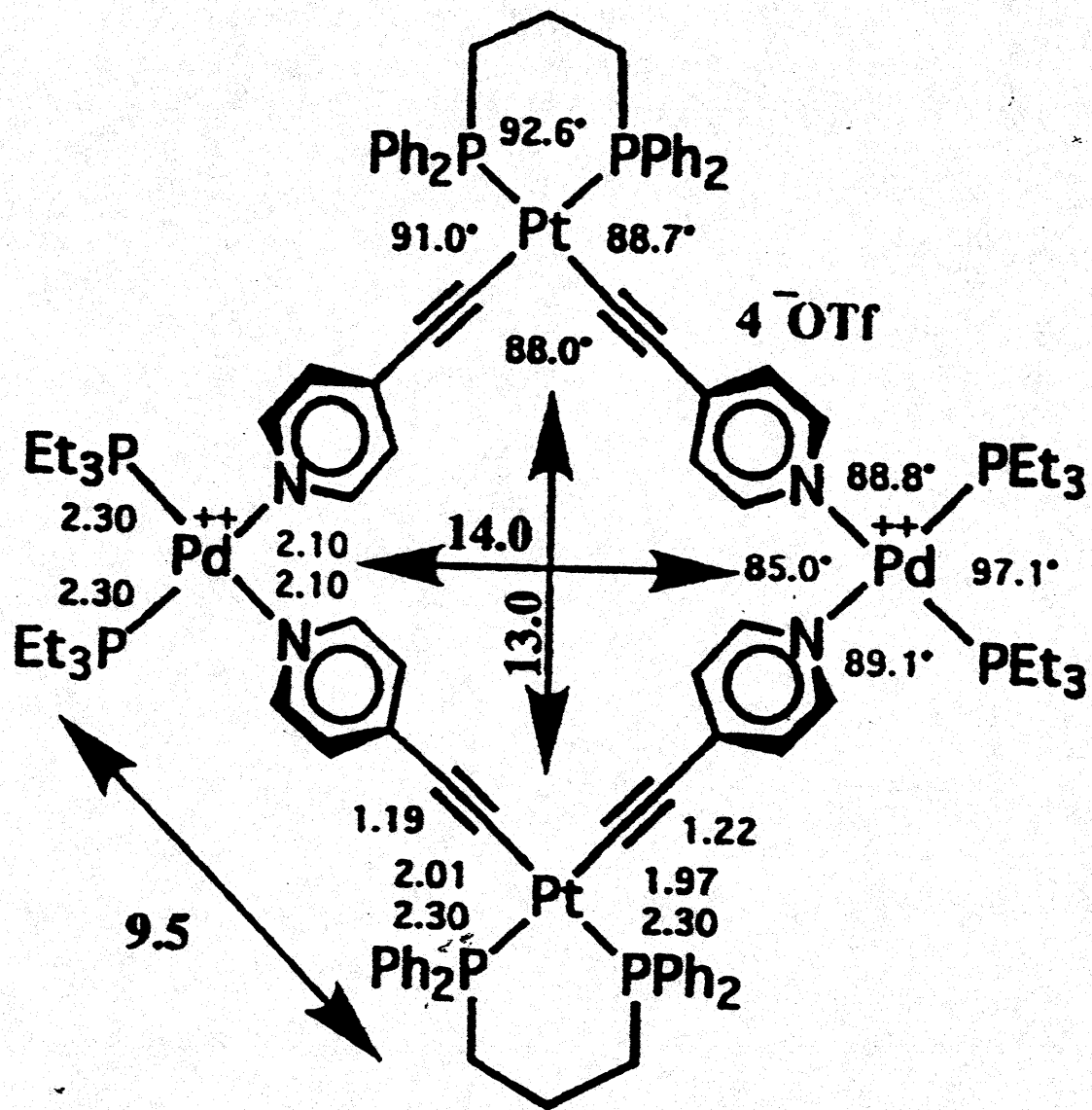


Figure 11.15. Molecular square formed by the self-assembly process of Fig. 11.14 showing bond angles, bond lengths, and interatomic distances expressed in angstrom (Å) units ($10 \text{ \AA} = 1 \text{ nm}$), obtained from a single-crystal X-ray diffraction study. The symbol Et denotes an ethyl group $-\text{C}_2\text{H}_5$ and Ph, a phenyl group $-\text{C}_6\text{H}_5$. The overall charge of the structure +4 is balanced by four $-\text{OSO}_2\text{CF}_3$ counterions. [From Stang and Olenyuk (2000), p. 181.]

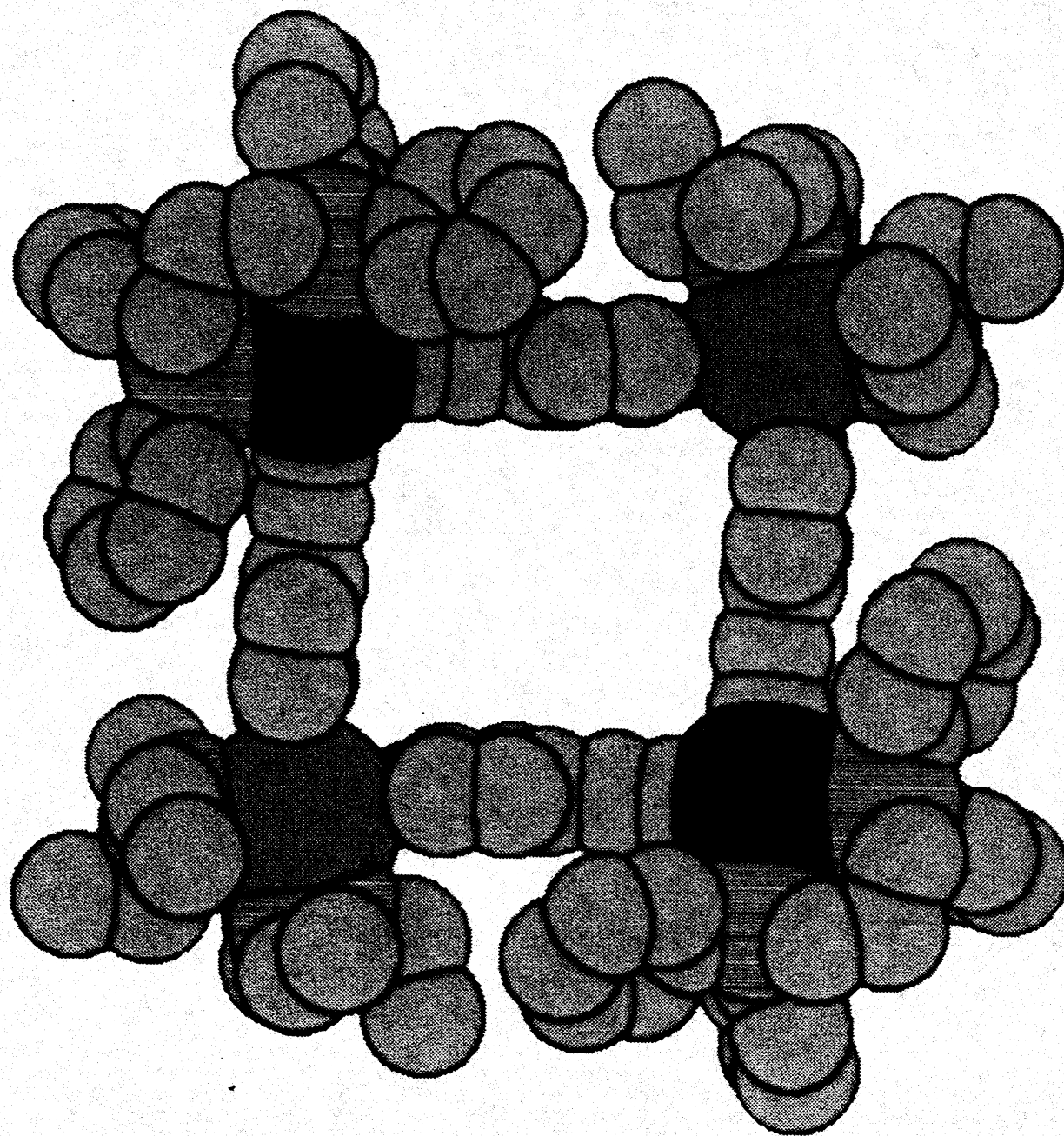


Figure 11.16. Space-filling model of the molecular square of Fig. 11.15, constructed from X-ray diffraction data. [From Stang and Olenyuk (2000), p. 182.]

ECE 417/517 NANO-ELECTRONICS

Spring 2007

Lecture 10: Carbon Nanotubes (CNTs)

- Introduction
- Fabrication
- Conduction & characteristics
- CNT transistors
- Complementary CNT circuits
- CNT resistor-transistor logic (RTL) circuits
- Miscellaneous

MULTI WALLED CARBON NANO TUBES

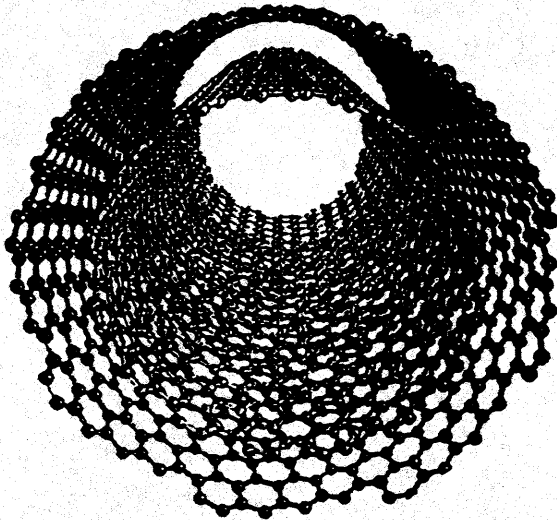


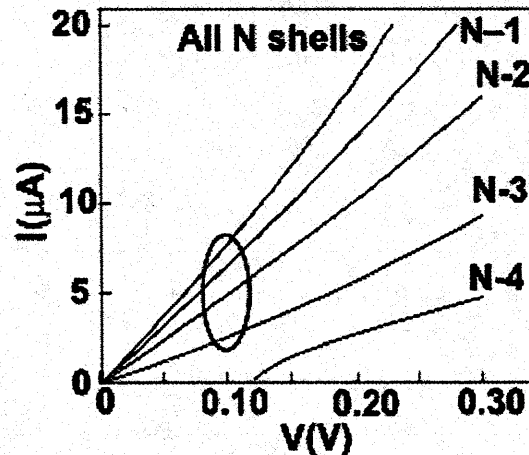
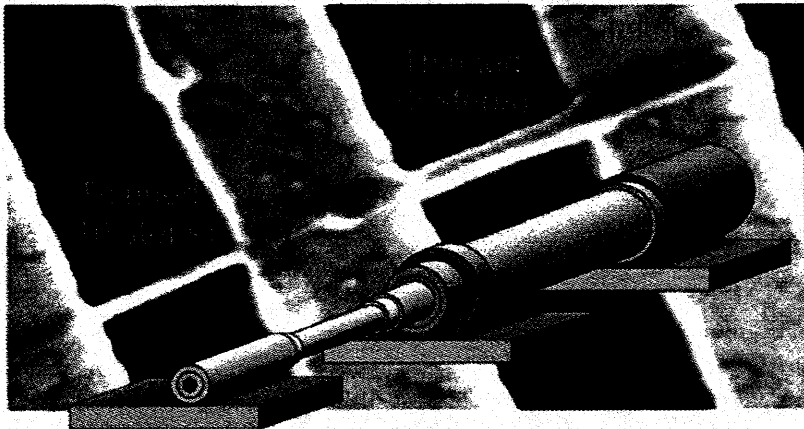
Figure 5.13. Illustration of a nested nanotube in which one tube is inside the another.

SWNT Single-walled nanotube
 MWNT Multi-walled nanotube

Each "shell" can have different indices, bandgaps, etc. Composite properties complicated.

Typically, outer shell conducts most current.

Contacts usually to outer shell



First 4 tube shells "coupled"

Fifth shell not coupled (≈ 0.1 v activation)

Figure 8^{8,14} - Thinned MWNT, layers removed, along with an I-V plot after removal of each shell

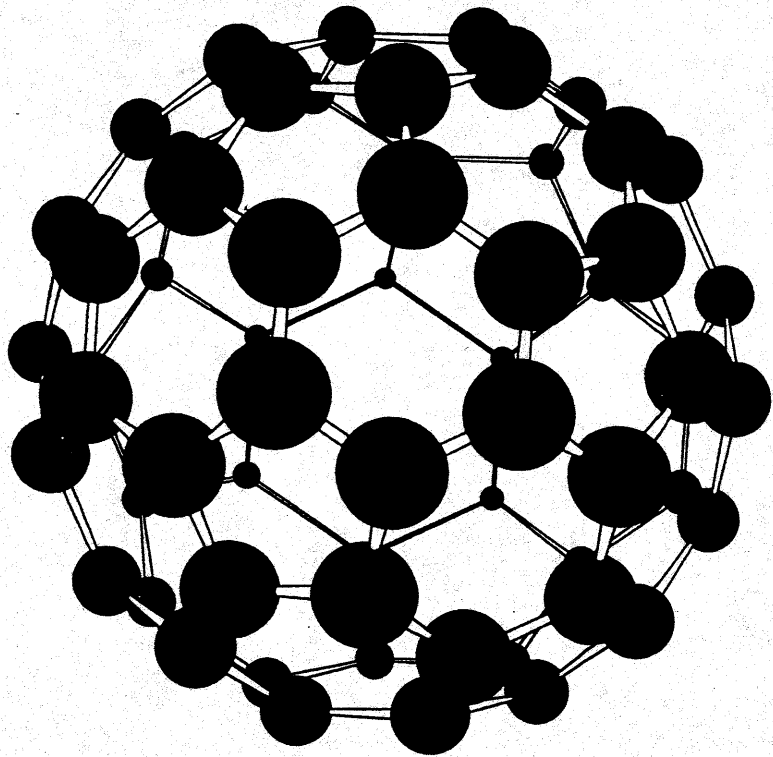


Figure 5.6. Structure of the C_{60} fullerene molecule.

Carbon \rightarrow graphite sheets

C_{60} fullerene [Buckminster Fullerene]

Doping \rightarrow alkali atoms
(superconductivity)

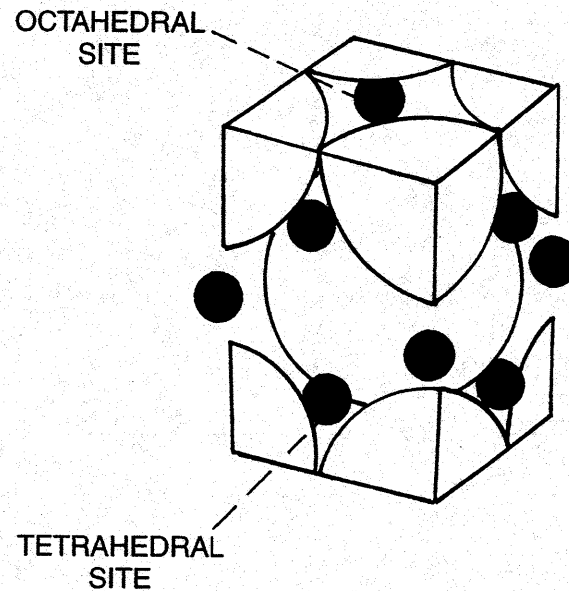
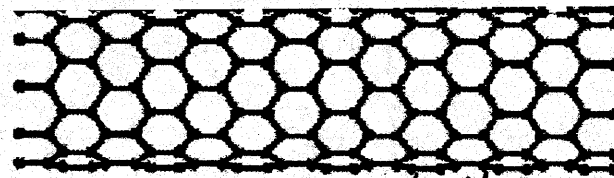
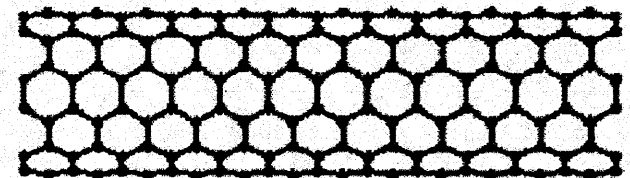


Figure 5.7. Crystal lattice unit cell of C_{60} molecules (large spheres) doped with alkali atoms (dark circles). [From F. J. Owens and C. P. Poole, Jr., *The New Superconductors*, Plenum, 1998.]

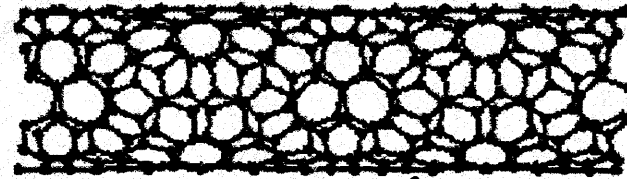
3 classifications



Armchair (Metallic) A
 $\theta = 30^\circ$

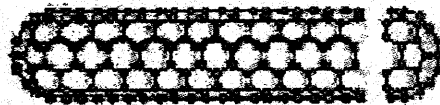


Zigzag B
 $\theta = 0^\circ$

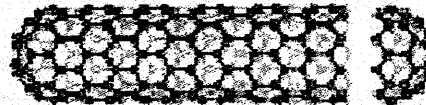


Chiral C
 $0^\circ < \theta < 30^\circ$

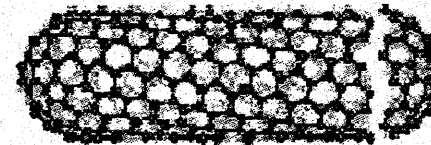
A simple way to determine if a carbon nanotube is metallic or semiconducting is to look at the indices that describe it, (n, m) . The nanotube will be metallic if $n = m$ or $n - m = 3i$, where i is an integer. Otherwise, the tube is semiconducting. The n and m indices can also be used to check which of the three categories a nanotube fits in, zigzag, armchair, or Chiral. Figure 5 shows examples of all three.



Zigzag
 $n = 0$ or $m = 0$



Armchair
 $n = m$



Chiral
 $n \neq m$

Figure 5¹¹ – Three types of Chirality.

The zigzag is characterized by its Zigzag shape, the armchair by its armchair shape, and the chiral by its twisted shape as highlighted. By combining figure 5 and the condition for type of conductor, armchair will always be metallic since $n = m$, while the others can be metallic or semiconductor. This is shown in figure 6.

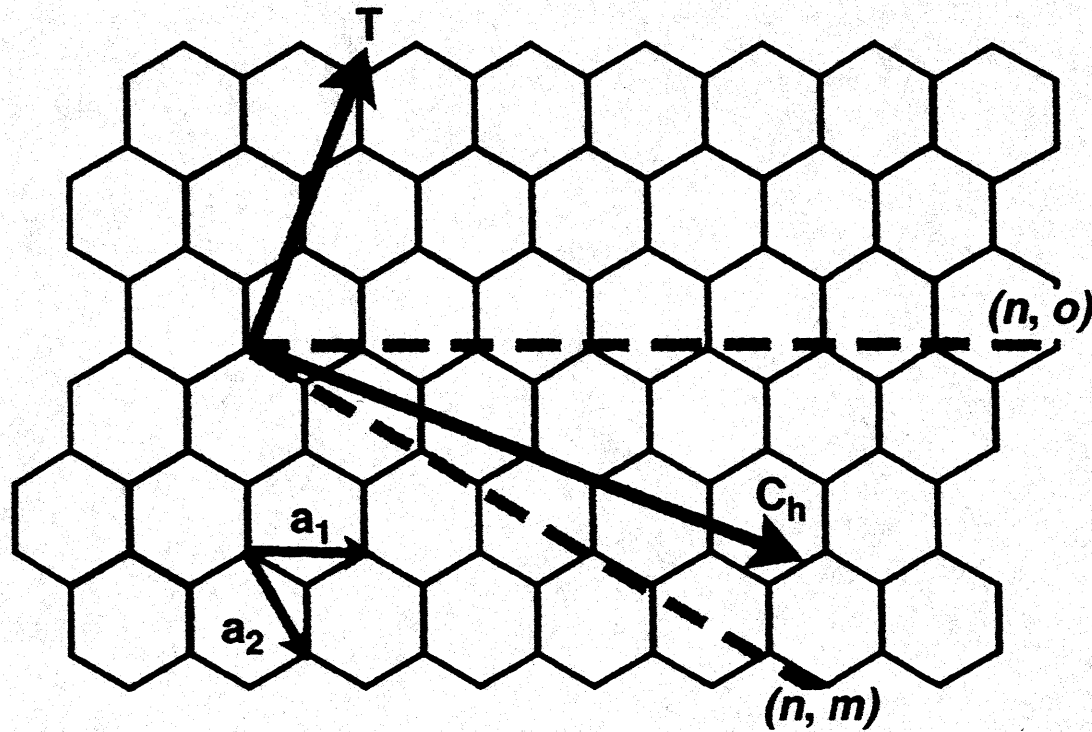


Figure 5.14. Graphitic sheet showing the basis vectors a_1 and a_2 of the two-dimensional unit cell, the axis vector T about which the sheet is rolled to generate the armchair structure nano-tube sketched in Fig. 5.11a, and the circumferential vector C_h at right angles to T . Other orientations of T on the sheet generate the zigzag and chiral structures of Figs. 5.11b and 5.11c, respectively.

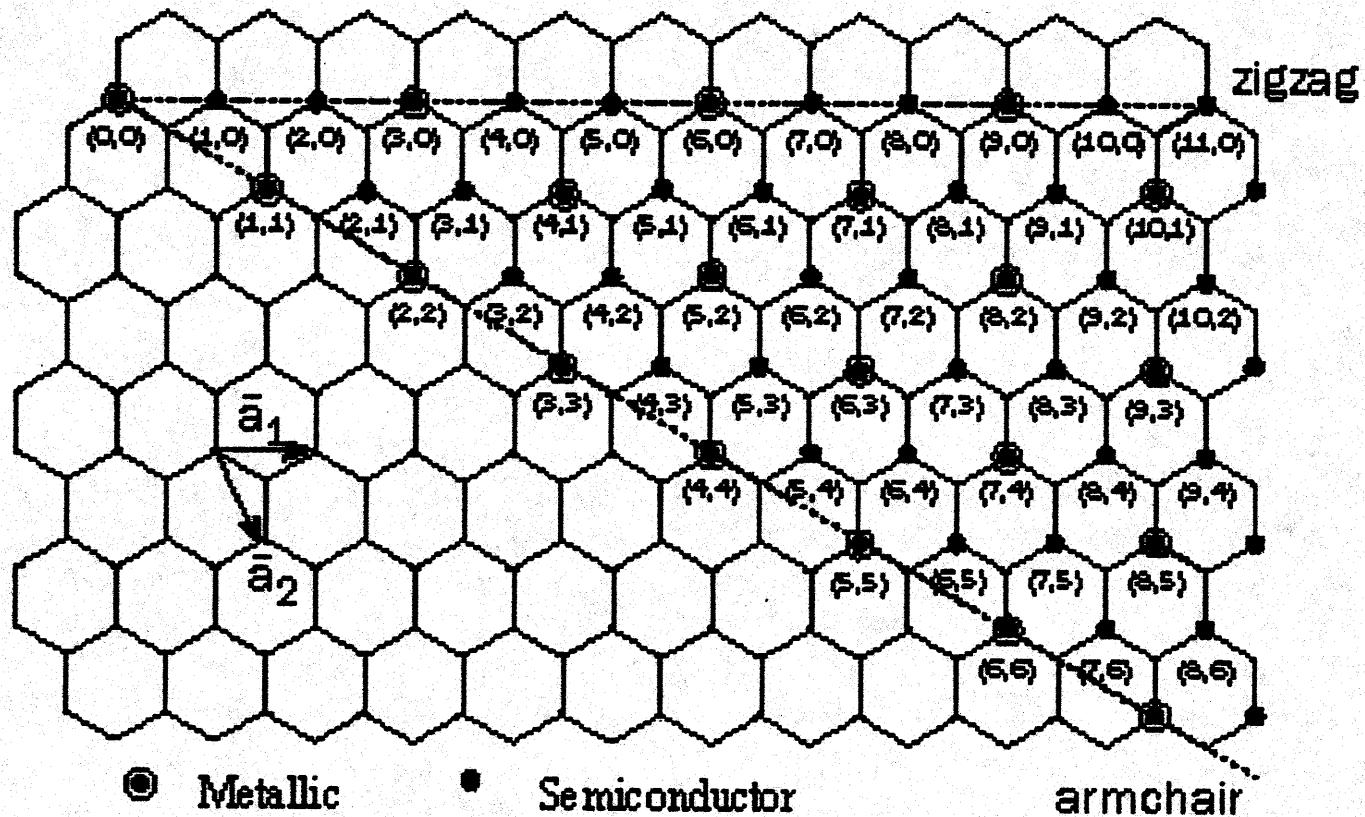


Figure 6⁹ – Metallic or semiconducting depending on which point the $(0, 0)$ point is rolled to.

If the $(0, 0)$ point is folded to any of the points along the armchair line, we get a metallic nanotube. However if it is folded along the zigzag line or in the chair area, which is the area between the zigzag and armchair, we get either semiconductor or metallic tube, depending on the n, m rules.

$$C = na_1 + ma_2, \quad (3.1)$$

where a_1 and a_2 are unit vectors of the graphene lattice, and the numbers n and m are integers.

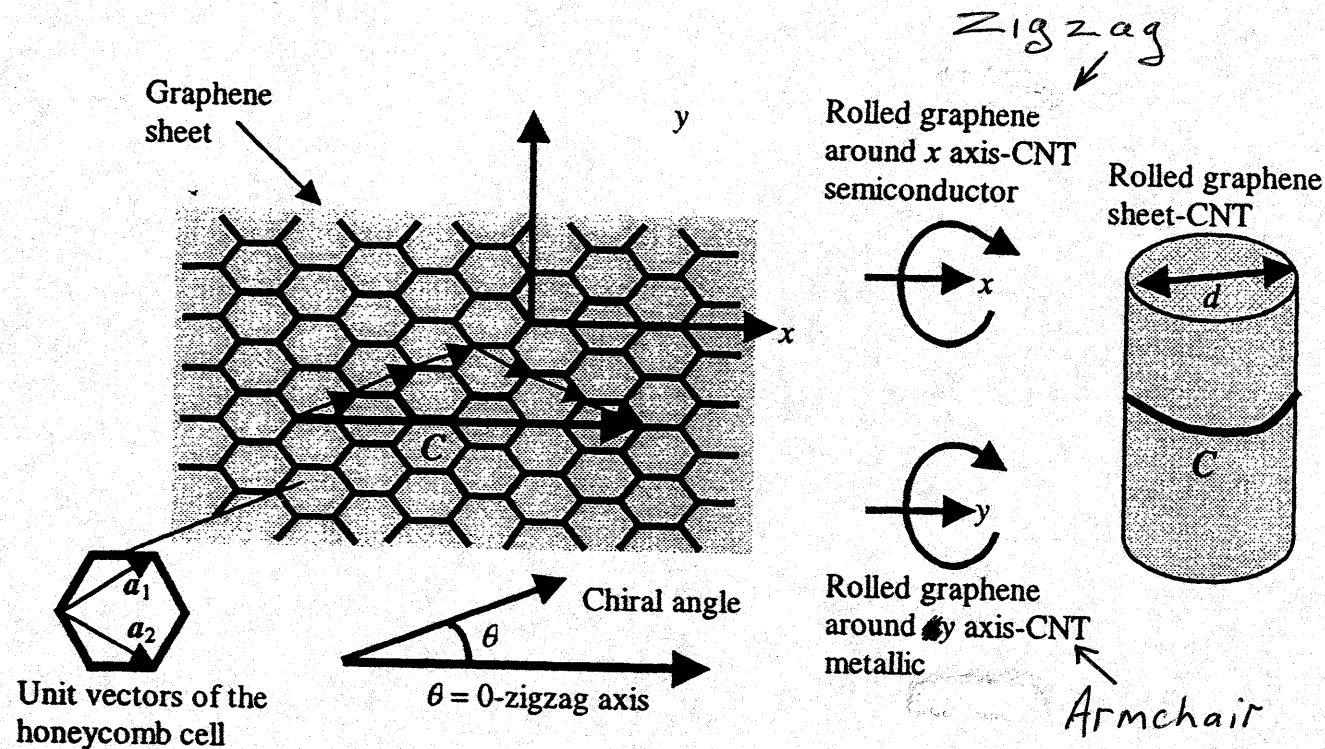


Figure 3.1 Schematic description of the CNT structure.

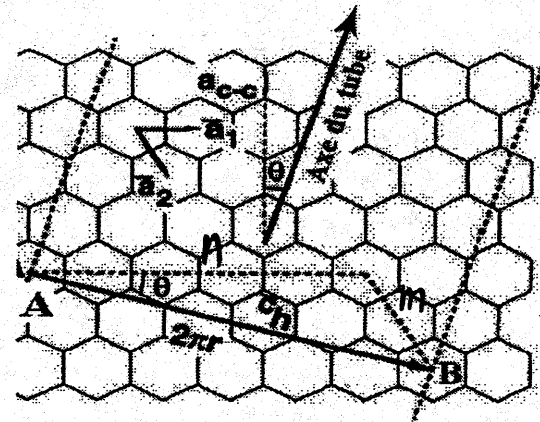
The set of integer numbers (n, m) describes entirely the metallic or the semiconducting character of any CNT. In general, the CNT is metallic if $n = m$, it shows a small bandgap (has allegedly a semimetallic character) if $n - m = 3i$, with $i = 1, 2, 3, \dots$, and is semiconducting when $n - m \neq 3i$ [1]. The most encountered situations are the (n, n) metallic CNTs, also called armchair CNTs, and the CNTs characterized by $(n, 0)$, which are semiconducting and are termed zigzag CNTs

A pair of indices (n,m) called the chiral vector is used to describe the way graphene being wrapped, the electrons become confined to the circumference of the nanotube as shown below. The integers n and m denote the number of unit vectors along two directions in the honeycomb lattice of graphene. The integer n represents the number of carbon atoms around the circumference of the tube, and the integer m means the number of atoms down the tube axis. This can also be illustrated by a quantization formula: $\vec{k}_c \cdot \vec{C} = 2\pi i$, where \vec{k}_c is the wavevector in the circumference direction, \vec{C} is the chirality vector, and i is an integer.

- Local basis (a_1, a_2)
- Its chiral vector $\vec{C}_h = \vec{AB} = \vec{R} = n\vec{a}_1 + m\vec{a}_2$
- Its Hamada indices (n, m)
- Its chiral angle θ $\cos \theta = \frac{(2n+m)}{2\sqrt{n^2+m^2+nm}}$
- Its diameter $d = AB = \frac{\|\vec{C}_h\|}{\pi} = \frac{a\sqrt{n^2+m^2+nm}}{\pi}$

(C_h is circumference)

- a) Therefore, knowing the m, n values, we can determine the CNT size and how twisted the CNT is.
- b) If $m=0$ or $n=0$, the nanotubes are called "zigzag". If $n=m$, the nanotubes are called "armchair". For all the other conditions, the nanotubes are called "chiral".
- c) Due to the symmetry and unique electronic structure of graphene, the structure of a nanotube strongly affects its electrical properties. For a given (n,m) nanotube, if $2n + m = 3q$ (where q is an integer), then the nanotube is metallic, otherwise the nanotube is a semiconductor. Thus all armchair ($n=m$) nanotubes are metallic, and nanotubes (5,0), etc. are semiconducting. An alternative (equivalent) representation of this condition is if $(n - m)/3 = \text{integer}$, then the SWNT is metallic. (ref.1)



$$n = 5, m = 2$$

A single graphene sheet and its characteristic parameters.

$$E_{Gap} = \frac{4\pi V_F}{3d}$$

d) Different (n,m) also affects the energy stability of the system. The following table indicates that by wrapping the Haeckelite sheet into a tubular structure, even one with a complex curvature, the energetic stability of the system increases. (ref.2)
 E: energy per atom; Eg width of the topological band gap

(n, m)	d (nm)	E (eV/atom)	Eg (eV)
(1, 0)	0.223	-6.38	-
(1, 1)	0.259	-6.81	-
(4, 0)	0.892	-7.00	-0.1
(4, 4)	1.038	-7.04	0.48
(0, 4)	0.665	-7.06	0.65
<i>Metallic</i> → (5, 2)	1.119	-7.02	-0.1

n-m = 3

Reference:

1. www.eng.auburn.edu/~Vagrawal/talks/nanotube_v3.1.pdf
2. László P Biró, Géza I. Márk, and Philippe Lambin "Regularly Coiled Carbon Nanotubes", IEEE TRANSACTIONS ON NANOTECHNOLOGY, VOL. 2, NO. 4,

High Frequency Effects

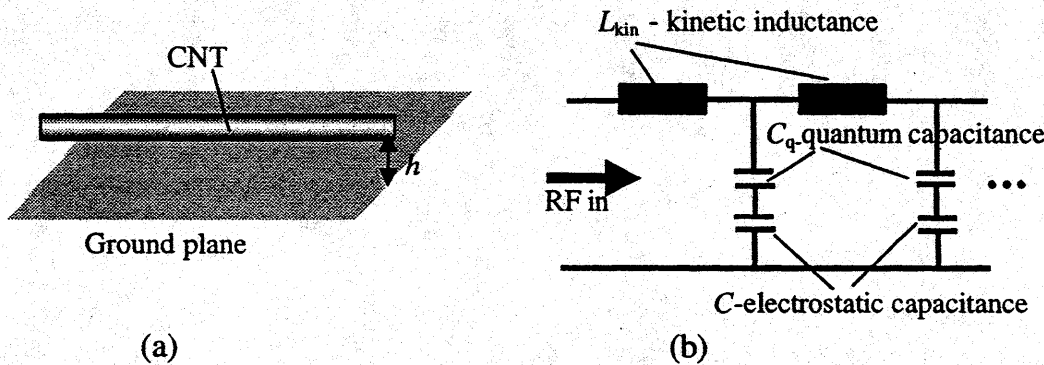


Figure 3.40 (a) The CNT transmission line, and (b) its equivalent circuit (After: [63]).

$L_{kin} \rightarrow$ Not magnetic field effect.
Electron inertia
Current delay \rightarrow

$$L_{kin} = h / 2q^2 v_F$$

$$v_F = 8 \times 10^5 \text{ m/s} \rightarrow \sim 16 \text{ nH}/\mu\text{m}$$

$$\gg L_{magnetic}$$

Add electrons to quantum states $> E_F$
 $\Delta E = h v_F / 2$

$$= e^2 / C_q$$

gives $C_q = 2q^2 / h v_F$

$$\therefore v_{CNT} = (L_{kin} C_q)^{-1/2} = v_F$$

But $\rightarrow (L_{kin} C_{tot})^{-1/2} > v_F$

for $C_{tot}^{-1} = C_q^{-1} + C^{-1}$

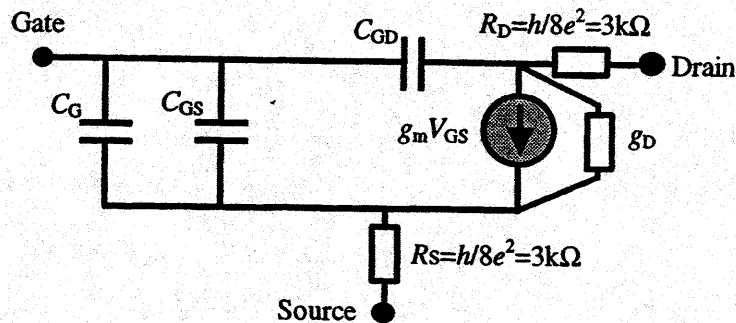
where $C = 2\pi\epsilon / \ln(h/d)$

$C_q \sim 100 \text{ aF}/\mu\text{m}$ $C \sim 50 \text{ aF}/\mu\text{m}$

$$Z = g (L_{kin} C_q)^{1/2} = g (h / 2q^2) = g / 12.5 \text{ k}\Omega$$

$$\sim 12.5 \text{ k}\Omega / \sqrt{3} \text{ for } C_q \sim 2C \text{ above}$$

Series R losses $\sim 1-10 \text{ k}\Omega/\mu\text{m}$



The simplified equivalent circuit of a CNTFET (After: [65]).

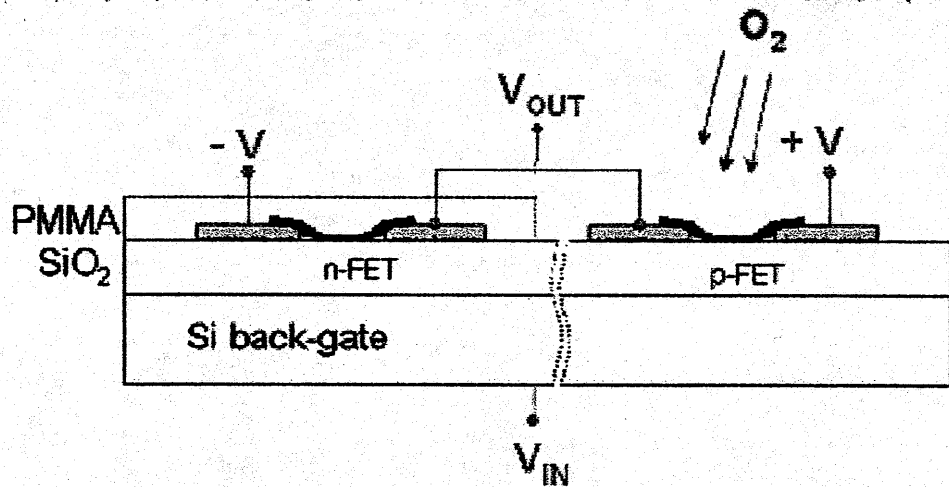
$$f_{RC} = (1/2\pi RC)^{-1} = 6.5 \text{ THz for } R = 6.25 \text{ k}\Omega, C = 4 \text{ aF}$$

$$C_{GS}^{-1} = C^{-1} + (4C_q)^{-1} \sim 50 \text{ aF}/\mu\text{m}$$

$$f_{gm} = \frac{g_m}{2\pi C_{GS}} \approx 0.5-3 \text{ THz}$$

for $g_m = 10 \rightarrow 60 \mu\text{S}$
 $\rightarrow 2.6 \text{ GHz for } 32 \text{ nm gate}$

COMPLEMENTARY INVERTER



Inverter created using annealing to create n-FET (n-type) and uses exposure to oxygen to convert to p-FET (p-type).

Fabrication A: Annealing

Start with identical devices (p-type)

Choose device to be n-type

Seal n-type device with PMMA

Anneal 200°C , 10 hours
(both now n-type)

Expose to O_2 , 10^{-3}T , 3 min
(unprotected device \rightarrow p-type)

Fabrication B: Doping

Seal both (initially p-type) devices with PMMA resist.

Open window above n-device with e-beam lithography

Dope with electron donor (eg. K)
(Adjust so thresholds overlap)

Sealed device remains p-type

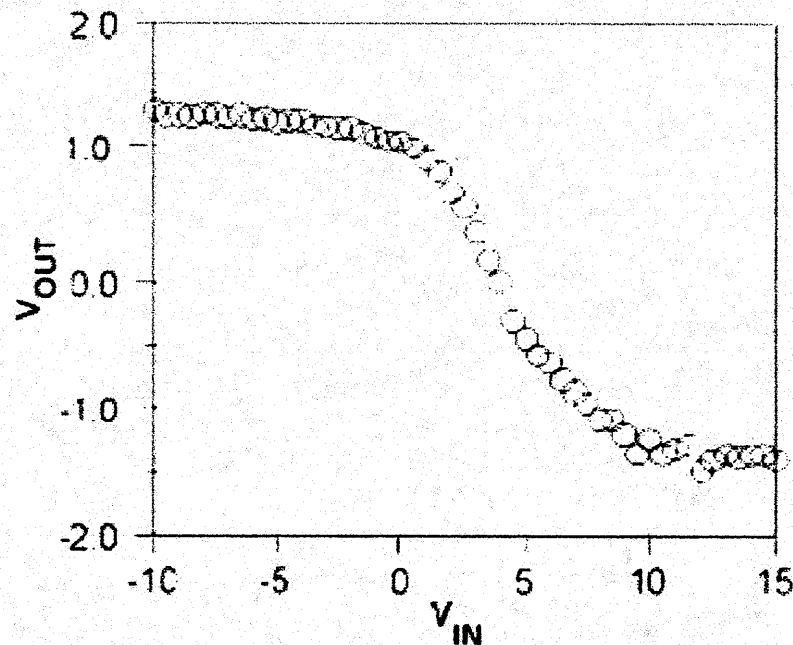


Figure 45²⁸ – Transfer curve of complementary CNFET inverter

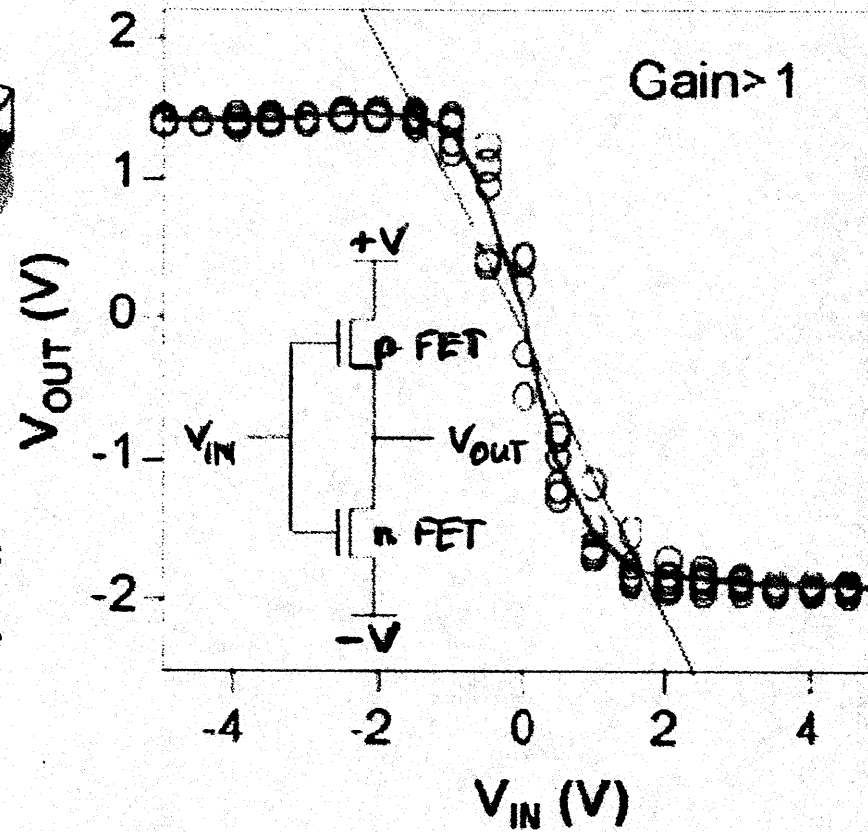
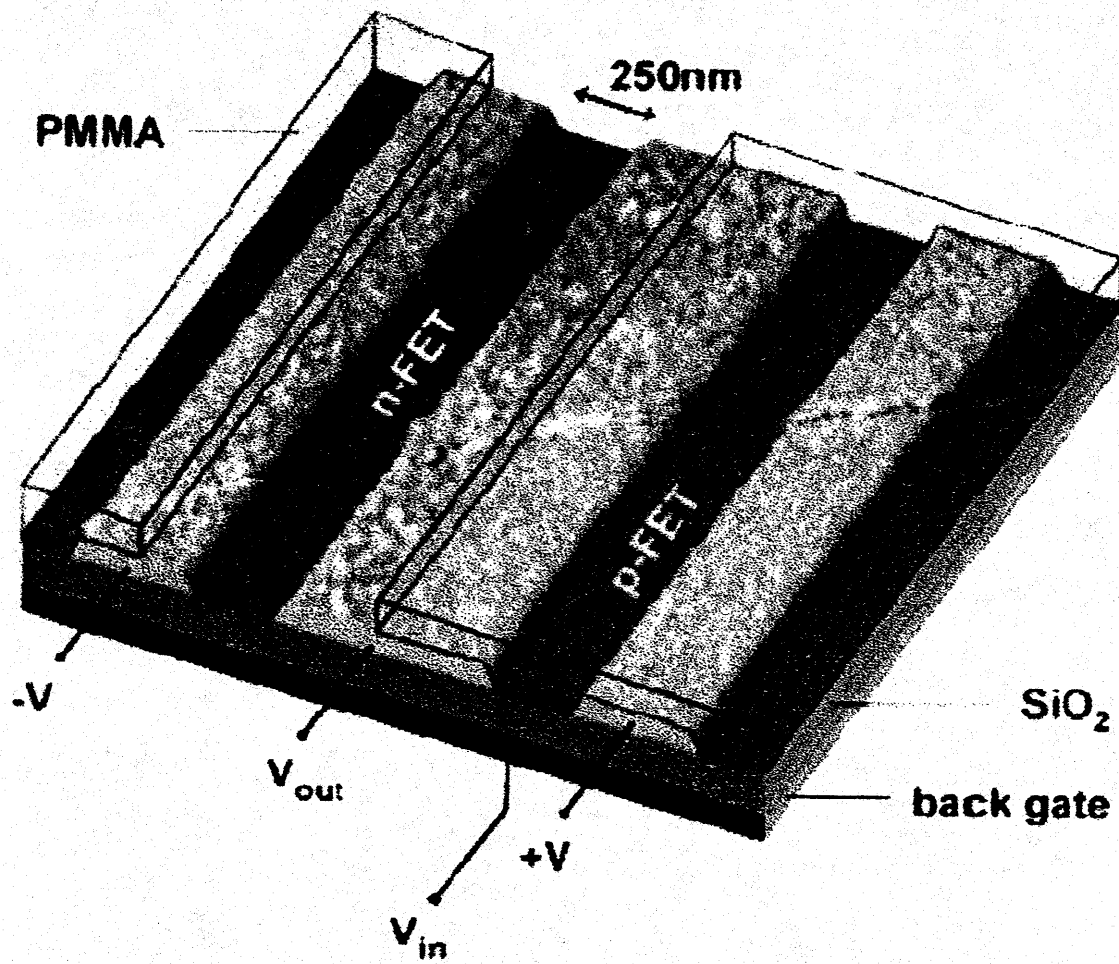


Figure 49²⁸ – Intra-nanotube inverter, n-FET left open for doping.

1.16.1.3 Resistor-Transistor Logic Inverter

Another way to create an inverter is to use Resistor-Transistor Logic (RTL). A schematic of an inverter in RTL logics is shown in figure 46.

General approach
which only needs
one type of device
(n-type or p-type)

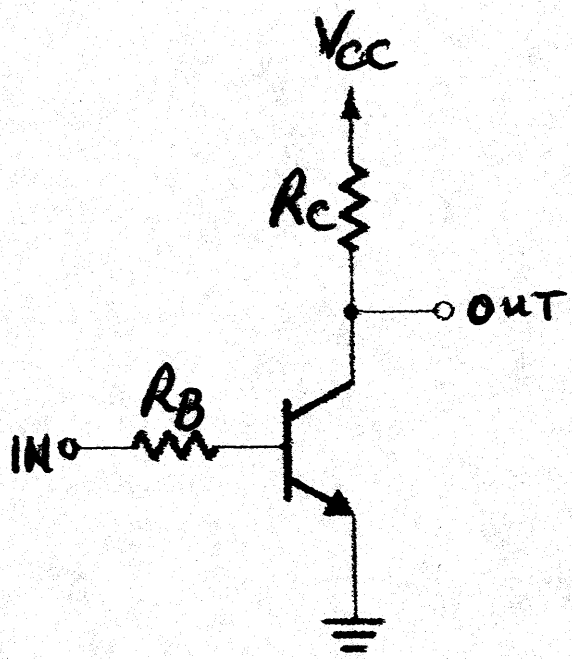


Figure 46²⁰ – Schematic of an inverter using RTL technology.

RTL - type Inverter

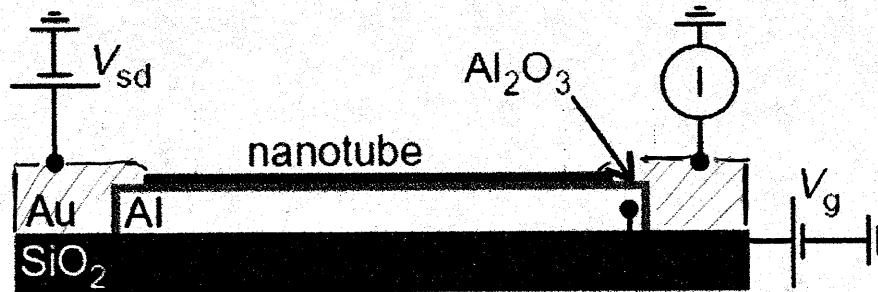
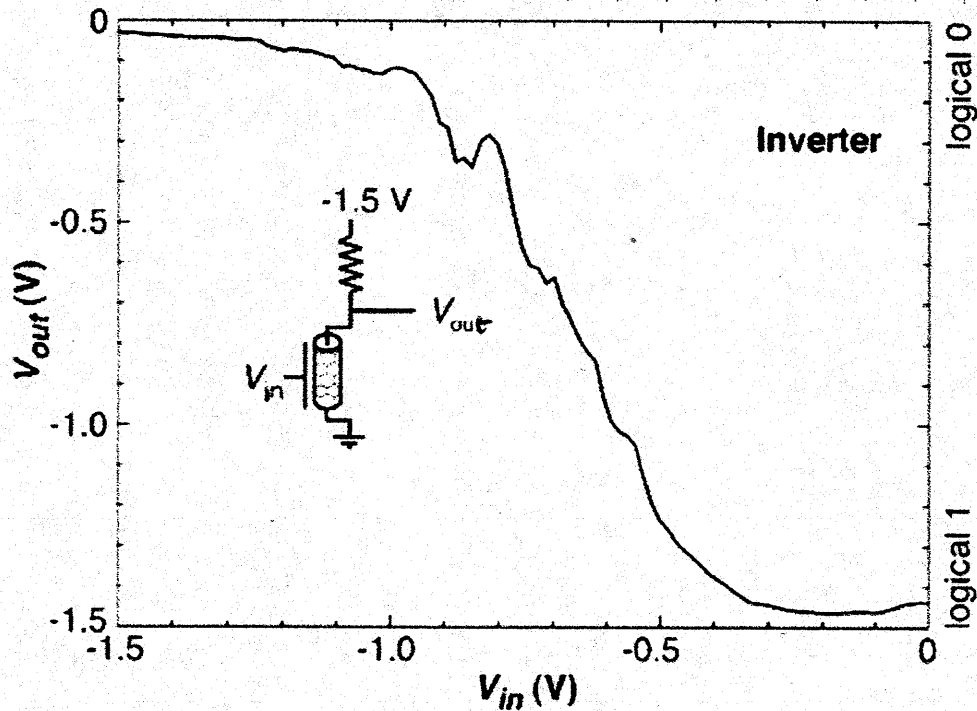
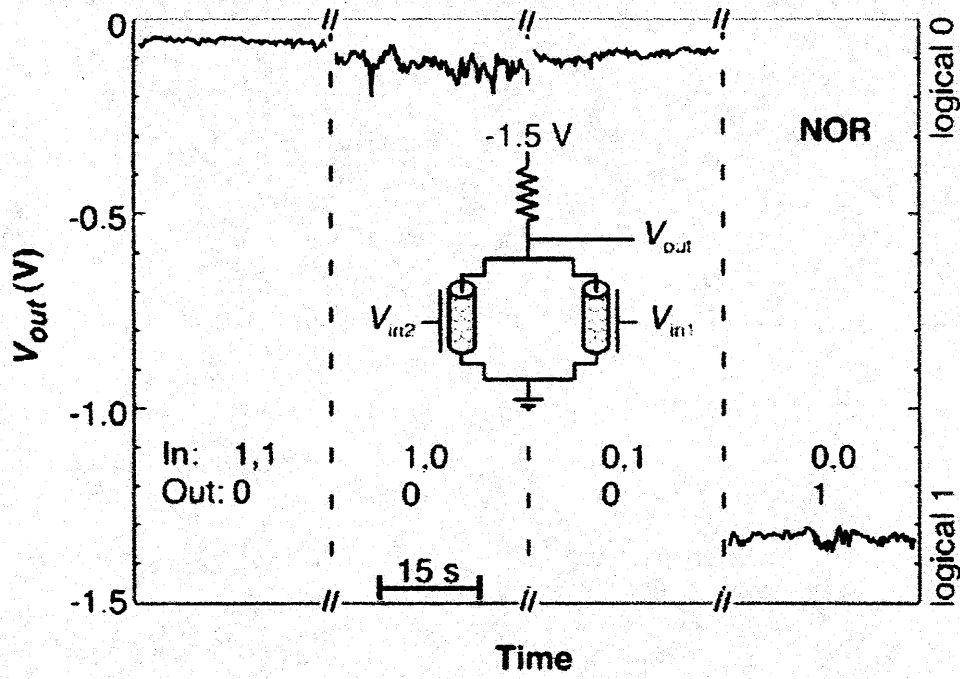


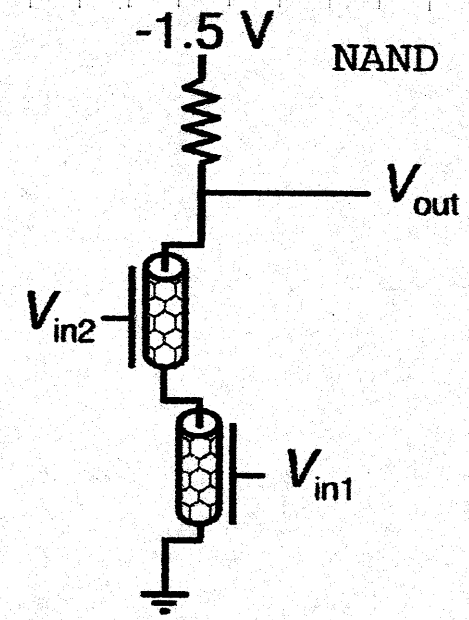
Diagram of an RTL inverter, using a hybrid design of the first and second generation.



- Transfer curve for a CNFET inverter, using RTL technology. Only a n-type CNFET is used.

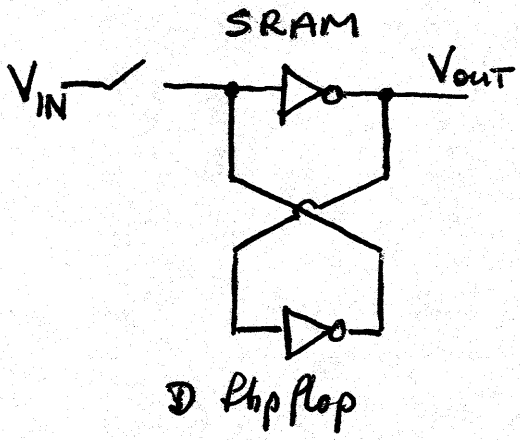


NOR gate

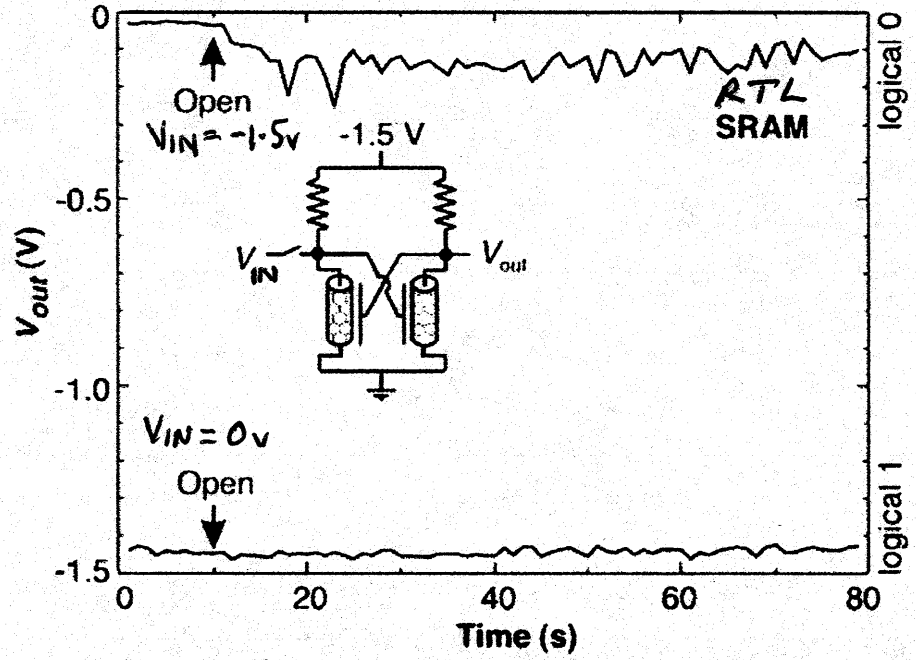


Schematic of a RTL NAND gate, using CNFETs

Schematic of a RTL inverter with CNFETs, along with its output voltage as a function of inputs.



1T1R SRAM



1T1R SRAM

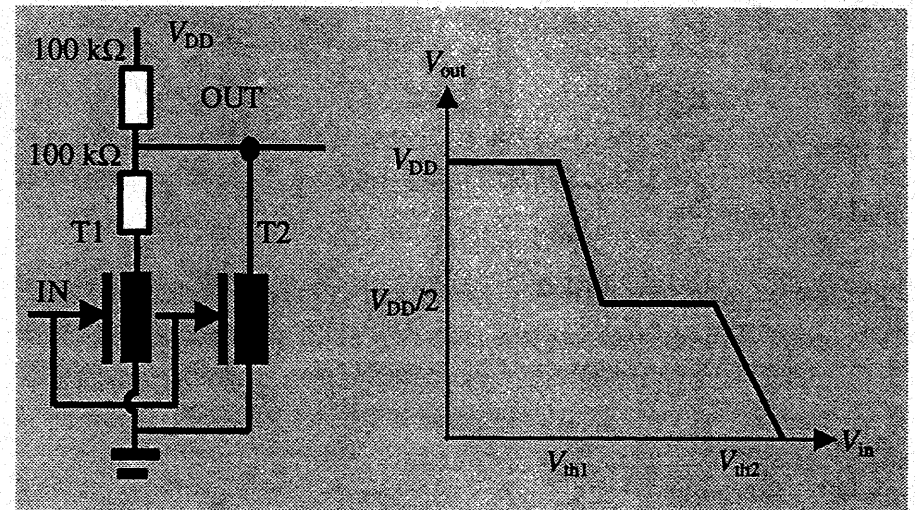
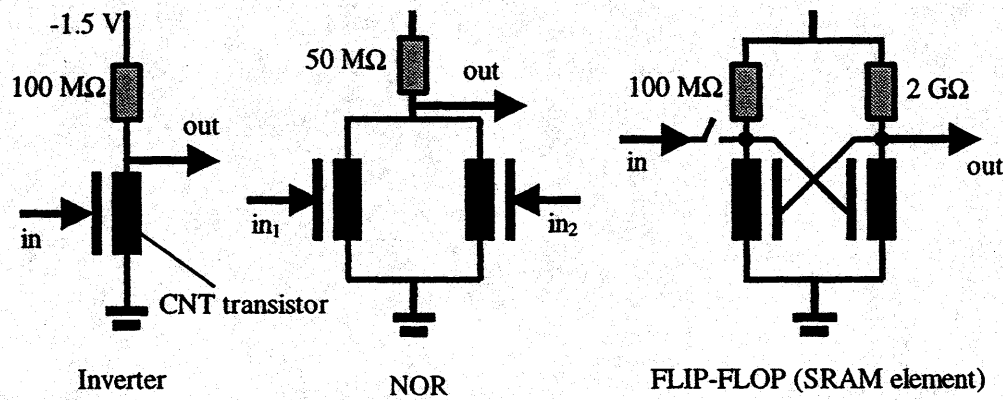


Figure 3.28 The implementation of the MVL complement operator using CNTFETs.

Intra-Nanotube OR

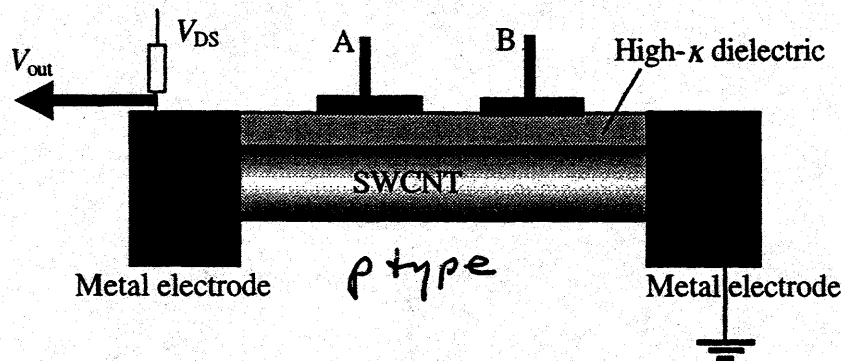
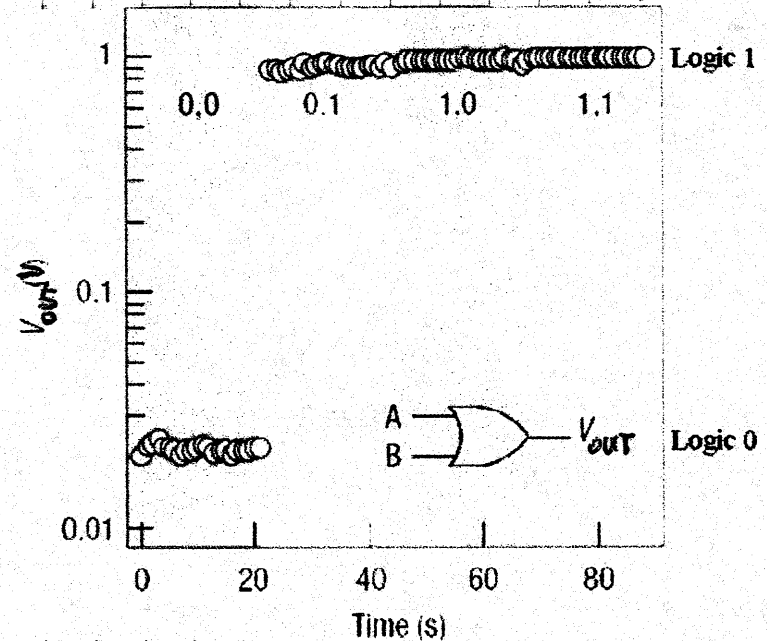


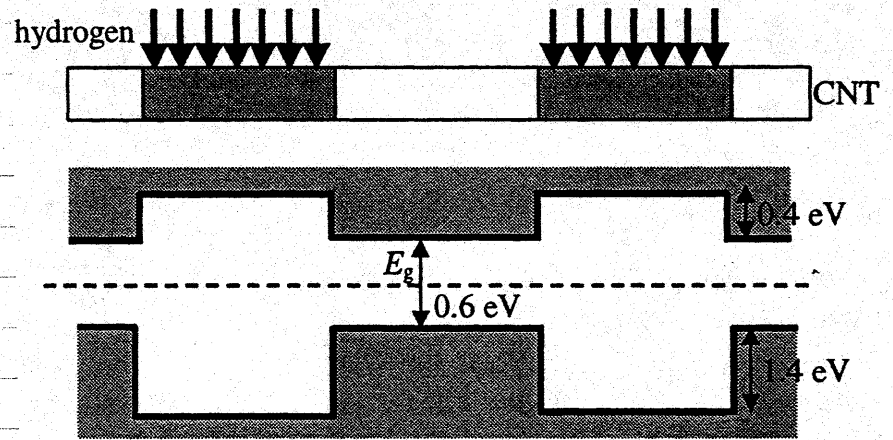
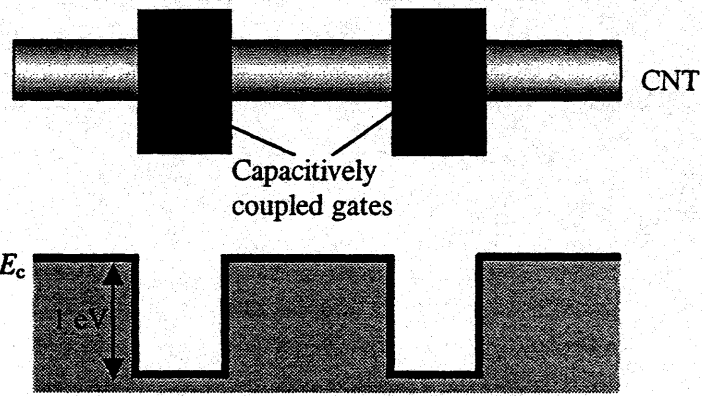
Figure 3.22 OR logic gate using a CNTFET with high- κ dielectric substrate.

For transistor ON, $V_{out} \rightarrow 0\text{v}$, Logic 0
 Needs both gates off, $V_A = V_B = 0\text{v}$

IF V_A or $V_B \rightarrow 1\text{v}$ (logic 1), transistor OFF, $V_{out} \rightarrow 1\text{v}$



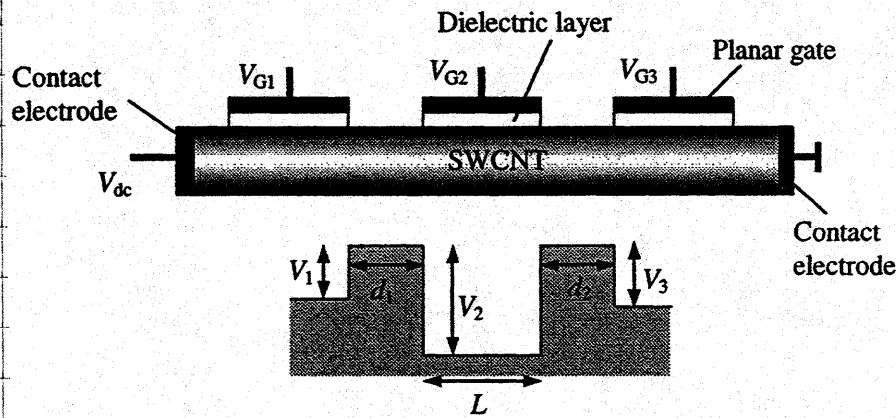
{ Note: For n-type transistor \rightarrow NOR gate }
 V_A or $V_B = 1\text{v}$, transistor ON, $V_{out} = 0\text{v}$
 V_A and $V_B = 0\text{v}$, transistor OFF, $V_{out} = 1\text{v}$



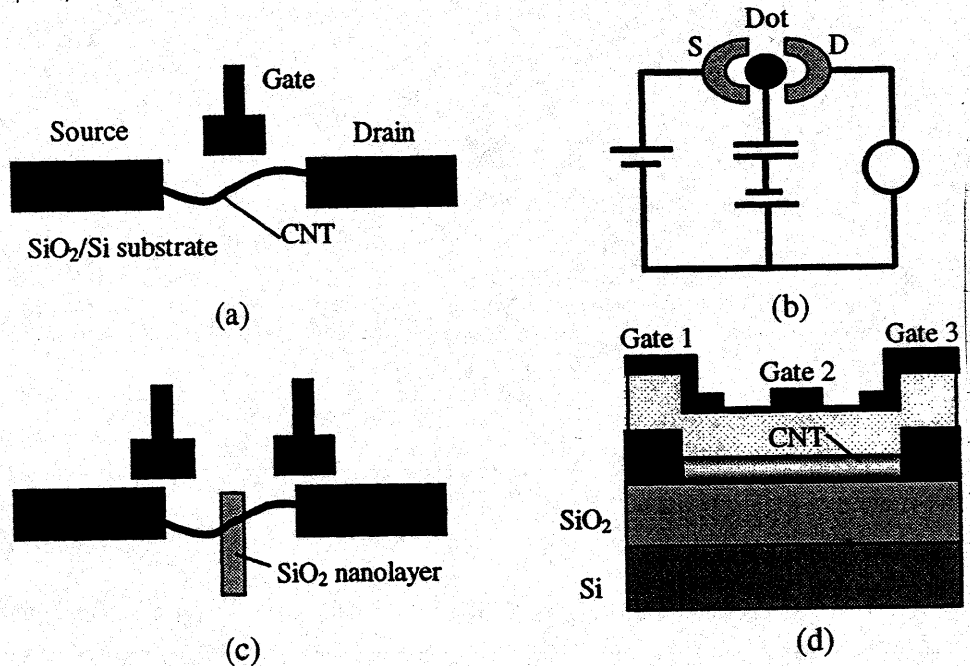
parametric electron pump created via capacitively coupled gates patterned onto a CNT.

Quantum CNT devices: RTD →

A quantum resonant tunneling structure realized by selective hydrogen absorption in a CNT



The THz CNT RTD (top) and its conduction energy band diagram (bottom)



SETs →

Figure 3.39 CNT-based quantum dot structures: (a) a single quantum dot, (b) its equivalent circuit, (c) double quantum dot, and (d) double quantum dots with local gates (After: [62]).

CNT SET

Structure #3

Buckled CNT

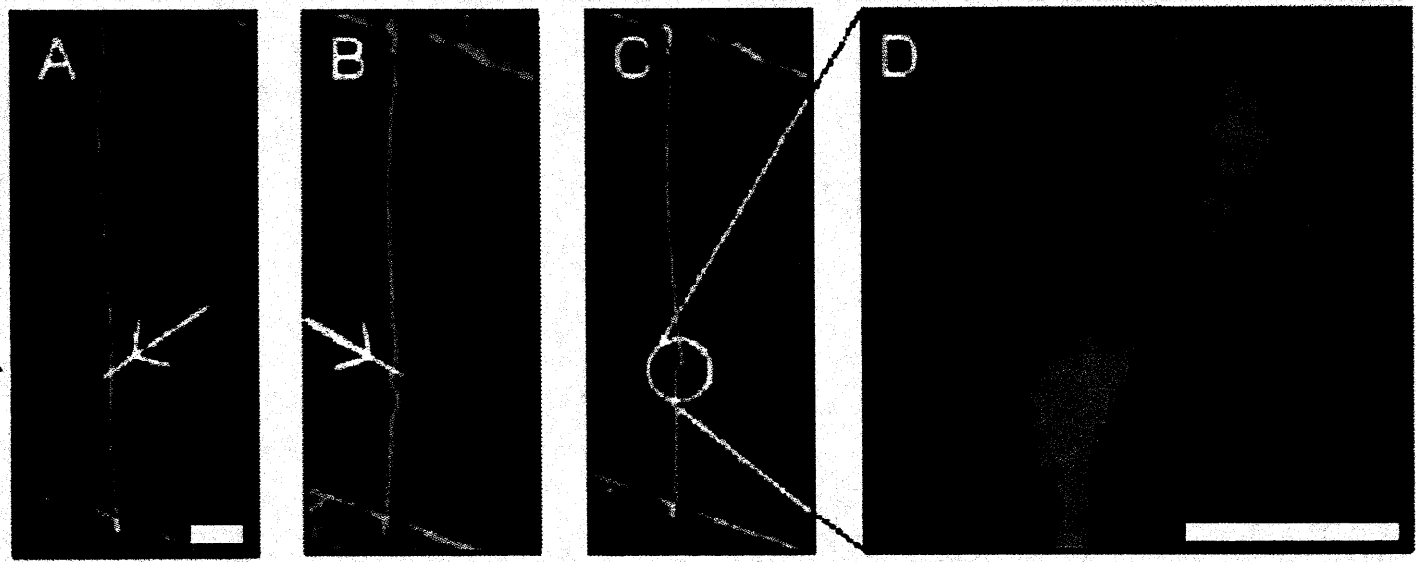
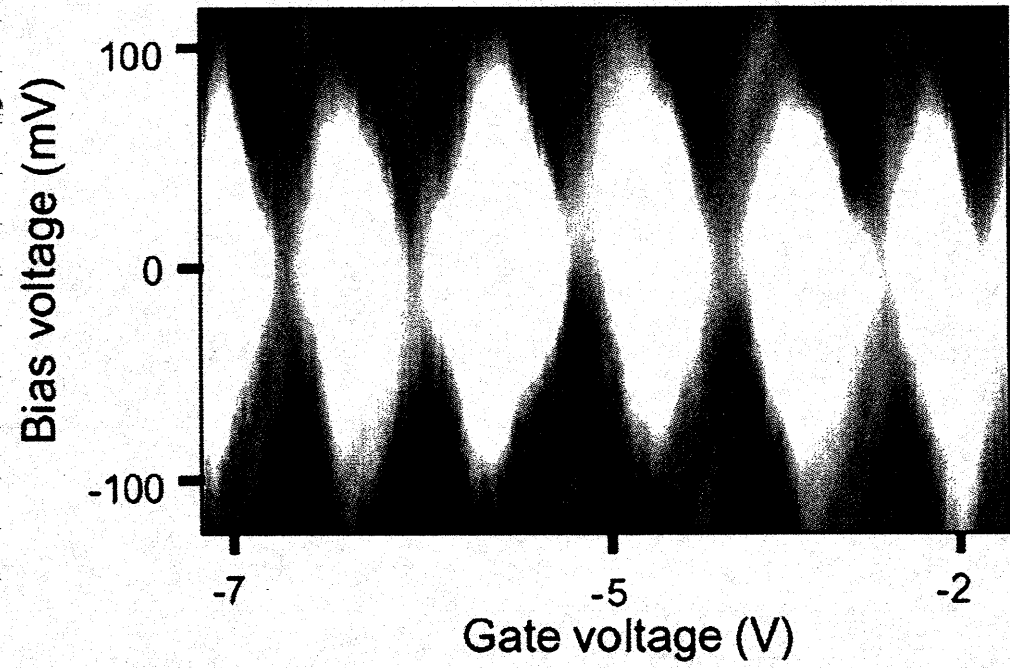


Figure 39²⁸ - Production of a SET through buckling of a nanotube

1. Drape CNT over contacts on substrate with oxide layer
2. Image with AFM.
3. Kink A with AFM tip
4. Kink B with AFM tip

See kink in C, D

Island between kinks
Substrate gate

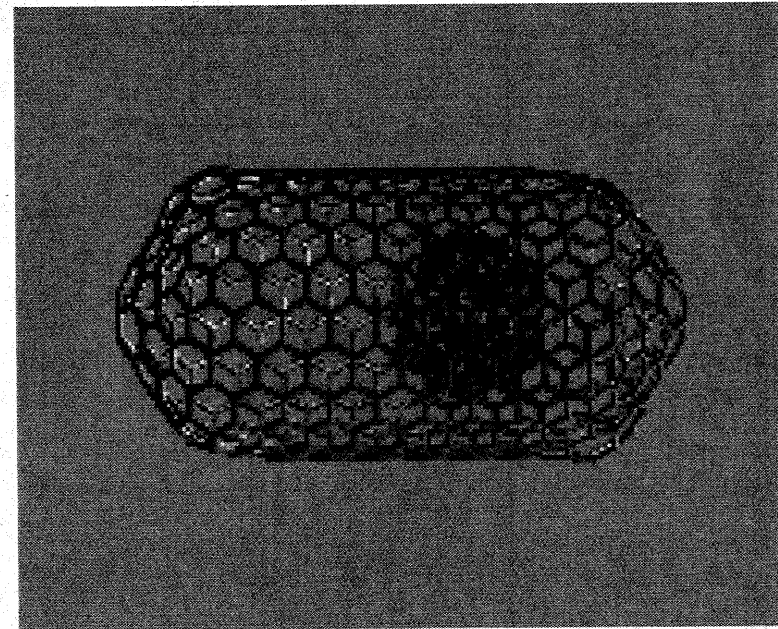
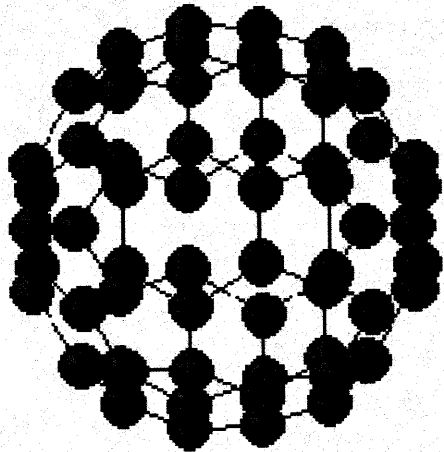


Kink small enough for room temperature operation

- Graph of conductance as bias voltage vs. gate voltage. White diamonds are coulomb blockade.

NanoMemory Device

- ◆ A new carbon structure, the buckyball (C_{60}), was discovered in 1985.



- ◆ A single-wall carbon nanotube would contain a charged (K^+) buckyball. That buckyball will stick tightly to one end of the tube or the other.

Source: M. Brehob "The Potential of Carbon-based Memory Systems", IEEE 1999

NanoMemory Device

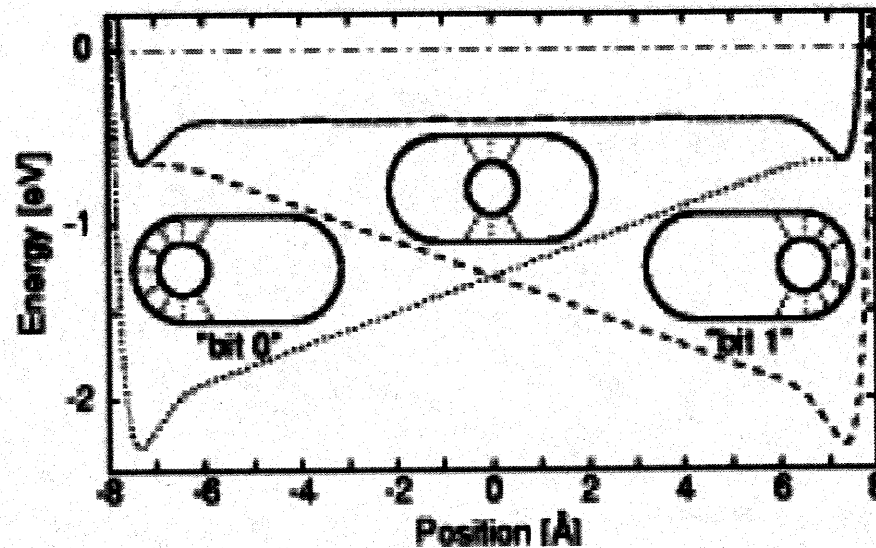


Figure 5 Potential energy of the shuttle at different locations in the capsule. The solid line is when no electric field is applied. The dashed lines are the potential energy when the two-volt potential difference is applied. [2]

- ✦ Assign the bit value of the device depending on which side of the tube the ball is. The result is a high-speed, non-volatile bit of memory.

Source: M. Brehob "The Potential of Carbon-based Memory Systems", IEEE 1999

NanoMemory Device

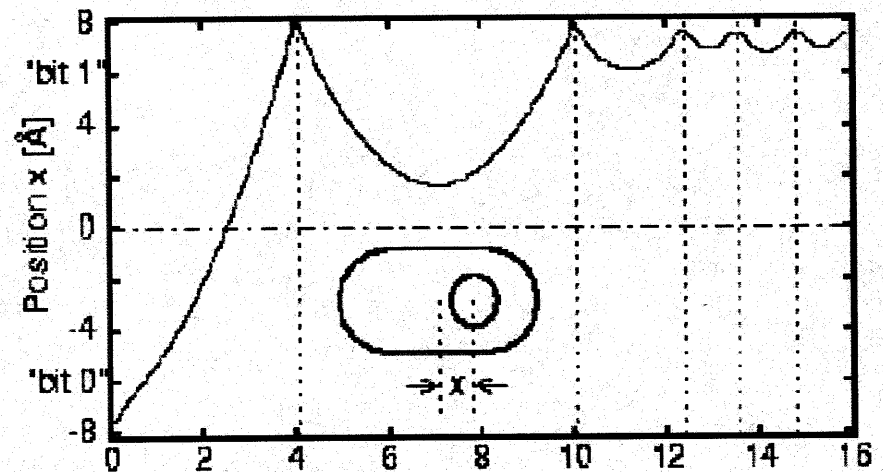
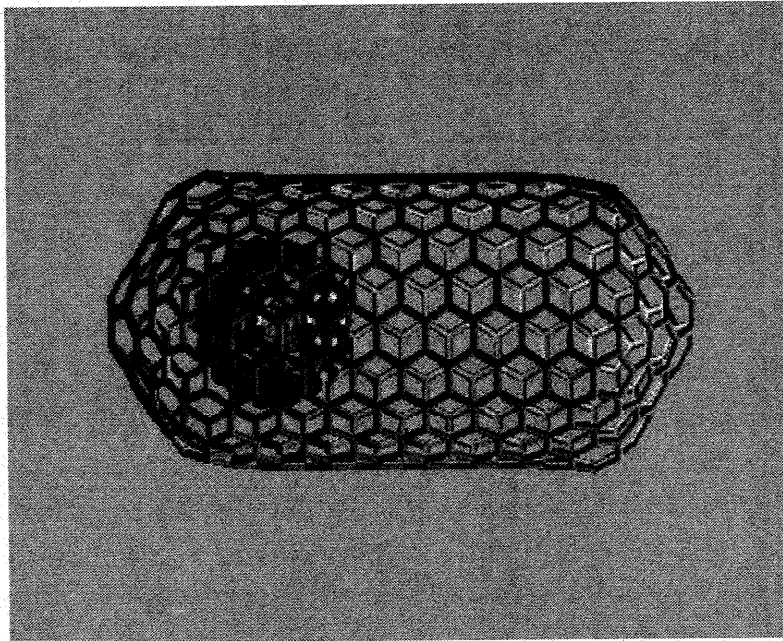


Figure 6 Location vs. time of the shuttle as a write is performed. Time is in picoseconds. [2]

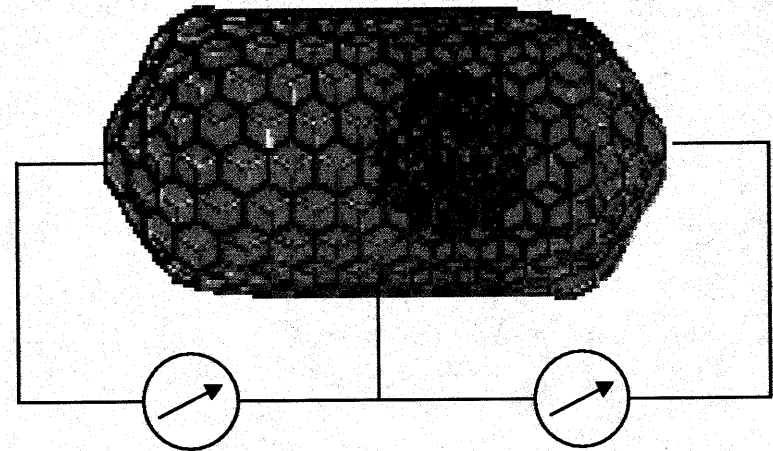
- ⊕ In general the amount of voltage which needs to be applied depends upon the length of the capsule.
- ⊕ A field of 0.1 volts/cm is sufficient to move the shuttle from one side of the tube to the other.
- ⊕ Write speed: 20 picoseconds

Source: M. Brehob "The Potential of Carbon-based Memory Systems", IEEE 1999

Problem: How to read???

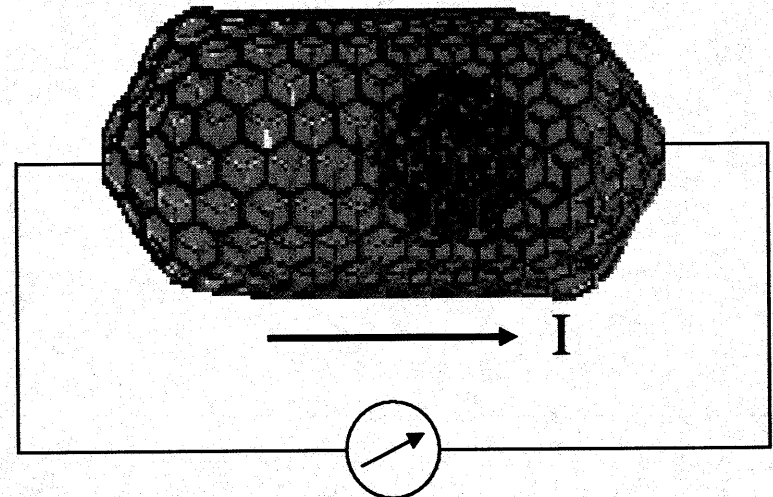
■ Three-wire detection

- ⊕ Monitor conductance
- ⊕ Hard to make middle wire connection



■ Current detection

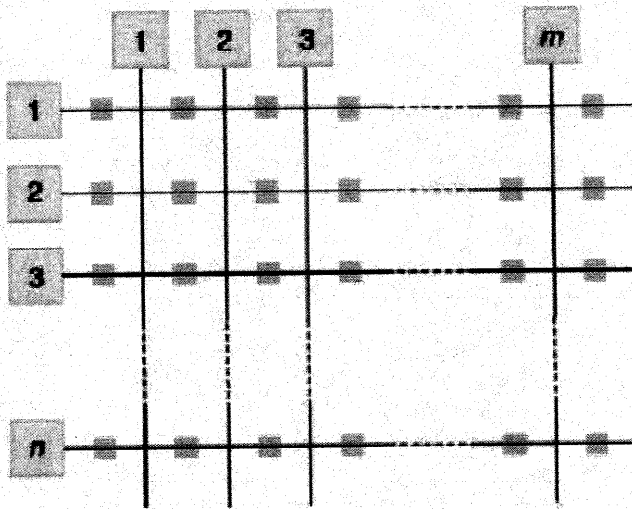
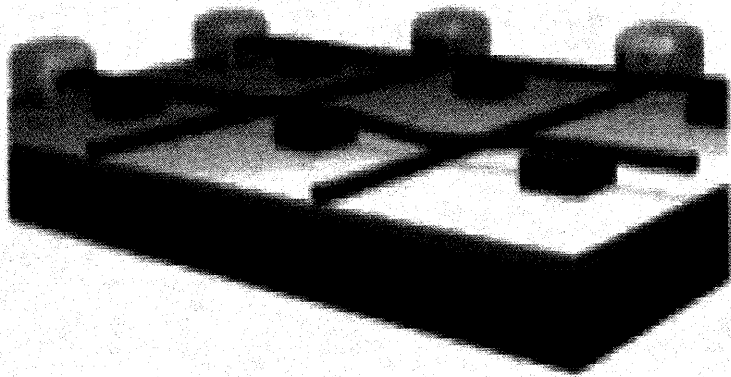
- ⊕ Done with writing
- ⊕ Use more shuttles
- ⊕ Long capsule



Bi-layer CNT RAM

- The clever thing is it combines both electronic and mechanical properties of single-wall nanotubes.
- Metallic nanotubes will bend toward a perpendicular semiconducting nanotube when electrically charged.
- When a metallic nanotube is one to two nanometers away from a semiconducting nanotube, the electrical resistance at the junction is low, creating an ON state. When the nanotubes are apart the resistance is much higher, creating an OFF state.

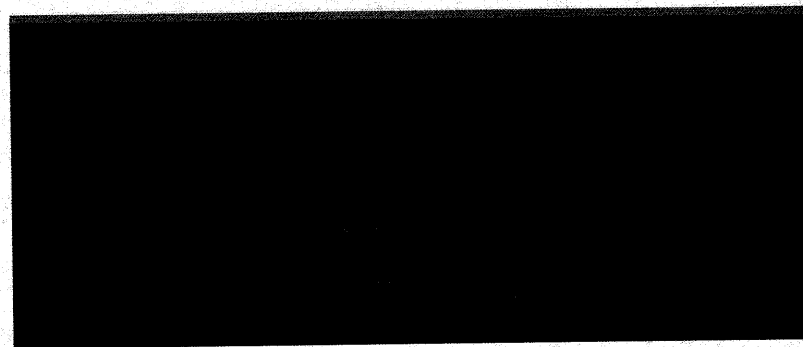
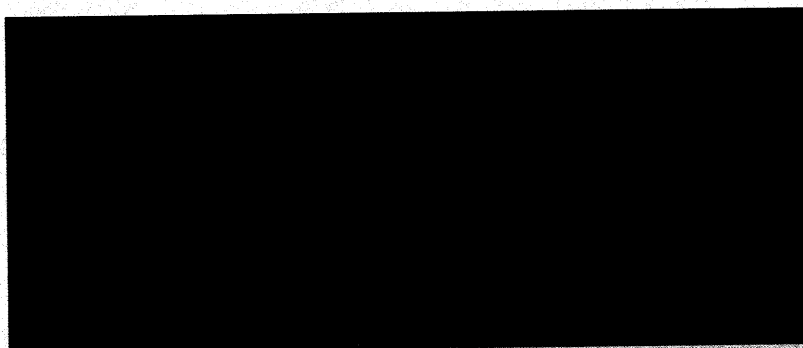
Structure



- ⊕ Nonconductive spacers keep the higher nanotubes flat and raised above the lower level. These spacers can be between five and ten nanometers in height to separate the layers of nanotubes.
- ⊕ These spacers must be tall enough to separate two layers of nanotubes from each other when both are at rest, yet short enough to allow small charges to attract and cause bends in the nanotubes.

Source: Thomas Rueckes, et al., "Carbon Nanotube Based Nonvolatile Random Access Memory for Molecular Computing", *SCIENCE*, VOL 289, 7 JULY 2000.

Working Principle

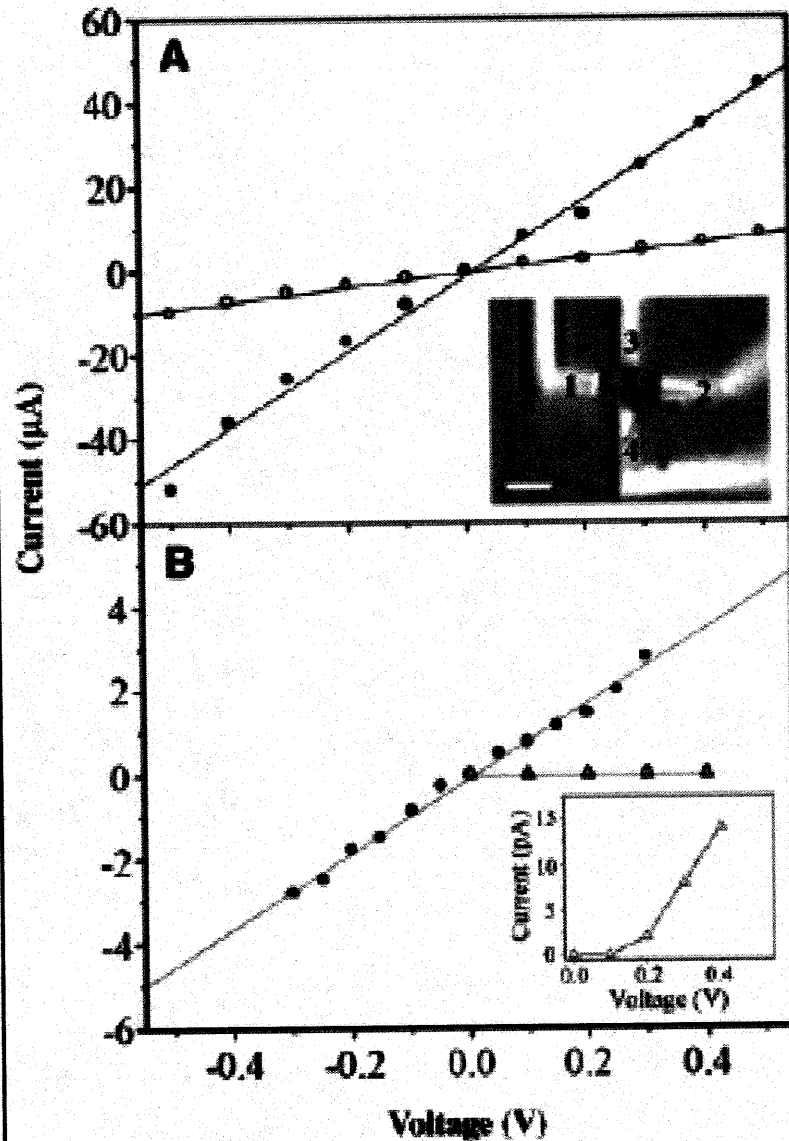


Bistable at NT crossing:

- ⊕ Top NT Suspended:
potential energy minimum
- ⊕ Top NT contacting lower NT:
van der Waals attraction

Source: Thomas Rueckes, et al., "Carbon Nanotube Based Nonvolatile Random Access Memory for Molecular Computing", SCIENCE, VOL 289, 7 JULY 2000.

I-V Characteristic



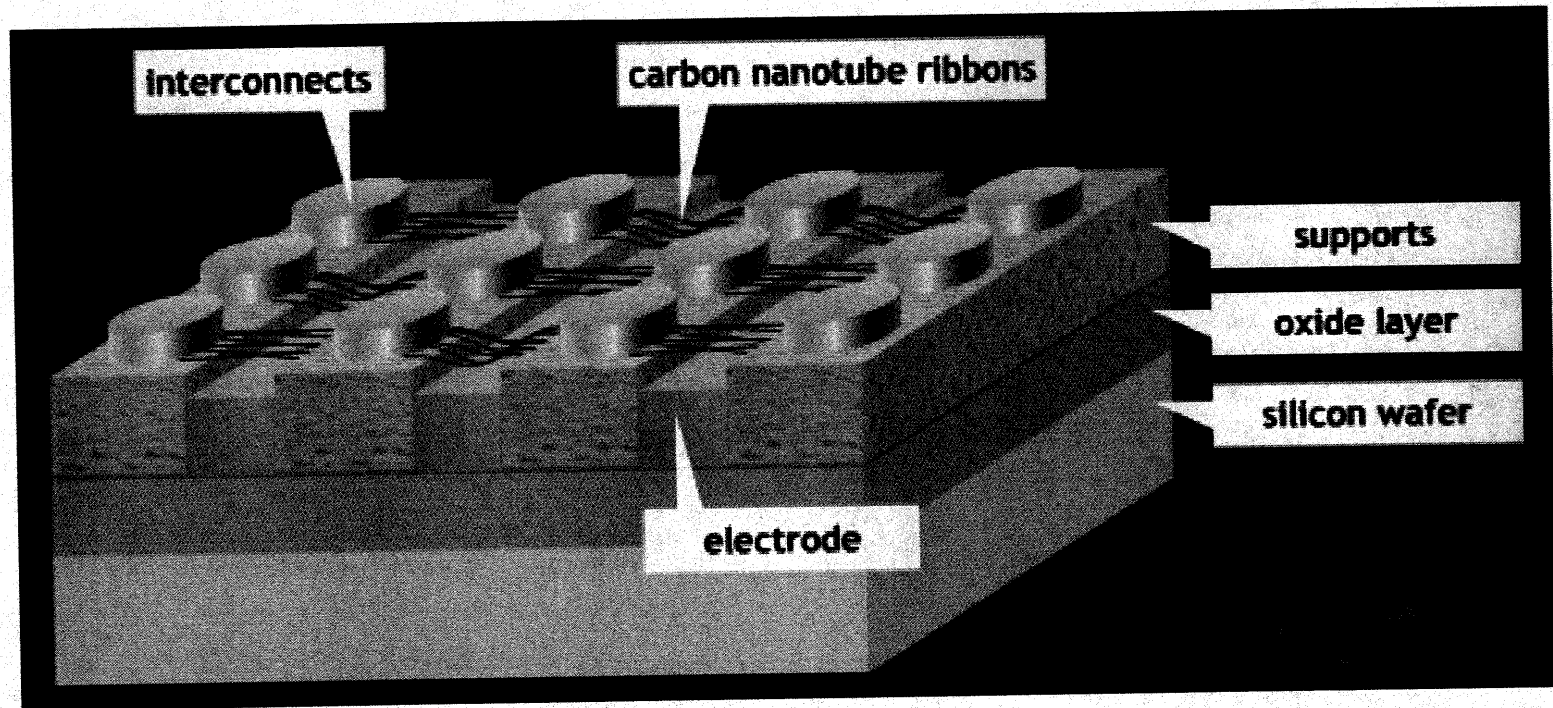
- The touching of two nanotubes decreases resistance between the two wires dramatically, yielding different I-V characteristics.
- Experimental results show 10X higher resistance for off state
- Bit value can be sensed by determining resistance with low voltage applied at electrodes
- Once a bend is made, it will remain until opposite charges are placed at the intersection.

Source: Thomas Rueckes, et al., "Carbon Nanotube Based Nonvolatile Random Access Memory for Molecular Computing", *SCIENCE*, VOL 289, 7 JULY 2000.

Problem

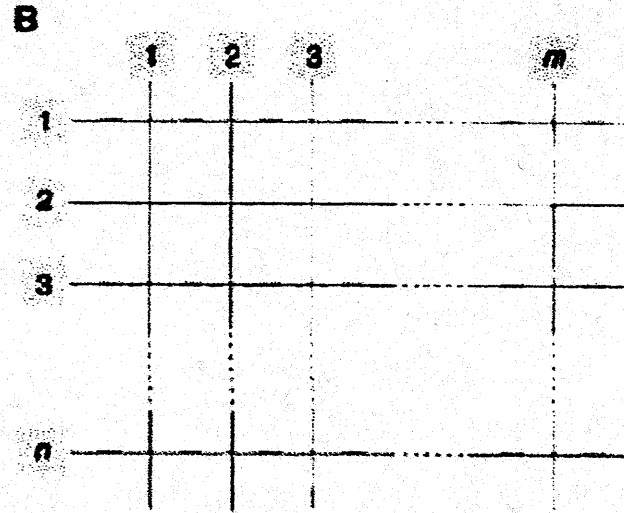
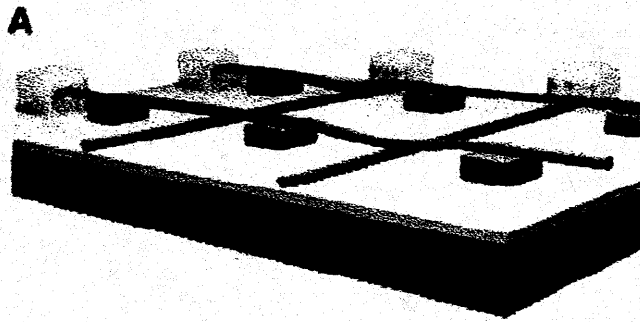
- ⊕ The distance between the crossed wires has to be controlled fairly precisely: one to two nanometers
- ⊕ Assemble and aligning a large number of these cross-wires. To make this pattern of nanotubes with precise control of distance is going to be the difficulty.
- ⊕ Not yet a reliable way to produce separate sets of metallic and semiconducting nanotubes.

NRAM™ by Nantero



- ⊕ Applied charge make CNT ribbons bend down to touch the substrate or bend up back to its original state.
- ⊕ Ribbon-up gives 'zero' and ribbon-down is 'one'.

Source: <http://www.nantero.com/nram.html>

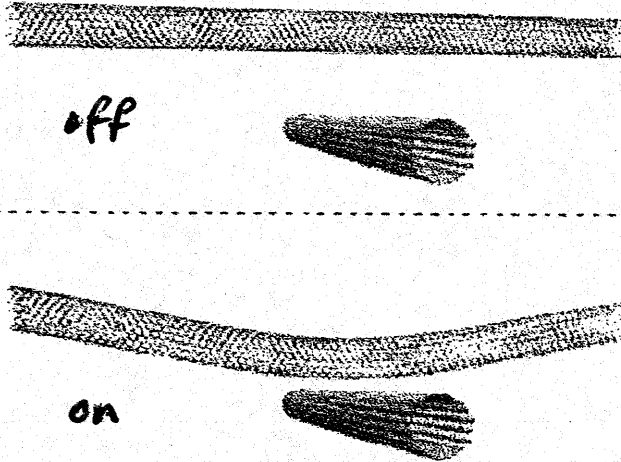


lines do read & write functions

Write

Charge to attract/repel

C



Read

High resistance

Low resistance (contacting)

Electromechanical CNT memory

Non-volatile

10^{12} bits/cm²

5nm elements →
~5ps switching
ie. ~200GHz

Figure 57³² – Memory device based on 2 layers of carbon nanotubes, in which the top layer is suspended above the lower layer. (A) A 3D view, gold structures are the contacts, and the black cubes are nonconductive supports. (B) A 2D view showing the matrix used each cross represents a bit. (C) The off state is a normal suspension, while the on state has the top layer bent down towards the bottom.

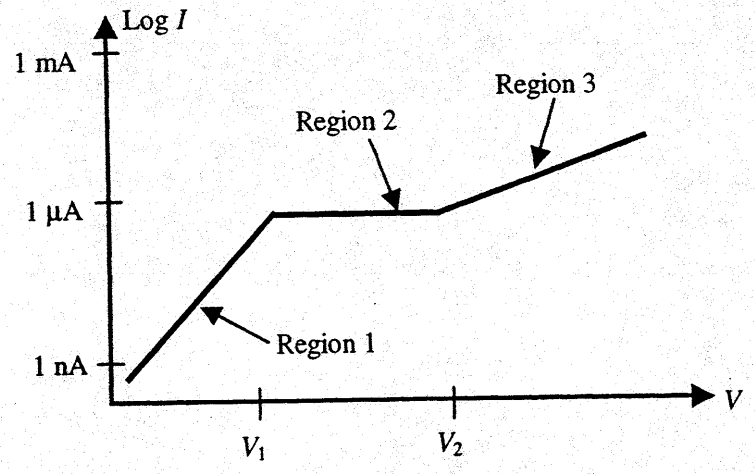
eg Nantero/LSI-Logic

Field emission devices

Electric field $\sim 2500 - 3000 \text{ V}/\mu\text{m}$
for metal $\phi \sim 5 \text{ eV}$

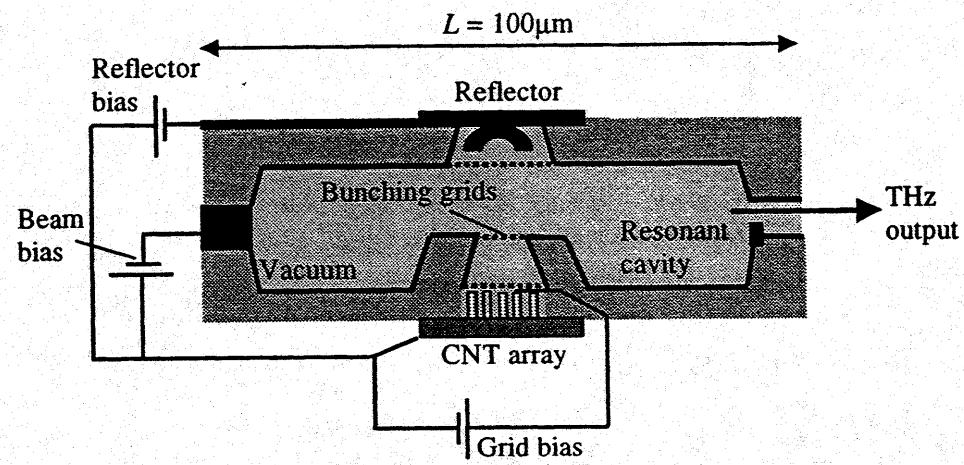
Field concentration $\beta = h/r$
 h - tip height
 r - radius of curvature

Arrays of CNTs $\rightarrow 1 \text{ mA}/\text{cm}^2$ for $\sim 5 \text{ V}/\mu\text{m}$
due to concentration $10^2 - 10^3$
Each CNT $\sim 1 \mu\text{A}$



The field emission I - V characteristic for a single SWCNT (After: [44]).

- Region 1 : Fowler Nordheim tunneling
- 2 : Saturation \rightarrow emission through (H_2O ?) surface adsorbate; states distort at $\sim 700 \text{ V}$
(No saturation for clean CNTs)
- 3 : Typical clean SWCNT



\leftarrow Application example

Figure 3.32 THz klystron with an array of ordered CNTs as a cold cathode (After: [48]).

ECE 417/517 NANO-ELECTRONICS

Spring 2007

Lecture 16: Miscellaneous Topics

- Spintronics
- Nanowires
- Nanosystems
 - Thermodynamics & Reliability

a fundamental nature and can not be overcome. This is true, with the reservation that the limits as seen today are not necessarily final ones because the research in physics continues. We can expect considerable progress in the field of quantum computing, which will move some limits far beyond current ones. Some of these physical limits that are presented for classical microelectronics are summarized below.

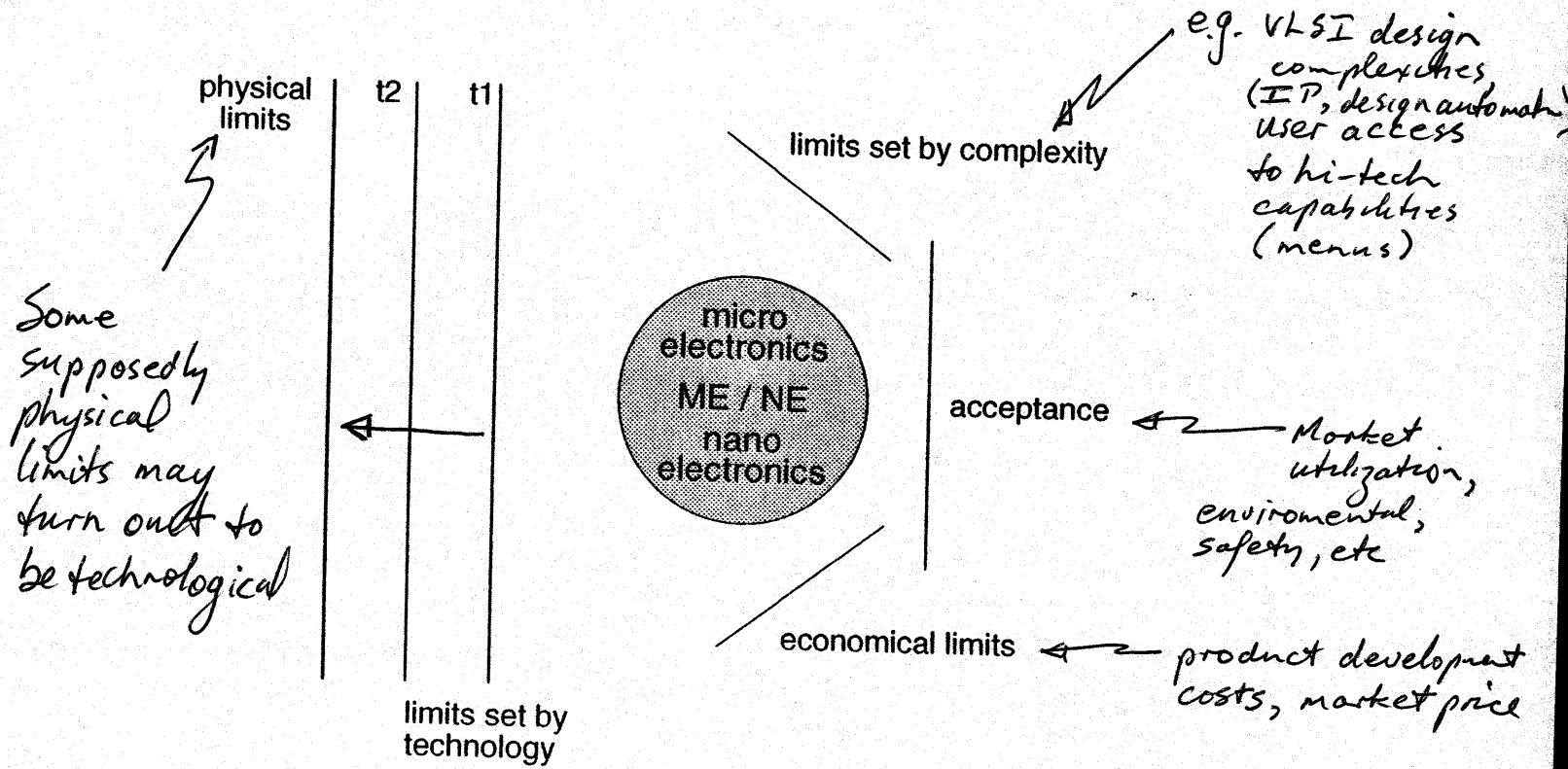


Fig. 15.1. Some limits of micro- and nanoelectronics ME/NE. Further development enlarges the circle ME/NE, so the borderline can reach different limits. The technological limit is indicated for the times t_1 and t_2

General Limits (I) → Mature technologies

... stop. Products
 t radio waves,
 so depends on
 only assumed
 these cases the
 mportance.
 y. A product
 uired. System
 ssful product.
 ent change of
 tion problem
 r indicate the

improvement
 been reduced
 stay mainly
 2. The yield
 read. Under
 lower costs
 perspective the
 out reaching

technologies. In this case the replacement of technologies with improved ones can be done sooner.

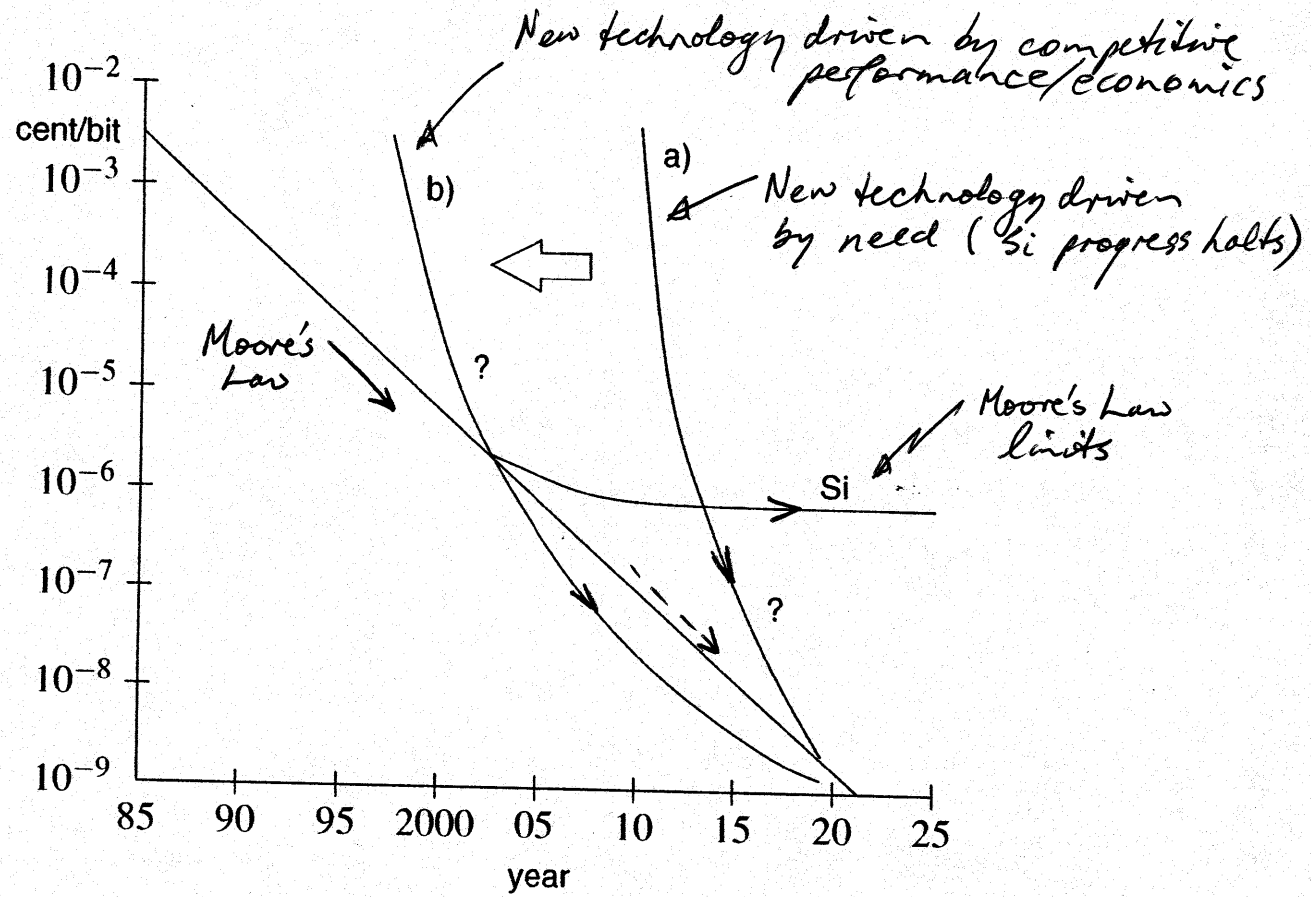
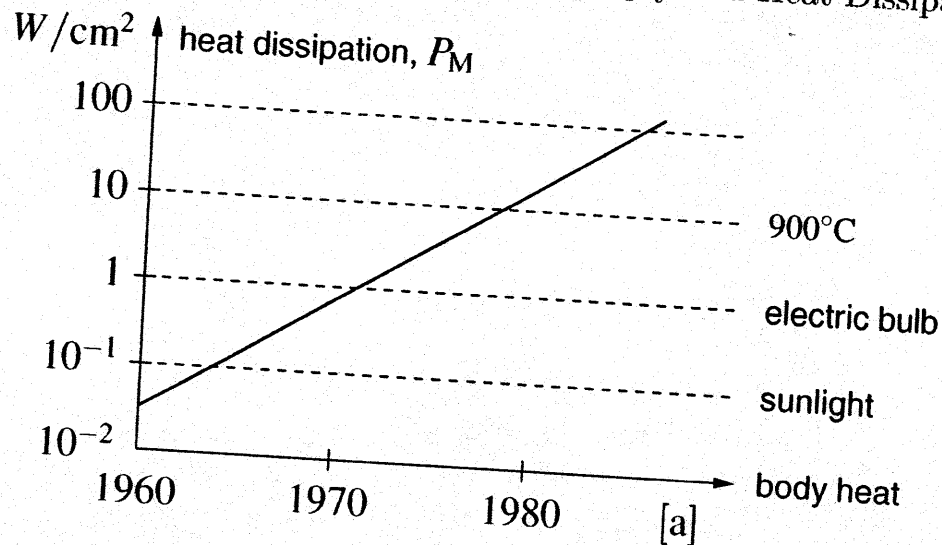


Fig. 15.2. Costs per device. The limit of silicon technology is expected for the year 2010. After this, new technologies will emerge (a). If these technologies are cheaper the change of a technology occurs sooner (b). The choice of technology is still uncertain (?)

General Limits (II) → New technologies



Thermal Limits
I

Fig. 15.4. Heat dissipation P_M of a module (electronic)

The power dissipation has its origin in the transistor itself. From there the power dissipation or heat has to pass through the chip and the module before the working environment is reached. Next to the improvement of microelectronics the heat conduction could also be improved, as denoted in Fig. 15.4. At the beginning the improvement was due to improved printed circuit boards and packaging. Heat conduction P_M could be increased to 1 W/cm^2 . The application of a ventilating fan increased this value to 10 W/cm^2 . The next step in the development was fin cooling where the chips on a module are cooled with water from the backside. The backside exhibits a number of grooves that are fabricated by micromechanical structuring. This results in a P_M of about 100 W/cm^2 , which is a typical value for high-performance microcomputers.

During the design of a microelectronic system the context between heat conduction P_M of a module and the technology-dependent power-delay product of a gate is of great importance [45]. This context is explained with the help of the following simple derivation. Let us assume a module containing n integrated devices as shown in Fig. 15.5. The module area A_M containing the

the limiting condition of (15.8) can be drawn on a $P_V - t_D$ chart.

Thermal Limits II

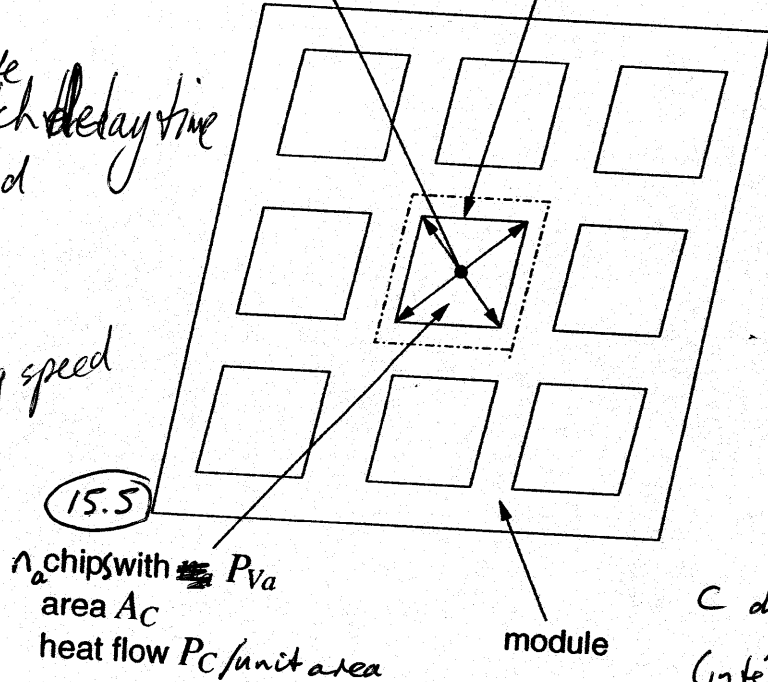
① $A_M \bar{P}_M > n_a P_{V_a}$

Signal delay $t_m < \overset{\text{Gate}}{\text{Switch delay time}} t_d$

$t_d > m_m \frac{\sqrt{A_m}}{v_m}$
 empirical \swarrow \nwarrow sig speed

$t_d^2 > \frac{m_m^2 n_a}{v_m^2 \bar{P}_m} P_{V_a}$

powerstage with P_{VL}
 area, A_M
 acceptable heat flow, $P_M/\text{unit area}$



C distributed capacitance /unit length (interconnect transmission line)

Power-delay due to heating limitations

Fig. 15.5. Heat dissipation on a module and on a chip

A fundamental restriction of aggressive scaling could be the heat conduction especially in those cases where the power dissipation per unit area increases. Today this problem is not of great interest in information-processing circuits. Nevertheless it is an important topic for power stages.

② For $A_C \bar{P}_C > P_{VL}$
 chip dissipation

$P_{VL} < \frac{1}{4} \frac{m_c^2 \bar{C}^2 v_B^2}{P_C} t_{DL}^2$ --- (15.8)

Energy transfer $P_{VL} t_{DL} = m_c \frac{1}{2} \sqrt{A_C} C v_B^2$
 substitute $A_C > P_{VL} / P_C$

If these reflections are passed onto integrated circuits and taking the switching time into account we get the chart of Fig. 15.6. This chart contains the limits for field effect transistors. The removal of heat is actually restricted to values around 100 W/cm^2 . The more devices integrated on a chip the lower must be the switching energy. Lowering the switching energy causes smaller dimensions, therefore the performance of the devices increases. On the other hand, the absolute limit of lowering the switching energy is set by thermodynamics of about $50 kT$. The uncertainty relation leads to the quantum-mechanical limit, which is important for single-electron transistors.

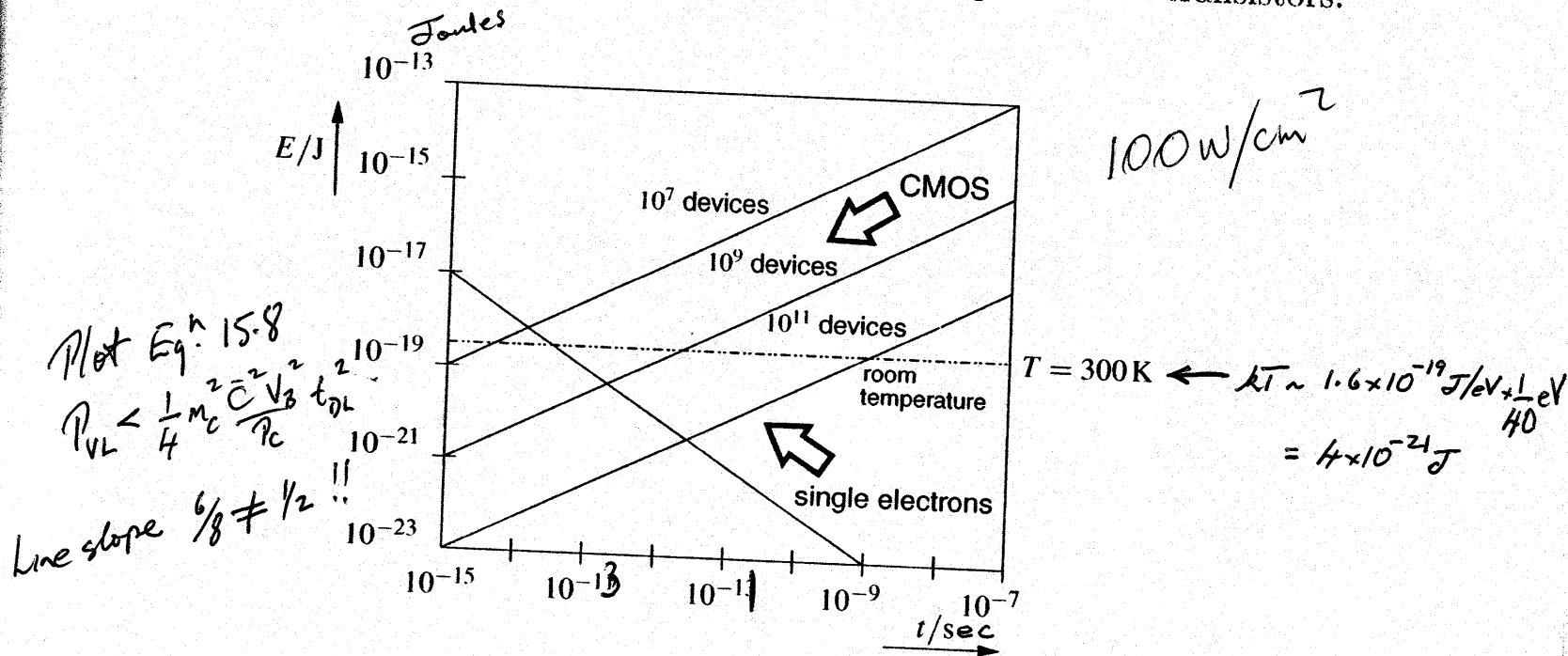


Fig. 15.6. Switching energy versus delay for SET and CMOS devices

Also important are the consequences of further scaling down the energy supply of the circuits. Even if scaling reduces the supply voltage to V/α , the currents on the supply lines increase due to an increase in the number of

Thermal Limits III

Parameter Spread Limits I

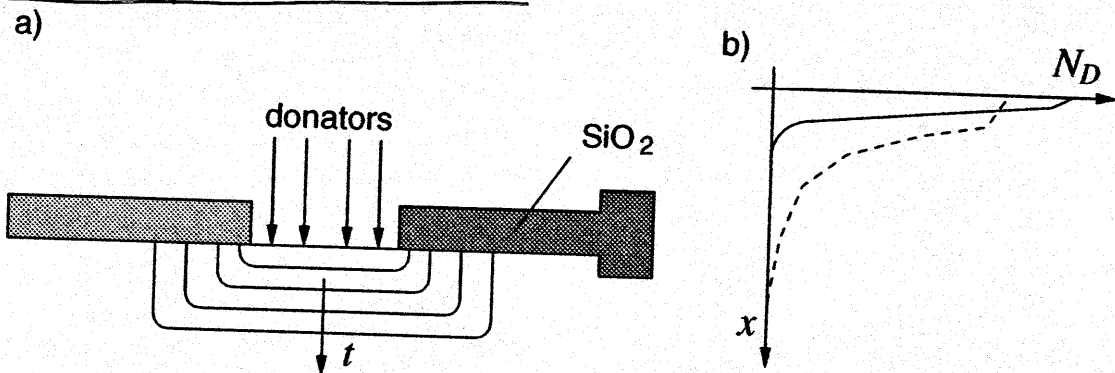


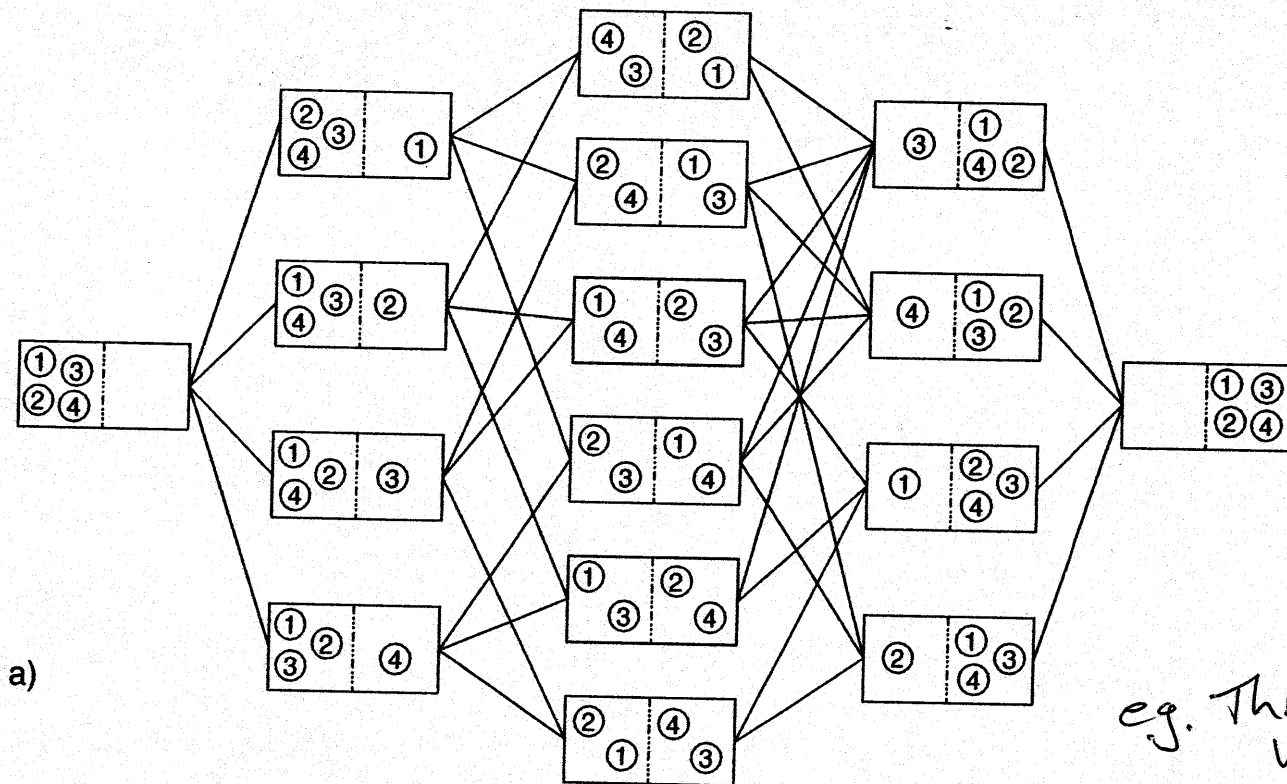
Fig. 15.7. Process of diffusion for the realization of semiconductor structures. (a) Diffusion process in a semiconductor and (b) the diffusion profiles as a function of time

Small dimensions → statistical variations greater

In (15.9) Q denotes the initial density of phosphorus atoms and D the diffusion constant. If the temperature is lowered the diffusion process does not stop but reduces its speed. This also indicates that the electrical parameters that are adjusted during the manufacturing process can vary with time and can sometimes cause device failures. Therefore the diffusion process is very important when the reliability of a device or system is of concern.

The equal-probability distribution of (15.9) is only a mean value. The other values of each pn-junction vary around this value. This results in a spread of the electrical and technological characteristics of the devices. This is a fundamental effect for microelectronics and is mostly detrimental to integrated circuits.

Volume	$(1 \text{ cm})^3$	$(1 \mu\text{m})^3$	$(0.1 \mu\text{m})^3$
Mean number doping atoms	10^{16}	10^4	10
Normalized std. deviation	10^{-8}	10^{-2}	$10^{-0.5}$
		(1%)	(30%)

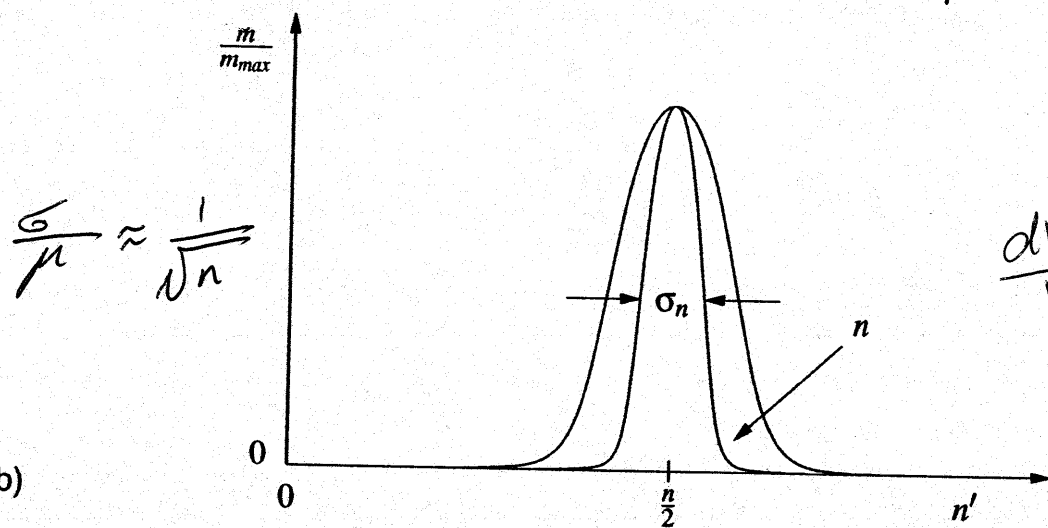


$m = 1$

4

6

4



eg. Threshold voltage variation

$$x = (2\epsilon\phi_s/NAq)^{1/2}$$

$$V_T = (q^2\epsilon\phi_s NA)^{1/2} / C_{ox}$$

$$\frac{dV_T}{V_T} = \frac{1}{2} \frac{dNA}{NA} = \frac{1/2}{\sqrt{NA} x(WL)}$$

$$\frac{\Delta V_T}{V_T} = \frac{1/2}{\sqrt{NA} x(WL)}$$

The thres

The variat
concentration

According

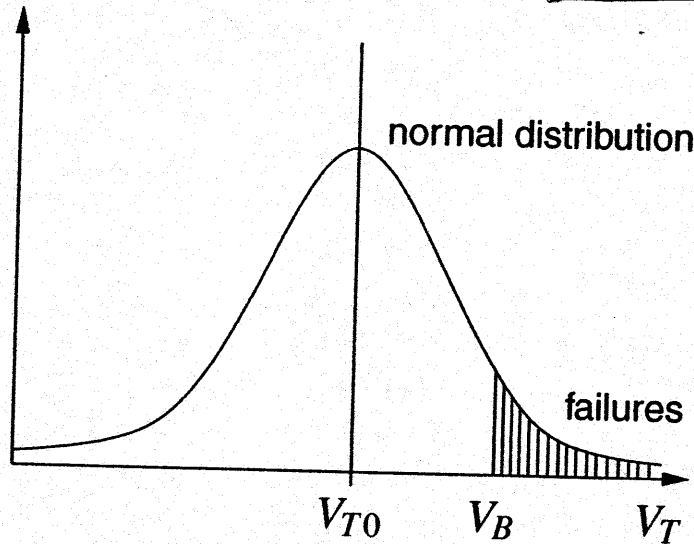
Equation (
doping atoms

The variat
and with lowe
According
operated at tl

The proba
scattering. Th
parameters. If

Fig. 15.8. Number m of possibilities to place four particles according to (15.11) (a)

$$\frac{\Delta V_T}{V_{T0}} \propto (WL)^{-1/2}$$



N_A variations
 $\rightarrow V_T$ variations
 Failure when
 V_T exceeds
 maximum available
 voltage (V_B)

Fig. 15.9. Impact of the parameter spread on the yield and reliability: If the threshold voltage is above the power supply voltage the inverter does not work. The shaded area denotes the probability of a failure

For an inverter chain with m stages the yield is considerably smaller,

$$Y_{St} = Y_I^m = (1 - P_I)^m \quad (15.20)$$

If one wants to achieve a given yield, P_I has to become sufficiently small. According to Fig. 15.9 the supply voltage V_B has to be increased. The minimum supply voltage is therefore not set by the nonlinear behavior of the characteristic curves but by parameter variations. Mead calculated this voltage for a given FET technology and for 10^7 inverters to be 700 mV. The problem of a reduction of the yield becomes more and more important for devices with decreasing feature sizes.

Although some experts see this problem as insuperable, engineers have found some answers to this problem, as stated in Chap. 2. The solution to this problem can be achieved by two approaches: The first approach wants

15.5 The I

These stochastic variations due to noise, these effects h

15.5.1 The I

The diffusion of carriers occurs thermodynamic field must can be explain

The potential integrating (15

This voltage conductor. The solution of the

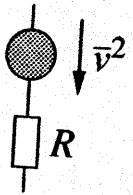
each degree
age energy of
ory the mean

(15.26)

culated with

(15.27)

b)



ivalent elec-

erature, and
r electronic
A figure of

provides an adequate model for the explanation [68].

The diffusion process always occurs at temperatures above 0K and increases with rising temperatures. The latter is advantageously used in the manufacture of integrated circuits. If a device is operated at working temperature the diffusion process is small enough that the lifetime of a device is hardly reduced. On the other hand, some failure mechanisms are based on the diffusion process. The lapse of time for this mechanism is very fast so further unwanted failures occur.

Reliability Limits I

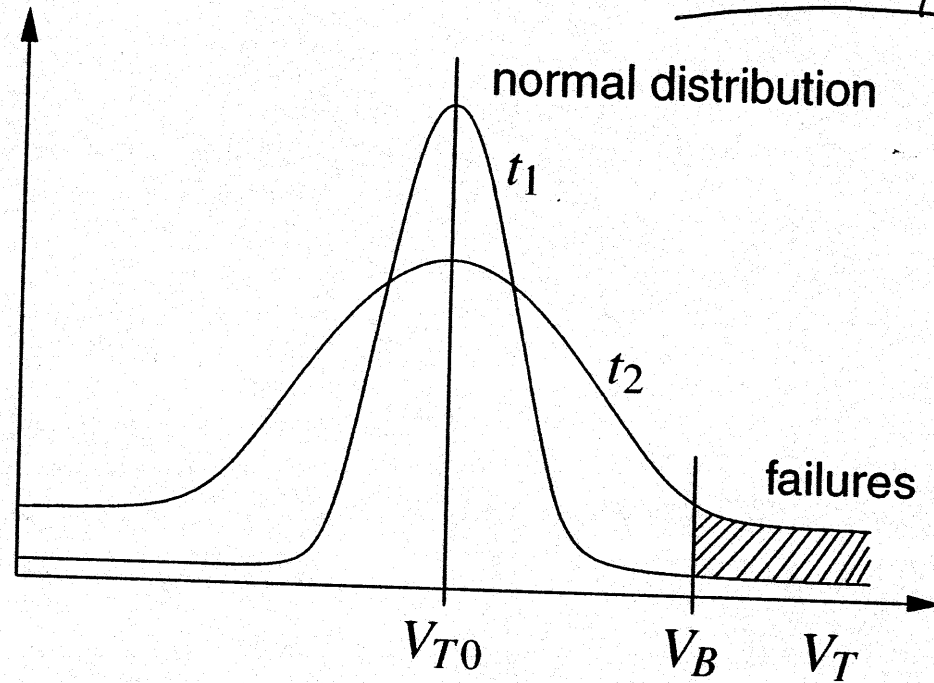


Fig. 15.11. With increasing time $t_1 \rightarrow t_2$ the failure rate increases. This is due to the enlargement of the distribution caused by the diffusion

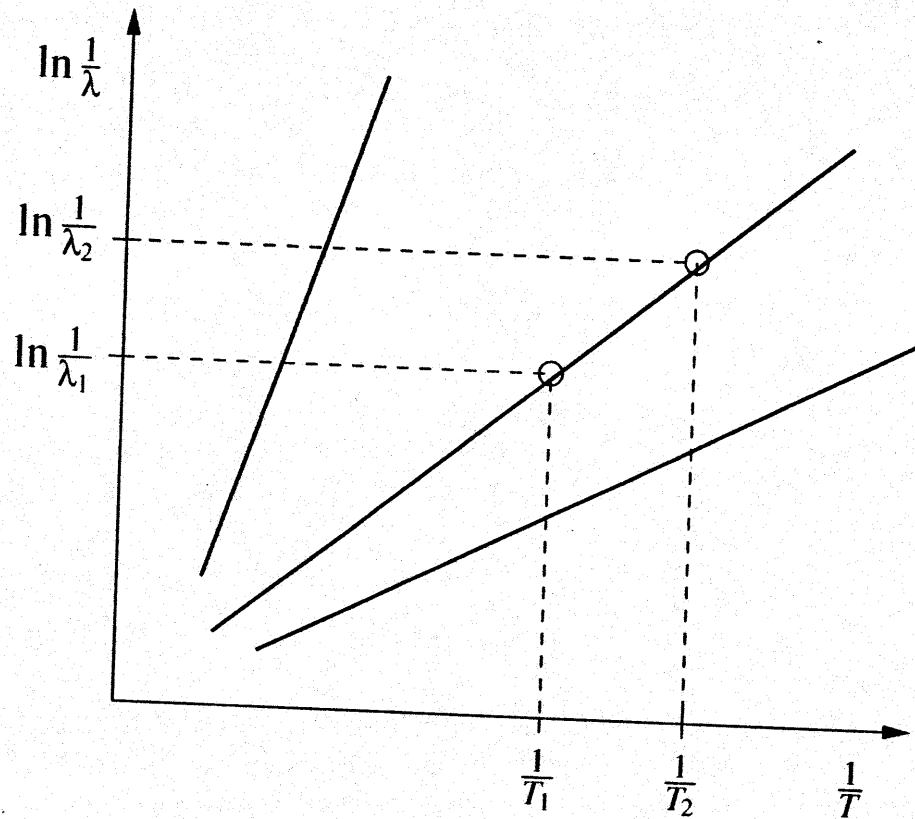
Diffusion
time const

$$\tau_z = \frac{x_0^2}{D} = C' \exp \frac{EA}{kT}$$

Reliability $N = N_0 \exp -\lambda t$, $\frac{1}{N} \frac{dN}{dt} = -\lambda$
 (λ^{-1} time const)

$$\lambda = C_A \exp -\frac{EA}{kT}$$

if $\lambda^{-1} \sim \tau_z$



Failure rates

λ_1, λ_2

at

T_1, T_2

$$\lambda_1 = C_A \exp(-E_A/kT_1)$$

$$\lambda_2 = C_A \exp(-E_A/kT_2)$$

$$E_A = \frac{k T_1 T_2}{T_2 - T_1} \ln \frac{\lambda_2}{\lambda_1}$$

Fig. 15.12. Dependence of λ of the temperature T and the activation energy E_A . E_A can be determined by two measurements with different temperatures

If (15.30) is converted into a difference equation

$$\Delta N = -\lambda N \Delta t \tag{15.33}$$

and if $\Delta N = 1$ we get the time Δt that passes until a failure on the average will occur,

$$\Delta t = \frac{1}{N \lambda} \tag{15.34}$$

A device with the failure rate λ stated in hours will fail on average in $1/\lambda$ h. The time until a failure in a system with N devices occurs is reduced with

tested devices in real-world application is of crucial importance for increasing the quality.

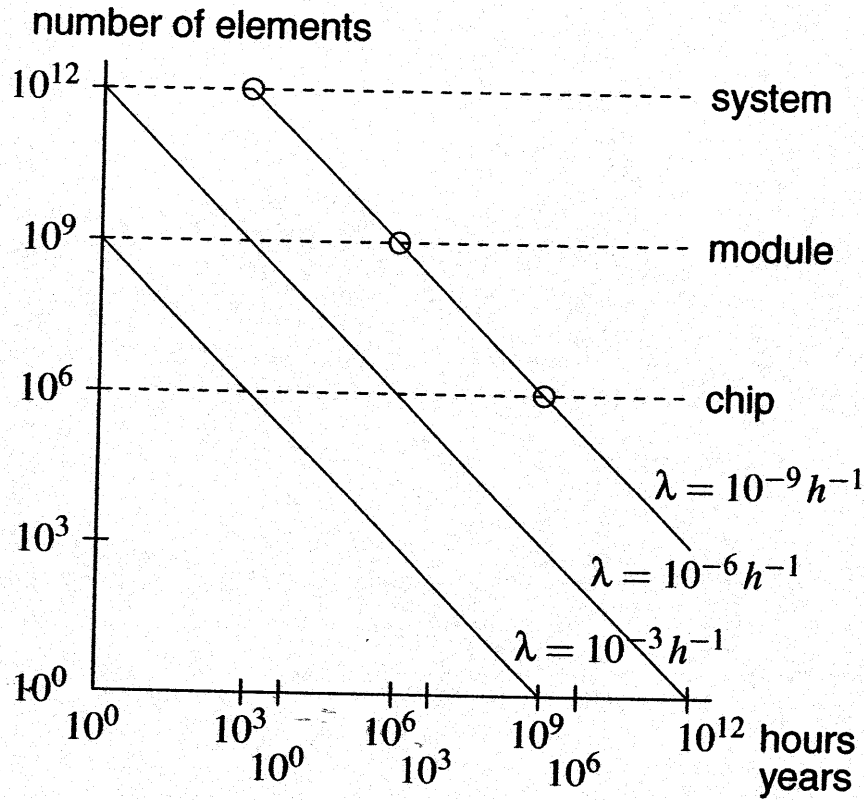


Fig. 15.13. MTBF in hours or years and the number of devices on the module or chip level for different failure rates λ . The markers correspond to the examples in the text

Nanosystems: Smaller devices \rightarrow larger scale systems. Need higher component reliability to maintain same system reliability.

A product has to function for many years. However, a lifetime above 10 years is not worth aspiring to due to increased costs. On the other hand, failures that occur in the first year of operation are troublesome. The reliability decreases from the system level down to the device level. To find the correct values at each level is not an easy task.

Redundancy architectures??

A faster comp
times have an
In practice
fundamental c

15.7 Physi

The preceding
limits of micro
important limi
quantum mech
shown in Fig.
for $1 \text{ fJ} = 10^{-1}$
acteristic for c
have been unde
Without any d

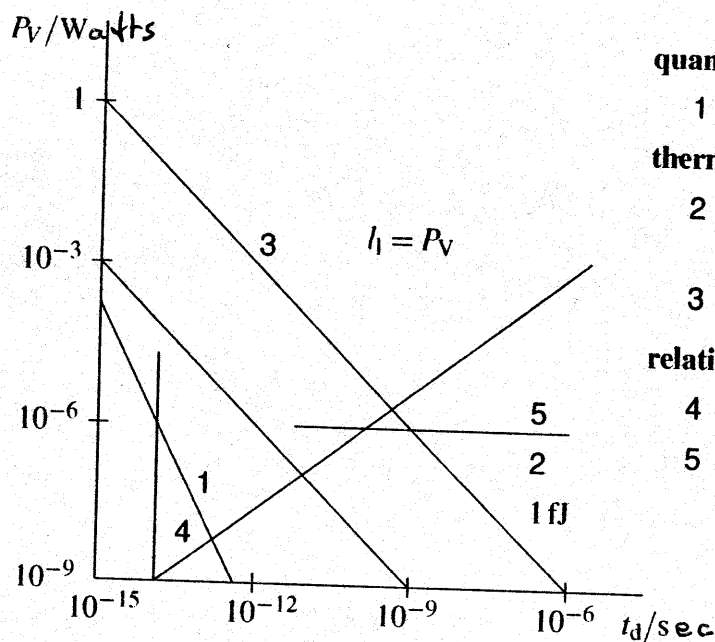
Some of the
mechanical asp
sults of any cor
the appropriate
believe that a
tunneling devic
done with a ne

All these id
computers such
presented below

mechanical aspects are used. When regarding the quantum computer the results of any computation are valid without any delay in time when applying the appropriate input signals and after a unitary transformation. Some people believe that a signal propagation as fast as the speed of light is possible in tunneling devices. Other theories suggest that information processing can be done with a negligible amount of energy.

All these ideas should be taken with caution because new concepts for computers such as those for the quantum computer could affect the limits presented below.

Physical Limits



Heisenberg $\omega_s \geq h/t_s$

quantum-mechanical limit $P_V = \frac{h}{t_d^2}$

thermodynamical limits

2 minimal voltage $V_{min} = rV_T$ ($r = 4 - \phi$)
 $P_{wire} = V_{min}^2 / Z_{1.0}$

3 therm. fluctuations $E_S = P_V t_d = ckT$
 $= 1 fJ = 10^{-15} \text{ W}\cdot\text{s}$
 for $c \approx 2.5 \times 10^8$

relativistic limits

4 delay $t_L = \frac{\sqrt{\epsilon_r \mu_r} l_L}{c}$

5 wave impedance $Z_L = \sqrt{\frac{\mu_r}{\epsilon_r}} Z_{1.0}$ (50kT?)
 $Z_{1.0} < \sqrt{\frac{\mu_0}{\epsilon_0}}$

$P_{wire} \sim \frac{(16-64)}{1600 \times 337} \sim (2.5-10) \times 10^{-5} \text{ W}$

Fig. 15.14. Physical limits for microelectronics with regard to power and delay

Also: Debye Length $\lambda_D \sim 100 \text{ nm}$ for Si at 300K.
 Noise $\rightarrow \bar{v}^2 = 4RkT\Delta f$ & R large at nanoscale
 (quantum resistance)
 (tunneling)

the module or
the examples in

time above 10
on other hand,
The reliability
and the correct

the hardware
can be easily
parts is area
fault-tolerant
ce, especially

ight be some-
es are deter-
the inside of
n exists. On
compounds,
re partly un-

esults of any
of a second.

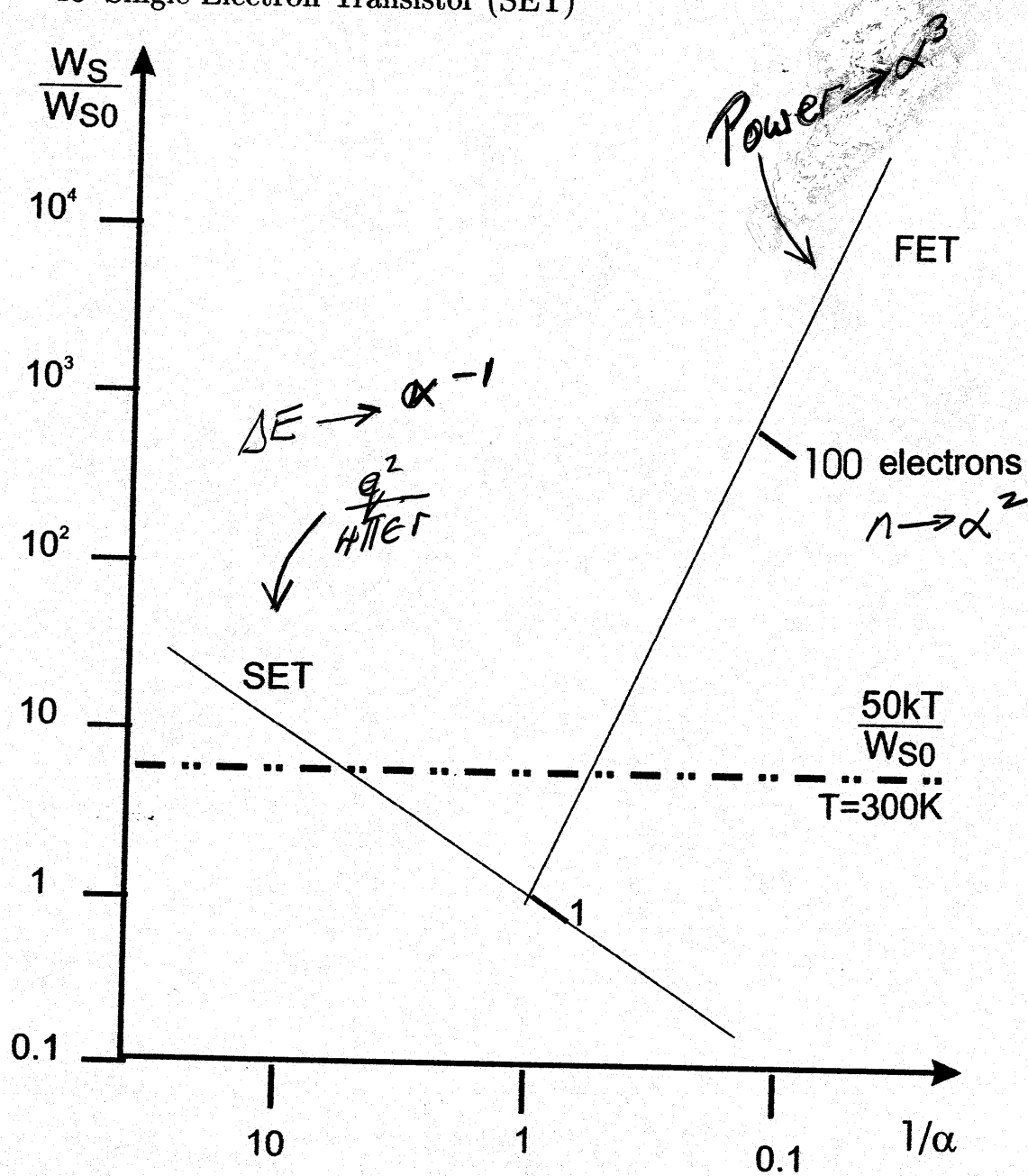


Fig. 13.17. The power-delay diagram reveals the impacts of scaling on the SET and FET

cooling. For si
 than the therm
 of the stored
 such as superc
 magnetic flux

13.4 Summr

Single electron
 since they can
 dimensions the
 moderate temp
 charge still rem
 improvements
 the developmen